Università degli Studi di Ferrara

ISTITUTO ITALIANO DI TECNOLOGIA

DOCTORAL COURSE IN
"Translational Neurosciences and Neurotechnologies"

CYCLE XXXII

COORDINATOR Prof. Luciano Fadiga

"microRNAs, gene networks and cell therapy: promises and challenges for treating epilepsies and their comorbidities"

Scientific/Disciplinary Sector (SDS) BIO/14

Candidate
Dott. Lovisari Francesca

Supervisor
Prof. Simonato Michele

Year 2016/2019

Abstract – English

Anti-epileptic drugs (AEDs) do not control seizures in about a third of epileptic patients. Moreover, epilepsy is not only seizures, as many may think: this disease is characterized by a plethora of neurologic and psychiatric comorbidities, that are often not even referred by the patients because of the strong stigma affecting epilepsy.

In the course of my PhD, I employed classical and holistic (systems genetics) approaches to try to tackle some of the major needs in epilepsy: 1) the identification of biomarkers of epileptogenesis, capable of identifying those individuals (estimated to be 10-20%) that will develop epilepsy following exposure to an epileptogenic insult like a brain trauma or an episode of status epilepticus; these biomarkers would be instrumental for the development of preventive therapies; 2) the treatment of seizures in drug-resistant patients; in particular, I focused on strategies to deliver therapeutic molecules that cannot cross the blood-brain barrier directly in the epileptogenic area; 3) the treatment of epilepsy comorbidities, that are generally not affected (and sometimes worsened) by currently available AEDs.

Epilepsy comorbidities. Using a systems genetics approach, Sestrin 3 (SESN3) was identified as a master regulator of a network of pro-epileptic genes that is up-regulated in hippocampal samples from temporal lobe epilepsy (TLE) patients. To better understand the effects of SESN3, we decided to evaluate the phenotype of SESN3-knock-out (SESN3-KO) rats, using different experimental models of TLE, and behavioral testing. As expected, SESN3-KO rats were less susceptible to chemoconvulsant-induced status epilepticus. In addition, both at P7 and at adult age, SESN3-KOs were found to have a lower tendency to anxious behaviors than wild-type animals. These results suggest an implication of SESN3 not only in seizure generation, but also in epilepsy comorbidities.

Biomarkers of epileptogenesis. A systems genetics approach was also applied to investigate biomarkers of epileptogenesis, by analyzing miRNA samples in plasma. A meta-analysis of data from 4 distinct epilepsy models identified the up-regulation of five miRNAs (three of which already known) in plasma samples of animals that would subsequently become epileptic, as compared with animals that would not become epileptic in spite of receiving an identical epileptogenic insult. Two of these miRNAs, namely miR-129-5p and miR-138-5p, were previously reported to be dysregulated in brain samples from experimental models of TLE and/or surgical resection of epileptic focus in patients.

Drug-resistant seizures. Brain-derived neurotrophic factor (BDNF) and glial-cell line derived neurotrophic factor (GDNF) may exert an anti-epileptic effect, because they are known to modulate mechanisms at the basis of epilepsy development and seizures occurrence. However, they cannot

cross the blood-brain barrier. We found that the delivery of these neurotrophic factors directly in the hippocampi of epileptic rats by using an encapsulated cell device highly decrease the frequency of epileptic seizures. Moreover, BDNF and GDNF treatment revert the cognitive impairment observed in the chronic phase of the disease.

Taken together, the data presented in this PhD thesis illustrate how traditional and new, holistic approaches can provide information on the mechanisms of epileptogenesis and contribute to the development of epilepsy treatments.

Abstract - Italiano

I farmaci anti-epilettici (*anti-epileptic drugs, AEDs*) non determinano controllo delle crisi in circa un terzo dei pazienti con epilessia. Quando si parla di epilessia, inoltre, sarebbe necessario tener presente la moltitudine di disturbi neurologici e comorbidità a essa correlate, di cui spesso nemmeno i pazienti parlano, per il timore del profondo stigma presente.
Durante il mio percorso di dottorato ho focalizzato l'attenzione su alcuni dei maggiori bisogni ancora oggi presenti in epilessia, applicando approcci tradizionali e alcuni più innovativi (genetica dei sistemi). Ciò di cui mi sono occupata è stato:
identificare biomarcatori di epilettogenesi, in grado di identificare preventivamente quegli individui (10-20% circa) a rischio di sviluppare epilessia, a seguito di un insulto epilettogeno quale trauma cranico o stato epilettico;
studiare nuovi approcci terapeutici potenzialmente utili in caso di farmaco-resistenza, valutando l'utilizzo di tecnologie innovative, che permettessero di somministrare direttamente nel focus epilettogeno alcune sostanze che, altrimenti, non sarebbero in grado di oltrepassare la barriera emato-encefalica;
valutare gli effetti di approcci terapeutici sulle comorbidità di epilessia, spesso non trattate dai comuni AEDs utilizzati.

Comorbidità di epilessia: il gene codificante la Sestrina 3 (SESN3) è stato identificato come regolatore di un network di geni pro-epilettici, sfruttando i principi della genetica dei sistemi: questi geni sono risultati infatti up-regolati in campioni di ippocampo di pazienti con epilessia del lobo temporale (TLE). Per prima cosa sono stati generati ratti SESN3 knocked-out (SESN3-KO), per permetterci di indagare a fondo sulle implicazioni di questo gene su epilessia e sue comorbidità. I nostri risultati dimostrano che gli animali SESN3-KO siano meno suscettibili all'induzione di Stato Epilettico (SE) a seguito di somministrazione di agenti chemo-convulsivanti. Inoltre, è stato possibile individuare una componente di minor suscettibilità nello sviluppo di ansia negli animali SESN3-KO, a partire da P7 fino all'età adulta. Presi insieme, questi risultati suggeriscono che il codificante per Sestrina 3 sia implicato sia nello sviluppo di crisi, ma anche nelle comorbidità associate ad epilessia.
Biomarcatori di epilettogenesi: le metodiche alla base della genetica dei sistemi sono state applicate anche per lo studio di biomarcatori di epilessia, nello specifico per lo studio di miRNA circolanti nel plasma. I dati, ottenuti a seguito dell'utilizzo di quattro diversi modelli di TLE, sono stati analizzati tramite il modello di meta-analisi; cinque miRNA diversi sono risultati up-regolati nel plasma di animali che, a posteriori, sarebbero diventati epilettici. Il confronto è stato svolto sia verso animali che, partendo dallo stesso tipo di insulto epilettogeno, non avrebbero sviluppato la

malattia, che verso animali naive. Due di questi cinque miRNA erano già stati descritti in ambito di epilessia: il miR-129-5p e il miR-138-5p.

Epilessia farmaco-resistente: dati di letteratura indicano che sia il brain-derived neurotrophic factor (BDNF) che il glial-cell derived neurotrophic factor (GDNF) possano avere azione anti-epilettica, in quanto in grado di modulare i meccanismi alla base dello sviluppo di crisi epilettiche. Questi due fattori neurotrofici, però, non possono essere somministrati per via periferica, in quanto impossibilitati ad oltrepassare la barriera emato-encefalica. Se somministrati però direttamente in ippocampo, tramite un sistema che utilizza cellule incapsulate all'interno di specifici devices, BDNF e GDNF sono in grado di modulare e diminuire la frequenza delle crisi epilettiche nel modello di TLE indotto da pilocarpina. Oltre al risultato positivo sulle crisi epilettiche, abbiamo inoltre osservato un miglioramento dell'impairment cognitivo, evidente in fase cronica di epilessia.

I dati esposti in questa tesi mirano quindi a dimostrare che è possibile utilizzare approcci tradizionali, ma anche olistici, per ottenere dettagliate informazioni inerenti i meccanismi alla base di epilettogenesi e che possano altresì essere sfruttati per identificare nuovi trattamenti per epilessia.

Table of contents

Structure of the thesis

This PhD thesis will be divided into different chapters:

- Chapter 1 will focus on epilepsy: etiology, epileptogenesis, treatments available and comorbidities
- Chapter 2 will focus on gene networks and systems genetics; it contains a brief review published in
- Chapter 3 will be about the implication of Sestrin 3 in epilepsy and comorbidities, it consists in a manuscript under submission

- Chapter 4 will focus on biomarkers of epileptogenesis, including a project we carried out in collaboration with other research laboratories throughout Europe
- Chapter 5 will elucidate the role of two different neurotrophic factors, BDNF and GDNF, on seizures reduction in a rat experimental model of TLE; papers are attached
- Chapter 6 will conclude and elucidate the future perspectives of my PhD projects
- In the end, there will be attached other works for which I co-worked.

Abstract

Anti-epileptic drugs (AEDs) do not control seizures in about a third of epileptic patients. Moreover, epilepsy is not only seizures, as many may think: this disease is characterized by a plethora of neurologic and psychiatric comorbidities, that are often not even referred by the patients because of the strong stigma affecting epilepsy.

In the course of my PhD, I employed classical and holistic (systems genetics) approaches to try to tackle some of the major needs in epilepsy: 1) the identification of biomarkers of epileptogenesis, capable of identifying those individuals (estimated to be 10-20%) that will develop epilepsy following exposure to an epileptogenic insult like a brain trauma or an episode of status epilepticus; these biomarkers would be instrumental for the development of preventive therapies; 2) the treatment of seizures in drug-resistant patients; in particular, I focused on strategies to deliver therapeutic molecules that cannot cross the blood-brain barrier directly in the epileptogenic area; 3) the treatment of epilepsy comorbidities, that are generally not affected (and sometimes worsened) by currently available AEDs.

Epilepsy comorbidities. Using a systems genetics approach, Sestrin 3 (SESN3) was identified as a master regulator of a network of pro-epileptic genes that is up-regulated in

hippocampal samples from temporal lobe epilepsy (TLE) patients. To better understand the effects of SESN3, we decided to evaluate the phenotype of SESN3-knock-out (SESN3-KO) rats, using different experimental models of TLE, and behavioral testing. As expected, SESN3-KO rats were less susceptible to chemoconvulsant-induced status epilepticus. In addition, both at P7 and at adult age, SESN3-KOs were found to have a lower tendency to anxious behaviors than wild-type animals. These results suggest an implication of SESN3 not only in seizure generation, but also in epilepsy comorbidities.

Biomarkers of epileptogenesis. A systems genetics approach was also applied to investigate biomarkers of epileptogenesis, by analyzing miRNA samples in plasma. A meta-analysis of data from 4 distinct epilepsy models identified the up-regulation of five miRNAs (three of which already known) in plasma samples of animals that would subsequently become epileptic, as compared with animals that would not become epileptic in spite of receiving an identical epileptogenic insult. Two of these miRNAs, namely miR-129-5p and miR-138-5p, were previously reported to be dysregulated in brain samples from experimental models of TLE and/or surgical resection of epileptic focus in patients.

Drug-resistant seizures. Brain-derived neurotrophic factor (BDNF) and glial-cell line derived neurotrophic factor (GDNF) may exert an anti-epileptic effect, because they are known to modulate mechanisms at the basis of epilepsy development and seizures occurrence. However, they cannot cross the blood-brain barrier. We found that the delivery of these neurotrophic factors directly in the hippocampi of epileptic rats by using an encapsulated cell device highly decrease the frequency of epileptic seizures. Moreover, BDNF and GDNF treatment revert the cognitive impairment observed in the chronic phase of the disease.

Taken together, the data presented in this PhD thesis illustrate how traditional and new, holistic approaches can provide information on the mechanisms of epileptogenesis and contribute to the development of epilepsy treatments.

Chapter 1: Epilepsy

Epilepsy is one of the most common neurological disorders, affecting more than 50 million people worldwide, with a higher impact in non-developed countries; for example, at least 5 million epileptic patients live in India [1]. A strong fear and stigma was conveyed to epilepsy since the ancient times, a stigma that even nowadays is not completely overcome.

The word epilepsy calls to mind the physical action to fall after a sudden perturbation, and its etymology derives from the word *Epilanbanein*, ("to be overwhelmed" in ancient Greek). Anyhow, this pathology was already known long before ancient Greece, again with a negative connotation: it was seen as sort of curse of the god of the moon. In addition, being epileptic meant not having rights such as the right to get married. Only Hippocrates, in 400 B.C., warned people about looking at epilepsy not as a damnation but as an illness of the brain.

Since the 18th century, epilepsy was also thought to be infectious, transmitted by contaminating people with the "evil's breath". Stigma and discrimination were not restricted to religious backgrounds: a large number of laws existed that inhibited epilepsy patients to live their lives freely: as an example, in the U.S epileptic patients were not allowed to enter restaurants, and marriage was allowed only in the mid of 20th century.

Things have fortunately changed and the level of misperception of epilepsy is not as severe as centuries ago, but a lot still needs to be done to allow patients to have a good quality of life: communication, education and support are needed for patients and their families. Even more importantly, issues related to the clinical aspects have to be solved. Among these clinical aspects, it is important to accelerate timing of diagnosis, and to avoid misdiagnosis and mistreatment for people who are developing epilepsy. In these respects, identification of biomarkers of epilepsy and epileptogenesis is a key issue.

1.1 Epidemiology and Classification

When talking about Epilepsies, the first thing people think about are seizures, but this is a common mistake: a seizure (the result of a parossistic excitability in the brain) is just a symptom, while the disease (epilepsy) entails many other aspects. In 2005, The International League Against Epilepsy (ILAE) redacted a first definition of epilepsy, stating it as a "disease characterized by an enduring *predisposition* to generate epileptic seizures and by the neurobiological, cognitive, psychological and social consequences of

this condition" [2]. This definition, not sufficiently detailed, was then revised in 2014 with a more practical definition that listed diagnosis criteria:

- At least two unprovoked seizures occurring more than 24 h apart; or
  One unprovoked seizure and a probability of further seizures similar to the general recurrence risk after two unprovoked seizures, occurring over the next 10 years.

The term "epilepsy" refers to a group of similar pathophysiological conditions, all characterised by an imbalance between excitatory and inhibitory circuitries in the brain, eventually leading to seizures.

An accurate classification of epilepsy is important to establish a proper diagnosis and therapy in the fastest time possible. From the early 60s a lot has been done to delineate a useful classification of the different types of seizures and epilepsies, and ILAE published in 2017 the latest revision of these classifications [3]. The classification of seizures is shown in Figure 1. the classification of the epilepsies takes into consideration seizure types, aetiologies and comorbidities.

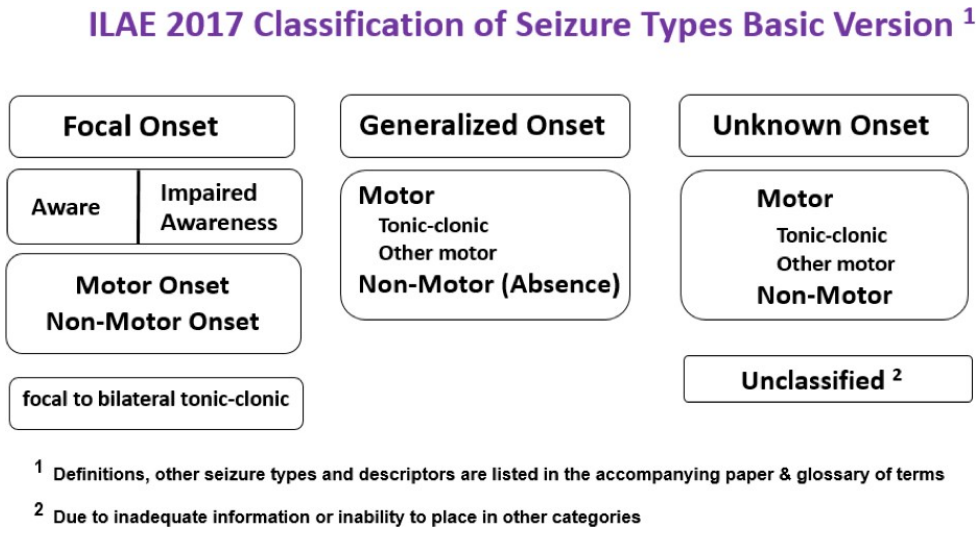

Fig.1: ILAE classification of seizures

Seizures can be divided in three categories: focal, generalized and of unknown onset.

Focal seizures are those originating in a strictly localized area of the brain, limited on one hemisphere only, not spreading across neuronal networks. Focal seizures often originate in subcortical regions. Analysing the symptomatology, focal seizures can be accompanied by motor activity, with rhythmic and repetitive spasms (tonic-clonic) or non-motor activity. Awareness may be impaired.

Generalized seizures are seizures that, even if originating in a specific brain area, rapidly spread to both hemispheres involving bilateral networks. Generalized seizures are always

accompanied by loss of awareness. They can be subclassified in non-motor seizures (absence or "petit-mal", characterized by a short-lasting loss of awareness) or motor seizures, which can vary from clonic, tonic or clonic-tonic activity.
Seizures of unknown onset are all the seizures that cannot be assigned to one of the two other categories.

1.2 Diagnosis and Treatment

Electroencephalography (EEG) recordings and imaging techniques, such as computerized tomography (CT), magnetic resonance imaging (MRI) and positron emission tomography (PET) are used to investigate brain function and anatomical alterations that can inform the diagnosis of epilepsy. Even when the patient is not experiencing a seizure, in fact, some EEG features may detected in an epileptic brain, for example interictal spikes.

Epilepsy drug therapy is not curative, meaning that anti-epileptic drugs (AEDs) only act on the symptoms. AEDs may have different mechanisms of action:
1) *Sodium Channel Blockers*: these channels permit the firing of an action potential in axons. They open in a voltage-dependent manner, allowing influx of Na^+ in the cell and generating action potentials. Their duration of opening is very short (ms) and is followed by a refractory period during which the channel is in an inactive state and action potential cannot be generated. Na^+ channel blockers stabilize the channels in this inactive state, limiting the firing rate of the neuron. This category includes Carbamazepine (CBZ), Oxacarbazepine, Lamotrigine and Phenytoin, which was one of the first drugs used to control epileptic seizures.
CBZ is one of the most used AEDs, both for partial and generalized seizures; it is normally well tolerated except for dose-related adverse effects mostly at the onset of therapy. CBZ can induce CYP3A4 and thereby interfere with the action of several all drugs metabolized by CYP3A4, such as tricyclic antidepressants, warfarin, oral contraceptives.
2) *Calcium Channel Inhibitors:* calcium channels can be found in different forms (L, N and T) in the human brain, where they lead to partial depolarization of the membrane by allowing Ca^{++} influx. T-channels are known to play an important role in absence seizures spike-and-wave discharges. AEDs that act on these channels control seizures by inhibiting this increased Ca^{2+} influx in the cell.
3) *Gamma-aminobutirric acid (GABA) signal enhancers*: GABA is the main inhibitory neurotransmitter in the brain. Benzodiazepines and barbiturates are positive allosteric modulators of $GABA_A$ receptors, that are Cl^--permeable channels, and thus facilitate

GABA-mediated hyperpolarization. Other AEDs prolong the effect of released GABA by blocking its reuptake (Tiagabine) or by inhibiting its catabolism by GABA transaminase (Vigabatrin).

Benzodiazepines (diazepam, lorazepam and clonazepam) and barbiturates (phenobarbital) are the most commonly used drugs of this group. Unfortunately, these drugs have many side effects: respiratory depression, sedation and psychomotor impairment. Tiagabine has also profound side effects, like asthenia, dizziness and emotional lability. Vigabatrin is linked to important visual side effects that can be irreversible.

4) *Glutamate signal inhibitors*: glutamate is the main excitatory neurotransmitter. When it binds its ionotropic receptors, glutamate induces the inflow of Na^+ (and Ca^{2+}) and the efflux of K^+, resulting in excitation. Drugs implicated in inhibiting the glutamate signal include AMPA/Kainate inhibitors (Perampanel) and blockers of presynaptic Ca^{2+} channels implicated in electro-secretory coupling in glutamatergic terminals (Gabapentin).

5) *SV2A-binding drugs:* the synaptic vesicle protein 2A (SV2A) is thought to play an important role in the dynamics of neurotransmitter vesicles Some effective AEDs (Levetiracetam) interact with this protein [4].

AEDs should be managed carefully, paying attention to their side effects (Table 1). Monotherapy is recommend as a first approach after diagnosis. However, polytherapy is most common in the vast majority of patients. Assessing the best therapeutic approach may take a lot of time and efforts and all the possible signs of toxicity must be analysed during drug treatment.

Somnolence and dizziness (Gabapentin, Lacosamide, Levetiracetam, Lamotrigine, Oxcarbazepine, Perampanel, Topiramate, Vigabatrin)	**Behavioral problems and psychotic episodes** (Gabapentin, Topiramate, Levetiracetam, Vigabatrin)	**Depression** (Vigabatrin, Levetiracetam)	**Cognitive impairment** (Topiramate, Oxcarbazepine)	**Teratogenic effects** (Valproate, Phenytoin)
Hypersensitivity (Topiramate, Lamotrigine, Oxcarbazepine)	**Weight loss** (Topiramate) **and weight gain** (Gabapentin, Vigabatrin, Valproic Acid)	**Leukopoenia** (Oxcarbazepine)	**Gastrointestinal problems and nausea** (Gabapentin, Levetiracetam, Oxcarbazepine, Valproate)	**Hepatic enzyme inducers** (Phenytoin, Carbamazepine, Barbiturates, Topiramate)

Tab 1: Side effects of AEDs

Despite the many available AEDs, 30% of patients still struggle to experience any benefit from the conventional drug therapy, thus becoming drug resistant. ILAE defines drug

resistant epilepsy (DRE) a condition in which seizures cannot be controlled with two AEDs, either in mono or poli-therapy.

In these cases, options to treat are limited to the surgical removal of the epileptogenic focus, when possible, or other approaches like vagal nerve stimulation (VNS), deep brain stimulation (DBS) or ketogenic diet.

- *Surgery*

Surgery for drug-refractory epilepsy consists in the removal of the epileptic focus. This option must be considered only after careful identification of the area where seizures arise, using EEG, MRI (to assess possible structural abnormalities) and also neuropsychological examination. The ideal condition in which the surgical approach is feasible is when the epileptogenic area is well localized and its removal would not cause any important deficit [5]. In 90% of the cases, surgery results in healing focal epilepsy but, even when total seizure control is not reached, patients experience a sensible improvement in their quality of life [6].

- *Vagal nerve (VNS) or deep brain stimulation (DBS)*

VSN was firstly proposed in 1880 by Nothnagle, who stated that electrically stimulating the vagus nerve could reduce venous hyperaemia in the brain, a condition that (in his view) may lead to epilepsy. In 1883, James Corning reported positive results on convulsions through the combination of specific devices, where compression of the carotid artery and stimulation of the vagal nerve decreased cerebral flow. VNS is approved by the FDA as epilepsy treatment in patients older than 4 years who suffer from intractable partial epilepsy. The exact mechanism through which it regulates seizure activity remains unclear. It seems probable that VNS efficacy is the result of the interaction of several mechanisms [7]. In any case, VNS proved to be well tolerated and helpful for different epileptic syndromes, such as Lennox-Gastault and absence epilepsy.

DBS consists in the implantation of deep electrodes inside the brain and low-amplitude stimulation activating axons in a programmed manner – as a sort of pacemaker – to help control brain activity. DBS efficacy to treat epilepsy, and its tolerability have been shown in a multicentric double-blind trial, named SANTE, where 110 epileptic patients, suffering from partial or generalized seizures, were randomized to DBS in the anterior nucleus of the thalamus during a three months window of time. A 40% reduction in the treated group was shown, compared to a 14% in the control, unstimulated group. Long-term follow-up of this trial, at 5 years after treatment, showed a further improvement in the reduction of severe seizures. Moreover, no cognitive decline or worsening of depression were reported [8].

- *Ketogenic Diet (KD)*

The ketogenic dietary approach, based on high-fats and low-carbohydrates food intake, is a non-pharmacological alternative therapy, widely used especially for childhood drug resistant epilepsy. Our cells, including neurons, use glucose as fuel; in a low-carbohydrate diet, that can be viewed as a hypoglicemic long-lasting, fuel and energy must be obtained from other macronutrients, such as ketones, the products deriving from splitting fat molecules. The real benefits of this therapeutic approach are still unclear, as well as the mechanism. The leading hypothesis is that changes in ATP production (i.e. glucose starvation) might have an incidence in the change of metabolic demand during seizures; other hypotheses relate to increase of adenosine levels and DNA methylation [9,10]. In any event, KD may ameliorate not only seizures but also comorbidities [11,12]. However, ketosis might lead to a toxic state and it is therefore of great importance that a therapeutic approach like KD must be prescribed very carefully.

1.3 Temporal Lobe Epilepsy

In the first paragraphs of this chapter, it was already stressed out that the term epilepsy includes a large variety of syndromes. Temporal lobe epilepsy (TLE) identifies a specific type of the disease hitting the temporal lobe of the brain. TLE is one of the most common acquired form of focal epilepsy in adults, with nearly 2/3 of epileptic patients suffering from intractable TLE undergoing surgery [13]. It always starts as a focal form of epilepsy, meaning it originates from a specific brain region of one hemisphere, but it can secondarily generalize into the other hemisphere.

There are two types of TLE:

1) lateral temporal lobe epilepsy (lTLE), the less common form, which originates in the neocortical temporal area and
2) mesial temporal lobe epilepsy (mTLE), the most common and most studied, that hits the inner regions of the temporal lobe: hippocampus, para-hippocampal gyrus and amygdala [14]. This specific form is often associated with structural modifications such as hippocampal sclerosis (HS), rearrangements in synaptic plasticity and aberrant gliosis and neurogenesis [15].

As illustrated in Fig. 2, the brain injury leading to the development of TLE might be caused by different external factors such as a brain trauma, stroke, infection, status epilepticus, febrile seizures during childhood and brain tumours; all of these represent

triggering factors for the reorganisations and modifications that lead a healthy brain to become an epileptic one. After a latency period during which no evident symptomatology can be identified, the patient experiences the first spontaneous seizures and only at this point it is possible to diagnose the disease. This latency period corresponds to the epileptogenesis phase.

TLE is responsible not only for the occurrence of spontaneous seizures, but patients can occasionally report problems with memory – in most cases not severe - and emotion consolidation, as these aspects are controlled by the limbic system; moreover, at least 40 to 80% of patients also have automatisms such as lip smacking and rubbing of hands.

The phenomenon of pharmaco-resistance, that hits nearly 40% of epilepsy patients, is widely common in TLE, and it worsens the on-going problems this disease determines on the general quality of life and personal health risks. Pharmacological therapy and non-pharmacological treatments chosen for TLE patients should take into consideration not only the type and origin of epileptic seizures, but also possible comorbidities and other problems related to the disease itself, and lot remains to be done in order to identify molecules acting on the triggering factors for the development of epilepsy: i.e., anti-epileptogenic and disease-modifying therapy. In this regard, research is working to investigate and understand the basis of the transformation of a healthy brain into an epileptic one, and to identify possible biomarkers to identify (and treat) patients before the onset of spontaneous seizures.

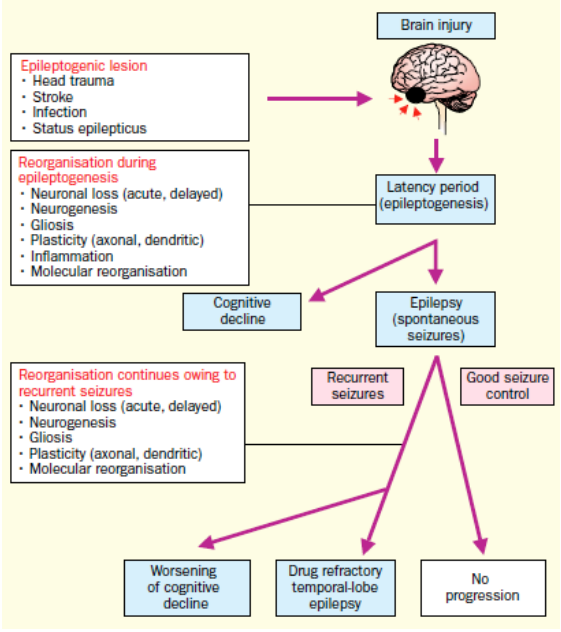

Fig. 2: The epileptic process in TLE (Pitkanen and Sutula, 2002)

1.4 Limbic system

The limbic system is composed of several cerebral structures: thalamus, hypothalamus, amygdala and hippocampus. These areas and their neuronal networks are responsible for memory consolidation, emotions, mood tone. Here we will focus on the hippocampal area, the one mostly associated with mTLE and with the epilepsy model we apply in our studies. The hippocampal area is composed of the hippocampus, subiculum, parasubiculum and prosubiculum – to which the majority of hippocampal neurons project – and the entorhinal cortex – from which the hippocampus receives excitatory and inhibitory inputs.

Two different anatomical areas can be identified in the hippocampus (Fig. 3): the Ammon' horn region, or *Cornu Ammonis* in latin (CA) subdivided in the CA1, CA2 and CA3 areas, and the dentate gyrus (DG).

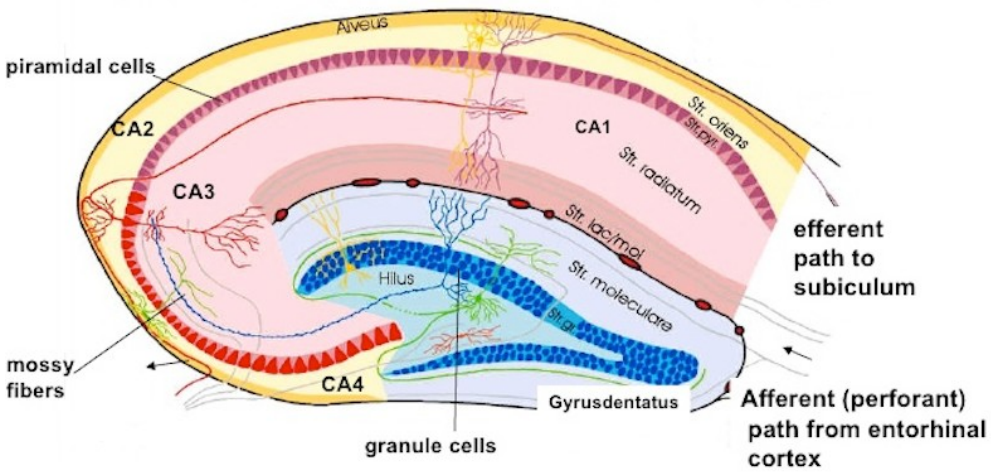

Fig 3: Anatomic organisation of the hippocampus

As members of a more complex system, hippocampal neurons communicate with other regions of the limbic system; excitatory inputs come from the entorhinal cortex through the perforant path, that project to DG granular cells and CA3 dendrites. Mossy fibers are the projections from the DG granular cells to the CA3 pyramidal neurons. The signal is then transmitted to the CA1 area through the Shaffer's collaterals, and finally to the subiculum through efferent fibers.

Gamma-aminobutyric acid (GABA) plays an important role on balancing excitatory information.

1.5 Epileptogenesis

The term "epileptogenesis" defines the processes leading to the transformation of a normal

healthy brain into an altered, epileptic tissue, that is capable of generating spontaneous seizures [16].

While for decades it was thought that the epileptogenesis identified the phase from the brain insult to the occurrence of the first spontaneous seizure that allows the diagnosis [17], in the last decades it has been recognized that epileptogenesis continues even after the occurrence of the first seizure. Indeed, many experimental and clinical studies suggest that molecular and cellular modifications that are triggered by the initial insult can progress and worsen after the diagnosis of epilepsy, rendering epileptogenesis a continuous and prolonged process; moreover, seizures per se may cause the worsening of morphological modifications [18] .

Even if no sign or symptom can be detected during the latency phase, lasting months to years, in patients that will eventually become epileptic a plethora of morphological and biological modifications do take place [19] . The most frequently observed molecular and cellular alterations include neurodegeneration and neuronal loss; neuroinflammation and recruitment of cytokines and interleukines; gliosis; aberrant neurogenesis; mossy fiber sprouting and dendritic remodelling; angiogenesis; loss of GABAergic interneurons, leading to downregulation in the inhibitory signals.

Neurodegeneration is mainly observed in the hilus of the DG and in CA1 and CA3 pyramidal cells and GABAergic interneurons, while it less commonly affects CA2 piramidal cells and the granular layer of the DG [20]. It is not only the hippocampus that shows neurodegeneration during epileptogenesis, but also other areas like the amygdala, entorhinal cortex, thalamus and cerebellum [21] . Neurodegeneration during epileptogenesis has a lot of consequences: it compromises the circuitry and the correct functionality of neuronal networks; it can contribute to pathological processes leading to epilepsy or to comorbidities; it triggers the instauration of inflammatory responses and astrogliosis.

With the activation of apoptotic factors like Bcl-2, astrocytes and microglial cells are activated and release pro-inflammatory molecules, such as cytokines. In particular, interleukin-1β (Il-1β) and Tumor Necrosis Factor-α (TNF-α) can interfere with glutamate re-uptake and, consequently, increase NMDA and AMPA receptor activation and levels of intracellular Ca^{2+}. All these factors together are responsible for increased seizure susceptibility and excitotoxicity [22].

Aberrant hippocampal neurogenesis is another feature often observed in TLE. It is known that the hippocampal region is one of the brain areas where neurogenesis is maintained throughout life. Seizures are responsible of the migration of newborn neurons into the

dentate hilus and the molecular layer; if not controlled, this process may modify the normal neuronal plasticity [23] .

Sprouted mossy fibers increase the number of excitatory connections between granule cells, contributing to the maintenance of chronic TLE [24]. Albeit it remains unclear how this process arises, a conspicuous number of studies, both in human tissue and in experimental models, confirm that mossy fibers sprouting is a common aspect of TLE.

1.6 Epilepsy comorbidities

A condition is defined comorbid when it occurs concomitantly with another disease. Many studies reported the high burden of comorbidities in epilepsy, reaching almost 50% of patients and heavily affecting the prognosis and the quality of life. Eighty percent of TLE patients experience a comorbid condition during life, and almost 80% of the comorbidities involve mood and the psychiatric context.

Identification of the mechanism of association is very important:

- Causative: the comorbidity takes place first and gives rise to epilepsy;
- Shared risk: there is no causal relation between comorbidity and epilepsy, but they share some underlying risk factor (genetic, environmental, structural or physiological);
- Resultant mechanism: epilepsy takes place first and causes the comorbidity;
- Bidirectional: the two conditions cause each other.

The role of genetics in epilepsy comorbidities can include causative or resultant associations. One example is the relation between epilepsy and auto-immune diseases like type 1 diabetes, because patients with both conditions often are diagnosed with the presence of GAD antibodies (80% of TD1 and 6% of epileptic patients).

As stated above, mood and psychiatric disorders are the most common comorbid conditions experienced by epileptic patients. Depression, anxiety and psychosis are the most common [25]. The link between epilepsy and mental disorders may be related to changes in neurotransmitter systems, such as decreased serotoninergic and glutamatergic signalling, that influence intracellular signalling pathways and induce neuronal hyperexcitability. Animal models of epilepsy are a great tool for understanding comorbidities: one example is a study in which lowering serotonergic transmission and noradrenergic transmission has been found to facilitate the occurrence of seizures in several animal models of epilepsy [26].

As already stressed pointed out, **depression** is one of the most common comorbidity

diagnosed in patients with epilepsy [27]; apart from TLE, in which the limbic system is involved, the causes might be related to AEDs side effects such as fatigue, sleep and eating difficulties, slowed thinking and decreased energy. Moreover, the stigma around epilepsy contributes to self-esteem and social isolation. However, different animal models demonstrate that epilepsy and depression can be related even when no pharmacological treatment is ongoing, and neurotransmitter disturbances may explain the link. Animal models of depression have demonstrated increased CNS glutamatergic activity, mediated by decrease expression of glutamate-transporters, as well as decreased GABAergic neurotransmission, all resulting in increased cortical hyperexcitability. Other mechanisms might be alterations in the hypothalamic–pituitary–adrenal axis or activation of proinflammatory cytokines like interleukin 1 beta (IL-1β), that have proconvulsant properties [26]. Recent studies have tried to identify a correlation between the development of depression and the localisation of the epileptic focus, without solid results [28]. It appears, instead, that depression in epileptic patients might be due to the presence of epilepsy itself, no matter the type and severity of the disease per se.

Another common psychological comorbidity is the Attention Deficit and Hyperactivity Disorder, known as **ADHD**: this condition is characterised by overactivity, behavioural problems and poor impulse control, as well as difficulties in attention and learning. Similar to depression, ADHD and epilepsy share common underlying pathophysiological mechanisms that may be responsible for the occurrence of the two conditions: disruption of lipid metabolism, norepinephrine system or dopamine transport system modifications.

Since the early thirties, **anxiety** has been recognized to be linked to epilepsy, contributing to a worsening in the quality of life. Anxiety may be a consequence of restrictions in everyday life due to the unpredictability of the disease and of the low self-esteem; however, it may also be caused by the pathophysiology underlying the two diseases. Several type of anxiety can be diagnosed in epilepsy patients, such as obsessive-compulsive disorder, generalized anxiety disorder or post-traumatic disorder. Depending on the temporal relation with spontaneous seizures, anxiety can occur before, during, in between or after having experienced a seizure. These disorders are more common in patients with epilepsies involving the limbic system [29] .

Cognitive functions may also be impaired in some forms of epilepsy, including TLE, being the hippocampus a crucial area for episodic, spatial and emotional memory

consolidation. Cognitive impairment in people with epilepsy might be due to neuronal cell loss occurring during the initial lesion, such as status epilepticus or brain trauma, or during spontaneous seizures. Moreover, chronic and intense dysfunctionality of the limbic system may worsen the cognitive impairment [30].

1.7 Experimental models of epilepsy

Epilepsy is a complex disease and its causes are yet not well known: animal models are thus useful tools to better understand pathophysiological mechanisms underpinning epilepsy development. As already described, TLE may arise following a brain trauma, brain infections, stroke, tumor or status epilepticus (SE). In rodents, SE can be induced using chemoconvulsant agents, such as pilocarpine or kainic acid, or by electrical stimulation. SE experimental models are continuously refined to identify the best model that permits to study the development of chronic epilepsy, the mechanisms underlying the synaptic reorganisation and neuronal death that are common during epileptogenesis, the changes in gene expression that arise after seizure induction and, of course, to study new anticonvulsant and anti-epileptic drugs.
The ideal SE animal model should reflect the pathophysiology of human TLE: it should exhibit a clear seizure phenotype, meaning a latency period between the initial brain insult and the occurrence of spontaneous seizures, and epileptogenesis should be characterized by neuropathological features of human TLE such as aberrant neurogenesis, astrogliosis, mossy fibers sprouting, neuronal death. Being TLE one of the most commonly pharmacoresistant epilepsy, epileptic animals must exhibit resistance to certain AEDs, in order to allow the screening of novel compounds. Moreover, an ideal experimental model of epilepsy should also display the same comorbid scenario observed in clinics.

One of the most widely accepted SE animal models is the kainic acid (KA) model, in which the chemoconvulsant, a cyclic analog of L-glutamate, is used because of its ability to bind and activate AMPA and KA glutamatergic receptors. Ben-Ari was the first scientist who described how, after an intra-amygdaloid injection of kainic acid, rodents display behavioral seizures and damage could be eventually reported in the CA4 region of the hippocampus [31]. The administration of KA may be performed via peripheral or intra-cerebral (hippocampus or amygdala) administration, and is followed by the development of a convulsive SE.

The pilocarpine model was first described by Turski in 1983: this chemical agent, binding M1 muscarinic receptors, results in Ca^{2+} levels alteration and consequent abnormal release of glutamate from presynaptic terminals, which binds N-methyl-D-aspartate (NMDA) glutamatergic receptors, inducing SE [32 33]. Activation of NMDA receptors also leads to an excitotoxic effects and cell death. Pilocarpine can be administered either peripherally or via intra-hippocampal injection, both in rats and mice, even if in the latter it is responsible for a high mortality rate. The induced SE is characterized by tonic-clonic seizures, and it is followed by a latent, seizure-free period, that corresponds to epileptogenic molecular and cellular modifications. After this latent period, spontaneous recurrent seizures arise.

More recently, the model has been refined into the lithium-pilocarpine model, in which pilocarpine is given in combination with lithium. The rationale is to lower the seizure threshold, allowing also to lower the pilocarpine doses by 10 times, with a decrease in mortality rate. Another refinement is the use of a drug cocktail to block SE, composed of one benzodiazepine, one barbiturate and a muscarinic antagonist. Multiple administration of these drugs terminates both behavioral and encephalographic seizures.

The intra-hippocampal or intra-amygdala kainate models and pilocarpine or lithium-pilocarpine models in rats are characterized, in the chronic period, by the occurrence of spontaneous recurrent seizures. When using these experimental models, in order to assess the severity of recorded spontaneous seizures, researchers usually refer to the Racine's scoring scale [34]. In this scale, seizures are classified in five different classes, from 1 to 5, dividing partial (classes from 1 to 3) to generalized seizures (class 4 and 5). These chronic models of TLE are useful also because they lead to the development of some of the most common neurological comorbidities of epilepsy, such as impairment in memory and cognition, anxiety and depression. All of these behavioral implications can be assessed using behavioral tests, opening the possibility to test novel therapeutic approaches that can be used for treating both epileptic seizures and comorbidities.

References

1. Pitkänen A, Lukasiuk K. Mechanisms of epileptogenesis and potential treatment targets. *The Lancet Neurology* 2011; **10**(2): 173-86.
2. <Fisher_et_al-2005-Epilepsia.pdf>.
3. Fisher RS. An overview of the 2017 ILAE operational classification of seizure types. *Epilepsy Behav* 2017; **70**(Pt A): 271-3.
4. <pq015268.pdf>.
5. Liu G, Slater N, Perkins A. Epilepsy: Treatment Options. *Am Fam Physician* 2017; **96**(2): 87-96.

6. Villanueva V, Carreno M, Herranz Fernandez JL, Gil-Nagel A. Surgery and electrical stimulation in epilepsy: selection of candidates and results. *Neurologist* 2007; **13**(6 Suppl 1): S29-37.
7. Fan JJ, Shan W, Wu JP, Wang Q. Research progress of vagus nerve stimulation in the treatment of epilepsy. *CNS Neurosci Ther* 2019.
8. Salanova V. Deep brain stimulation for epilepsy. *Epilepsy Behav* 2018; **88S**: 21-4.
9. Lusardi TA, Akula KK, Coffman SQ, Ruskin DN, Masino SA, Boison D. Ketogenic diet prevents epileptogenesis and disease progression in adult mice and rats. *Neuropharmacology* 2015; **99**: 500-9.
10. Caraballo R, Vaccarezza M, Cersosimo R, et al. Long-term follow-up of the ketogenic diet for refractory epilepsy: multicenter Argentinean experience in 216 pediatric patients. *Seizure* 2011; **20**(8): 640-5.
11. Chen F, He X, Luan G, Li T. Role of DNA Methylation and Adenosine in Ketogenic Diet for Pharmacoresistant Epilepsy: Focus on Epileptogenesis and Associated Comorbidities. *Front Neurol* 2019; **10**: 119.
12. Freeman JM, Kossoff EH, Hartman AL. The ketogenic diet: one decade later. *Pediatrics* 2007; **119**(3): 535-43.
13. Blair RD. Temporal lobe epilepsy semiology. *Epilepsy Res Treat* 2012; **2012**: 751510.
14. Allone C, Lo Buono V, Corallo F, et al. Neuroimaging and cognitive functions in temporal lobe epilepsy: A review of the literature. *J Neurol Sci* 2017; **381**: 7-15.
15. Thom M. Review: Hippocampal sclerosis in epilepsy: a neuropathology review. *Neuropathol Appl Neurobiol* 2014; **40**(5): 520-43.
16. Pitkanen A, Lukasiuk K, Dudek FE, Staley KJ. Epileptogenesis. *Cold Spring Harb Perspect Med* 2015; **5**(10).
17. Dudek FE, Staley KJ. The Time Course and Circuit Mechanisms of Acquired Epileptogenesis. In: th, Noebels JL, Avoli M, Rogawski MA, Olsen RW, Delgado-Escueta AV, eds. Jasper's Basic Mechanisms of the Epilepsies. Bethesda (MD); 2012.
18. Kadam SD, Smith-Hicks CL, Smith DR, Worley PF, Comi AM. Functional integration of new neurons into hippocampal networks and poststroke comorbidities following neonatal stroke in mice. *Epilepsy Behav* 2010; **18**(4): 344-57.
19. Bertram E. The relevance of kindling for human epilepsy. *Epilepsia* 2007; **48 Suppl 2**: 65-74.
20. Pitkanen A, Sutula TP. Is epilepsy a progressive disorder? Prospects for new therapeutic approaches in temporal-lobe epilepsy. *Lancet Neurol* 2002; **1**(3): 173-81.
21. Jutila L, Immonen A, Partanen K, et al. Neurobiology of epileptogenesis in the temporal lobe. *Adv Tech Stand Neurosurg* 2002; **27**: 5-22.
22. Webster KM, Sun M, Crack P, O'Brien TJ, Shultz SR, Semple BD. Inflammation in epileptogenesis after traumatic brain injury. *J Neuroinflammation* 2017; **14**(1): 10.
23. Shetty AK. Hippocampal injury-induced cognitive and mood dysfunction, altered neurogenesis, and epilepsy: can early neural stem cell grafting intervention provide protection? *Epilepsy Behav* 2014; **38**: 117-24.
24. Santhakumar V, Aradi I, Soltesz I. Role of mossy fiber sprouting and mossy cell loss in hyperexcitability: a network model of the dentate gyrus incorporating cell types and axonal topography. *J Neurophysiol* 2005; **93**(1): 437-53.
25. Kanner AM. Management of psychiatric and neurological comorbidities in epilepsy. *Nat Rev Neurol* 2016; **12**(2): 106-16.
26. Korczyn AD, Schachter SC, Brodie MJ, et al. Epilepsy, cognition, and neuropsychiatry (Epilepsy, Brain, and Mind, part 2). *Epilepsy & Behavior* 2013; **28**(2): 283-302.

27. Sankar R, Mazarati A. Neurobiology of Depression as a Comorbidity of Epilepsy. In: th, Noebels JL, Avoli M, Rogawski MA, Olsen RW, Delgado-Escueta AV, eds. Jasper's Basic Mechanisms of the Epilepsies. Bethesda (MD); 2012.
28. Rider FK, Danilenko OA, Grishkina MN, et al. Depression and Epilepsy: Comorbidity, Pathogenetic Similarity, and Principles of Treatment. *Neuroscience and Behavioral Physiology* 2017; **48**(1): 78-82.
29. Vazquez B, Devinsky O. Epilepsy and anxiety. *Epilepsy & Behavior* 2003; **4**: 20-5.
30. Mazarati A. Epilepsy and forgetfulness: one impairment, multiple mechanisms. *Epilepsy Curr* 2008; **8**(1): 25-6.
31. Ben-Ari Y, Pradelles P, Gros C, Dray F. Identification of authentic substance P in striatonigral and amygdaloid nuclei using combined high performance liquid chromatography and radioimmunoassay. *Brain Res* 1979; **173**(2): 360-3.
32. Hamilton SE, Loose MD, Qi M, et al. Disruption of the m1 receptor gene ablates muscarinic receptor-dependent M current regulation and seizure activity in mice. *Proc Natl Acad Sci U S A* 1997; **94**(24): 13311-6.
33. Turski WA, Cavalheiro EA, Schwarz M, Czuczwar SJ, Kleinrok Z, Turski L. Limbic seizures produced by pilocarpine in rats: behavioural, electroencephalographic and neuropathological study. *Behav Brain Res* 1983; **9**(3): 315-35.
34. Racine RJ, Gartner JG, Burnham WM. Epileptiform activity and neural plasticity in limbic structures. *Brain Res* 1972; **47**(1): 262-8.

Chapter 2: Systems Biology and Gene Networks

Cells, tissues and organs work together as a complex biological system. Therefore, it is not surprising that a mutation or loss-of-function affecting a gene does not only cause a single protein to function improperly; the mutation can trigger a cascade of events hierarchically distributed from molecular to behavioral, that may ultimately lead to the development of a disease. In other words, when studying a disease we should look at its complexity. In the field of Systems Biology, complex networks research can be described as the characterization, analysis and simulation of complex systems, taking into account different elements of connections [1]. General systems theory dates back to Beralanffy who, seeking a way to study the organism as a whole and not as single compartments, proposed the unification of mathematical models and biology [2] .

Complex systems are by definition non-linear and hierarchically self-organized: this means that a perturbation of the system can cause an alteration in the way the system is organized, influencing its final behavior that, therefore, cannot be understood by analyzing the single components. In general, it is easier to predict the impact of a perturbation at higher level of the hierarchy because fewer non-linear steps should be taken into account, whereas a perturbation at the lower levels of the hierarchy may trigger compensatory mechanisms or interactions more difficult to predict.

Systems Genetics is a small part of Systems Biology, that aims to "understand how genetic information are integrated, coordinated and ultimately transmitted through molecular, cellular and physiological networks, to enable the higher-order functions and emergent properties of biological systems" [3]. Systems genetics studies multiple genetic perturbations rather than individual ones, giving an idea of the general architecture of complex traits and into the flow of biological information [4].

References

1. Mahoney JM, Mills JD, Muhlebner A, et al. 2017 WONOEP appraisal: Studying epilepsy as a network disease using systems biology approaches. *Epilepsia* 2019; **60**(6): 1045-53.
2. Kesic S. Systems biology, emergence and antireductionism. *Saudi J Biol Sci* 2016; **23**(5): 584-91.
3. Nadeau JH, Dudley AM. Genetics. Systems genetics. *Science* 2011; **331**(6020): 1015-6.

4. Civelek M, Lusis AJ. Systems genetics approaches to understand complex traits. *Nat Rev Genet* 2014; **15**(1): 34-48.
5. Simonato M. Epilepsy an Update on Disease Mechanisms: The Potential Role of MicroRNAs. *Front Neurol* 2018; **9**: 176.

Epilepsy & Behavior xxx (xxxx) xxx

Contents lists available at ScienceDirect

Epilepsy & Behavior

journal homepage: www.elsevier.com/locate/yebeh

Review

Gene networks and microRNAs: Promises and challenges for treating epilepsies and their comorbidities

Francesca Lovisari [a], Michele Simonato [a,b,*]

[a] Section of Pharmacology, Department of Medical Sciences, University of Ferrara, Italy
[b] School of Medicine, University Vita-Salute San Raffaele, Milan, Italy

article info

Article history:
Received 5 July 2019
Revised 6 August 2019
Accepted 8 August 2019
Available online xxxx

Keywords:
Epileptogenesis
Seizures
Systems biology
Sestrin3
miRNA

abstract

Neurobiology research has used an essentially reductionist approach for many years, dissecting out the brain in more simple elements. Recent technical advances, like systems biology, have made now possible to embrace a more holistic vision and try to tackle the complexity of the system. In this short review, we describe how these approaches, in particular analyses or gene networks and of microRNAs, may be useful for epilepsy research. We will describe and discuss recent studies that illustrate how these research approaches can lead to the identification of therapeutic targets and pharmacological strategies to prevent or treat some forms of epilepsy. We aim to show that studying epilepsy and its comorbidities within a complex system framework is a promising integration to the traditional reductionist approaches, and that it will become more and more important in the future for developing new therapies.

This article is part of the Special Issue "NEWroscience 2018."

1. Systems biology

The approach to research in neurobiology has changed in the past few decades: the historic reductionist approach is now paired with a more holistic vision. Reductionism can be traced back to Bacon and Descartes: the first stated that laws derived from specific cases should be used to elaborate general predictions, while the second proposed to divide a problem in many little case studies and solve them one by one [1]. From the early 50's, more integrated approaches gained importance in molecular biology and more recently, starting with the Human Genome Project, new, holistic systems biology approaches were developed. Reductionism gives significance to one factor at a time and considers systems as linear and predictable [1]. Systems biology views at different factors as capable of describing a behavior, and considers systems as nonlinear and nonpredictable on the basis of knowledge of their single components. An initial theory of systems was proposed by Beralanffy [2], who was seeking a way to study the organism as a whole and not as the sum of individual parts, and proposed means to unify mathematical models and biology. It must be emphasized that, without the results obtained using reductionist approaches, important notions about genes, molecules, and processes would not exist. Thus, the aim of systems biology is not to substitute more traditional approaches but, rather, to find connecting links at higher levels, prioritizing networks against single elements (for example, molecules or cells).

In a reductionist framework, a mechanism underlying a disease is identified within the components of the system itself. This could lead to misinterpretations, because it is well-known that, for example, a loss of function or a mutation of a single gene may not be sufficient to produce a disease and complex diseases are the results of multiple mechanisms that interfere one with another. Therefore, analyzing single components may be insufficient to clarify the mechanisms of disease in complex biological systems.

A complex system is any system featuring large numbers of interacting components whose aggregate activity is nonlinear (not derivable from the summation of the activities of the individual components) and that exhibits hierarchical self-organization. The brain is a quintessential complex system (Fig. 1). Important features of complex systems include the following: no level is biologically more relevant than any other; each level is required for the level above it and may feedback to the level below it (hierarchy); prediction of how a level will behave as a function of a change in a

* Corresponding author at: Section of Pharmacology, Department of Medical Sciences, University of Ferrara, Via Fossato di Mortara 17-19, 44121 Ferrara, Italy.
E-mail address: michele.simonato@unife.it (M. Simonato).

https://doi.org/10.1016/j.yebeh.2019.106488

Please cite this article as: F. Lovisari and M. Simonato, Gene networks and microRNAs: Promises and challenges for treating epilepsies and their comorbidities, Epilepsy & Behavior, https://doi.org/10.1016/j.yebeh.2019.106488

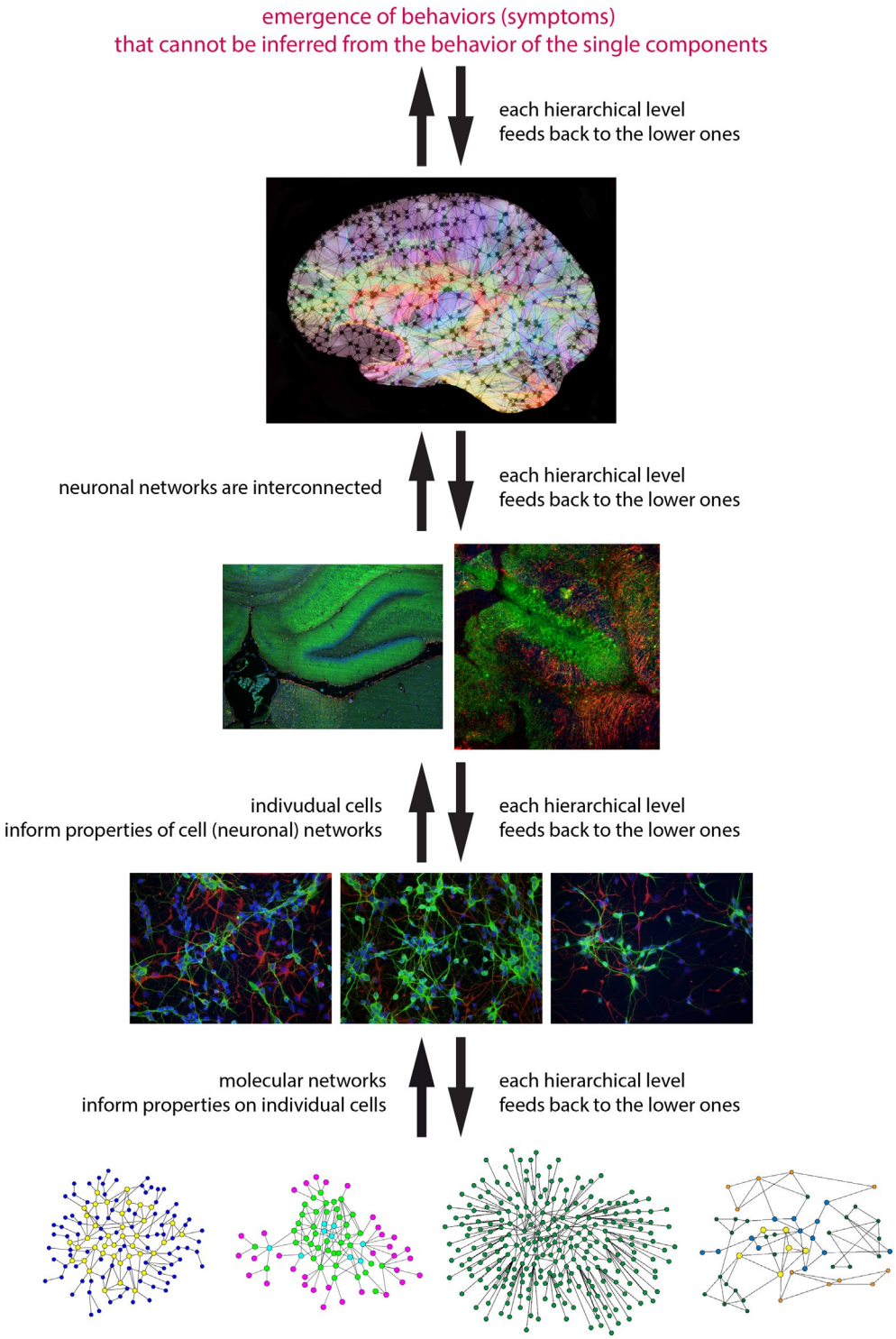

Fig. 1. The brain as a complex system. At the most basal level, the system can be represented as a collection of networks where different types of molecules (nucleic acids, proteins) interact. These molecular networks entail the essential properties of complex systems (emergency of properties that cannot be found in its individual elements; capacity to maintain the main functions or readapt under environmental perturbations; high connection of elements sharing similar functions). They produce emerging properties that affect the hierarchically higher levels (individual cells, neuronal networks, whole brain), and these higher levels feedback on the organization of the molecular networks. See text for further details.

lower/upper level is uncertain because of compensatory mechanisms, redundancy, interactions (nonlinearity); the impact of interventions at higher levels of the hierarchy could be easier to predict as there are fewer nonlinear steps; a complex system spontaneously acquires order without direction from external agents (self-organization); modification of an input will alter the way the system self-organizes, and this will influence the characteristics of the emergent behavior.

2. Systems genetics

Systems genetics is the part of systems biology that aims to "understand how genetic information are integrated, coordinated, and ultimately transmitted through molecular, cellular, and physiological networks, to enable the higher-order functions and emergent properties of biological systems" [3]. Through systems genetics it is possible

Please cite this article as: F. Lovisari and M. Simonato, Gene networks and microRNAs: Promises and challenges for treating epilepsies and their comorbidities, Epilepsy & Behavior, https://doi.org/10.1016/j.yebeh.2019.106488

to study multiple genetic perturbations rather than individual ones [4]. Well-established qualitative techniques have been paired with quantitative ones, such as next generation sequencing (NGS), which permit to study the whole transcriptome of a given cell, also offering the opportunity to discover novel transcripts or to reveal sequence variations. Transcriptome sequencing can be seen as a molecular fingerprint, and finding perturbations in the gene expression networks may lead to the discovery of disease mechanisms [5]. Data derived from sequencing studies can be put together in genome-wide associations studies (GWAS) to search for small variations within the genome analyzed; normally, the most common type of genetic variation is single nucleotide polymorphisms (SNPs) [6].

At the most basal level, biological systems can be represented as networks where different types of molecules (nucleic acids, proteins) interact. Coherently with the general features of complex systems, these molecular networks entail some essential properties [7]:

1) emergence: the links between the elements of the network can lead to the emergency of properties that cannot be found in its individual elements;
2) robustness: biological systems are capable of maintaining their main functions under perturbations driven by the environment, or readapt and create new interactive networks;
3) modulation: elements sharing similar functions are highly connected one with another.

In must be kept in mind, as already stated above, that molecular networks are at the basis of the pyramid. They have their internal organization and produce emerging properties that affect the hierarchically higher levels, but these higher levels feedback on the organization of the molecular networks. Therefore, a gene mutation may cause a protein to function improperly and trigger a cascade of events that may lead to the development of a disease [8]. However, it may not necessarily lead to that disease, because the system as a whole may generate effective counter-mechanisms to oppose those generated by the pathological protein. For the same reason, even pathological molecular networks may not necessarily lead to development of a disease.

3. Relevance for epilepsy

Epilepsy is an example of a complex disease: not only because it is a neurological disease, and the brain is the most complex organ, but also because of its enormous heterogeneity. In the past few years, thousands of genetic variations have been identified in clinical and preclinical studies that associate with epileptic phenotypes. A major unresolved issue is why a single mutation can lead to many different outcomes: a gene variant in a single molecular pathway can in fact be associated with different types of epilepsy in different patients [8]. Even though it can be difficult to identify identical mutations across different patients affected by the same form of epilepsy, different mutations may affect the same functional pathway(s), which can be identified by mapping interactions of the different causal genes, that is, searching modules enriched with the altered genes. Within this approach, regulatory factors capable of orchestrating the activation of the pathological module may be proposed as therapeutic targets.

Below, we describe how this approach may be exploited, taking as examples findings to which our lab has contributed.

3.1. *Epilepsy gene networks*

One example of how systems biology and gene-network study approaches have been employed in epilepsy research is the work by Johnson and colleagues [9], that let to identification of Sestrin 3 (SESN3) as a master regulator of a gene network module associated with epilepsy.

The starting question was if the transcriptome in the epileptic hippocampus is organized into gene coexpression networks. In order to pursue an answer, whole-genome expression profiles were obtained from surgically resected hippocampi from 129 patients with temporal lope epilepsy (TLE). Graphical Gaussian Models (GGMs, tools to study gene association networks) were used to analyze the data and identified a large coexpression network comprising 442 genes. To establish if this network was causally related to epilepsy, data were integrated with genetic susceptibility data. Genome-wide associations studies data from a separate cohort of patients (1429 patients with TLE) were compared to 7358 healthy controls: the TLE network as a whole was highly enriched for genetic associations to epilepsy compared with genes not in the network, indicating a causal involvement of the TLE-network in epilepsy etiology. This coexpressed gene network clustered into two functionally homogenous transcriptional modules (i.e., subnetworks of highly correlated genes): Module-1, comprising 69 genes enriched for gene ontology (GO) categories related to inflammation (IL-1 signaling cascade and TLR-signaling pathway); and Module-2, comprising 54 genes enriched for cell-to-extracellular matrix adhesion processes. These subnetworks, and in particular Module-1, were conserved across species, as the genes were found upregulated also in an animal model of epilepsy. However, the key step was to identify genetic variants that regulate the gene coexpression modules (i.e. regulatory 'hotspots'). Evidence of genetic regulation of module expression can be obtained using genome-wide Bayesian expression mapping of quantitative trait loci (QTL), i.e. DNA loci that correlate with variations of a phenotypic trait. This analysis identified a locus on chromosome 11q21 associated with Module-1 expression. Among the protein-coding genes contained in this locus, SESN3 was most strongly and positively correlated with Module-1 gene expression in the human and in the mouse epileptic hippocampus. In vitro experiments of silencing and overexpression of SESN3 confirmed its role as regulator of the proconvulsant Module-1 genes. In addition, zebrafish larvae microinjected with SESN3 morpholinos (SESN3 knocked-down), in comparison with control larvae, exhibited a sustained reduction in locomotor activity following exposure to the convulsant agent pentylenetetrazol.

Sestrin 3 belongs to the sestrin family of proteins, 3 proteins that guide the intracellular response to reactive oxygen species (ROS). Sestrins are involved in the deposit of adipose cells, cell metabolism, and mammalian target of rapamycin (mTOR) regulation. SESN1 and 2 are a link between oxidative stress, aging, and aging-associated conditions like cancer, diabetes, neurodegenerative diseases, muscular dystrophy, chronic inflammation. Sestrin 3 is the least characterized member of the family [10,11].

The following steps, on which we are currently engaged, are to elucidate the role of SESN3 in mammalian epilepsy. To this aim, we generated SESN3 knock-out rats and are currently carrying out a detailed phenotypization, in terms of susceptibility not only to epilepsy and seizures, but also to neuropsychiatric comorbidities, such as anxiety, depression, and cognitive impairment. Such analysis is being performed both in pups and in adults, using an extended battery of tests and epilepsy models (Lovisari et al., in preparation).

These studies illustrate the power of systems genetics applied to epilepsy research: starting from surgically-removed brain tissue of patients with epilepsy, we identified a module of coexpressed genes regulated by a specific factor, SESN3, which may represent a new therapeutic target. The key point is that SESN3 was identified not through its direct effect on a specific parameter (e.g. membrane excitability), but by its relationship to an epileptic gene coexpression network.

Another example of this approach is the study conducted by Delahaye-Duriez and colleagues [12]. Here, a genome-wide coexpression analysis was performed from human brains, autoptic samples from patients that did not experience neurological disorders as compared with a database of mutations known to exist in epileptic encephalopathies. The modules identified were then tested for enrichment of association with other common forms of epilepsy. In this way, a module of genes was identified (named M30), enriched for de novo mutations and functionally relevant for synaptic transmission, gamma-aminobutyric acid

Please cite this article as: F. Lovisari and M. Simonato, Gene networks and microRNAs: Promises and challenges for treating epilepsies and their comorbidities, Epilepsy & Behavior, https://doi.org/10.1016/j.yebeh.2019.106488

(GABA) signaling and conduction of nerve impulses. One other interesting result was that, when performing a GWAS analysis using data from the International League against Epilepsy (ILAE), the M30 module resulted significantly enriched of association with focal and generalized epilepsy [12]. Microarrays and RNA-Seq studies showed that M30 genes are downregulated in murine and human epileptic hippocampi. Finally, valproic acid proved capable of restoring expression levels of M30 genes, emphasizing the possibility to employ these systems genetics approaches to develop new pharmacological treatments.

Genome-wide analysis has also been applied to other types of variants, not only SNPs, such as ribonucleic acid (RNA) editing events. RNA editing is any posttranscriptional variation that alters nucleotide composition, thereby modifying protein function. Srivastava and colleagues [13] were the first to perform a GWAS study on differential RNA editing (DRE) using an acquired epilepsy model: RNA-Seq of samples from 100 epileptic mice, and 100 healthy controls were analyzed and investigated for functional enrichment with GO or phenotype terms relevant for epilepsy. Genome-wide associations studies analysis identified a set of 256 DRE sites between epileptic and control mice, 134 of which were clustered together. Moreover, GO analysis suggested that the editing affected genes enriched for functional terms related to neural processes, leading to hypothesize a DRE role in epileptogenesis [13].

3.2. Gene networks and miRNAs

Other interesting object of study of the mechanisms leading to the transformation of a healthy into an epileptic brain is the microRNAs (miRNAs). MicroRNAs are small noncoding RNAs (22-25 nucleotides), acting at posttranscriptional level by binding complementary sites on target messenger RNAs (mRNAs) and thereby inhibiting transcription or leading to target RNA degradation, and ultimately controlling protein levels [7]. One single miRNA can target multiple mRNAs, and one mRNA can be regulated by many miRNAs. These characteristics might be exploited to modulate several targets at once, increasing the effect on complex and multidimensional pathologies like epilepsy, but also increasing the risk of off-target mediated side effects [14]. Indeed, recent studies suggest that these molecules play a key role in the pathogenesis of epilepsy and might be targeted for novel therapeutic approaches [14,15].

The question is how to identify the miRNA(s) that represent optimal therapeutic targets for epilepsy. In a microarray study in the pilocarpine model, we identified clusters of miRNAs in the dentate gyrus that separated control and chronic phase rats from those sacrificed during latency or after the first spontaneous seizure [16]. Comparison with data from epileptic patients identified at least 3 miRNAs that were upregulated in both the human and rat epileptic hippocampus. In addition, an overlap could be observed between miRNAs differently expressed during epileptogenesis in our study with those found in other studies that employed a similar approach in different epilepsy models [17,18].

In order to select those miRNA that were altered in a disease- and not simply model-dependent manner, we thought to combine data from these 3 studies in a meta-analysis [19].

This led to the identification of 26 miRNAs differentially expressed during epileptogenesis, 11 of which were not identified in individual studies, and of 5 miRNAs differentially expressed in the chronic period, 11 of which not identified in the individual studies. We also pursued identification of the mRNA targets of these miRNAs. For that, we first performed target prediction using a web-accessible database (miRWalk), but that retrieved a huge number of targets. We than looked for inverse relationship between our miRNAs and mRNAs identified in separate epileptogenesis studies in the same models [20]. We found inverse relationship between 22 (of our 26) miRNAs, and 112 predicated gene targets.

Although these findings potentially disclose mechanisms of epileptogenesis and therapeutic targets that should now be investigated and validated, the number and heterogeneity of identified mRNAs suggest that therapies focused on a single miRNA may not be sufficient to reverse or ameliorate the epileptogenic process. Rather, proper combinations of miRNAs should be targeted together. Nonetheless, existing data suggest that modulation of even a single miRNA may be sufficient to produce significant effects. For example, Jimenez-Mateos and colleagues demonstrated that inhibiting miR-134 after induction of status epilepticus can prevent the occurrence of spontaneous seizures [21].

4. Conclusions

The few examples described in this minireview support the notion that studying epilepsy and its comorbidities within a complex systems framework is a promising integration to the traditional reductionist approaches. It should be emphasized that we do not suggest (nor we expect) that the reductionist approaches should be abandoned, because they will certainly continue to advance our knowledge and to contribute new treatments. However, we believe that the concept of network disease is important for improving our understanding of epilepsy, and that the use of techniques that allow a more holistic vision of the changes occurring in complex systems (like systems genetics) will become more and more important for developing new pharmacological therapies, as illustrated by the studies discussed in this article.

Acknowledgments

The authors' work was supported by a grant from the European Community FP7 [grant agreement no. 602102 (EPITARGET)].

Declaration of competing interest

The authors have nothing to disclose.

References

[1] Fang FC, Casadevall A. Reductionistic and holistic science. Infect Immun 2011;79(4):1401–4.
[2] Kesic S. Systems biology, emergence and antireductionism. Saudi J Biol Sci 2016;23(5):584–91.
[3] Nadeau JH, Dudley AM. Genetics. Systems genetics. Science 2011;331(6020):1015–6.
[4] Civelek M, Lusis AJ. Systems genetics approaches to understand complex traits. Nat Rev Genet 2014;15(1):34–48.
[5] Goksuluk D, Zararsiz G, Korkmaz S, Eldem V, Zararsiz GE, Ozcetin E, et al. MLSeq: machine learning interface for RNA-sequencing data. Comput Methods Prog Biomed 2019;175:223-31.
[6] Markowetz F, Boutros M. An introduction to systems genetics. In: Markowetz F, Boutros M, editors. Systems Genetics: Linking Genotypes and Phenotypes (Cambridge Series in Systems Genetics. Cambridge: Cambridge University Press; 2015. p. 1-11. https://doi.org/10.1017/CBO9781139012751.001.
[7] Bartel DP. MicroRNAs: genomics, biogenesis, mechanism, and function. Cell Press 2004;116(2):281-97.
[8] Mahoney JM, Mills JD, Muhlebner A, Noebels J, Potschka H, Simonato M, et al. WONOEP appraisal: studying epilepsy as a network disease using systems biology approaches. Epilepsia 2017;60(6):1045-53.
[9] Johnson MR, Behmoaras J, Bottolo L, Krishnan ML, Pernhorst K, Santoscoy PLM, et al. Systems genetics identifies Sestrin 3 as a regulator of a proconvulsant gene network in human epileptic hippocampus. Nat Commun 2015;6:6031.
[10] Wang M, Xu Y, Liu J, Ye J, Yuan W, Jiang H, et al. Recent insights into the biological functions of Sestrins in health and disease. Cell Physiol Biochem 2017;43(5):1731-41.
[11] Dalina AA, Kovaleva IE, Budanov AV. Sestrins are gatekeepers in the way from stress to aging and disease. Mol Biol 2018;52(6):823-35.
[12] Delahaye-Duriez A, Srivastava P, Shkura K, Langley SR, Laaniste L, Moreno-Moral A, et al. Rare and common epilepsies converge on a shared gene regulatory network providing opportunities for novel antiepileptic drug discovery. Genome Biol 2016;17(1).
[13] Srivastava PK, Bagnati M, Delahaye-Duriez A, Ko JH, Rotival M, Langley SR, et al. Genome-wide analysis of differential RNA editing in epilepsy. Genome Res 2017;27(3):440-50.
[14] Henshall DC, Hamer HM, Pasterkamp RJ, Goldstein DB, Kjems J, JHM Prehn, et al. MicroRNAs in epilepsy: pathophysiology and clinical utility. Lancet Neurol 2016;15(13):1368-76.
[15] Cattani AA, Allene C, Seifert V, Rosenow F, Henshall DC, Freiman TM. Involvement of microRNAs in epileptogenesis. Epilepsia 2016;57(7):1015-26.
[16] Roncon P, Soukupovà M, Binaschi A, Falcicchia C, Zucchini S, Ferracin M, et al. MicroRNA profiles in hippocampal granule cells and plasma of rats with

Please cite this article as: F. Lovisari and M. Simonato, Gene networks and microRNAs: Promises and challenges for treating epilepsies and their comorbidities, Epilepsy & Behavior, https://doi.org/10.1016/j.yebeh.2019.106488

pilocarpine-induced epilepsy – comparison with human epileptic samples. Sci Rep 2015;5(1).
[17] Bot AM, Debski KJ, Lukasiuk K. Alterations in miRNA levels in the dentate gyrus in epileptic rats. PLoS One 2013;8(10):e76051.
[18] Gorter JA, Iyer A, White I, Colzi A, van Vliet EA, Sisodiya S, et al. Hippocampal subregion-specific microRNA expression during epileptogenesis in experimental temporal lobe epilepsy. Neurobiol Dis 2014;62:508-20.
[19] Srivastava PK, Roncon P, Lukasiuk K, Gorter JA, Aronica E, Pitkänen A, et al. Meta-analysis of MicroRNAs dysregulated in the hippocampal dentate gyrus of animal models of epilepsy. eneuro 2017;4(6) [ENEURO.0152-17.2017].
[20] Dingledine R, Coulter DA, Fritsch B, Gorter JA, Lelutiu N, McNamara J, et al. Transcriptional profile of hippocampal dentate granule cells in four rat epilepsy models. Sci Data 2017;4:170061.
[21] Jimenez-Mateos EM, Engel T, Merino-Serrais P, McKiernan RC, Tanaka K, Mouri G, et al. Silencing microRNA-134 produces neuroprotective and prolonged seizure-suppressive effects. Nat Med 2012;18(7):1087-94.

Please cite this article as: F. Lovisari and M. Simonato, Gene networks and microRNAs: Promises and challenges for treating epilepsies and their comorbidities, Epilepsy & Behavior, https://doi.org/10.1016/j.yebeh.2019.106488

Chapter 3: Sestrin 3

Implication of Sestrin3 in epilepsy and its comorbidities

Francesca Lovisari,[1]* Paolo Roncon,[2]* Marie Soukoupova,[1] Giovanna Paolone,[1] Maryline Labasque,[1] Selene Ingusci,[1] Chiara Falcicchia,[1] Michael Johnson,[3] Enrico Petretto,[4] Rafal Kaminski,[5] Ben Moyon,[6] Zoe Webster,[6] Michele Simonato[1,2**] and Silvia Zucchini[1**]

[1] Department of Medical Sciences, Section of Pharmacology, University of Ferrara, Italy
[2] Division of Neuroscience, University Vita-Salute San Raffaele, Milan, Italy
[3] Division of Brain Sciences, Imperial College London, United Kingdom
[4] Duke-NUS Medical School, Singapore
[5] Neuroscience TA, UCB Biopharma SPRL, Braine l'Alleud, Belgium
[6] Es Cell and Transgenics, Medical Research Council, Imperial College London, United Kingdom

* Both authors contributed equally to this paper.
** Both senior authors.

Address correspondence to:
Silvia Zucchini, PhD
Department of Medical Sciences, Section of Pharmacology
University of Ferrara
Via Fossato di Mortara 17-19
44121 Ferrara, Italy
Email: silvia.zucchini@unife.it

Abstract

Epilepsy is a serious neurological disorder affecting about 1% of the population worldwide. Despite evidence that most epilepsies have a genetic base, both genome wide association studies (GWAS) and exome sequencing approaches have so far provided limited insights into its mechanisms. Recently, we used a systems biology approach to investigate transcriptional networks and pathways within the hippocampus of temporal lobe epilepsy (TLE) patients who underwent the surgical resection of the epileptic focus, and identified a transcription program that is overexpressed in the TLE hippocampus and promotes expression of epileptogenic signaling pathways. The Sestrin-3 (SESN3) gene was identified as an activator of this transcriptional program. In this study, we investigated the phenotype of SESN3 knock out (KO) rats in terms of susceptibility to seizures, and observed a significant delay in status epilepticus (SE) onset in SESN3 KO compared to control rats. This finding confirms in vitro and in vivo evidence indicating that SESN3 may favor occurrence and/or exacerbate seizures. We also analyzed the phenotype of SESN3 KO rats for anxiety, depression, and cognitive impairment, i.e. the common comorbidities of epilepsy. SESN3 KO rats proved less anxious compared to control rats in an array of behavioral tests. Taken together, the present results suggest that SESN3 may be a master regulator of the expression of molecules involved in the pathogenesis of epilepsy and of its comorbidities.

3.1 Introduction

Epilepsies are complex group of neurological diseases, each differing in many aspects: etiology (genetic, lesional or cryptogenic), localization of the epileptic focus, symptomatology. The common feature of every epilepsy is the occurrence of spontaneous seizures, triggered by a paroxysmal excitatory activity in neuronal networks. However, epilepsy is not just seizures: it is important to take into consideration the deep impact that this condition has on the general quality of life. The majority of epileptic patients report the occurrence of other medical problems [35,36] and, in fact, a number of comorbidities are linked to epilepsy, including psychiatric disorders such as anxiety, depression and cognitive impairment. These comorbidities have a major impact on every-day social life [37].

The burden of epilepsy comorbidities is incredibly high: at least 50% of adult patients suffer from one comorbid disorder [38]. There is no striking evidence that epilepsy causes the onset of a specific comorbidity or vice-versa, but it is thought that common pathogenic mechanisms are at the basis of both [25]. Several causative mechanisms linking epilepsy and depression have been proposed, for example a decrease in function of specific neurotransmitters (serotonin, noradrenaline, dopamine, GABA); tissue atrophy; morphological alterations in limbic areas; higher cytokine concentrations (IL-1beta) [25,28]. Comorbidities represent a burden also for the healthcare system, because they require additional, expensive medical interventions, and can also aggravate the severity of epilepsy or the side effects of anti-epileptic drugs (AEDs).

It would be important to explain the physiological mechanisms at the basis of both comorbidities and epilepsy in order to find the appropriate therapeutic intervention, because AEDs may at best control seizures, but do not affect the development of comorbidities. One approach could be using animal models. In fact, a relationship between epilepsy and depression has been described also in animal models of mesial temporal lobe epilepsy (mTLE): for example, rats treated systemically with pilocarpine or electrically kindled in the amygdala develop a depression-like state [39,40]. Animal models of mTLE also provide evidence of the presence of anxiety-related behavior [41].

Using a systems genetics approach, we have identified a pro-epileptic gene network that is orchestrated by sestrin 3 (SESN3), a member of the sestrin family of stress-inducible proteins [42].The pro-epileptic effect of SESN3 was indeed confirmed in non-mammalian species [42]. This observation was actually unexpected, because other sestrins may exert anti-epileptic effects. By upregulating the nuclear factor erythroid 2-related factor 2 (NRF2) signaling, in fact, SESN1 and 2 inhibit the mechanistic target of

rapamycin complex 1 (mTORC1), attenuating reactive oxygen species (ROS) accumulation [43]. mTORC1 inhibition, as obtained with the prototype inhibitor rapamycin, can prevent development of epilepsy [44 45]. However, mTORC1 activation seems to be required for ketamine-induced anti-depressant effects [46], indicating that SESN1 and 2 may worsen epilepsy comorbidities.

In this work, we asked if SESN3 has a similar double-edge effect on epilepsy and epilepsy comorbidities. To explore this issue, we generated SESN3 knockout (SESN3 KO) rats and studied in detail their phenotype, not only in terms of susceptibility to seizures, but also to anxiety and depression.

3.2 Materials and methods

3.2.1 Animals

SESN3-KO and wild type (WT) rats in a Sprague-Dawley (SD) background (Harlan, Italy) were used for all experiments. They were housed under standard conditions: constant temperature (22-24°C) and humidity (55-65%), 12h light/dark cycle, water and food ad libitum. The ARRIVE (Animal Research: Reporting *In Vivo* Experiments) guidelines have been followed. Procedures involving animals and their care were carried out in accordance with European Community, national and local guidelines, laws and policies. The University of Ferrara Ethical Committee approved all experimental protocols for Animal Experimentation and by the Italian Ministry of Health (n.953/2016-PR). All animals were euthanized by anesthetic overdose.

3.2.2 SESN3-KO rat generation

SESN3-KO rats were generated at the Imperial College, London, exploiting a zinc finger nucleases (ZFN) engineered plasmid (Sigma Aldrich) implanted into single cell SD embryos. The ZFN technique permitted to cut at a specific site of the SESN3 gene, leading to complete knocking down of the gene. Heterozygous rats were then mated to give birth to WT and SESN3-KO rats.

The foster females aged 8 to 12 weeks have been injected intraperitoneally (i.p.) with 40 µg (0.2 ml) of Lutenizing Hormone - Releasing Hormone (LH-RH) agonist 4 days prior to mating. On the day of mating, the recipients were individually placed with males. The following day, the females were de-mated and examined for the presence of

copulation plug. The females presenting a plug have been used as embryo recipient for embryo transfer surgery.

SD females aged 4 to 6 weeks have been used as embryo donors. Two days before mating, the females were injected with 30 IU of pregnant mare's serum gonadotropin (PMSG, i.p.). On the day of mating, the females have been injected with human pregnancy urine chorionic gonadotropin (HCG, 40 IU, i.p.) and placed individually with SD males. The following day, the females were separated, culled and the oviducts removed. The embryos were then collected and left in incubator at 37°C, 5% CO_2 until used for pro nuclear injections.

The embryo recipients were anesthetized with a mix of ketamine and xylazine (1:1, i.p.) and a painkiller (Carprofen, 5 mg/kg s.c.). The female rats were placed under the microscope, the incision area between flank and ribcage was shaved and an incision was made through the skin and peritoneal wall. After having injected the embryos, the peritoneal wall sutured. The female rats were then placed back in their cages on a heat pad at 37°C, until recovery from anesthesia.

After having generated the first colony of rats, animals were to the laboratory of the University of Ferrara, where the breeding was conducted in heterozygosis, by mating SESN3-KO males and SD females.

3.2.3 SESN3-KO rats genotyping

Genotyping was conducted via PCR analysis. DNA was obtained by harvesting ear punch biopsies from 21 days rats, from both female and male rats, and put into 1.5 ml tubes. Samples were then immerged in 25 µl OB protease and 180 µl lysis buffer (55°C, overnight) to enhance tissue digestion.

The day after, DNA was extracted with Tissue DNA Kit (Omega bio-tek) and PCR-amplified. After amplification, a specific nuclease was added to the DNA samples (IDT Suveyor Mutation Detection Kit), that is able to recognize the cutting sites of the DNA chain of samples from SESN3-KO rats. Finally, samples were run in a 2% agarose gel: WT bands were observed at 400 kb, SESN3-KO bands at 200 kb.

Male WT and SESN3-KO homozygous littermates were employed for all experiments.

3.2.4 Behavioral testing in pups

Observational screens and simple behavioral tests were performed 7 days after birth to assess general health and developmental milestones. We rapidly screened rats for the

appearance of the fur, whiskers and posture and we tested them for neurological and sensory reflexes and non-complex motor activities through a battery of simple tests: the postural flexion test, the righting reflex test, the response to fear test, the negative geotaxis test and the placing responses test.

Postural flexion test. Pups were lifted by the tails at 30 cm height from a horizontal plan. If the proprioceptive system is functioning correctly, pups perceive the gravity and turn around in the natural posture. We recorded the time employed by the pups to turn around, with a cut-off of 1 min, and the side by which they turned.

Righting reflex test. Pups were laid supine on a horizontal plan. The time required to turn procumbent and the side by which the pup turned was noted by the experimenter.

Response to fear test. Pups were placed near the edge of a plan, facing the empty space. The time required for turning to the opposite side or for evaluating the intention to explore the empty (i.e. jumping from the plan) was recorded, with a 60 s cut off.

Negative geotaxis test. Pups were put facing down on a 30° inclined plane, and the experimenters noted the time employed to turn up, with a cut off of 60 s. Pups that failed to turn face up, or that slipped down, were assigned 60 s.

Response to stimulus test. This test evaluates the capacity of the pups to react to an external stimulus. The experimenter, leaving its paws free to move, holds the animal. Using an iron spatula, the experimenter touches both the right and the left anterior part of the rat's paw and notes if the animal moves the paw after the stimulus.

3.2.5 Behavioral testing in adults

A battery of behavioral tests was conducted in adult (8 week old) WT and SESN3 KO male rats, to assess anxiety and depressive-related behavior, motor and cognitive functions. We employed the following tests: Elevated Plus Maze (EPM), Open Field (OF), Novel Object Recognition (NOR), Rotarod and Forced Swimming (FS). Since the FS test cause a high level of stress, only a subgroup of rats (WT n=11, SESN3-KO n=8) was employed for it and not used in further experiments. Tests in adults were performed using only male rats. Animals performed just one test per morning, under artificial diffused red light. Behavioral experiments were conducted in a soundproof room, into which animals were moved at least 30 min before testing. Every rat was used to be handled by researchers before being employed in behavioral tests.

Elevated-plus maze test. The test was performed as described by Tchekalarova and colleagues in, 2015 [47] . The apparatus consisted of two open arms (50 x 10 cm) and two closed arms (50 x 10 x 50 cm) connected through a central platform (10 x 10 cm). The

apparatus was 50 cm above floor level. Luminosity was checked using a luminometer, and found to be nearly 1 in the open arms and close to zero in the closed arms. At the beginning of the test, rats were placed in the central part of the platform, facing an open arm. The test lasted 5 min. The calculated measures were: number of entries in open arms; number of entries in closed arms; time spent in open arms; time spent in closed arms; number of stretched-attend postures (SAP), i.e. how many times the rat looked at the open arms while being with the body in the closed arm; number of head dippings (HD), i.e. how many times the rat looked down from the open arms of the EPM apparatus; and number of rearings, i.e. how many times the rat looked up leaning against the walls of the closed arms. After each test the EPM apparatus was cleaned with 0.1% ethanol solution.

Open field test. The test was performed as described before [47] . The apparatus consisted of a gray box (100 x 100 cm) divided into two compartments: outer (periphery) and inner (center). The rat was placed in the center of the box and was allowed to explore it for 20 min. The calculated measures were: total distance traveled (in cm); time spent in the center; number of entries in the center; time spent in the corners; and number of entries in the corners. After each test, the OF apparatus was thoroughly cleaned with 0.1% ethanol solution to prevent any odor traces. The test was recorded using a video camera IR (DSS1000 video recording system V4.7.0041FD, AverMedia Technologies, USA), and then videos were analyzed using the Any Maze software (Ugo Basile S.R.L., Gemonio VA, Italy).

Forced swimming test. The forced swimming test was employed to investigate the despair-like behavior [48] . The test was performed using a plexiglass cylinder (50 x 20 cm) filled by three forth with water kept at 25±1°C. Two swim sessions were conducted: 15 min of training followed (24 h later) by a 5-min test session. After each test, the rat was dried and kept warm by a heating device for 10 min. Two different experienced observers recorded (i) the time of immobility, which occurred when the rat floated in the water without struggling and (ii) the time of climbing or movements made by the rat to keep its head above the water. The time spent immobile has been related to a depressive behavior [49].

Novel object recognition test. The NOR test was performed as described by Ennaceur and Delacour [50] (1988). The test consisted of three phases: habituation, acquisition and test. The OF test, conducted the day before NOR, was used as habituation phase. The day after habituation, the acquisition trial was conducted by placing the rat in the field, in which two identical objects were positioned at the corners of the arena, approximately 10 cm from the walls. Rats were allowed to explore the two objects for 5 min, and exploratory activity (i.e.

the time spent exploring each object) was recorded. After 2 h, rats were placed again in the arena, where one object was substituted with a novel one, not used in the acquisition phase. Again, the time that each animal spent exploring each object was measured. We consider a valid exploratory behavior when the rat directly interacts with the object. The choice of objects as novel or familiar was carried out in a random way, and the position of each object was also alternated between trials. After each test, the arena and the objects were thoroughly cleaned with 0.1% ethanol solution.

Rotarod test. The test has been run in a three-day trial. The rotarod apparatus is composed of a rotating cylinder, divided into different compartments, one for each animal. The cylinder rotates and the speed was been increased by steps of 5 rpm every three min. Maximum duration of the test was 30 min. The operator recorded every fault, i.e. when rats fell down from the cylinder or hung to the cylinder without running. The test was considered finished if the animal made 4 continuous errors.

3.2.6 Models of epilepsy

Pilocarpine. Both WT and SESN3-KO animals were randomly assigned to two groups: pilocarpine treated and controls. The former received a single injection of methyl-scopolamine (1 mg/kg, s.c.) 30 min prior to pilocarpine (370 mg/kg, i.p.), whereas the latter received a single injection of methyl-scopolamine 30 min prior to vehicle (0.9% NaCl solution). Thereafter, experienced researchers observed the animals for at least 6 h, taking note of convulsive activity based on the Racine scoring scale [34] (Racine et al., 1972). Usually, about the 80% of WT rats develop seizures evolving into convulsive status epilepticus (SE) within the first 20-25 min after pilocarpine injection [51]. The experimenters also recorded the time required to enter convulsive SE. SE has been interrupted 3 h after its onset by administration of diazepam (20 mg/kg, i.p.).

Intrahippocampal kainic acid. We also assessed susceptibility to SE in the intra-hippocampal kainic acid (KA) model [52]. Because KA was administered in awake animals, to allow proper observation of SE, guide cannulas were implanted one week before KA administration in the right ventral hippocampus for insertion of the injecting needle.

Stereotaxic surgery was thus performed to implant 20 G guide cannulas (PlasticsOne, USA) in the ventral hippocampus of both WT and SESN3-KO rats, following Paxinon's Atlas (coordinates from bregma AP= 5.6; ML= +4.5; D=+3.5). Anesthesia was induced with ketamine/xylazine (87 and 13 mg/kg i.p.) and maintained with isoflurane (1.5% in oxygen). After placing the rat in the stereotaxic frame, the skull was exposed and a burr hole was drilled after at the above coordinates. Six other smaller

holes were drilled to position screws. The guide cannula was then inserted, dental cement was used to fix cannula and screws to the skull, and the scalp was sutured with stitches. Animals were treated with tramadol and antibiotics before and after the stereotaxic surgery and then checked daily to monitor their well-being.

After a week of recovery, rats were injected with KA (0.4 µg/0.2µl) using a 30 G needle connected to a 5 µl Hamilton syringe. After KA administration, rats were video-monitored and SE severity was recorded using the Racine's scale. If SE did not resolve within 2.5 h, diazepam (10 mg/kg i.p.) was administered to stop seizure activity.

Kindling. Rats were anesthetized with mixed Ketamine Imalgene and Domitor in water (v/v; 50 mg/kg and 0.5 mg/kg respectively; intramuscular injection, 2 ml/kg) and implanted with a bipolar stimulation/recording electrode into the right basolateral amygdala with the following coordinates: AP-2.3, L-4.8, V-8.5 (9), all measured from bregma. The electrode consisted of two twisted Teflon-coated stainless-steel wires. An electrode in the left occipital cortex served as the indifferent reference electrode. Bipolar, reference and ground electrodes were connected to plugs and the electrode assembly and anchor screws were held in place with dental acrylic cement (Grip Cement Liquid, Dentsply International Inc., USA) applied to the exposed skull surface. After 50 min, awakening was facilitated with an intramuscular administration (2.5 ml/kg) of Antisedan, 1.25 mg/kg, prepared at the final concentration of 10% in water. Following surgery, the rats were kept individually in Makrolon cages (Model 4, 480 x 375 x 210 mm) and were allowed ad libitum access to standard dry pellet food and tap water before random assignment to experimental groups.

After a postoperative period of 3 weeks, rats were placed in individual boxes and stimulated in the amygdala with increasing stimulation intensities, 1 ms monophasic square wave pulses, 50 Hz for 1 s. We started at sub-maximal electrical intensity to determine the afterdischarge (AD) seizures threshold for each animal. We used a range of stimulation intensities from 20 to 444 µA with increasing steps of 20%.

Three days after initial threshold determination, rats were stimulated once daily, 5 days per week, in the amygdala with 500 µA. Kindling was defined as the appearance of 10 consecutive stage 4 or 5 seizures according to the scale of Racine where:

0 = no reaction

1 = stereotype mouthing, eye blinking, mild facial clonus

2 = head nodding, severe facial clonus

3 = myoclonic jerks in the forelimbs

4 = clonic convulsions in the forelimbs with rearing

5 = generalized clonic convulsions associated with loss of balance

Scores 0-2 were considered to reflect the focal phase and scores 3-5 the generalized phase of the motor seizures.

3.2.7 Structure analysis and immunofluorescence

Rats were killed by decapitation after an anesthetic overdose. Brains were removed and immersed in 10% formalin for 48 h. They were then processed using a standard protocol (VTP 300, Bio-Optica, Milan, Italy) and paraffin embedded. Coronal sections of 7 µm were cut across the hippocampus and mounted onto polarized slides (Superfrost slides, Diapath Martinengo, BG, Italy). Sections were de-waxed with 2 washes in xylol (10 min each), 5 min in ethanol 100%, and rehydrated in ethanol 95%, ethanol 80% and phosphate buffered saline (PBS) 1% (5 min each). Antigens were unmasked with a solution of citric acid and sodium citrate in a microwave oven at 750 watts (3 min), then at 350 watts (2 cycles of 5 min).

To analyze potential differences in tissue architecture, we performed a hematoxylin/eosin staining. Sections were immersed in hematoxylin for 5 min, washed in tap water, then stained with eosin for 2 min and washed again. For immunofluoresce, sections were incubated with 5% bovine serum albumin (BSA) and 5% serum of the species in which the secondary antibody was produced, for 30 min at room temperature. They were then incubated in a humid plastic box with primary antibodies, overnight at 4°C. The primary antibodies were: anti-IBA-1, diluted 1:200 (rabbit monoclonal, #234003, Synaptic System, Gottingen, Germany) for microglia staining, anti-GFAP 1:100 (mouse monoclonal, #MAB12029, Immunological Science, Rome, Italy) for astrocyte staining, anti-β3-tubulin 1:400 (mouse monoclonal, #4466X, Cell Signaling Technologies, MA, USA) for neuron staining. Two washes in 1xPBS and a 30 min incubation in 0.3% Triton X-100 were performed before applying the secondary antibody, 488 or 594 Alexa-Fluor anti-mouse or anti-rabbit (diluted 1:250 in 1x-PBS) depending on the species of the primary antibody. Sections were left in a dark chamber under controlled humidity conditions for 3 h before proceeding with DAPI staining (0.0001% in 1xPBS for 15 min; Santa Cruz, Texas, USA) to label nuclei. Coverslips were mounted using an aqueous anti-fading mounting gel (Sigma).

3.2.8 Real Time qPCR

Total RNA was extracted from frozen hippocampi of WT and SESN3-KO rats, by using the RNeasy Lipid Tissue Mini Kit (Exiqon, #74804), following the manufacturer's

instructions. RNA was quantified using Nanodrop and diluted to 150 ng/ul, then retro-transcribed to cDNA using the SuperScript IV First-Strand Synthesis System (Thermo Fisher Scientific, #18091050) and stocked at -20°C. Real Time q-PCR was run to evaluate the expression of IL-1β, TNFα, c-fos, c-jun and Sesn1. Data were normalized to alpha-tubulin. The reverse transcription protocol was set up following Biorad Kit indications, while the primers recognizing the gene sequencing for the final quantification were purchased from Exiqon.

3.2.9 Statistical analysis

All experiments were run and analyzed by blinded experimenters. Animals have been ordered randomly during the behavioral tests: only during NOR test, in fact, the researchers followed a pre-imposed order because following the correct timing and order of animals is pivotal for the test to succeed.

To test for statistical significance between two groups (i.e. SESN3-KO vs WT rats) a two-tailed unpaired *t* test has been applied to parametric data and a two-tailed Mann-Whitney U test has been used for non-parametric data. The Welch's correction has been used when parametric data showed different standard deviations. In addition, when the statistic test reached significance, we run a post-hoc power analysis considering the number of animals and the "effect size" was calculated. Fold change difference analysis after Real Time qPCR was performed using the Livorak formula.

Statistical test analyses have been performed and graphs prepared with GraphPad Prism (6.0 version). Power calculations have been made using the G power software (version 3.1).

3.3 Results

3.3.1 Pups behavior

To investigate the neurological development of SESN3-KO rats, we performed a battery of behavioral tests on KO and WT littermate pups, that provide information on proprioception, movement execution, general neurological development and fear. Seven days after birth, both male and female rats were evaluated in all tests. First, pups were tested for postural flexion and righting reflex to test proprioceptive and cognitive functions. These two tests explore the capacity of the rat to return to its normal position after being posed in an unnatural position by the operator. WT pups spent less than 10 s to

complete the tasks: in the postural flexion test they spent 9.6±1.0 s to rotate by 45° when suspended by the tail (Supplementary Figure 1A), whereas in the righting reflex test they spent 5.0±0.5 to rotate from a supine to prone position (Supplementary Figure 1B). KO pups performed in a similar manner (no significant differences), as shown in Supplementary Figure 1. Next, we tested the ability to respond to an external stimulus represented by a touch with a small metal spatula to the left and the right anterior paw. Pups should retrieve their paw when touched. KO rats displayed a significantly higher percentage of correct answers (86.2%) compared to the WT littermates (62.8%; P=0.003; power= 0.77; Figure 1A).

Finally, we performed two tests to analyze fear and anxiety-related behavior. In both tests, the pup is forced to an unnatural position, i.e. positioned facing down on a 45° inclined plane in the negative geotaxis test, and on the edge of a table facing the empty space, in the response to fear test. In the negative geotaxis test, SESN3-KO rats were much faster in completing their task compared to WT (P<0.001; power=0.99; Figure 1B). Interestingly, 20 of 46 WT and 3 of 46 SESN3-KO pups froze and stayed immobile for more than 60 s (the cut off time). These rats were included in the analysis with a time of 60 s. We observed a similar situation in the response to fear test. Indeed, SESN3-KO pups returned in the middle of the table, escaping from the empty space, significantly faster than the WT (P=0.008; power=0.92; Figure 1C). However, 11 KO and 2 WT pups (out of 46 per group) attempted to jump off the table. Together, these data highlight a fearless-like attitude of SESN3-KO pups compared to WT littermates that, instead, displayed a passive reaction to the tests. This behavior may be linked to a less anxious phenotype, and capacity to cope more successfully with life challenges.

3.3.2 Adult rats' behavior

Elevated Plus Maze. The EPM test aimed to evaluate anxiety. During this test, normal, WT rodents prefer the most protected and safest areas of the apparatus, i.e. the closed arms. Thus, the greater the time spent in the open arms, the lesser the animal may be considered anxious. In this test, we observed a highly significant difference between the two groups both in terms of time spent (P=0.004) and entries (P<0.001; power=0.97) in the open arms, as SESN3-KO rats spent more time (+28%; Figure 2A) and entered more frequently in the open arms (+78%; Figure 2B).

During the 5-minute testing, we also explored other behavioral traits, such as the number of stretched-attended postures (SAP), i.e. the number of times the rat extended itself from a closed to an open arm, the number of head dipping (HD), i.e. the movement of

the animal looking from the open arm towards the basement, and the number of rearings, i.e. exploration towards the ceiling when the rat stands on its posterior paws. The comparison between SESN3-KO and WT rats showed a similar number of HD and rearings (Figure 2C and 2D), whereas a significantly increased number of SAP was observed in the KO group (P=0.003, power=0.76; Figure 2E). These findings may reflect a proactive attitude towards danger situations.

Open field. In order to better characterized this less anxious phenotype of SESN3-KO rats, we tested the two groups in the OF test. This test provides additional information on susceptibility to anxiety, based on the number of entries and the time spent in the central area of the arena, that is perceived as a dangerous area of the apparatus. The SESN3-KO rats spent slightly more time in the central area compared to WT littermates (P=0.023, power=0.64, Figure 3A), while entered the central area the same number of times (Figure 3B). However, the average time per entry was alightly, but not significantly increased in SESN3-KO rats (Figure 3C). Both groups spent a similar time (Figure 3E) and entered a similar number of times in the corners (Figure 3F). Importantly, the behavioral profile observed in the EPM and OF is not due to an increased motor activity, because SESN3-KO and WT rats walked similar total distances in the OF arena during the test (Figure 3F).

Forced swim test. The two parameters taken into consideration were the climbing and the immobility time (Figure 4). During the 5 min testing, SESN3-KO rats displayed a slight, but non-significant tendency to keep trying to escape from the water cylinder and staying less immobile compared to WT rats. A higher number of animals maybe could have permitted reaching significance. However, we had to limit numbers for this highly stressful test.

Novel object recognition. We performed the novel object recognition (NOR) test to evaluate if cognitive impairment was also found in SESN3-KO rats. During the testing trial, in which one object (familiar) was substituted by a novel one, both WT and SESN3-KO rats explored for a longer time the novel than the familiar object. No difference between the two groups could be observed (Figure 5A).

Rotarod. Finally, to further verify that changes in motor activity could account for the findings in the EPM and OF, we performed the Rotarod test. No differences were observed between the two groups (Figure 5B).

3.3.3 Seizure susceptibility

Systemic pilocarpine. The epileptic phenotype was first explored by inducing status epilepticus (SE) by administration i.p. of pilocarpine. Eleven of 13 SESN3-KO rats (85%)

did not develop SE within 30 min after pilocarpine injection, and were administered a second half dose of the chemoconvulsant. In contrast, only 4 of 15 WT rats (27%) did not develop SE within the first 30 min and received a second half dose. Altogether, SESN3-KO rats needed significantly more time (and higher doses of pilocarpine) to develop the SE compared to WT (p=0.008; power= 0.92; Figure 6A).

Intra-hippocampal KA. Because of a progressive accumulation of fat tissue, SESN3-KO animals tend to have a greater body weight in adulthood compared with WT rats. This may affect the distribution of peripherally administered drugs, including pilocapine. Therefore, we decided to verify the above findings using a SE model in which the chemoconvulsant is directly administered in the brain, namely intra-hippocampal KA. Consistent with pilocarpine, the onset of convulsive was delayed in SESN3-KO than in WT rats (P=0.041; power= 0.61; Figure 6B).

Kindling. Because both the pilocarpine and the KA model are chemically-induced, we decided to investigate also the electrical kindling model. However, we did not find any difference in AD threshold or kindling development between SESN3-KO and WT rats (Figure 6C and 6D).

3.3.4 Morphology and immunohistochemistry

No differences in the structure of the hippocampus was detected, based on hematoxylin-eosin staining (data not shown). The number and morphology of neurons, astrocytes and microglial cells was also not detectably altered (Figure 7).

3.3.5 Real Time q-PCR

Levels of expression in the hippocampus of selected Module-1 genes (IL-1β, TNFα, c-fos, c-jun) has been quantified as Cycle Threshold (CT) number using the Bio-Rad software. No significant difference between the two groups was observed. We therefore hypothesized that compensatory mechanisms may be set in motion by knocking-out SESN3. In fact, Sesn1 expression levels were slightly higher in SESN3-KO animals than in WT controls, even if not in a significant manner (data not shown).

3.4 Discussion

The analysis of the phenotype of SESN3-KO rats presented here supports the notion that SESN3 promotes not only epileptogenesis and seizure development, but also the generation of some comorbidities of epilepsy (anxiety), but not others (cognitive impairment).

SESN3-KO rats and their WT littermates were subject to a battery of behavioral tests assessing anxiety, depression, cognition and motor function. The most striking result was that both pups and adult SESN3-KO rats manifested increased ability to face danger and unknown situations, such as the exploration of the empty space at the edge of a table, or when being placed into the open area of an arena. These trait indicate that these animals are less prone to the fear and anxiety that normally guide animals to stay away from situations that are perceived as potentially dangerous. Importantly, this is not due to an unspecific stimulation of motor activity, because the distance walked in the open field during a test session was identical in KO and WT rats.

Based on these findings, we hypothesized that SESN3-KO rats would have been also less prone to depression. This idea was tested using the FST, a rather dramatic test which induces a state of desperation due to the impossibility to escape a life-threatening situation. While a lower tendency to desperation (i.e. continued attempts to escape and less immobility) was observed in SESN3-KO rats, this was not statistically significant. In addition, we did not observe any improvement in cognitive tests like novel object recognition.

Next , we thought to confirm in mammals the observation previously made in in a Zebrafish model, that knocking down SESN3 can reduce seizure susceptibility [42]. As a first study test we employed the pilocarpine model, and found that, in keeping with the expectations, susceptibility to SE was reduced in SESN3-KO rats, because they required higher doses and more time than WT to enter SE. In our WT group, these parameters were identical to those reported in the literature [53] . However, a limitation in this experiment is that the pharmacokinetics (PK) of pilocapine may be altered in adult SESN3-KO rats, because these animals tend to gain weight and, in particular, accumulate fatty tissue [54,55,56]. In addition, other authors have reported the opposite result that knocking down SESN3 using a different approach (namely, intra-hippocampal injection of lentivectors expressing a small interfering RNA against SESN3) aggravates pilocarpine-induced acute seizures [57]. Therefore, we thought to employ a model in which a convulsant agent (KA) is directly injected in the brain, thus avoiding the PK confounding factor [58]. This approach confirmed

our data. In addition, we also decided to test an electrical model of epilepsy, amygdala kindling. However, we did not observe any difference in AD threshold or kindling development between the two groups.

In sum, these data suggest the presence of a phenotype characterized by reduced anxiety and fear, as well as lower susceptibility to seizures. However, only some of these traits are clearly evident, while others are more subtle and not confirmed when using additional tests. One possible interpretation of these inconsistencies may be that, being the model we employed one in which the gene is constitutively knocked out, compensatory mechanisms may take place during development. In fact, we found that the hippocampal levels of SESN1 were increased in SESN3 KO rats.

As stated in the Introduction, the finding that SESN1 and 2 inhibit mTORC1 suggest an anti-epileptic but also a pro-depressant effect [46 44 45]. Our present data support the notion that SESN3 may have both a pro-epileptic effect (confirming our previous findings [42]), and an anxiogenic effect. Whereas the former effect is likely due to activation of expression of a module of pro-epileptic genes [42], the second remains to be investigated. SESN3 is primarily regulated by FoXO1 and FoXO3 [59]. FoxO proteins are expressed in the limbic system, in particular in the hippocampus, amygdala and nucleus accumbens, areas implicated in the regulation of mood and emotions [60]. Indeed, FoxO3 was hypothesized to be a pro-depression gene, because FoxO3-deficient mice are less prone to develop depressive-like behavior [61]. These effects of FoxO3 may be mediated by activation of SESN3 expression that, in turn, will increase expression of the genes in the pro-epileptic module, many of which (for example IL-1b [62] may exert anxiogenic and/or depressant effect.

In conclusion, the present data suggest that SESN3 may represent a common mechanism of epilepsy and anxiety (maybe depression), i.e. some co-morbidities of epilepsy. Identifying common mechanisms of epilepsy and its comorbidities would be important to develop therapies that are not purely anti-seizure and, in some cases, may even worsen comorbidities [25]. The present findings are informative in that direction. However, the limitations of this study should be also carefully considered. First, testing was performed in normal animals. It will be important in the future to extend it to chronically epileptic animals in which anxiety, depression and cognitive impairment are already present. Second, part of the phenotype may have been obscured in our experiments by compensatory mechanisms that occurred during development. Therefore, another important future goal will be to modulate SESN3 expression in key brain areas and at

specific time points. These limitations notwithstanding, the present study identifies a possible therapeutic target to hit both epilepsy and its psychiatric comorbidities.

3.5 References

1. Gaitatzis A, Sisodiya SM, Sander JW. The somatic comorbidity of epilepsy: a weighty but often unrecognized burden. *Epilepsia* 2012; **53**(8): 1282-93.
2. Pitkanen A, Ekolle Ndode-Ekane X, Lapinlampi N, Puhakka N. Epilepsy biomarkers - Toward etiology and pathology specificity. *Neurobiol Dis* 2019; **123**: 42-58.
3. Taylor RS, Sander JW, Taylor RJ, Baker GA. Predictors of health-related quality of life and costs in adults with epilepsy: a systematic review. *Epilepsia* 2011; **52**(12): 2168-80.
4. Keezer MR, Sisodiya SM, Sander JW. Comorbidities of epilepsy: current concepts and future perspectives. *The Lancet Neurology* 2016; **15**(1): 106-15.
5. Kanner AM. Management of psychiatric and neurological comorbidities in epilepsy. *Nat Rev Neurol* 2016; **12**(2): 106-16.
6. Rider FK, Danilenko OA, Grishkina MN, et al. Depression and Epilepsy: Comorbidity, Pathogenetic Similarity, and Principles of Treatment. *Neuroscience and Behavioral Physiology* 2017; **48**(1): 78-82.
7. Steimer T. Animal models of anxiety disorders in rats and mice: some conceptual issues. *Dialogues Clin Neurosci* 2011; **13**(4): 495-506.
8. Chen SD, Wang YL, Liang SF, Shaw FZ. Rapid Amygdala Kindling Causes Motor Seizure and Comorbidity of Anxiety- and Depression-Like Behaviors in Rats. *Front Behav Neurosci* 2016; **10**: 129.
9. Hesdorffer DC, Ishihara L, Mynepalli L, Webb DJ, Weil J, Hauser WA. Epilepsy, suicidality, and psychiatric disorders: a bidirectional association. *Ann Neurol* 2012; **72**(2): 184-91.
10. Johnson MR, Behmoaras J, Bottolo L, et al. Systems genetics identifies Sestrin 3 as a regulator of a proconvulsant gene network in human epileptic hippocampus. *Nat Commun* 2015; **6**: 6031.
11. Rhee SG, Bae SH. The antioxidant function of sestrins is mediated by promotion of autophagic degradation of Keap1 and Nrf2 activation and by inhibition of mTORC1. *Free Radic Biol Med* 2015; **88**(Pt B): 205-11.
12. Citraro R, Leo A, Constanti A, Russo E, De Sarro G. mTOR pathway inhibition as a new therapeutic strategy in epilepsy and epileptogenesis. *Pharmacol Res* 2016; **107**: 333-43.
13. Talos DM, Jacobs LM, Gourmaud S, et al. Mechanistic target of rapamycin complex 1 and 2 in human temporal lobe epilepsy. *Ann Neurol* 2018; **83**(2): 311-27.
14. Li N, Lee B, Liu RJ, et al. mTOR-dependent synapse formation underlies the rapid antidepressant effects of NMDA antagonists. *Science* 2010; **329**(5994): 959-64.

15. Tchekalarova J, Moyanova S, Fusco AD, Ngomba RT. The role of the melatoninergic system in epilepsy and comorbid psychiatric disorders. *Brain Res Bull* 2015; **119**(Pt A): 80-92.
16. Porsolt RD. Animal model of depression. *Biomedicine* 1979; **30**(3): 139-40.
17. D'Aquila PS, Panin F, Serra G. Long-term imipramine withdrawal induces a depressive-like behaviour in the forced swimming test. *Eur J Pharmacol* 2004; **492**(1): 61-3.
18. Ennaceur A, Delacour J. A new one-trial test for neurobiological studies of memory in rats. 1: Behavioral data. *Behav Brain Res* 1988; **31**(1): 47-59.
19. Racine RJ, Gartner JG, Burnham WM. Epileptiform activity and neural plasticity in limbic structures. *Brain Res* 1972; **47**(1): 262-8.
20. Roncon P, Soukupova M, Binaschi A, et al. MicroRNA profiles in hippocampal granule cells and plasma of rats with pilocarpine-induced epilepsy--comparison with human epileptic samples. *Sci Rep* 2015; **5**: 14143.
21. Raedt R, Van Dycke A, Van Melkebeke D, et al. Seizures in the intrahippocampal kainic acid epilepsy model: characterization using long-term video-EEG monitoring in the rat. *Acta Neurol Scand* 2009; **119**(5): 293-303.
22. Curia G, Longo D, Biagini G, Jones RS, Avoli M. The pilocarpine model of temporal lobe epilepsy. *J Neurosci Methods* 2008; **172**(2): 143-57.
23. Dalina AA, Kovaleva IE, Budanov AV. Sestrins are Gatekeepers in the Way from Stress to Aging and Disease. *Molecular Biology* 2018; **52**(6): 823-35.
24. Narasimhan SD, Mukhopadhyay A, Tissenbaum HA. InAKTivation of insulin/IGF-1 signaling by dephosphorylation. *Cell Cycle* 2009; **8**(23): 3878-84.
25. Narasimhan SD, Yen K, Tissenbaum HA. Converging pathways in lifespan regulation. *Curr Biol* 2009; **19**(15): R657-66.
26. Huang LG, Zou J, Lu QC. Silencing rno-miR-155-5p in rat temporal lobe epilepsy model reduces pathophysiological features and cell apoptosis by activating Sestrin-3. *Brain Res* 2018; **1689**: 109-22.
27. Bragin A, Wilson CL, Almajano J, Mody I, Engel J, Jr. High-frequency oscillations after status epilepticus: epileptogenesis and seizure genesis. *Epilepsia* 2004; **45**(9): 1017-23.
28. Budanov AV. Stress-responsive sestrins link p53 with redox regulation and mammalian target of rapamycin signaling. *Antioxid Redox Signal* 2011; **15**(6): 1679-90.
29. Wang H, Quirion R, Little PJ, et al. Forkhead box O transcription factors as possible mediators in the development of major depression. *Neuropharmacology* 2015; **99**: 527-37.
30. Polter A, Yang S, Zmijewska AA, et al. Forkhead box, class O transcription factors in brain: regulation and behavioral manifestation. *Biol Psychiatry* 2009; **65**(2): 150-9.
31. Pineda EA, Hensler JG, Sankar R, Shin D, Burke TF, Mazarati AM. Interleukin-1beta causes fluoxetine resistance in an animal model of epilepsy-associated depression. *Neurotherapeutics* 2012; **9**(2): 477-85.

3.6 Figures

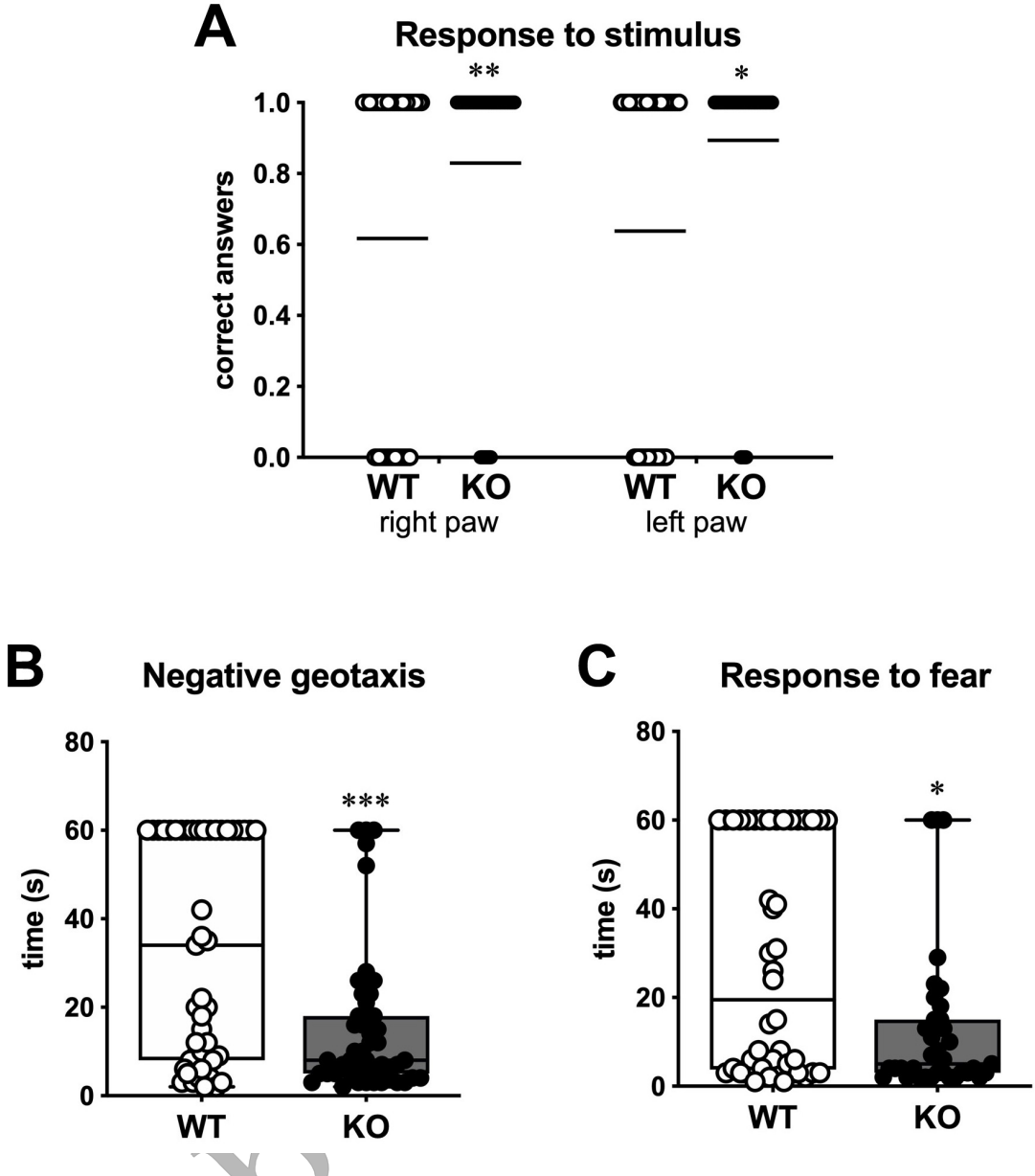

Figure 1. Behavioral testing on pups. (A) Response to stimulus. Scatter dot plot of all responses. On the left is shown the percentage of the correct responses following a stimulus to the left anterior paw of WT (open circles) and of the SESN3-KO rats (solid circles) and, on the right, the correct responses after a stimulus to the right anterior paw of the same animals (n=46). Horizontal lines indicate the percentage of correct responses. Statistical analysis: Mann-Whitney U test. (B) Negative geotaxis test. Time spent by WT and SESN3-KO rats to turn from down to up on the 45° inclined plan (n=46). (C) Response to fear. Time spent by WT and SESN3-KO rats to turn from the edge to the center of the plan (n=46). Statistical analysis in B and C: unpaired *t* test with Welch's correction. * P<0.05; ** P<0.01; *** P<0.001.

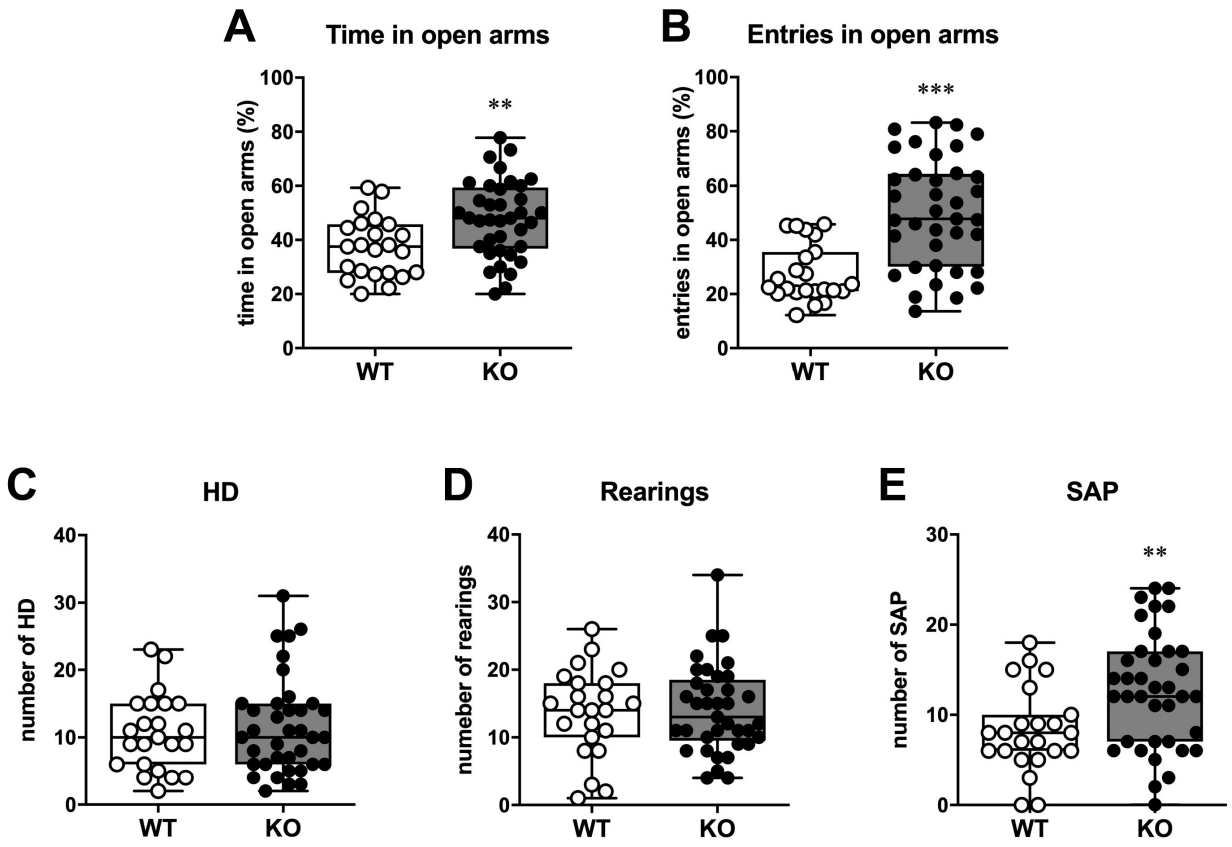

Figure 2. Elevated plus maze test. (A) Percent of time spent exploring the open arms over the total time of exploration. (B) Percent of entries in the open arms over the total number of entries. (C) Number of HD during the 5 min of testing. (D) Number of rearings during the 5 min of testing. (E) Number of SAP during the 5 min of testing. Statistical significance has been calculated with the Unpaired T test with the Welch's correction. In all panels, open circles represent WT (n=23) and solid circles represent SESN3-KO rats (n=37). Statistical analysis in A and B: Mann-Whitney U test. Statistical analysis in B and C: unpaired *t* test with Welch's correction. ** P<0.01; *** P<0.001.

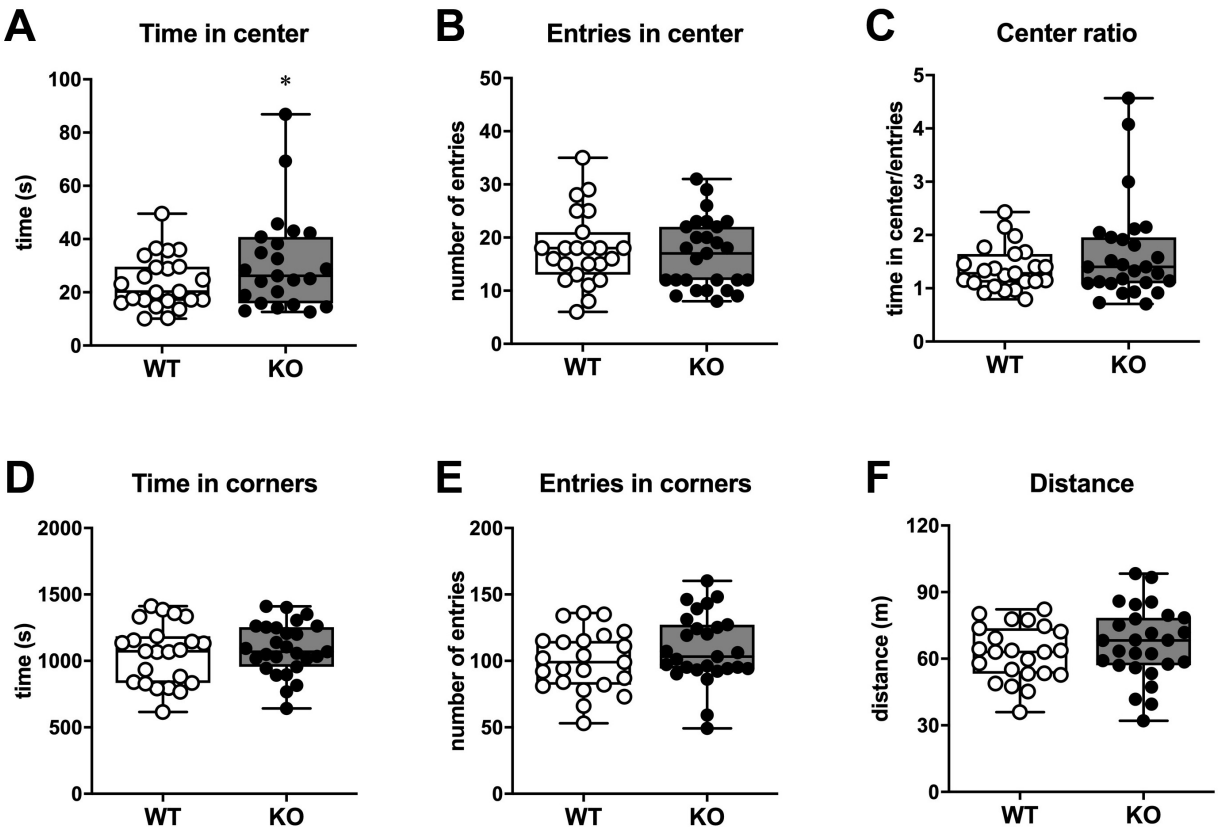

Figure 3. Open field test. (A) Time, in seconds, spent in the center of the arena. (B) Number of entries in the center of the arena. (C) Time spent in the center of the arena per entry. (D) Time spent in the corners of the arena. (E) Number of entries in any of the 4 corners of the arena. (F) Total distance in meters run by the rats. In all panels, open circles represent WT (n=23) and solid circles represent SESN3-KO rats (n=27). Statistical analysis: unpaired *t* test with Welch's correction. * P<0.05.

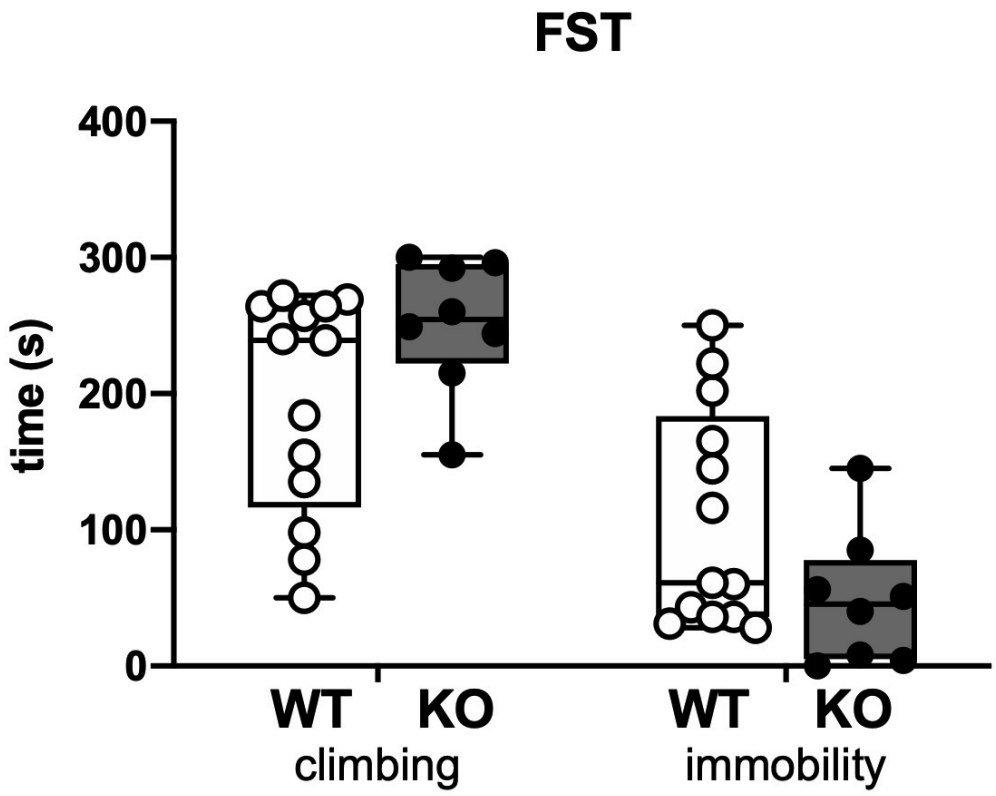

Figure 4. Forced swimming test. The plot shows the time spent by the rats in trying to climb the cylinder or swimming in an attempt to find an escape (climbing) and the time spent floating immobile (immobility). Open circles represent WT (n=13) and solid circles represent SESN3-KO rats (n=8).

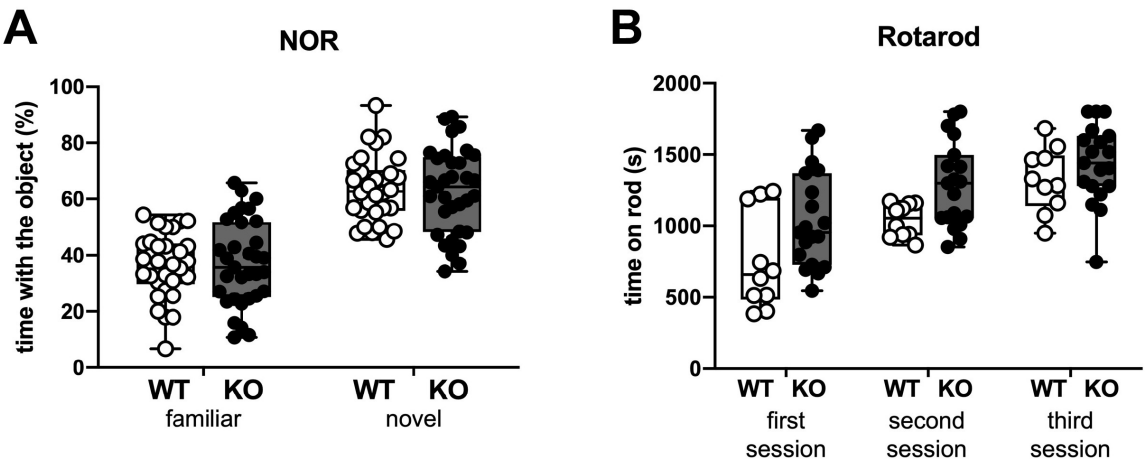

Figure 5. (A) Novel object recognition. Percentage of time spent interacting with the familiar and the novel object in 30 WT and 33 SESN3-KO rats. (B) Rotarod. Time spent on the rods during in 3 trials of testing. Open circles represent WT (n=10) and solid circles represent SESN3-KO rats (n=19).

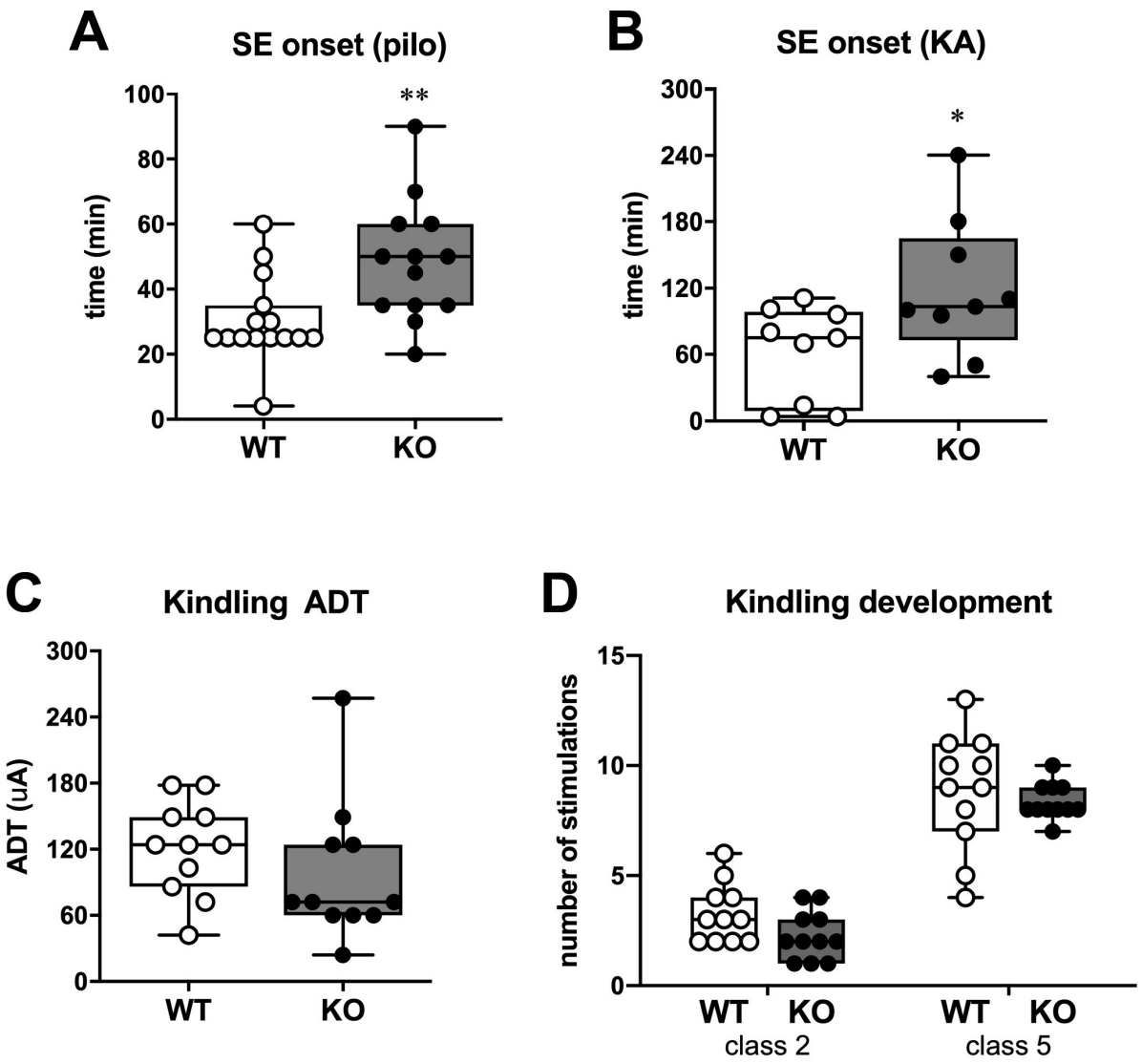

Figure 6. Seizures susceptibility. (A) Time to SE onset after i.p. pilocarpine injection onset in 15 WT and 13 SESN3-KO rats. (B) Time to SE onset after intra-hippocampal injection of KA in 9 WT rats and 9 SESN3-KO rats. (C) ADT associated with minimal behavioral symptoms (i.e. 1-2 on Racine scale score, n=11 per genotype) (D) Kindling development. Days to reach class 2 or class 5 seizures according to the Racine's scoring scale, in 11 animals per genotype. In all panels, open circles represent WT and solid circles represent SESN3-KO rats. Statistical analysis: unpaired *t* test with Welch's correction. * P<0.05; ** P<0.01.

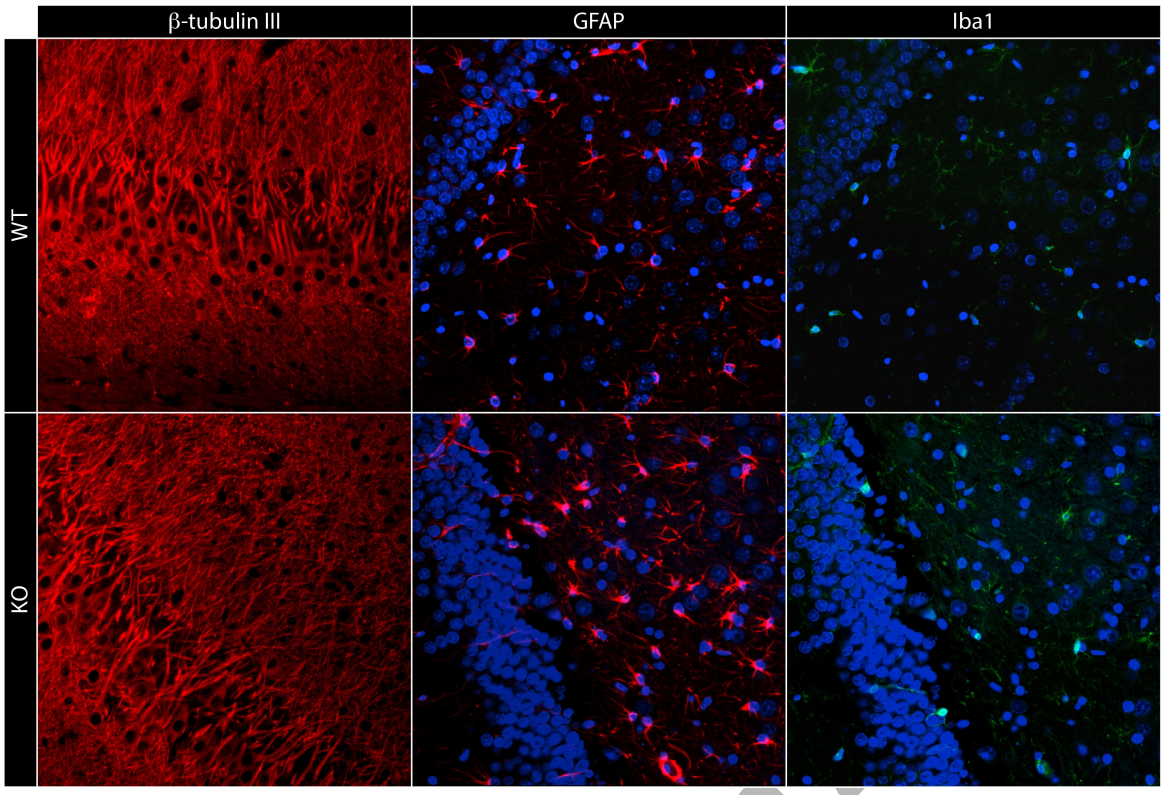

Figure 7. Immunohistochemical analysis of microglial cells (A-B, labeled in green with an Iba-1 antibody), astrocytes (C-D, labelled in red with a GFAP antibody) and neurons (E-F, labelled in red with a β-tubulin 3 antibody). Shown are representative sections from WT (A,C,E) and SESN3-KO rats (B,D,F). DAPI staining in blue for all images. 40x magnitude.

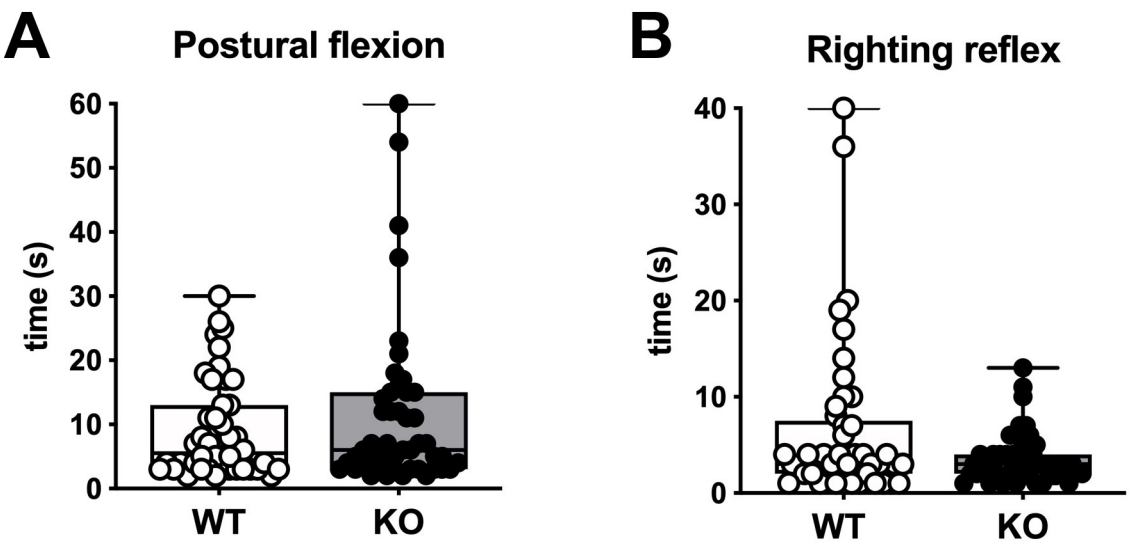

Supplementary Figure 1: Behavioral tests on pups. A) Postural Flexion test: time, in seconds, spent to complete a rotation of 45° when suspended by the tail; B) Righting reflex test: time, in seconds, spent to complete a rotation from a supine to prone position. Open circles represent WT rats, solid circles represent SESN3-KO rats.

Chapter 4: Biomarkers of epileptogenesis

4.1 Introduction

4.1.1 MicroRNA

MicroRNAs (miRNAs) are endogenous small non coding RNAs, about 22 nucleotides long, that can regulate gene expression at a post-transcriptional level [63]. Many different molecules can influence protein translation, promoting (enhancers) or inhibiting (silencers) translation. miRNAs are known as silencers, since they bind complementary un-translated mRNA sequences, leading to reduced translation and protein levels. miRNAs effect on protein expression can thus be responsible for mechanisms underlying disease development. Regarding epilepsy, miRNAs dysregulation could, for example, influence the translation of neurotrophic factors by decreasing their levels, or can lead to an increase in pro-apoptotic and pro-inflammatory levels if the miRNAs controlling anti-apoptotic factors are upregulated [64].

Literature data report that there is a canonical pathway of miRNA biogenesis, that starts from DNA sequences transcribed into primary miRNAs (pri-miRNAs), consequently processed into precursors (pre-miRNAs) and then in mature miRNAs. The processing phase, described in Fig.1, is driven by a complex consisting of a RNA binding protein, named DGCR8 and a ribonuclease III enzyme, Drosha [65]. The DGCR8 protein recognizes the amino acidic motif of the pri-miRNA, while Drosha cleaves the pri-miRNA duplex at the base of the hairpin complex. Pre-miRNAs are transported from the nucleus to the cytoplasm and here are further modified by the RNAse III endonuclease Dicer, that removes the terminal loop, generating the mature miRNA duplex structure [65,66]. miRNAs have different nomenclatures, depending on the directionality of their strand: the 3p or 5p strand arise from the 3' end or the 5' end of the pre-miRNA hairpin [67].

Independent of the strand, mature miRNAs are loaded into the Argonaute (AGO) protein in an ATP-dependent manner and then transported to the target mRNA. MiRNA-mediated gene regulation is made possible by interaction between miRNAs and the 3'UTR region of target mRNAs – even if there are cases of interaction with other regions such as the 5'UTR or even coding sequences [68]. To better understand how miRNAs act, it is necessary to explain the role of the minimal miRNA-induced silencing complex (miRISC). This complex consists in the guide strand (3' or 5') and the AGO protein. The

target specificity of the miRISC complex is due to sequence complementary with the target mRNA (known as MREs)[68]. The miRISC complex can interfere in different ways with protein expression: it can repress mRNA target translation or it can act by degrading the mRNA itself.

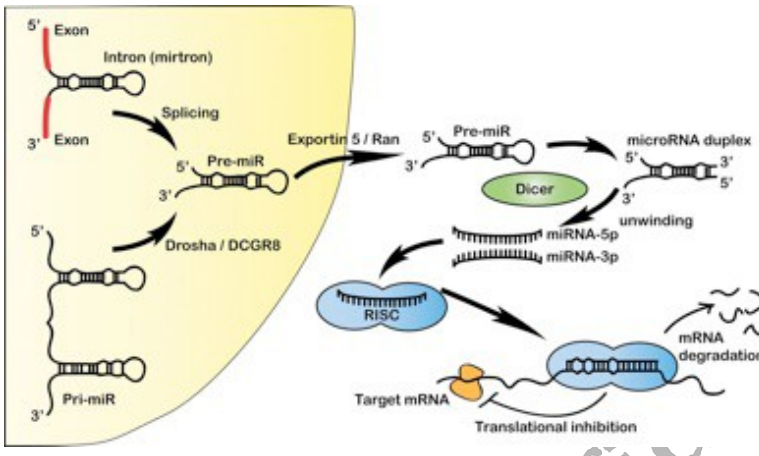

Figure 1: Biogenesis of miRNA.

4.1.2 Biomarkers

A biomarker is a "defined characteristic that is measured as an indicator of normal biological processes, pathogenic processes or responses to an exposure or intervention" [36] . Biomarkers can be classified in different classes:

- **Diagnostic**: biomarkers used to detect or confirm the presence of a disease, or to redefine the classification of the disease. Examples of this category are imaging-base or molecules that can identify tumors.
- **Monitoring**: markers that indicate the modification in the status of a medical condition; one example is HbA1C in diabetic patients.
- **Pharmacodynamics/response biomarkers:** change after the exposure to a drug or an environmental agent.
- **Predictive**: predicts a favorable or unfavorable effect after the exposure to a drug or environmental agent. They are very useful for enrichment strategies in clinical trials.
- **Prognostic**: their change in expression is directly linked to the likelihood that a disease or event occurs, when the medical condition is already present.
- **Safety**: indicate the presence or extent of toxicity.
- **Susceptibility/risk**: indicate the potential development of a disease or medical condition in people that do not appear to be ill.

Biomarkers can be molecules found in biofluids (plasma, serum, CSF); electrical traces (EEG or ECG); images as magnetic resonance (RMI).

Before being used in clinics, biomarker must be validated in pre-clinical studies. Whatever the biomarker, a stringent statistical analysis is mandatory. Sensitivity and specificity are the key parameters to be considered. Sensitivity is the probability that a biomarker is positive when the disease is present, whereas specificity is the probability that a biomarker is negative when the disease is not present [69]. Following these criteria, it is possible to divide subjects tested for a biomarker into four different categories: True Positive (TP), False Positive (FP), True Negative (TN) and False Negative (FN) [36]. Sensitivity can thus be calculated by applying the formula TP/(TP+FN), while specificity can be identified by TN/(TN+FP). The receiver operating characteristics (ROC) analysis is a standard method to determine the sensitivity and specificity of a proposed biomarker. It is a plot of sensitivity versus 1-specificity for the different cutoff points of a diagnostic test. Accuracy of the diagnostic test is based on the area under the curve (AUC) of the ROC plot (the closer the AUC to 1, the better the test). A value of 0.8 is typically considered the minimal value for a biomarker to have any clinical value.[36].

4.1.3 Biomarkers of epileptogenesis

The World Health Organization estimates that every 13 seconds one patient is diagnosed with epilepsy, leading to a total of 2.4 million new cases per year [70]. The epileptogenic area, where changes take place, may express and release molecules that might be used as biomarkers. Research on biomarkers for epilepsy has become more and more important in the last years, focusing on diagnostic and prognostic biomarkers [71]. Table 1 shows some of the biomarkers recently linked to epileptogenesis and epilepsy development.

Reference	Class of biomarker	Type of analysis	Biomarker
Bragin et al., 1999; Andrade-Valenca et al., 2011	Diagnostic for localization of epileptic focus	Deep EEG analysis	HFOs
Pollard et al., 2012	Diagnostic for focal epilepsy	Plasma	sICAM5
Wang et al., 2015	Diagnostic for pharmacoresistant epilepsy	Serum	Dysregulated miRNAs
Roncon et al., 2015	Diagnostic for mTLE	Plasma and tissue	Dysregulated miRNAs
Walker et al., 2017	Prognostic biomarker	Plasma	HMGB1

Table 1: Potential biomarkers of epilepsy

Diagnostic biomarkers, as already described, are those that can be used to identify the presence of the condition of interest, in our case epilepsy or epileptogenesis. As already

stated, not only molecules can serve as biomarkers of epilepsy, but also EEG patterns, such as high frequency oscillations (HFOs) or imaging outcomes, for example MRI observation of reduced amygdala relaxation times (T2) [72].

Cerebrospinal fluid (CSF) molecules could be one good option, because of proximity to the brain parenchyma. However, withdrawal of CSF is invasive. Therefore, epilepsy research is focusing on biomarkers in other more accessible fluids, such as plasma and serum. Walker and colleagues demonstrated that high levels of plasma High Mobility Group Box 1 (**HMGB1**) protein are linked to epilepsy [73]. The de-acetylated form of HMGB1 is passively released by necrotic cells, whereas the active form is released during inflammation [74]. High levels of HMGB1, released during inflammation by cells of the epileptic focus, may be thus claimed as prognostic biomarker of epilepsy. The **sICAM5** protein, better known as telencephalin, has been studied as biomarker of epilepsy for its anti-inflammatory role; this protein is expressed in glutamatergic neurons, but it is also stable in blood. It has been demonstrated that sICAM5 levels in blood are 5 times lower in pharmaco-resistant epilepsy patients as compared with healthy volunteers [75].

miRNAs are small nucleic acids (20-25 nucleotides) that regulate protein expression inhibiting mRNA translation, while **circular RNAs** act as sponges by grabbing miRNAs and thus preventing inhibition of protein production [76]. These molecules could serve as biomarkers: they cross the BBB, can be transported in biofluids via exosomes or bound to proteins, and are easily detectable. One study conducted in our laboratory has demonstrated changes in miRNA levels in brain tissue and blood from both animal models of epilepsy and human samples of epileptic patients [51]. We found that miR-9a-3p levels increase dramatically during latency, and then return to baseline after the first spontaneous seizure [51]. Others have also explore changes in plasma miRNAs during epilepsy development in animal models. For example, **miR-124** levels were found reduced in blood samples of rats during acute status epilepticus; because miR-124 is known to have neuroprotective effects, its down-regulation may be seen as an alarm to expect neuronal death [64,77].

4.2 Materials and Methods

4.2.1 Animals

Sprague-Dawley male rats were used for all the experiments. They were housed under standard conditions: constant temperature (22-24°C) and humidity (55-65%), 12h light/dark cycle, water and food ad libitum. The ARRIVE (Animal Research: Reporting *In Vivo* Experiments) guidelines have been followed. Procedures involving animals and their care were carried out in accordance with European Community, national and local guidelines, laws and policies. All experimental protocols for Animal Experimentation were approved by the University of Ferrara Ethical Committee and by the Italian Ministry of Health (D.M. 371/2016-PR). All animals were euthanized by anesthetic overdose.

4.2.2 Multicentric study

This study was designed as a multicentric project (Fig. 2) involving four laboratories throughout Europe, each one using a different model of TLE. The final goal was to find one or more dysregulated miRNAs circulating in plasma of epileptic animals, that could serve as biomarkers of epileptogenesis. The key point was to use plasma from animals that would or would not subsequently develop epilepsy after an identical brain damage.

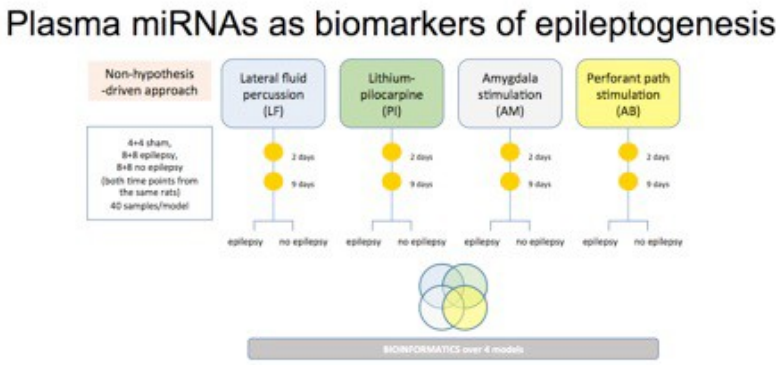

Figura 2. Multicentric plan

The model proposed by our laboratory was the lithium-pilocarpine model, a refinement of the well-consolidated pilocarpine model [53,78]. As described by Brandt and colleagues, the use of lithium before pilocarpine and of a drug cocktail to interrupt SE leads to total recovery of the rats after SE and, by modifying the duration of SE itself, it permits to obtain two separate phenotypes: rats developing spontaneous recurrent seizures (SRS) and rats that do not show any sign of paroxysmal activity in the brain area involved in TLE. To obtain a good percentage of rats not developing epilepsy, we interrupted SE after 60 minutes, as explained below[78]. Since the window of time identifying epileptogenesis, in

the animal models used in this study, lasts at least 10 days, we decided to sample blood at day 2 and day 9 after insult, as shown in Fig. 3.

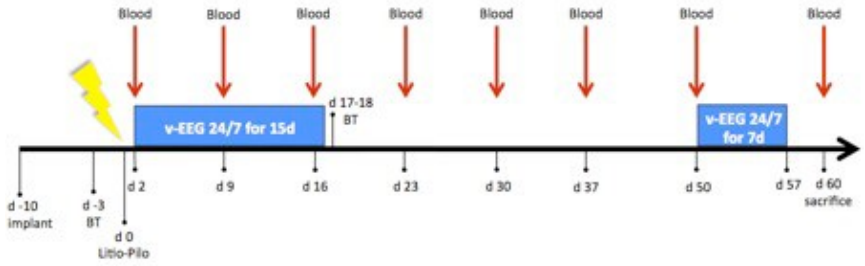

Figure 3. Timeline of the experiment.

4.2.3 Lithium-Pilocarpine model of TLE

Lithium (127 mg/kg) was orally administered 14-15 h before pilocarpine; pilocarpine (34 mg/kg) was administered through intraperitoneal injection, 30 min after methyl-scopolamine (1 mg/kg, s.c.), a muscarinic antagonist that is used to limit peripheral adverse effects [53]. Animals were then observed until the development of status epilepticus (SE), taking note of convulsive activity based on the Racine scoring scale [34] [34]. SE was interrupted 60 min after its onset by administration of a drug cocktail including diazepam (10 mg/kg i.p.), phenobarbital (25 mg/kg i.p.) and scopolamine (1 mg/kg i.p.), repeated 4 h after the first injection. At 8 hours from the first drug cocktail, a last injection was given that did not include the barbiturate to avoid excessive respiratory depression [79].

4.2.4 Electrode implantation

Ten days before SE induction, a bipolar electrode was implanted in the right dorsal hippocampus of each rat, via stereotaxic surgery. Rats were anaesthetized using a ketamine/xylazine solution (87 mg/kg, 13 mg/kg i.p.) and then positioned in the stereotaxic frame. During surgery, anesthesia was kept using 2% isoflurane. A hole was drilled in correspondence of the dentate gyrus (DG) of the right hippocampus (from bregma, AP: -3,9; ML: -1,7; P: +3,5, Paxinos Atlas). Other four holes were drilled to implant stainless steel screws, needed to stabilize the implantation. All was then fixed with dental cement. From two days before to three days after surgery, rats were treated with an antibiotic to prevent any infection (Enrofloxacine, 5mg/kg ip); an analgesic drug (Tramadol, 5 mg/kg i.p.) was also given immediately after the implantation, to prevent post-surgical pain.

4.2.5 Plasma sampling

In order to obtain comparable results, plasma was sampled following a common protocol by all laboratories involved in this study [80]. Before starting the procedure, the tail was immersed in hot water (42°C) for 2 min, to allow dilatation of the vessels, and then gently wiped with cotton soaked with ethanol 70%. Blood withdrawal was performed using a 23 G butterfly needle, inserted in the lateral tail vein; blood drops were collected in 0.5ml K_2EDTA coated Vacutainers (Becton Dickinson, USA) and stored at 4°C until centrifugation.

Samples were centrifuged at 1300 g for 10 min at 4°C. Soon after separation, plasma was stocked at -80°C in a 0.2 ml Eppendorf tube. Plasma quality was another critical point of the study, because it was essential to avoid hemolysis of red cells. Plasma was checked for hemolysis using a spectrophotometer (Eppendorf Biospectrometer), using as cut-off level of hemoglobin (Hg) absorbance a value of 0.25 nm. All samples with A>0.25 nm were discarded.

4.2.6 Video-EEG and video-monitoring

To correctly allocate rats to the epileptic or non-epileptic group, two weeks of video-EEG monitoring took place, starting from day 3 post-SE. The implanted bipolar electrode was associated to an amplification system (MP150 System, Biopac): the recorded signal was analyzed through the AcqKnowledge 5.0 system (Biopac). One EEG (partial) seizure was defined as a paroxysmal electrical activity characterized by three-times higher amplitude than baseline, lasting at least 5 s, with more than 5 spikes/sec. The amplifier was supported by cameras recording the behavior of the animals. Rats were considered epileptic after at least two EEG seizures and one generalized convulsive seizure (class 4 or 5 according to Racine's scale) [34] were detected.

4.2.7 Behavioral tests

A battery of behavioral tests was performed to assess the presence of epilepsy comorbidities, such as anxiety and cognitive impairment, before SE and in the chronic period.

Elevated Plus Maze (EPM). EPM is a well characterized behavioral test used to assess the susceptibility to anxiety[47]. The test is run on an apparatus kept 50 cm from ground, consisting of two open arms (50 x 10 cm) and two closed arms (50 x 10 x 50 cm) connected through a central platform (10 x 10 cm). At the beginning, rats were placed in the central part of the platform, facing an open arm. Different parameters were noted

during the 5 min test: number of entries in open arms; number of entries in closed arms; time spent in open arms; time spent in closed arms; number of stretched-attend postures (SAP), i.e. how many times the rat looked at the open arms while being with the body in the closed arm; number of head dippings (HD), i.e. how many times the rat looked down from the open arms of the EPM apparatus; and number of rearings, i.e. how many times the rat looked up leaning against the walls of the closed arms.

Novel Object Recognition (NOR). The NOR test was performed as described by Ennaceur and Delacour [50]. The test consisted of three phases: habituation, acquisition and test. The habituation phase, taking place 24 h before the acquisition and testing phases, consisted in the exploration of the arena were the NOR test is performed, for 10 min. The day after, the acquisition trial was conducted by placing the rat in the field, in which two identical objects were positioned at the corners of the arena. Rats were allowed to explore the two objects for 5 min, and exploratory activity (i.e. the time spent exploring each object) was recorded. After 2 h, rats were placed again in the arena, where one object was substituted with a novel one. The exploration time with the two different objects was noted.

4.2.8 MicroRNAs quantification

A total of 180 plasma samples were collected for the two time points relating to the epileptogenesis phase:

- 8 from non-epileptic animals per experimental model, at day 2 and day 9;
- 8 from epileptic animals per experimental model, at day 2 and day 9;
- 4 sham animals per experimental model, at day 2 and day 9.

Every plasma sample was shipped to the colleagues of the Amsterdam research group. Total RNA was extracted using miRCURY™ RNA Isolation and miRCURY™ biofluids kits (Exiqon). RNA-Seq was performed to identify the number of count reads, and thus investigate the presence of dysregulated miRNAs. The analysis was performed by an external company (GenomeScan B.V., Amsterdam). Before running the analysis in a Next-Generation Sequencing (NGS) platform (Illumina technology), plasma quality check was performed again, by looking at absorbance levels using a Nanodrop.

A meta-analysis was performed to combine the effect size (ES) of the four different studies, i.e. the four different animal models. Before performing it, preventive calculations were performed:

- Data filtering: miRNAs with less than 10 counts were discarded, since their weight is too low to have an impact on the ending point of the analysis;

- Voom Transformation and Normalization, to provide an estimate of the mean-variance relationship of the log-counts in order to calculate precision weights for each observation. The raw count data is transformed into log2-counts per million values (logCPM), and logCPM numbers are then normalized using the quantile normalization method;
- Higgins heterogeneity index (I2), that describes the variability in the effect size estimates.

4.3 Results

4.3.1 Animals phenotyping

A total of 48 rats were used for our part of this experiment, of which 26 developed epilepsy. As stated above, animals were considered epileptic after the observation of at least two EEG seizures (Fig. 4) and one generalized seizure (Fig. 5). The mean latency to the occurrence of the first spontaneous seizure in the epileptic group was 18 days after SE.

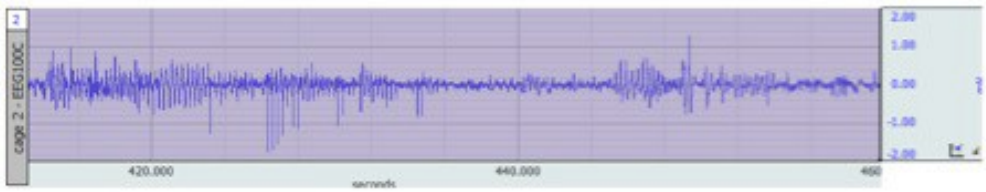

Figure 4. EEG of a partial seizure (class 2 Racine's scale).

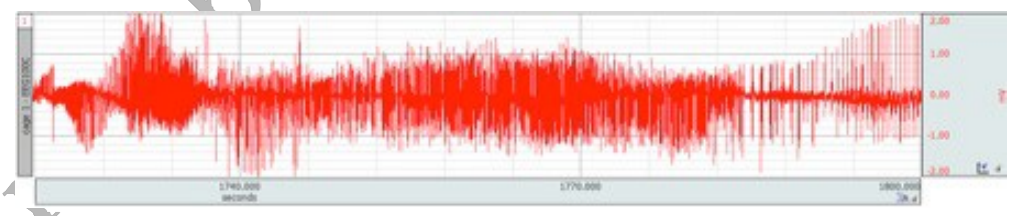

Figure 5. EEG of a generalized seizure (class 5 Racine's scale)

Elevated Plus Maze (EPM)

Naive animals spend more time in the closed arms, associated with a safer environment. The time spent in open (A) and closed (B) arms, and number of entries into the open (C) and closed (D) arms are shown in Fig. 6. Epileptic animals (dark grey bars), spent significantly more time into the open arms than sham (p=0.0218) and non-epileptic

animals (p=0.0154); as a consequence, epileptic animals spent significantly less time into the closed arms (p<0.0001). These results indicate a propensity of epileptic animals to explore unknown and unsafe areas of the apparatus; this behavior can be related to an anxiety or hyperactivity disorder.

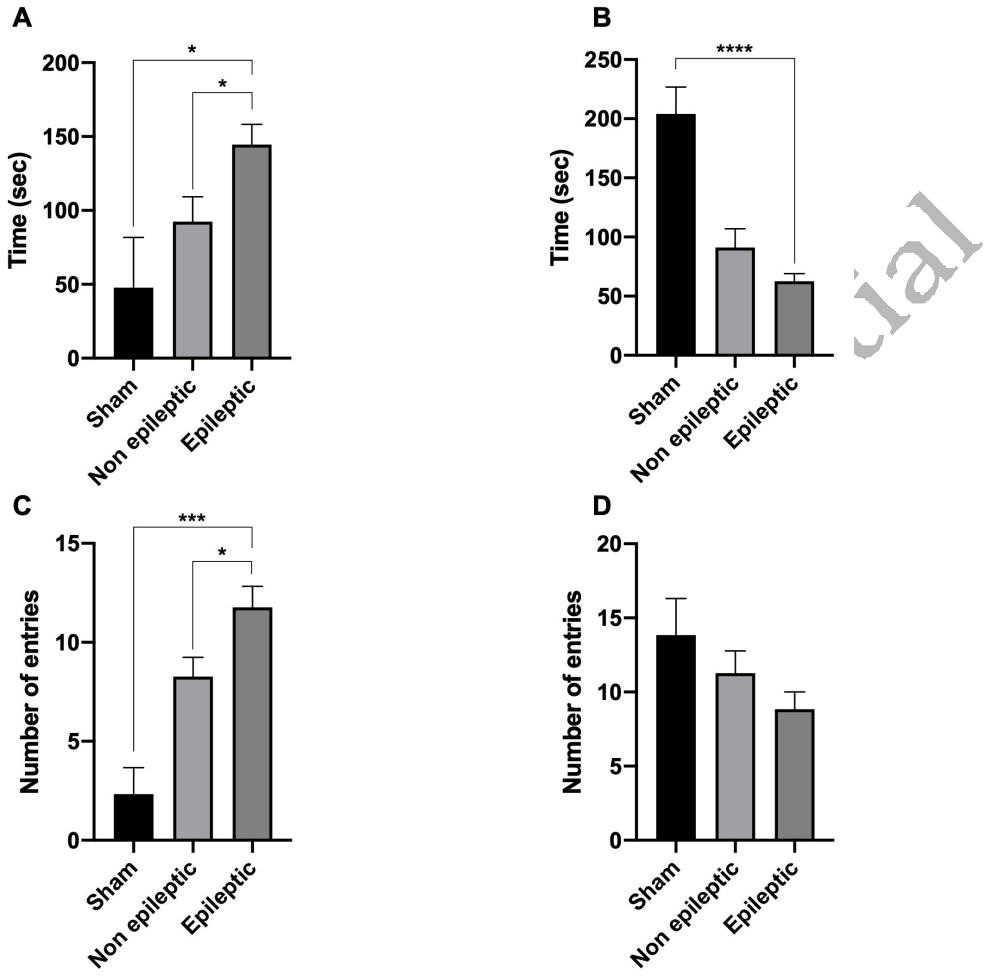

Figure 6 EPM **A.** Time spent into the open arms. **B.** Time spent into the closed arms. **C.** Number of entries into the open arms. **D.** number of entries into the closed arms. Data are the mean±SEM of 6 sham (black bars), 11 non epileptic (light grey) and 13 epileptic (dark grey). *P<0.05; **P<0.01; ***P<0.001, Mann-Whitney U test.

Novel Object Recognition (NOR)

The NOR test evaluates the cognitive ability of rodents. The protocol can be adapted based on the specific cognitive function to be studied; in our case, we chose to evaluate short memory consolidation, by doing the testing phase two hours after familiarization. To avoid any possible bias due to positioning of the objects or preferences of color or shape, the objects were chosen randomly, and to avoid preferences of placing, the two objects were moved after each test to cover all the corners of the arena. Exploration time with familiar and novel object, during the testing phase, is reported in Fig. 7A, while the total exploration time is in Fig. 7B. At day 18 post SE, epileptic animals cannot discriminate which object is the novel one, an ability that is instead maintained in non-epileptic and

sham rats. In fact, the exploration time of the novel object is significantly higher compared to the familiar one for both sham (p=0.0078) and non-epileptic animals (p=0.0413).

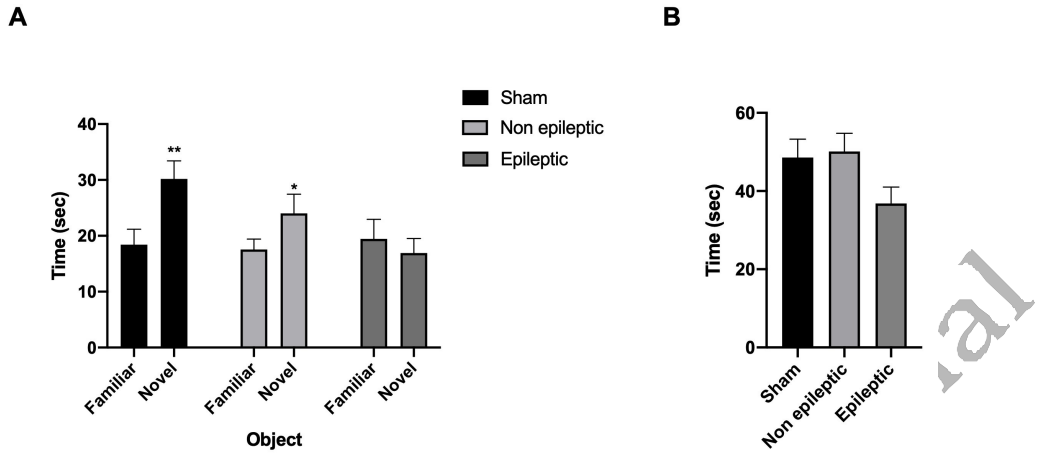

Figure 7. NOR test. **A.** Exploration time of the two objects. **B.** Total exploration time. Data are the mean±SEM of 6 sham (black bars), 11 non epileptic (light grey) and 13 epileptic (dark grey). *P<0.05; **P<0.01; Mann-Whitney U test.

4.3.2 Dysregulated miRNAs evaluation and meta-analysis

No common miRNA alterations were observed across all 4 models (Fig. 8). Only a few (boxed in yellow in Fig. 8) were common to 2 models. Therefore, it was initially decided to run an extra analysis focusing on isomiRs. Recent studies have shown that a single miRNA locus can generate a series of functionally distinct miRNA variants. These miRNAs variants, known as isomiRs, are produced when the 5' or 3'-end of the miRNA is modified through the addition of new nucleotides or through shortening of the mature miRNA sequence [81] While little is currently understood about the exact functional role of these isomiRs, it is known that they are abundantly expressed throughout a variety of biofluids, including plasma [82] Further, it has been shown in disease contexts that isomiRs have a higher level of specificity and sensitivity when compared to the canonical miRNAs [82]. However, no isomiR alteration was observed across the different models.

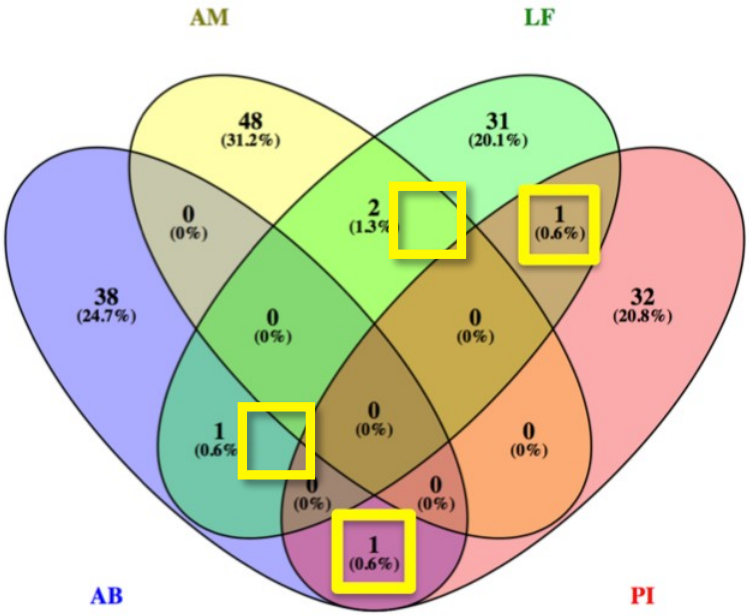

Figure 8. Venn diagram. Red: lithium-pilocarpine (PI) model; green: lateral fluid percussion (LF); yellow: amygdala stimulation (AM); blue: angular bundle (AB) stimulation.

It was then decided to run a meta-analysis of the data. Because differences between samples may arise through animal models, tissue collection methods etc., we tested heterogeneity of effect-size estimates using Cochran's Q statistics and quantified heterogeneity using I2 statistics. We found that there is low variation between the effect sizes and, therefore, a fixed effect model (FEM) may be appropriate. FEM meta-analysis identified 5 miRNAs that were significantly different between epileptic and non-epileptic animals at 2 d post insult (EL). Three of these were already known (namely miR-129-5p, miR-138-5p and miR-3085) and two were not (ENSRNOG00000054305 and ENSRNOG00000054389). Interestingly, miR-129-5p inhibition has been associated with synaptic downscaling in vitro and reduced epileptic seizure severity in vivo [83] and miR-129-5p is upregulated in different epileptic models [51,84]. In addition, miR-138-5p is a potential regulator of memory performance, a candidate regulator of P53 (involved in cell cycle, proliferation and apoptosis), and it is down-regulated in several phases of epilepsy [85,51,84]. Forest plots for miR-129-5p, miR-138-5p and miR-3085 are shown in Figs. 9 to 11.

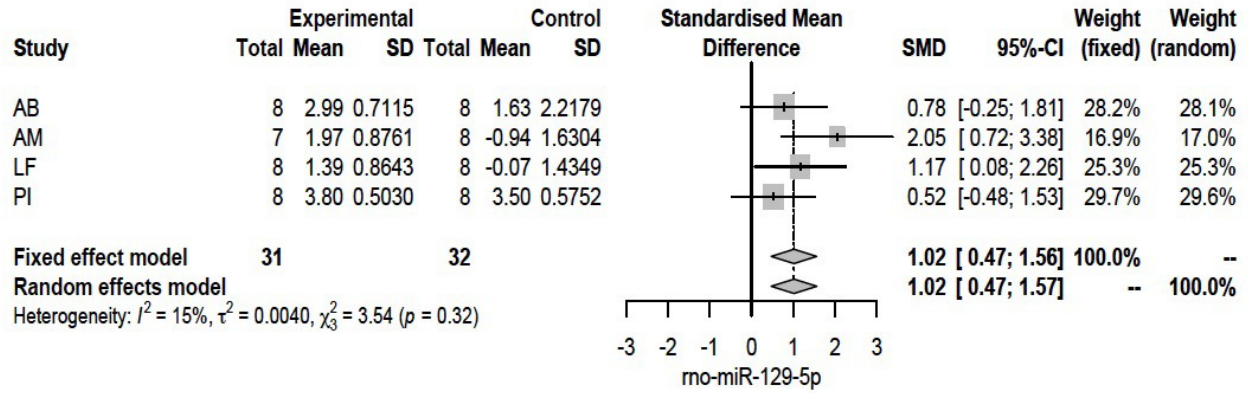

Figure 9. Forest plot of miR-129-5p.

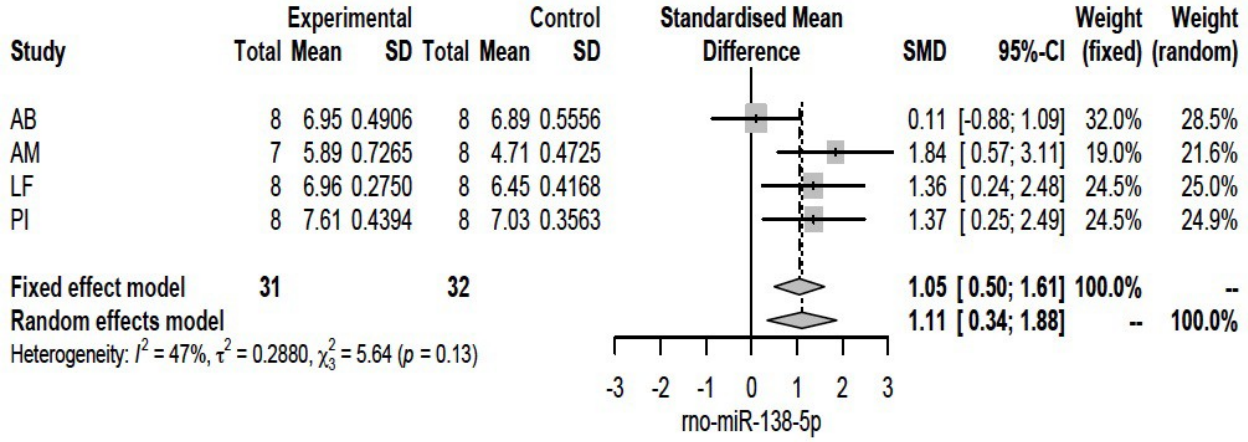

Figure 10. Forest plot of miR-138-5p.

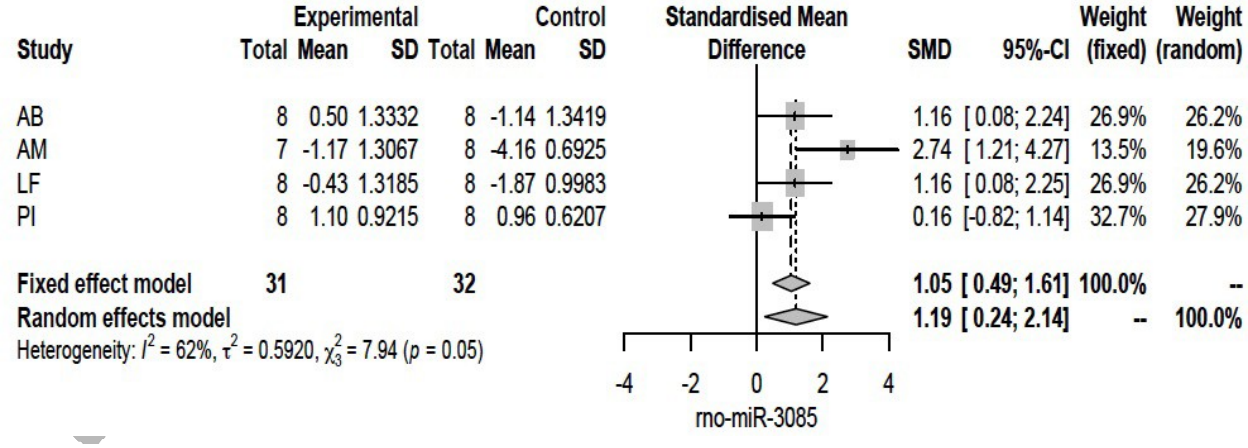

Figure 12. Forest plot of miR-3085.

4.4 Discussion

The final goal of this multicentric study was to identify one or more miRNA that could be used as biomarker of epileptogenesis. We aimed to discover biomarkers that could be detected using non-invasive techniques, and plasma sampling was thus the best choice. It is in fact an urgent medical need to identify those patients who, after a status epilepticus, a brain trauma, a stroke, or a brain infection, will eventually develop epilepsy, and those who will not. This would help to develop preventive treatments.

The dysregulation of miRNA plasma levels has gain more and more importance as prognostic and diagnostic marker of diseases in the past few years. In 2015, our research group published the results of the analysis of dysregulated miRNAs expression in samples of hippocampal tissue derived from animal models of epilepsy or human tissue collected after surgical removal of the epileptic focus [51]. That study encouraged us to follow the idea that miRNAs could serve as biomarkers of epileptogenesis, but we had to overcome its limitations: i) the control group of both preclinical and human samples was from healthy individuals; ii) the invasiveness of the techniques used to obtain the samples.

The present study has thus been designed to use truly informative control group, i.e. rats that experienced SE but did not become epileptic, and a non-invasive approach, i.e. blood withdrawal. The lithium-pilocarpine model of TLE, as well as the other models employed in this study, actually allow to obtain two well defined groups of animals: one developing and one not developing the disease.

The application of a meta-analysis was mandatory in an attempt to identify common biomarkers of the development of epilepsy. Meta-analysis allowed to compare the data from the four different models of epilepsy, considering them as independent studies. In fact, the term epilepsy does not refer to a single disease but, rather, to multiple neurologic conditions, and our aim was to find biomarkers identifying more than one type of epilepsy.

The meta-analysis revealed that miR-129-5p, miR-138-5p and miR-3085 were all up-regulated in plasma samples of animals that were to become epileptic at day 2 post brain insult. It should be made clear that these miRNAs are not necessarily implicated in the pathogenesis of the disease, since their regulation was not studied in the epileptic focus, i.e. in brain tissue. It is, however, interesting to look at the biological pathways that these miRNAs are known to control.

miR-129-5p dysregulation has already been linked to epilepsy, being this miRNA implicated in the synaptic downscaling phenomena in epileptic tissue. Its inhibition decreases the severity of spontaneous seizures in a mice model of kainic acid injection [83]. In addition, its up-regulation has been described in the brain of other models of TLE, until at least 72 h after SE [51,83]. The molecular targets of miR-129-5p include Atp2b4 and Doublecortin (Dcx), respectively a gene coding for a Ca^{2+} pump and a proteins associated with neurogenesis and cellular migration [83].

miR-138-5p interacts with the MAP kinase family of proteins, and specifically with Map3k14: this protein may exert a pro-epileptogenic role by inhibiting NF-κB, a transcription factor with neuroprotective effects [85]. A down-regulation of miR-138-5p has been observed in epileptic tissue during latency [51,84,85], reinforcing the hypothesis that lowered levels of this miRNA could be linked to reduced neuroprotection.

As for **miR-3085**, this is the first time that this miRNA is linked to epilepsy.

In conclusion, we identified 3 circulating miRNAs that may represent diagnostic biomarkers of epileptogenesis (i.e. prognostic biomarkers of epilepsy). We are currently running technical validation of these findings using a different analytical approach (digital droplet PCR) and biological validation of these candidates in an extended cohort of animals and epilepsy models. If these further experiments will provide positive results, some of these miRNAs may become eligible for testing in human epilepsy.

4.5 References

1. Zucchini S, Marucci G, Paradiso B, et al. Identification of miRNAs differentially expressed in human epilepsy with or without granule cell pathology. *PLoS One* 2014; **9**(8): e105521.
2. Tiwari D, Peariso K, Gross C. MicroRNA-induced silencing in epilepsy: Opportunities and challenges for clinical application. *Dev Dyn* 2018; **247**(1): 94-110.
3. Denli AM, Tops BB, Plasterk RH, Ketting RF, Hannon GJ. Processing of primary microRNAs by the Microprocessor complex. *Nature* 2004; **432**(7014): 231-5.
4. Zhang H, Kolb FA, Jaskiewicz L, Westhof E, Filipowicz W. Single processing center models for human Dicer and bacterial RNase III. *Cell* 2004; **118**(1): 57-68.
5. Meijer HA, Smith EM, Bushell M. Regulation of miRNA strand selection: follow the leader? *Biochem Soc Trans* 2014; **42**(4): 1135-40.
6. O'Brien J, Hayder H, Zayed Y, Peng C. Overview of MicroRNA Biogenesis, Mechanisms of Actions, and Circulation. *Front Endocrinol (Lausanne)* 2018; **9**: 402.
7. Pitkanen A, Ekolle Ndode-Ekane X, Lapinlampi N, Puhakka N. Epilepsy biomarkers - Toward etiology and pathology specificity. *Neurobiol Dis* 2019; **123**: 42-58.

8. Pitkanen A, Henshall DC, Cross JH, et al. Advancing research toward faster diagnosis, better treatment, and end of stigma in epilepsy. *Epilepsia* 2019; **60**(7): 1281-92.
9. Engel J, Jr. Epileptogenesis, traumatic brain injury, and biomarkers. *Neurobiol Dis* 2019; **123**: 3-7.
10. Pitkänen A, Löscher W, Vezzani A, et al. Advances in the development of biomarkers for epilepsy. *The Lancet Neurology* 2016; **15**(8): 843-56.
11. Choy M, Dube CM, Patterson K, et al. A novel, noninvasive, predictive epilepsy biomarker with clinical potential. *J Neurosci* 2014; **34**(26): 8672-84.
12. Walker LE, Frigerio F, Ravizza T, et al. Molecular isoforms of high-mobility group box 1 are mechanistic biomarkers for epilepsy. *J Clin Invest* 2017; **127**(6): 2118-32.
13. Maroso M, Balosso S, Ravizza T, et al. Toll-like receptor 4 and high-mobility group box-1 are involved in ictogenesis and can be targeted to reduce seizures. *Nat Med* 2010; **16**(4): 413-9.
14. Pollard JR, Eidelman O, Mueller GP, et al. The TARC/sICAM5 Ratio in Patient Plasma is a Candidate Biomarker for Drug Resistant Epilepsy. *Front Neurol* 2012; **3**: 181.
15. Hsiao KY, Sun HS, Tsai SJ. Circular RNA - New member of noncoding RNA with novel functions. *Exp Biol Med (Maywood)* 2017; **242**(11): 1136-41.
16. Roncon P, Soukupova M, Binaschi A, et al. MicroRNA profiles in hippocampal granule cells and plasma of rats with pilocarpine-induced epilepsy--comparison with human epileptic samples. *Sci Rep* 2015; **5**: 14143.
17. Brennan GP, Dey D, Chen Y, et al. Dual and Opposing Roles of MicroRNA-124 in Epilepsy Are Mediated through Inflammatory and NRSF-Dependent Gene Networks. *Cell Rep* 2016; **14**(10): 2402-12.
18. Curia G, Longo D, Biagini G, Jones RS, Avoli M. The pilocarpine model of temporal lobe epilepsy. *J Neurosci Methods* 2008; **172**(2): 143-57.
19. Brandt C, Tollner K, Klee R, Broer S, Loscher W. Effective termination of status epilepticus by rational polypharmacy in the lithium-pilocarpine model in rats: Window of opportunity to prevent epilepsy and prediction of epilepsy by biomarkers. *Neurobiol Dis* 2015; **75**: 78-90.
20. Racine RJ, Gartner JG, Burnham WM. Epileptiform activity and neural plasticity in limbic structures. *Brain Res* 1972; **47**(1): 262-8.
21. Brandt C, Rankovic V, Tollner K, Klee R, Broer S, Loscher W. Refinement of a model of acquired epilepsy for identification and validation of biomarkers of epileptogenesis in rats. *Epilepsy Behav* 2016; **61**: 120-31.
22. van Vliet EA, Puhakka N, Mills JD, et al. Standardization procedure for plasma biomarker analysis in rat models of epileptogenesis: Focus on circulating microRNAs. *Epilepsia* 2017; **58**(12): 2013-24.
23. Tchekalarova J, Moyanova S, Fusco AD, Ngomba RT. The role of the melatoninergic system in epilepsy and comorbid psychiatric disorders. *Brain Res Bull* 2015; **119**(Pt A): 80-92.
24. Ennaceur A, Delacour J. A new one-trial test for neurobiological studies of memory in rats. 1: Behavioral data. *Behav Brain Res* 1988; **31**(1): 47-59.
25. Bofill-De Ros X, Yang A, Gu S. IsomiRs: Expanding the miRNA repression toolbox beyond the seed. *Biochim Biophys Acta Gene Regul Mech* 2019: 194373.
26. Nemeth K, Darvasi O, Liko I, et al. Comprehensive analysis of circulating microRNAs in plasma of patients with pituitary adenomas. *J Clin Endocrinol Metab* 2019.

27. Rajman M, Metge F, Fiore R, et al. A microRNA-129-5p/Rbfox crosstalk coordinates homeostatic downscaling of excitatory synapses. *EMBO J* 2017; **36**(12): 1770-87.
28. Korotkov A, Mills JD, Gorter JA, van Vliet EA, Aronica E. Systematic review and meta-analysis of differentially expressed miRNAs in experimental and human temporal lobe epilepsy. *Sci Rep* 2017; **7**(1): 11592.
29. Srivastava PK, Roncon P, Lukasiuk K, et al. Meta-Analysis of MicroRNAs Dysregulated in the Hippocampal Dentate Gyrus of Animal Models of Epilepsy. *eNeuro* 2017; **4**(6).

Chapter 5: Cell based therapy and neurotrophins

Epilepsy research is not only oriented in a complex system view. More empirical approaches are still applied and a good portion of epilepsy research groups still invest in finding ways to develop anti-epileptogenic or anti-epileptic treatments, targeting well-known pathways. I analysed the effects of two different neurotrophic factors (NTFs), Brain-Derived-Neurotrophic-Factor (BDNF) and Glial-cell line Derived Neurotrophic Factor (GDNF), in reducing spontaneous seizures in a model of TLE [86,87].

NTFs are a family of proteins that have gained strong interest in epilepsy research in the last decade, because of their potential role in many biological processes involved in TLE [88]. However, the study of these molecules must be undertaken carefully because they can exert a double role in epileptogenesis: both good – i.e. contrasting it – or bad – i.e. worsening it. As described in the Introduction, epileptogenesis is characterized by neuronal loss and damage, eventually leading to Hippocampal Sclerosis (HS), that may be both cause or consequence of epileptogenesis; modifications of the circuitry, including mossy fiber sprouting, increased neurogenesis and potentiation of glutamatergic synapses, again cause or consequence of epileptogenesis [20 89 90]. Because NTFs exert an important trophic activity and are involved in stem cells proliferation and differentiation, their study might help identifying therapeutic tools to intervene during epileptogenesis [91].

NTFs divided into three classes of proteins: neurotrophins, glial cell-line derived neurotrophic factors family ligands (GFLs) and neuropoietic cytokines. Among these groups, the best known are the neurotrophins, a family of six proteins: NGF, brain-derived neurotrophic factor (BDNF), and neurotrophins (NT) 3, 4/5, 6 and 7 [92]. Even if they share nearly 50% homology, variability is observed mainly in the N- and C-termini: in particular, the high variability in the N-terminus region has been evaluated as essential to determine receptor binding [93 94] .Neurotrophins can activate different receptors belonging to the high-affinity tropomyosin-receptor kinase (Trk) family and the low-affinity p75 neurotrophin receptor (p75NTR) [95 96] . In addition to the effects mentioned above on neuronal cell survival, axonal and dendritic growth and guidance, they can also regulate neurotransmitter release, differentiation in the developing nervous system and synaptic plasticity.

The GFLs include GDNF, neurturin (NRTN), artemin (ARTN), and persephin (PSPN). They also support the survival and regulate the differentiation of many peripheral and

central neurons, including sympathetic, parasympathetic, sensory, enteric neurons, as well central dopaminergic neurons [97]. GFLs act by binding a receptor complex, consisting of a high affinity glycosylphosphatidylinositol-anchored binding component (GFR1-GFR4) and the receptor tyrosine kinase (RET) [98]. Each GFL binds preferentially to a different GFR receptor type.

We have chosen to test BDNF and GDNF activity because of the emerging literature confirming their role in epilepsy. BDNF was shown to contribute to changes in axons and dendrites leading to a decrease in GABAergic inhibition in a neocortical model of epilepsy. These findings support the idea that BDNF may exert an anti-epileptic effect by interacting with parvalbumin interneurons [99]. GDNF was also shown to exert anti-epileptic effects in a model of chemically-induced SE, since its mRNA (and also mRNA coding its receptor) were found upregulated in granule and pyramidal cells after SE, suggesting the hypothesis that it might play a role in contrasting the hyperexcitability [100]. A proof of this hypothesis was that intraventricular infusion of GDNF suppressed seizures in both the KA-induced model [101] and electrically-induced kindling [102]. Subsequent studies have shown that viral-vector-dependent-delivery of GDNF in the hippocampus of epileptic rodents reduce occurrence of spontaneous seizures [91].

Although BDNF and GDNF are attractive candidates for epilepsy treatment, their delivery into the central nervous system after systemic administration is complicated because they are large proteins that do not cross the blood-brain-barrier. Different strategies have been tested to overcome this problem, in particular the use of viral vectors or invasive surgeries. We employed an innovative technique, the Encapsulated Cells Biodelivery (ECB) system. This technique allows to continuously produce and secrete the NTFs in the hippocampus of epileptic rats. It consists in a device composed of a biocompatible matrix containing engeneered-ARPE19 cells producing the NTF, protected by a semipermeable polymer membrane that allows the exit of BDNF or GDNF in the extracellular environment and the entrance of oxygen and nutrients, while preventing immunologic reactions [103].

Our goal was to demonstrate that BDNF and GDNF have a role in chronic epilepsy, not only in reducing the number of spontaneous seizures, but also in reverting neuronal damage and aberrant neurogenesis. Furthermore, we investigated a possible positive role in reverting epilepsy-associated cognitive and memory impairment.

References

1. Falcicchia C, Paolone G, Emerich DF, et al. Seizure-Suppressant and Neuroprotective Effects of Encapsulated BDNF-Producing Cells in a Rat Model of Temporal Lobe Epilepsy. *Mol Ther Methods Clin Dev* 2018; **9**: 211-24.
2. Paolone G, Falcicchia C, Lovisari F, et al. Long-Term, Targeted Delivery of GDNF from Encapsulated Cells Is Neuroprotective and Reduces Seizures in the Pilocarpine Model of Epilepsy. *J Neurosci* 2019; **39**(11): 2144-56.
3. Simonato M, Tongiorgi E, Kokaia M. Angels and demons: neurotrophic factors and epilepsy. *Trends Pharmacol Sci* 2006; **27**(12): 631-8.
4. Pitkanen A, Sutula TP. Is epilepsy a progressive disorder? Prospects for new therapeutic approaches in temporal-lobe epilepsy. *Lancet Neurol* 2002; **1**(3): 173-81.
5. Sutula TP, Hermann B. Progression in mesial temporal lobe epilepsy. *Ann Neurol* 1999; **45**(5): 553-6.
6. Parent JM, Yu TW, Leibowitz RT, Geschwind DH, Sloviter RS, Lowenstein DH. Dentate granule cell neurogenesis is increased by seizures and contributes to aberrant network reorganization in the adult rat hippocampus. *J Neurosci* 1997; **17**(10): 3727-38.
7. Simonato M, Zucchini S. Are the neurotrophic factors a suitable therapeutic target for the prevention of epileptogenesis? *Epilepsia* 2010; **51 Suppl 3**: 48-51.
8. Gotz R, Koster R, Winkler C, et al. Neurotrophin-6 is a new member of the nerve growth factor family. *Nature* 1994; **372**(6503): 266-9.
9. Kullander K, Carlson B, Hallbook F. Molecular phylogeny and evolution ofthe neurotrophins from monotremes and marsupials. *J Mol Evol* 1997; **45**(3): 311-21.
10. Mowla SJ, Farhadi HF, Pareek S, et al. Biosynthesis and post-translational processing of the precursor to brain-derived neurotrophic factor. *J Biol Chem* 2001; **276**(16): 12660-6.
11. Curtis R, Adryan KM, Stark JL, et al. Differential role of the low affinity neurotrophin receptor (p75) in retrograde axonal transport of the neurotrophins. *Neuron* 1995; **14**(6): 1201-11.
12. Binder DK, Scharfman HE. Brain-derived neurotrophic factor. *Growth Factors* 2004; **22**(3): 123-31.
13. Sariola H, Saarma M. Novel functions and signalling pathways for GDNF. *J Cell Sci* 2003; **116**(Pt 19): 3855-62.
14. Baloh RH, Enomoto H, Johnson EM, Jr., Milbrandt J. The GDNF family ligands and receptors - implications for neural development. *Curr Opin Neurobiol* 2000; **10**(1): 103-10.
15. Gu F, Parada I, Shen F, et al. Structural alterations in fast-spiking GABAergic interneurons in a model of posttraumatic neocortical epileptogenesis. *Neurobiol Dis* 2017; **108**: 100-14.
16. Kokaia Z, Airaksinen MS, Nanobashvili A, et al. GDNF family ligands and receptors are differentially regulated after brain insults in the rat. *Eur J Neurosci* 1999; **11**(4): 1202-16.
17. Martin D, Miller G, Rosendahl M, Russell DA. Potent inhibitory effects of glial derived neurotrophic factor against kainic acid mediated seizures in the rat. *Brain Res* 1995; **683**(2): 172-8.
18. Li S, Xu B, Martin D, Racine RJ, Fahnestock M. Glial cell line-derived neurotrophic factor modulates kindling and activation-induced sprouting in hippocampus of adult rats. *Exp Neurol* 2002; **178**(1): 49-58.

19. Emerich DF, Orive G, Thanos C, Tornoe J, Wahlberg LU. Encapsulated cell therapy for neurodegenerative diseases: from promise to product. *Adv Drug Deliv Rev* 2014; **67-68**: 131-41.

Molecular Therapy
Methods & Clinical Development
Original Article

Seizure-Suppressant and Neuroprotective Effects of Encapsulated BDNF-Producing Cells in a Rat Model of Temporal Lobe Epilepsy

Chiara Falcicchia,[1,2] Giovanna Paolone,[1,2] Dwaine F. Emerich,[2] Francesca Lovisari,[1] William J. Bell,[2] Tracie Fradet,[2] Lars U. Wahlberg,[2] and Michele Simonato[1,3]

[1]Department of Medical Science, Section of Pharmacology, Neuroscience Center, University of Ferrara and National Institute of Neuroscience, Ferrara, Italy; [2]NsGene Inc., Providence, RI, USA; [3]School of Medicine, University Vita-Salute San Raffaele, Milan, Italy

Brain-derived neurotrophic factor (BDNF) may represent a therapeutic for chronic epilepsy, but evaluating its potential is complicated by difficulties in its delivery to the brain. Here, we describe the effects on epileptic seizures of encapsulated cell biodelivery (ECB) devices filled with genetically modified human cells engineered to release BDNF. These devices, implanted into the hippocampus of pilocarpine-treated rats, highly decreased the frequency of spontaneous seizures by more than 80%. These benefits were associated with improved cognitive performance, as epileptic rats treated with BDNF performed significantly better on a novel object recognition test. Importantly, long-term BDNF delivery did not alter normal behaviors such as general activity or sleep/wake patterns. Detailed immunohistochemical analyses revealed that the neurological benefits of BDNF were associated with several anatomical changes, including reduction in degenerating cells and normalization of hippocampal volume, neuronal counts (including parvalbumin-positive interneurons), and neurogenesis. In conclusion, the present data suggest that BDNF, when continuously released in the epileptic hippocampus, reduces the frequency of generalized seizures, improves cognitive performance, and reverts many histological alterations associated with chronic epilepsy. Thus, ECB device-mediated long-term supplementation of BDNF in the epileptic tissue may represent a valid therapeutic strategy against epilepsy and some of its comorbidities.

INTRODUCTION

Because one-third of the epilepsies are refractory to medical treatment, it is highly important that new therapies with novel mechanisms of action are developed.[1] Neurotrophic factors like brain-derived neurotrophic factor (BDNF) represent interesting therapeutic candidates, because an extensive literature demonstrates their involvement in the cellular alterations observed in the epileptic tissue. In fact, the trophic effects of BDNF suggest an involvement in cell death, neurogenesis, and axonal sprouting; in addition, BDNF exerts effects at the synaptic level, with distinct modulatory actions at excitatory and inhibitory synapses.[2] Moreover, an important function of BDNF includes the control of short- and long-lasting synaptic interactions that influence memory and cognition.[3] With specific reference to chronic epilepsy, electrophysiological experiments in a model of neocortical epileptogenesis support the notion that reduction in trophic support by BDNF may contribute to regressive changes in axons and dendrites of fast-spiking interneurons and decreased GABAergic inhibition, suggesting that supplying BDNF to the injured brain may reverse structural and functional abnormalities in parvalbumin interneurons and provide an antiepileptic therapy.[4]

The development of BDNF-based therapeutic approaches for epilepsy, however, is complicated, because it exerts both beneficial and deleterious effects in models of epilepsy.[2] These variable results may depend on multiple factors, including the period of BDNF therapy in the natural history of the disease; specific alterations in some of its biological properties including biosynthesis, processing, and subcellular localization, and the method of delivery.[5–7] In particular, the method of delivering BDNF to the brain is a critical issue, given that its optimal effectiveness likely requires a specific targeting of the temporal lobe in a robust and prolonged manner. No traditional small-molecule drug with suitable pharmacokinetics and capability to act as either a selective agonist or antagonist to high-affinity BDNF receptors (the tropomyosin receptor kinase B [TrkB] receptors) has been developed and, in any event, such drugs would not act only in the epileptogenic region but throughout the brain, with risk of unwanted side effects. Other delivery strategies, based on cell grafts or viral vectors, may only provide a relatively short-term treatment, whereas, by their very nature, chronic diseases like epilepsy require long-term treatments. In addition, cell or gene therapy approaches do not generally offer a reversible strategy after inoculation in case of undesired effects.

Received 20 December 2017; accepted 5 March 2018;
https://doi.org/10.1016/j.omtm.2018.03.001.

Correspondence: Chiara Falcicchia, Department of Medical Sciences, Section of Pharmacology, University of Ferrara, Via Fossato di Mortara 17-19, 44121 Ferrara, Italy.
E-mail: chiara.falcicchia@unife.it

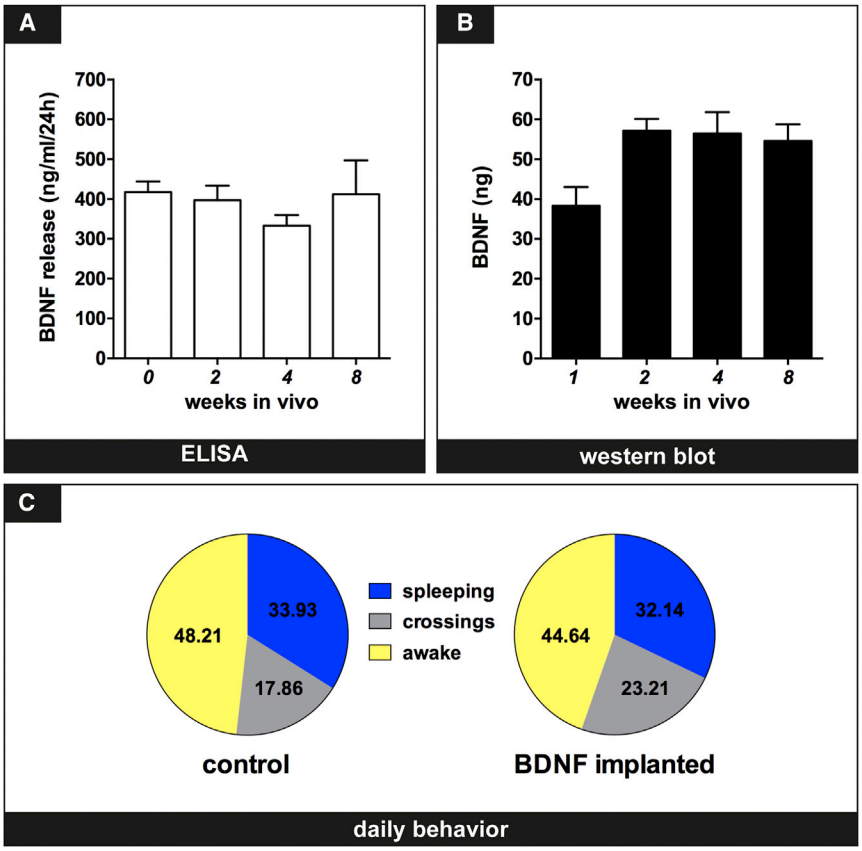

Figure 1. Long-Term BDNF Delivery Does Not Impact General Activity of Naive Rats

(A) BDNF release from devices (as measured using ELISA) prior to implantation and after 2, 4, and 8 weeks *in vivo*. See Materials and Methods for details on experimental design. (B) Levels of BDNF protein in the implanted hippocampus (as measured using ELISA) after 2, 4, and 8 weeks *in vivo*. (C) Daily behavioral activity of naive rats (left) and BDNF-treated rats (right), measured as percentage of the time spent awake, sleeping, or moving (crossings) for 20 min a day over a 24-week period. Data in (A) and (B) are expressed as mean ± SEM of eight devices and hippocampi per group. Data in (C) were obtained from 24 rats per group.

Here, we describe the beneficial effects of encapsulated cell biodelivery (ECB) devices loaded with BDNF-secreting cells and implanted into the hippocampus of pilocarpine-treated rats. In this approach, a human cell line is engineered to secrete BDNF, encapsulated in a biocompatible matrix and kept separated from the adjacent host brain tissue by a thin polymer membrane. The membrane possesses pores that allow BDNF to diffuse into the surrounding tissue and also allow oxygen and nutrients to enter from the surrounding brain to nourish the encapsulated cells. Immunological reactions are obviated because the semipermeable membrane prevents the host immune system from gaining access to cells, thereby preventing their rejection. Not only do ECB devices offer the advantage of long-term, local delivery of BDNF, but they also offer the possibility of easy removal if necessary or desired. We report here that these features were associated with a dramatic reduction of seizures and associated cognitive impairment, as well as normalization of many histological alterations associated with chronic epilepsy. These data provide support for continuing the development of this approach as a potential treatment for drug-resistant patients affected by focal epilepsy.

RESULTS

Long-Term BDNF Secretion and Tissue Levels of BDNF

We first evaluated the potential for long-term delivery of BDNF from encapsulated cells after implantation of ECB devices into the hippocampus of naive rats. Devices were assessed for BDNF output both before implantation and following retrieval after 2, 4, or 8 weeks *in vivo*. The implanted devices were easily retrieved from the brain with no host tissue adhering to the capsule wall. All capsules remained intact, with no evidence that any capsule broke either during implantation, while *in situ* or during the retrieval procedure. As described in the Materials and Methods section, devices were then transferred to culture medium for quantitation of BDNF secretion. As shown in Figure 1A, BDNF levels in the medium (that is, BDNF release capacity) were very stable, ranging from approximately 350–400 ng/device/24 hr at all time points.

This continuous delivery of BDNF to the hippocampus significantly elevated tissue concentrations of BDNF, as determined by ELISA (Figure 1B). Tissue levels of BDNF appeared to increase in the first 2 weeks following implantation and thereafter to remain relatively constant. Parallel studies (data not shown) confirmed that the secretion of BDNF from the devices and the elevated tissue levels of BDNF remained relatively stable for at least 6 months (the longest time period evaluated). Within this time frame, no differences in activity or sleep/wake patterns (Figure 1C) or body weight were found between implanted and unimplanted control animals.

Effect on Spontaneous Seizures

A schematic representation of the *in vivo* experiments is shown in Figure 2. All animals were continuously video monitored between day 10 and day 20 after status epilepticus (SE) (early chronic period) to verify occurrence of spontaneous generalized seizures.[8] Twenty days after SE, at the end of the first monitoring epoch, all animals were randomly assigned to one of four experimental groups: one group was not treated at all (no device), the second group was bilaterally implanted with empty ECB devices, the third group with two devices filled with parental ARPE-19 cells, the last group with ECB

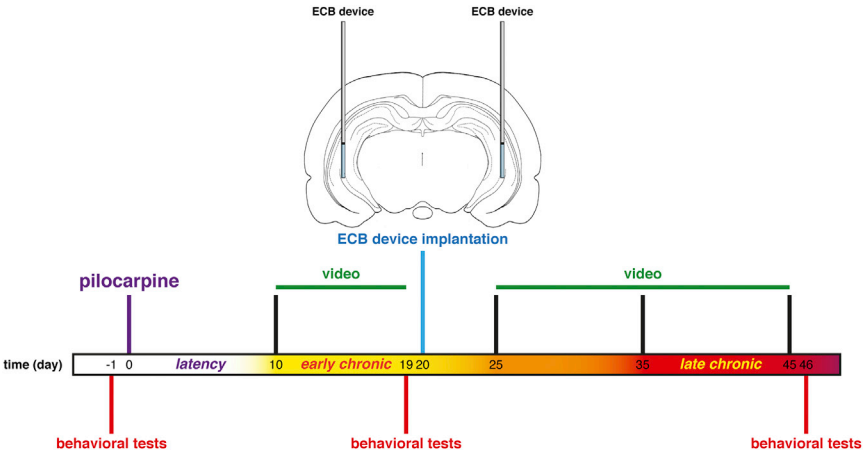

Figure 2. Timeline and Schematic Representation of the *In Vivo* Experiments

The top coronal brain slice illustrates the ECB device implant location. The bottom timeline depicts the sequence of behavioral testing (OF, NOR), video monitoring, and device implantation. In all cases, timing (days) is relative to pilocarpine treatment.

devices filled with ARPE-19-BDNF cells. Randomization was based on seizure frequency.

Surgical implantation did not impact seizure frequency. Between day 25 and 35 after SE, control animals (no device, empty device, or device with parental cells) displayed about three generalized seizures per day (Figure 3A). No difference in any of the parameters analyzed in this study were observed between the no-device and control implant groups, and therefore they were pooled together for statistical analysis and collectively termed the "control" group. In contrast, animals treated with BDNF devices exhibited a marked and significant reduction in seizures, displaying on average less than one seizure per day (Figure 3A). This benefit became even more apparent between days 35 and 45 after SE (late chronic period) as control rats exhibited a progression of the disease with an increased seizure frequency that was not observed in treated animals. In this time frame, treated animals exhibited a 90% reduction in seizure frequency. In contrast, the forelimb clonus duration was only moderately, but not significantly, reduced (Figure 3B).

At the conclusion of video monitoring, devices were removed and BDNF secretion was confirmed. Pilocarpine treatment did not impact device secretion. Before implantation, the average BDNF concentration in the medium was 206 ± 11 ng/24 hr, while after 2 weeks *in vivo* it was increased to 463 ± 43 ng/24 hr incubation (Figure 4A). Moreover, hippocampal levels of human mBDNF were investigated by western blot and expressed as BDNF protein levels relative to recombinant BDNF. Tissue levels of human mBDNF were elevated within hippocampi implanted with the ARPE-19 BDNF cell-loaded device (37.56 ± 4.59 relative BDNF protein level) whereas, as expected, they were negligible in all controls (Figure 4B).

Behavioral Effects

The effects of ECB-released BDNF were further evaluated on behavioral tests. In the open-field test, the control group spent increasing amounts of time in the center of the arena with the progression of the disease. In contrast, the BDNF-implanted animals remained in the center region for significantly shorter times even 46 days after SE, i.e., 4 weeks after the bilateral implant of the ARPE-19 BDNF-filled devices (Figure 5A). Moreover, the control rats displayed a progressively increased number of entries into the central area that was not evident in BDNF-treated animals. This difference became statistically significant in the late chronic period (32 ± 7 versus 18 ± 3 entries to center; Figure 5B). No difference was observed between groups in the distance covered during the test period. In sum, epileptic BDNF-treated animals appeared more "normal" than epileptic controls, because they displayed a behavior indistinguishable from that of naive rats.

Recognition memory was evaluated using the novel object recognition (NOR) test (Figure 6A). As expected, all animals spent more time exploring the novel object during the baseline phase, before the epileptogenic insult (SE). Establishment of an epileptic condition (early chronic phase) was associated with impairment of memory in this test (Figure 6B, yellow bars). However, increased exploration of the novel object (that is, improved memory) was observed in epileptic BDNF-treated rats but not in controls in the late chronic time point ($p < 0.01$; Figure 6B, purple bars). In addition, whereas a decrease in the total interaction time with the objects was observed in control rats from baseline to the early chronic to the late chronic time point, no such progression was observed in BDNF-treated animals (Figure 6C). Together, these findings suggest that the treatment with BDNF significantly improved memory function.

Histology

Neuron Survival and Hippocampal Volume

Neuronal survival was estimated by counting NeuroTrace-positive cells. Quantification of NeuroTrace-positive cells in the hippocampus revealed that pilocarpine-induced epilepsy led to significantly reduced neuronal numbers in the control group (55.2% ± 8.6% compared to naive animals). In contrast, BDNF-treated rats displayed only a modest, non-significant decrease (Figures 7A and 7B). No statistical differences were found between the hippocampi, nor in hippocampal subareas (Table S1), even when ECB devices were implanted unilaterally. In fact, we implanted a subset of epileptic animals in a single hippocampus with the intent of using the contralateral one as an internal control but, unexpectedly, all histological examinations described in this section (not only NeuroTrace) underwent identical changes in both the implanted and the non-implanted hippocampus.

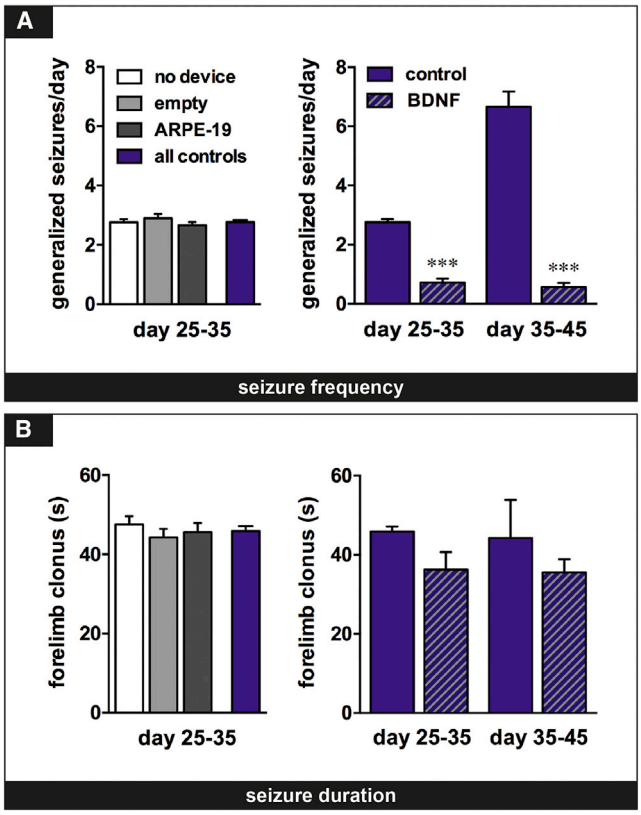

Figure 3. BDNF-Secreting Devices Reduce Frequency of Spontaneous Seizures

(A) Average daily frequency of spontaneous generalized seizures (class 4 or 5) in the chronic period (25–35 days after pilocarpine/SE and 5 days after device implantation) and in the late chronic period (35–45 days after SE). Controls received either no device, empty devices, or devices loaded with non-modified parental cells. To facilitate graphical and statistical representation, the controls were combined into a single control group. Interaction $F(1,18) = 47.74$; treatment $F(1,18) = 223.90$; time $F(1,18) = 41.08$. ***$p < 0.001$ versus control; two-way ANOVA and Sidak post-hoc test. (B) Average daily forelimb clonus duration of spontaneous generalized seizures in the chronic and late chronic period expressed in seconds. Data are expressed as mean ± SEM of 10 animals per group.

A pronounced hippocampal atrophy was observed in control epileptic animals, with a volume reduction of about 30% compared with naive rats. In contrast, no significant change in this parameter was observed after BDNF treatment.

Astrocytosis

Epilepsy-associated astrocytosis was evaluated using GFAP immunofluorescence. The density of GFAP-positive cells in the hippocampus was not altered in chronically epileptic animals, not even after implantation of BDNF devices (Figure 8A). However, whereas many of the GFAP-positive cells in epileptic controls displayed short, thick processes, an indication of active astrocytosis (Figure 8C, inset), GFAP-positive cells of BDNF-treated rats were similar to those of naive animals, with a small cell body and thin processes (compare Figures 8B and 8D insets).

Inhibitory Interneurons

Consistent with previous reports, pilocarpine-induced epilepsy was associated with a significantly reduced number of parvalbumin-positive interneurons in the hippocampus (Figure 9A; 49.8% ± 1.5% as compared with naive). BDNF treatment partially reverted this loss, parvalbumin-positive cells being 77.9% ± 4.6% of those found in naive hippocampi. This effect was especially prominent in the dentate gyrus (Table S2).

Neurodegeneration and Neurogenesis

BDNF-induced reversal of neuronal death may depend on reduction of continued, ongoing neurodegeneration in the chronically epileptic brain and/or on induction of neurogenesis. To explore the first possibility, we used Fluoro-Jade C (FJC) staining. FJC identified numerous degenerating cells in CA1, CA3, and in the hilus of the dentate gyrus in control epileptic rats (Figures 10A and 10C), while a very limited number of FJC-positive cells were observed after BDNF treatment (Figures 10A and 10D). Similar results were obtained analyzing the entire hippocampus or the single subareas (Table S3).

To evaluate neurogenesis, we counted doublecortin (DCX)-positive cells. The effect of the BDNF devices on neurogenesis was remarkable, as shown in Figure 11A. While pilocarpine alone significantly decreased the numbers of DCX-positive cells, this effect was largely reverted by BDNF. An increased number of DCX-positive cells was observed with BDNF especially in the dentate gyrus, where they were almost double the number found in control epileptic animals, which in turn were about 40% of those in naive rats (Figure 11C). Moreover, DCX-positive cells in control epileptic animals did not have elaborate elongations and tended to aggregate into clusters (morphological aspects of aberrant neurogenesis; Figure 11Ab). In contrast, DCX-positive cells in BDNF-treated epileptic hippocampi had more elongations projecting across the granular layer and did not aggregate in clusters (Figure 11Ac).

Target Engagement

Finally, we verified that the BDNF treatment with ECB devices could indeed lead to activation of TrkB, the high-affinity BDNF receptors. To do so, we compared the expression of TrkB with that of its phosphorylated (activated) form (p-TrkB^{Y515}) and calculated the ratio between p-TrkB^{Y515} and TrkB in the different conditions (naive, control epileptic, and BDNF-treated epileptic). BDNF-treated epileptic rats exhibited a highly significant increased TrkB^{Y515}/TrkB ratio compared to naive and control epileptic rats (Figure 12C). Similar results were obtained in each hippocampal subarea (Table S4), arguing that the effects observed in this study are likely dependent on TrkB engagement.

DISCUSSION

We show here that intrahippocampal implants of ECB devices secreting BDNF highly significantly decrease the frequency of spontaneous seizures in chronically epileptic rats. Considering that only a subset of spontaneous seizures originate from the hippocampus in the pilocarpine model,[9] this effect may be even greater than reported

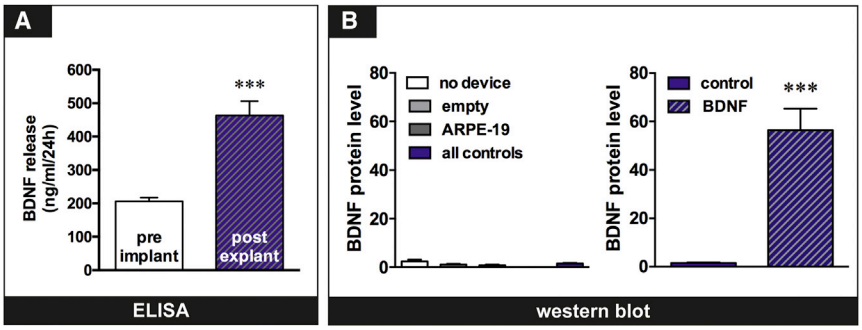

Figure 4. BDNF Release from Devices Explanted from Pilocarpine-Treated Animals

(A) BDNF release (ELISA) from devices explanted after 2 weeks *in vivo*. (B) Concentrations of BDNF protein (western blot) in the hippocampus. The mature BDNF (mBDNF) signal was normalized to α-actin for quantification. As in Figure 3, controls received either no device, empty devices, or devices loaded with non-modified parental cells devices. Data are expressed as mean ± SEM of 10 animals per group. ***$p < 0.001$ versus control; Mann-Whitney U test.

here. An accurate EEG mapping of electrical seizure activity in multiple brain areas will be needed to clarify this point. In this study, however, we decided to avoid inserting electrodes, because inserting two ECB devices is an invasive procedure for the rat brain, and we did not want to take the risk of altering behavior because of an overload of materials in the brain. In fact, the decrease in seizure frequency associated with dramatic improvements in recognition memory and with normalization of the hippocampal architecture.

BDNF-mediated TrkB activation has been found to exert contrasting effects on seizures, depending on the epilepsy model, the time of administration in the natural history of the experimental disease, and the TrkB activation or inhibition strategy. For example, many studies support a pro-epileptogenic effect of TrkB activation,[10,11] but others suggest an anti-epileptogenic effect of BDNF supplementation.[12,13] More relevant to the present study, i.e., in the chronic epileptic period, BDNF was found to reduce $GABA_A$ receptor desensitization in the human and in the murine epileptic hippocampus[14,15] but, in contrast with these and with the present findings, a herpes simplex vector-mediated supplementation of BDNF in the hippocampus of epileptic rats did not alter spontaneous seizure frequency or severity.[12] However, some major differences exist between this previous report and the present study. First, the BDNF delivery method differed (endogenous cells infected by the vector producing and secreting BDNF versus ECB). Second, in the study by Paradiso et al.,[12] BDNF was expressed together with fibroblast growth factor 2 (FGF-2) by the viral vector. Third, the viral vector induced expression of the transgenes (BDNF and FGF-2) only in the dorsal hippocampi, whereas ECB devices were implanted bilaterally in the ventral hippocampus and likely released BDNF in a wider area. Therefore, an insufficiently broad supplementation of BDNF with the viral vector may have led to an apparent lack of effect.

In the present experimental settings, we also found that BDNF delivery improved the performance in behavioral tests of memory and spontaneous activity. This is an important finding, because cognitive and behavioral abnormalities are the most common and severe co-morbidities of epilepsy,[16] and can greatly reduce the quality of life of patients.[17]

Several studies have shown that spontaneous recurrent seizures seriously affect cognitive ability[17] in animal models of epilepsy. On the other hand, it is also known that hippocampal BDNF is implicated in spatial and recognition memory,[18,19] and that BDNF delivery to the entorhinal cortex prevents learning and memory impairment in rodent and primate models of Alzheimer disease.[20] Our data confirm the involvement of BDNF in memory functions, showing that ECB devices secreting BDNF, when implanted in the hippocampus of chronically epileptic rats, significantly improve recognition memory, reverting the learning and memory deficits of epileptic rats.

Exploratory behavior was tested using the open-field test. Rodents are spontaneously thigmotaxic and prefer the safer and darker periphery of the arena over the central and bright part of the apparatus. In accordance with previous studies,[21,22] we found that epileptic animals spent a progressively increasing amount of time in the aversive central part of the field, indicating a hyperactive and disinhibited state. In contrast, rats implanted with BDNF devices had a behavior indistinguishable from that of naive rats.

All together, these data support a strongly positive effect of ECB-mediated supplementation of BDNF in the epileptic hippocampus. However, a difficult issue to clarify is the genuine BDNF-dependence of the observed effects. Unfortunately, no small molecule TrkB antagonist with suitable pharmacokinetics for peripheral administration is currently available, and the ECB device does not allow practical space for intra-hippocampal injection in the area where it releases BDNF. However, the mature BDNF isoform, binding to the high-affinity TrkB receptor, initiates its dimerization and auto-phosphorylation of intracellular tyrosine residues, which results in formation of phosphorylated-TrkB receptors that activate intracellular signaling cascades.[23] Therefore, to begin to explore the mechanistic basis of our data, we analyzed the activation of TrkB by measuring the ratio of phosphorylated to non-phosphorylated TrkB. We found that TrkB activation was increased in all subareas of the hippocampi implanted with BDNF releasing devices. These data do not directly demonstrate that the observed effects are TrkB dependent, but they do clearly show that the employed procedure leads to target engagement.

What then are the consequences of TrkB receptor activation in the epileptic hippocampus that lead to reduced frequency of seizures and amelioration of co-morbidities? The present data support the idea that neurotrophic effects play a key role. A prevention of further

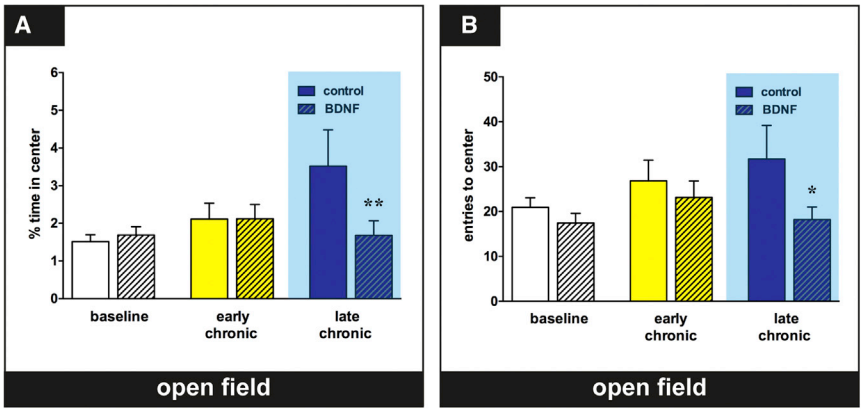

Figure 5. BDNF Normalizes Exploratory Behavior in an Open-Field Test

Shown here are the times spent in the center of an open-field arena (A) and the number of entries into the center of the arena (B) for epileptic control (empty bars) and BDNF-treated rats (hashed bars). Note that animals were not yet holding devices (either control or BDNF) at baseline and in the early chronic period. Because randomization was based on seizure frequency, the two bar types (empty and hashed) are shown also at these time points to show data on animals that will be subsequently allocated in the control or BDNF group. Over time, pilocarpine controls displayed a tendency toward increased time spent in the center and entries in the center (compare empty bars), which was not evident in BDNF-treated animals. Data are expressed as mean ± SEM of 14 or 15 animals/group. Data in (A), but not in (B), were found to be normally distributed based on the D'Agostino-Pearson and the Shapiro-Wilk tests. **$p < 0.01$ versus control; Student's t test for unpaired data. *$p < 0.05$ versus control; Mann-Whitney U test.

damage that is ongoing in this epileptic model, together with an increased neurogenesis (and, in particular, with increased production of GABA cells) may favor a normalization of hippocampal cytoarchitecture and circuitries, including regression of astrocytosis. Although there may be a key basic mechanism that leads to all these positive outcomes, it would be quite difficult to track it down with the currently available tools. An alternative interpretation may be that all of the identified effects are important and combine in a complex and non-linear way to impact the behavior of the neural network. This alternative view is in line with the emerging concept of network neuroscience.[24,25]

The SE-damaged hippocampus exhibits a loss of neuronal cells.[26] We found that, while pilocarpine-induced epilepsy was associated with a dramatic reduction of hippocampal volume, reduction in the total number of neurons (as estimated using NeuroTrace) and continuing neuronal degeneration (as estimated using FJC), all these parameters were attenuated or normalized after ECB-mediated BDNF supplementation. In addition, chronic epilepsy is known to lead to reduced neurogenesis,[27] and in fact we observed that pilocarpine-induced epilepsy resulted in a dramatic decrease in DCX-positive cells. Again, this was reversed by BDNF treatment.

BDNF has been reported to exert a specific role in the development and maturation of GABAergic cells, in particular of parvalbumin-positive interneurons.[28] Indeed, we found that ECB device-mediated BDNF supplementation can lead to a robust increase in the number of parvalbumin-positive cells in the hippocampus, returning them to nearly control levels. Parvalbumin interneurons are known to degenerate in both patients[29] and animal models of temporal lobe epilepsy (TLE)[30–33] recently provided experimental evidence that selective, permanent inhibition of parvalbumin interneurons reduce perisomatic feed-forward inhibition *in vivo*, resulting in a decrease in seizure threshold and the development of spontaneous seizures (i.e., epilepsy). Based on our data, it is intriguing to hypothesize that ECB device-mediated BDNF supplementation can activate neurogenesis to produce (among others) new parvalbumin interneurons that contribute to decreased seizure frequency.

Implantation of BDNF devices did not alter the density of GFAP-positive cells in chronically epileptic rats but normalized their morphology, indicating an attenuation of reactive astrogliosis. Whether this effect is an indirect consequence of the other effects discussed above (i.e., of a general amelioration/normalization of hippocampal cytoarchitecture) or, vice versa, those effects are a consequence of a primary action on astrocytes, remains uncertain. Future studies will be needed to define the precise mechanism of the therapeutic effects of direct BDNF delivery to the hippocampus.

Another interesting observation that deserves further investigation is that all histological benefits were observed in both hemispheres even when the implants were performed unilaterally, suggesting a complex interplay between hemispheres during epilepsy. While the spread of epileptiform activity to the contralateral side is well known in human and experimental epilepsy, the symmetrical amelioration of histological impairments after treatment of a single site is more difficult to explain. Even if it is known that BDNF and other neurotrophic factors can undergo anterograde transport in neurons, thereby potentially reaching distant areas, the existence and precise nature of such mechanisms in the present experimental settings remain a mere hypothesis.

In spite of uncertainties regarding a mechanistic interpretation of the effects downstream target activation, a strength of the present findings is their clinical translatability. These findings demonstrate that ECB devices represent an effective means of exogenous long-term delivery of BDNF to the hippocampus,and that this strategy can reduce the frequency of seizures and the epilepsy comorbidities. The ECB device approach has been developed into a practical, clinically validated means of overcoming the obstacles associated with delivering to the brain molecules that cannot cross the blood-brain barrier.[34] This system has

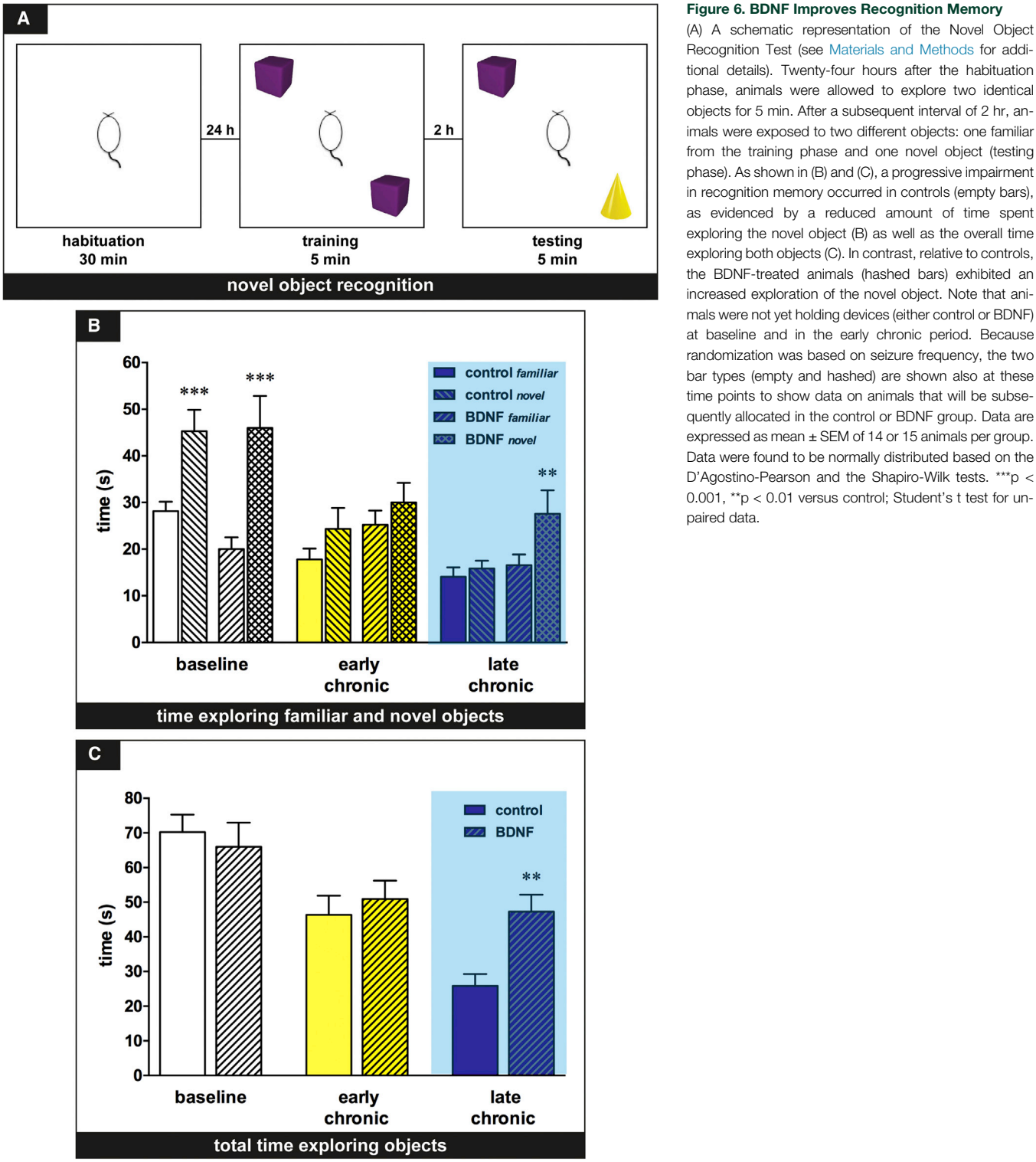

Figure 6. BDNF Improves Recognition Memory

(A) A schematic representation of the Novel Object Recognition Test (see Materials and Methods for additional details). Twenty-four hours after the habituation phase, animals were allowed to explore two identical objects for 5 min. After a subsequent interval of 2 hr, animals were exposed to two different objects: one familiar from the training phase and one novel object (testing phase). As shown in (B) and (C), a progressive impairment in recognition memory occurred in controls (empty bars), as evidenced by a reduced amount of time spent exploring the novel object (B) as well as the overall time exploring both objects (C). In contrast, relative to controls, the BDNF-treated animals (hashed bars) exhibited an increased exploration of the novel object. Note that animals were not yet holding devices (either control or BDNF) at baseline and in the early chronic period. Because randomization was based on seizure frequency, the two bar types (empty and hashed) are shown also at these time points to show data on animals that will be subsequently allocated in the control or BDNF group. Data are expressed as mean ± SEM of 14 or 15 animals per group. Data were found to be normally distributed based on the D'Agostino-Pearson and the Shapiro-Wilk tests. ***$p < 0.001$, **$p < 0.01$ versus control; Student's t test for unpaired data.

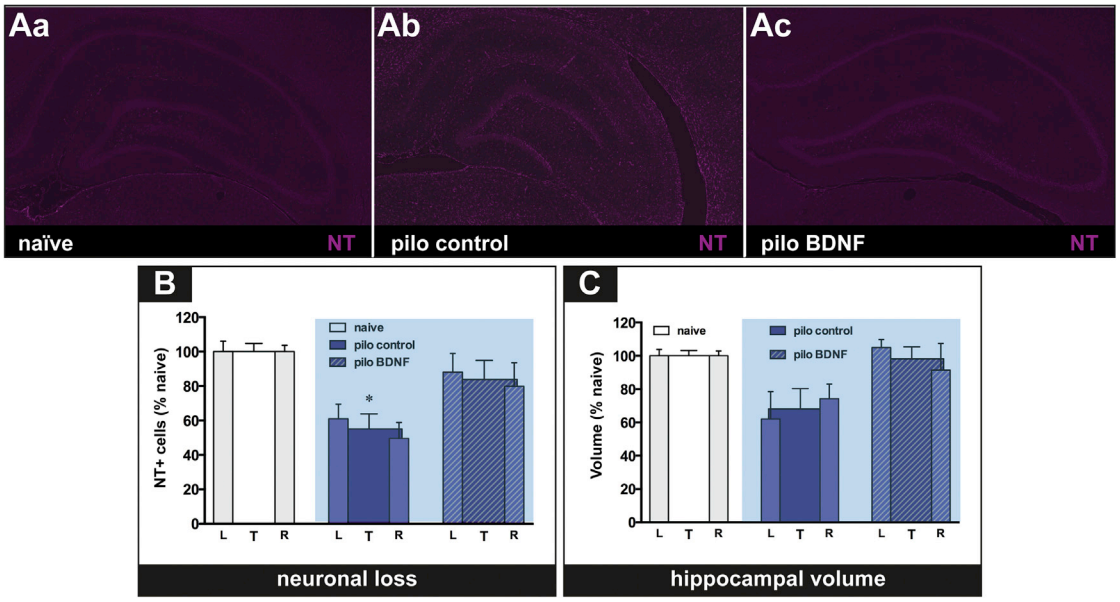

Figure 7. BDNF Treatment Reduces Hippocampal Atrophy and Neuronal Cell Loss

(A) Representative hippocampal sections stained for NeuroTrace from naive rats (a), control epileptic rats (b), and BDNF-treated epileptic rats (c) illustrates pronounced neuronal cell loss and hippocampal atrophy in control epileptic, but not in BDNF-treated epileptic rats. (B) Quantification of the NeuroTrace-positive cells confirmed this observation in both hemispheres. While the control group exhibited a 44.8% loss of cells, the BDNF-treated animals showed only a 16.1% loss. (C) The normalization of neuron numbers was associated with a normalization of the overall hippocampal volume, as control epileptic rats exhibited a 28.6% volume reduction, whereas the BDNF-treated animals did not show any change in hippocampal volume. Data are expressed as mean ± SEM percentage of naive animals obtained from a total of five animals/group. L, left hippocampus; R, right hippocampus; and T, total (both hippocampi combined). **$p < 0.01$ versus naive; ANOVA and post-hoc Dunnett test.

already been tested for safety in large animal models and, most importantly, has been tested clinically in Alzheimer patients using NGF-secreting cells. In this clinical study, up to four devices were well tolerated when implanted bilaterally into the cholinergic basal forebrain and then easily and safely retrieved intact 12 months later.[35,36]

Several other aspects of the present findings are worthy of note with regard to human translation. First, the implantation of ECB devices was performed under conditions that reproduce the clinical situation: chronic patients with surgically treatable TLE. Patients who planned to undergo a two-step surgery may be an ideal population to clinically test this approach because the ECB device could be implanted together with recording electrodes and, should it prove ineffective, it could be removed and the patient would undergo surgery as originally planned. The use of conventional stereotactic procedures for ECB implantation inherently provides a means of selectively targeting those areas of the brain where BDNF will be therapeutic, while reducing exposure of other anatomical regions of the brain where it could produce side effects. Because multiple implants can be used within the same target region, it is possible to achieve far greater spread of protein throughout the targeted region than can be achieved with crude infusion of protein.

In conclusion, the present data suggest that BDNF, continuously released in the epileptic hippocampus, reduces the frequency of generalized seizures and improves co-morbidities while producing a robust neuroprotective effect. This approach may be directly applicable to patients that are selected for surgical resection of the epileptic hippocampus and are undergoing implantation of depth electrodes to define the epileptogenic area before respective surgery. ECB device(s) may be implanted together with these electrodes: if ineffective, they would be removed and the patient would undergo surgery as originally planned; if effective, the patient would have the option of avoiding surgery.

MATERIALS AND METHODS

Cells and Devices

Cell Culture

ARPE-19 cells, a spontaneously immortalized human retinal pigment epithelial cell line, were cultured using standard plating and passaging procedures in T-175 flasks with growth medium; DMEM + glutamax (1×) supplemented with 10% fetal bovine serum (Gibco). Routine culture consisted of feeding the cells every 2–3 days and passaging them at 70%–75% confluence. Cells were incubated at 37°C, 90% humidity, and 5% CO_2.

Human BDNF-Secreting Cell Line Establishment

We generated clonal BDNF-secreting ARPE-19 cell lines using the sleeping beauty (SB) transposon expression system, as described elsewhere.[37] In brief, ARPE-19 cells were co-transfected with the plasmid pT2.CAn.hopp.BDNF, containing the entire pre-pro BDNF sequence, and the SB vector pCMV-SB-100x. Clones were selected using G418 (Sigma-Aldrich, Germany), and cells were isolated and

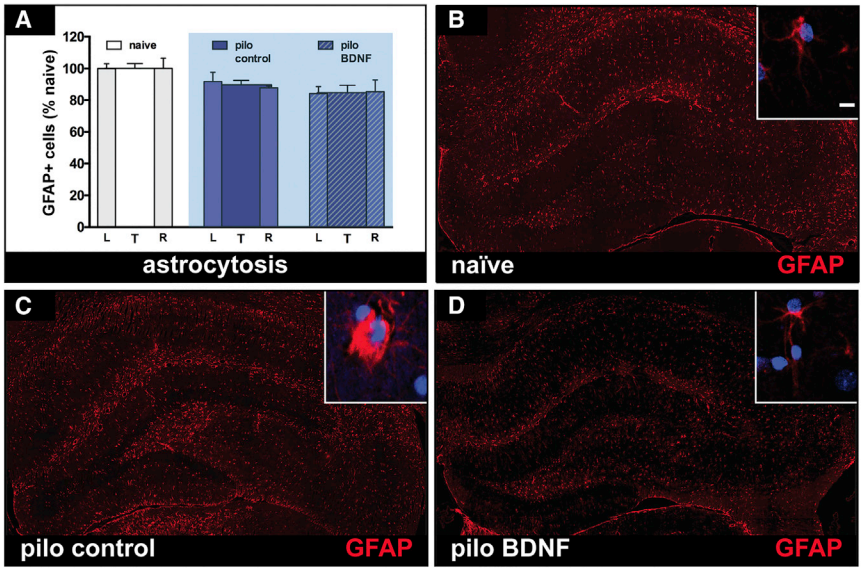

Figure 8. Effects on Astrocytosis

(A) GFAP-positive cells in the hippocampus of naive, epileptic control, and BDNF-treated epileptic rats. While no significant changes in the total number of GFAP-positive cells were found following either pilocarpine alone or pilocarpine + BDNF, clear qualitative differences were apparent (higher magnification insets). Numerous GFAP-positive cells in control epileptic animals (C) displayed short, thick processes, while the cells of BDNF-treated rats (D) were notably similar to those of the naive group (B) with a small cell body and long, thin processes. Nuclei were counterstained using DAPI (blue). Horizontal bar: 10 μm. Data are expressed as mean ± SEM of five animals per group. L, left hippocampus; R, right hippocampus; and T, total (both hippocampi combined).

expanded based on their BDNF release levels. Clonal cell lines producing high and stable levels of BDNF were further characterized *in vitro* and *in vivo* in ECB devices and the BDNF clone used in the experiments was selected based on high BDNF secretion and long-term function in ECB devices *in vivo*.

Encapsulation of Cells in the ECB Device

Devices for cell culture experiments were built as follows: 7-mm-long semipermeable polysulfone hollow fibers (NsGene, USA), with an inner diameter of approximately 500 μm, were internally fitted with filaments of polyethylene terephthalate yarn scaffolding for cell adhesion. Prior to filling, ARPE-19-BDNF cells were cultured in growth medium. Prior to encapsulation, cells were dissociated and suspended in human endothelial serum-free medium (HE-SFM; Invitrogen) at a density of 100,000 cells/μL. Five microliters of cell solution (5×10^4 cells in total) were injected into each device using a custom manufactured automated cell-loading system. Devices were kept in HE-SFM at 37°C and 5% CO_2 for 2–3 weeks prior to surgical implantation. Devices loaded with non-modified ARPE-19 cells or without cells were treated in the same manner and included as negative controls.

These cells replicate until contact inhibited and remain stable thereafter. They do not have tumorigenic potential *in vivo* when injected naked into the brain. Membrane and cell scaffolds were prepared under rigorous, well-controlled manufacturing processes, and all the devices were removed at the end of the experiments and proved to be intact.

BDNF Release In Vitro

The amount of BDNF released by each capsule over a 24-hr period in HE-SFM was measured using the Human BDNF Quantikine ELISA Kit (R&D systems, Minneapolis, USA). Standards and samples were assayed in duplicate according to the manufacturer instructions, and results were expressed in ng/24 hr.

BDNF Release In Vivo

Following device removal, the left and right hippocampi were dissected and processed to extract total RNA, genomic DNA, and proteins using the RNeasy Lipid Tissue Mini Kit (QIAGEN, Germany). RNA extraction was performed following the manufacturer instructions. Proteins and genomic DNA were isolated after RNA extraction using the phenol phase. In brief, genomic DNA was precipitated from the phenol phase with ethanol, and pellets were washed with sodium citrate ethanol solution and stored in 75% ethanol at −80°C. After DNA precipitation, proteins were isolated from the supernatant ethanol-phenol by isopropanol precipitation. Proteins were then washed several times with 0.3 M guanidine HCl-95% ethanol solution before being air-dried and resuspended in a rehydration buffer (62 mM Tris-HCl [pH 6.8], 2% SDS, 10% glycerol, 12.5 mM EDTA, 50 mM DTT, β-mercaptoethanol, protease inhibitor cocktail) by a 20 min incubation at 95°C and three rounds of 30 s sonication.

Proteins were quantified using the Bradford method using the Bio-Rad protein assay kit (Bio-Rad Laboratories, CA, USA) and a biospectrometer (Eppendorf, Germany) and then analyzed by western blotting. Protein samples (2 μg) were diluted in SDS-gel loading buffer, boiled for 10 min, and centrifuged before loading. Samples were then electrophoretically separated onto a 12% SDS-PAGE and transferred to nitrocellulose membranes. After blocking in a buffer (PBS-Tween 20) containing 5% dried milk, membranes were incubated with the primary antibody in another buffer containing 2.5% dried milk overnight at 4°C. After three washings, incubations were performed with the secondary antibody in buffer/dried milk at room temperature for 1 hr. The mature BDNF protein was revealed using a polyclonal chicken anti-hBDNF antibody (Promega, WI, USA; dilution 1:500) and actin using a rabbit anti-actin monoclonal antibody (Sigma, MO, USA; 1:1,000). The chicken polyclonal antibody was revealed using a rabbit anti-chicken horseradish peroxidase (HRP)-conjugated secondary antibody (Dako, Denmark; dilution 1:1,250) and the rabbit monoclonal antibody by a swine anti-rabbit HRP-conjugated secondary antibody (Dako; dilution 1:3,000). The

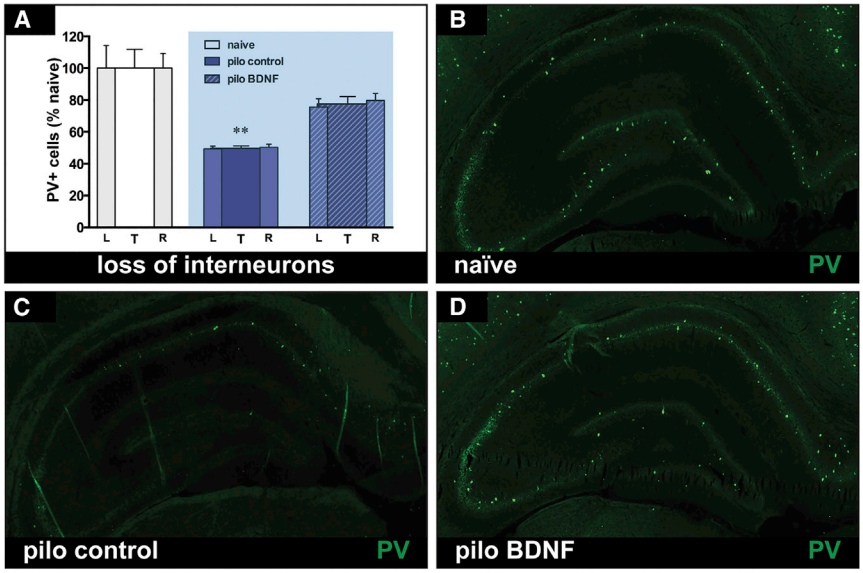

Figure 9. BDNF Preserves Hippocampal Parvalbumin Interneurons

(A) Quantification of parvalbumin-positive cells in the hippocampus of naive, control epileptic, and BDNF-treated epileptic rats. While pilocarpine significantly reduced the numbers of parvalbumin cells throughput the hippocampus (A and C) relative to naive controls (B), BDNF treatment substantially reversed this pathological effect (A and D). While the control epileptic group exhibited a 50.3% loss of cells, BDNF-treated animals displayed only a 22.5% loss. Data are expressed as mean ± SEM percentage of naive animals and were obtained from five animals/group. L, left hippocampus; R, right hippocampus; and T, total (both hippocampi combined). ***$p < 0.001$ versus naive; ANOVA and post-hoc Dunnett test.

immunocomplexes were detected using the ECL western blot detection kit (GE Healthcare, NJ, USA) and ChemiDoc XRS (Bio-Rad) for electronic blot pictures. Quantification was performed using the Image Lab software (Bio-Rad).

Animals

A total of 78 animals were employed in this study. Male Sprague-Dawley rats (250–350 g; Harlan, USA) were used for all experiments. The experiments involving animals were conducted in accordance with European Community (EU Directive 2010/63/EU) and national and local laws and policies. The IACUC of the University of Ferrara approved this research that was authorized by the Italian Ministry for Heath (D.M. 246/2012-B). The ARRIVE (Animal Research: Reporting *In Vivo* Experiments), the NC3Rs (National Centre for the Replacement, Refinement and Reduction of Animal Research), and the National Institutes of Health guidelines were followed.[38,39] Animals were housed under standard conditions: constant temperature (22°C–24°C) and humidity (55%–65%), 12 hr light/dark cycle, free access to food and water.

Long-Term BDNF Secretion

Separate sets of naive animals (n = 16) were used to verify the long-term, continued secretion of BDNF. Devices were bilaterally implanted into the hippocampus, as described below, removed 1, 2, 4, and 8 weeks post-implant, and immediately incubated at 37°C in HE-SFM prior to measuring BDNF levels using ELISA.

Immediately after device removal, the previously implanted hippocampi were dissected, placed in 1 mL of Tissue Protein Extraction Reagent (T-PER; Thermo Scientific, Rockford, IL, USA), and flash frozen in liquid nitrogen. For ELISA analysis, samples were thawed and placed in 1.5 mL tissue protein extraction reagent (T-PER) plus 0.5 mL of a modified buffer[40] containing 100 mM Tris-HCL (pH 7.2), 400 mM NaCl, 4 mM EDTA, 0.05% sodium azide, 0.5% gelatin, 0.2% Triton X-100, 2% BSA, and complete protease inhibitor cocktail (Sigma, P8340). Tissues were homogenized with a polytron for 10 s and supernatants from pulverized and centrifuged tissue samples were assessed for BDNF levels using ELISA.

The same naive animals implanted with BDNF-secreting devices were monitored over the implant period for alterations in body weights and general activity, as rated by a blind observer using the Ellinwood and Balster[41] behavioral rating scale.

Pilocarpine Treatment

Pilocarpine was administered intraperitoneally (i.p.) (340 mg/kg), 30 min after a single subcutaneous injection of methyl-scopolamine (1 mg/kg, to prevent peripheral effects of pilocarpine), and the rats' behavior was monitored for several hours thereafter, using the scale of Racine:[8] (1), chewing or mouth and facial movements; (2), head nodding; (3), forelimb clonus; (4), generalized seizures with rearing; (5), generalized seizures with rearing and falling. Within the first hour after injection, all animals developed seizures evolving into recurrent generalized (stage 4 and higher) convulsions (SE). SE was interrupted 2 hr after onset by administration of diazepam (10 mg/kg, i.p.). All animals began experiencing spontaneous behavioral seizures 10 ± 1 days after SE.

Surgery

In all efficacy studies, surgery for ECB device implantation was performed 20 days after SE (Figure 2), between two video monitoring sessions (as described below). Rats were anaesthetized using isoflurane (3%–4%) and positioned in a stereotaxic frame (Stoelting, Dublin, Ireland). A midline incision was made in the scalp, and two bilateral holes were drilled through the skull. Devices filled with ARPE-19 BDNF cell (n = 20), filled with non-modified ARPE-19 cells (n = 20) and empty devices (n = 20) were bilaterally implanted in hippocampus in a vertical position using a cannula mounted to the stereotaxic frame. The implantation coordinates, with respect

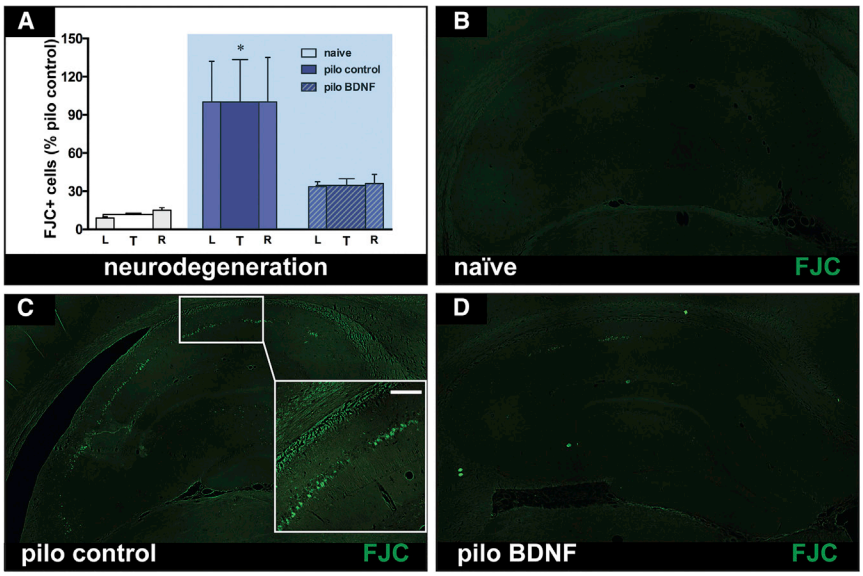

Figure 10. BDNF Reduces Ongoing Neuronal Degeneration

Quantitative analysis of Fluoro-Jade C (FJC)-positive cells (A) revealed that the numbers of degenerating cells were highly increased in epileptic controls (C) but not in the BDNF-treated animals (D) and naive animals (B). Data are expressed as mean ± SEM percentage of naive animals and were obtained from five animals/group. L, left hippocampus; R, right hippocampus; and T, total (both hippocampi combined). *$p < 0.05$ versus naive; ANOVA and post-hoc Dunnett test. Scale bar in (C) inset, 150 μm.

to bregma, were as follows: AP, −4.8; ML, ±4.6; and DV, −7.0. A subset of epileptic rats was unilaterally implanted with devices filled with ARPE-19 BDNF cells (n = 5) for histological analyses. After implantation, the skin was sutured closed. Continued secretion of BDNF was verified at the end of all experiments. Devices were removed by placing the anesthetized animal into the stereotactic frame, visualizing the proximal tip of the implant and gently removing it using microforceps. Devices were immediately incubated at 37°C in HE-SFM prior to processing for BDNF levels using ELISA.

Video Monitoring

Video monitoring was performed using a Swann 4 channel system (Swann, Santa Fe Springs, California USA). The first video-monitoring session was between day 10 and day 20 after SE (Figure 2), when animals began experiencing spontaneous seizures.[12] The second video-monitoring session was after implantation of the ECB devices, between days 25 and 45 after SE. Seizure severity was scored using the scale of Racine[8] by investigators that were blind of the treatment administered to the different rats.

Open-Field Test

Rats were placed for 30 min in an open-field arena measuring 75 cm in length, 75 cm in width, and 45 cm in height. The whole area was divided into 36 squares of 12.5 × 12.5 cm by black lines and the four central squares (25 cm from the walls) were defined as the central area. Each rat was placed at the center of the apparatus and, using the ANY Maze video software, we counted the total number of crossings in the central area and measured the time (in seconds) spent in the center of the arena by each rat over 30 min. The test was repeated at three different time points: baseline (1 day before pilocapine-induced SE), at the end of early chronic period (i.e., before surgery, at day 19 after SE), and at the end of late chronic period; 46 days after SE (Figure 2). The apparatus was cleaned with 5% ethanol between each animal testing.

Novel Object Recognition Test

The novel object recognition test (NOR) was used to assess recognition memory at three different time points, as above (Figure 2). The open-field squared box was used. NOR testing consisted of three parts: habituation, training/object familiarization, and novel object recognition testing, which were recorded using a video camera placed above the box. All objects and the open-field box were cleaned with 5% ethanol between each rat testing. During the habituation session, rats were placed in the empty arena, in the absence of objects, and allowed to move freely and explore the environment. On the next day, rats were put in the arena containing two identical objects and the total time spent exploring each object was recorded for 5 min. Then, after a 2-hr interval, animals were returned to the apparatus with a familiar and a novel object. Object recognition was assessed as more time spent interacting with the novel rather than the familiar object.

All behavioral testing was performed only if no spontaneous seizures were observed for at least 2 hr before the test; if seizures occurred during this pre-test period, the rat was placed back into its home cage and the trial was repeated after 2 hr.

Histology

Immunohistochemistry

Brains were rapidly removed, immersed in 10% formalin, and paraffin embedded after 48 hr. Coronal sections (8 μm thick) were cut with a Microtome (Leica RM2125RT, Germany) across the entire hippocampus, and mounted onto polarized slides (Superfrost slides, Diapath). One section every 500 μm was used for each stain. These sections were dewaxed (two washes in xylol for 10 min, 5 min in ethanol 100%, 5 min in ethanol 95%, 5 min in ethanol 80%) and re-hydrated in distilled water for 5 min. All antigens were unmasked using a commercially available kit (Unmasker, Dia-path), according to the manufacturer's instructions. After washing in PBS, sections were incubated with Triton x-100 (Sigma; 0.3% in 1× PBS, room temperature, 10 min), washed twice in 1× PBS, and incubated

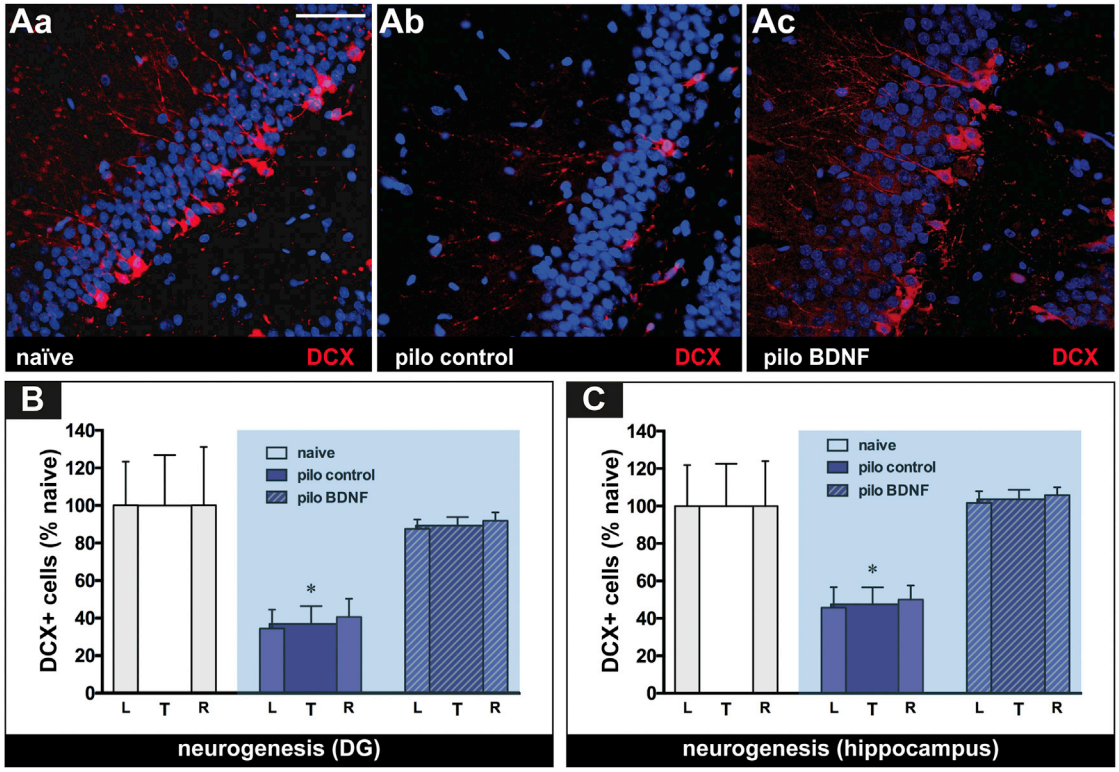

Figure 11. BDNF Normalizes Hippocampal Neurogenesis

Pilocarpine significantly reduced the numbers of doublecortin-positive (DCX) cells in the dentate gyrus and hippocampus (Ab, B, and C) relative to naive animals. When quantified, this effect manifested as a loss of, respectively, 63.0% and 52.4% in the dentate gyrus and in the whole hippocampus of epileptic controls versus naive animals. In contrast, the loss was only 10.6% in the dentate gyrus, and no loss in the whole hippocampus of BDNF-treated rats. The benefits of BDNF were also apparent on qualitative morphological observation, with the DCX-positive cells of BDNF-treated animals having a normal morphology (Ac), in contrast with those of epileptic controls (Ab). Data are expressed as mean ± SEM percentage of naive animals and were obtained from five animals/group. L, left hippocampus; R, right hippocampus; and T, total (both hippocampi combined). *$p < 0.05$ versus naive; ANOVA and post-hoc Dunnett test. Immunofluorescence (dentate gyrus) for DCX is shown in red with nuclei labeled in blue with DAPI. Scale bar in (Aa), 75 μm.

with 5% BSA and 5% serum of the species in which the secondary antibody was produced, for 30 min. Sections were incubated overnight at 4°C in a humid atmosphere with a primary antibody specific for different cellular markers: glial fibrillaryacid protein (GFAP; mouse polyclonal, Sigma) 1:100; DCX (rabbit polyclonal, Cell Signaling, MA, USA) 1:400; parvalbumin (mouse monoclonal, Swant, Switzerland) 1:100; TrkB (rabbit polyclonal, Santa Cruz) 1:50; phosphor Y515-TrkB (rabbit polyclonal, AbCam) 1:100. After 5-min rinses in PBS, sections were incubated with Triton (as above, 30 min), washed in PBS, and incubated with a goat anti-mouse Alexa 594 or Alexa 488 secondary antibody (1:250, Invitrogen) for mouse primary antibodies, or with a goat anti-rabbit, Alexa 488 or Alexa 594 secondary antibody (1:250; Invitrogen) for rabbit primary antibodies, at room temperature for 3 hr. NeuroTrace (1:250; Invitrogen) was included in the secondary antibody incubation. After staining, sections were washed in PBS, counterstained with 0.0001% DAPI (Santa Cruz, Texas, USA) for 15 min, and washed again. Coverslips were mounted using anti-fading, water-based Gel/Mount (Sigma).

FJC Staining

For FJC (Millipore, Massachusetts, USA) staining, slides were first dewaxed as described above and then immersed for 5 min in a basic alcohol solution consisting of 1% sodium hydroxide in 80% ethanol. They were then rinsed for 2 min in 70% ethanol, for 2 min in distilled water, and then incubated in 0.06% potassium permanganate solution for 10 min. Slides were then transferred for 20 min to a 0.001% solution of FJC followed by three washes in distilled water for 1 min each. Finally, the slides were air dried on a slide warmer at 50°C for 5 min and cleared in xylene for 1 min. Coverslips were mounted using DPX (Sigma) mounting media.

Quantitative Analysis of Histological Staining

All quantifications were performed by two investigators that were blinded to the experimental condition. The analysis included 10 coronal sections cut at 500-μm intervals across the entire hippocampus, between −1.8 mm and −6.3 mm from bregma (Figure S1A; Paxinos[42]). Quantifications of cell numbers were performed in the whole hippocampus and in regions of interest (ROI) corresponding to the

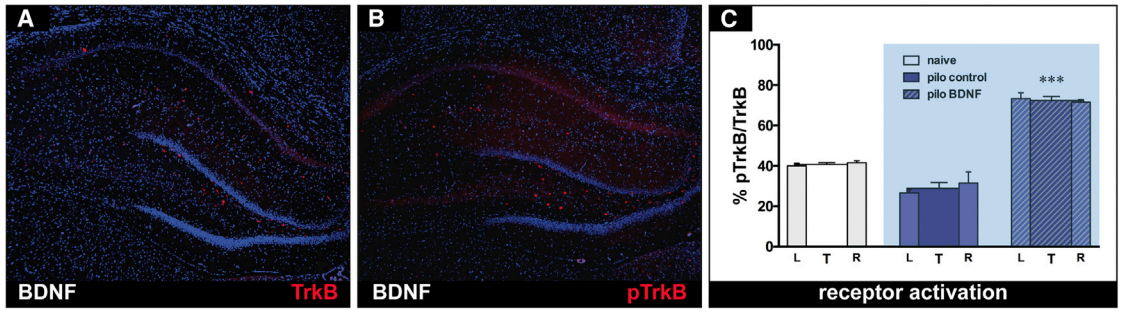

Figure 12. Hippocampal TrkB Is Activated following ECB Device-Mediated BDNF Treatment

Representative sections illustrating immunofluorescence (in red) of TrkB (A) and pTrkB^{Y515} (B). DAPI was used to counterstain nuclei in blue. (C) Percent ratio between phosphorylated and non-phosphorylated TrkB receptors. L, left hippocampus; R, right hippocampus; and T, total (both hippocampi combined). Data are expressed as mean ± SEM of five animals per group. ***$p < 0.001$ versus naive; ANOVA and post-hoc Dunnett test.

various hippocampal subareas (dentate gyrus; CA3; CA1–2), as shown in Figures S1B and S1C. All images were captured using a Leica microscope (DM RA2, Leica), and analyses were performed using the ImageJ software (NIH) and the MetaMorph Image Analysis software, respectively, for cell quantification and for hippocampal volume estimation.

To quantify the cells positive for the different markers (NeuroTrace, Parvalbumin, FJC, DCX, TrkB, and p-TrkB), we employed a method based on the thresholding of each digital image. The 10 full-color images of both hippocampi of each rat were captured using a Leica microscope, and transformed into grayscale. A fixed threshold for each staining was set to allow the software to recognize positive pixels and calculate the number of positive cells based on pre-defined recognition parameters. As stated above, one section every 500 μm across the entire hippocampus was quantified; thus, ten coronal sections regularly spanning 5-mm were examined for each rat. The number of positive cells obtained from the 10 coronal sections was summed to obtain a single estimate for each animal. All analyses were independently performed by two investigators, and the two estimates were averaged to obtain a single number for each animal. Finally, data have been reported as percentage of average cell number in naive rats.

The volume of the hippocampus was calculated using the 10 coronal sections from each rat (from −1.8 mm to −6.3 mm from bregma), stained with DAPI. The hippocampal area in each section was drawn and calculated using the MetaMorph Image Analysis software. The volume of the cone between two progressive sections was then calculated using the Cavalieri's principle. The sum of these values provided an estimation of the hippocampal volume for each rat. Finally, data were expressed as percentage of the average volume in naive rats.

Statistical Analysis

Results were expressed as the mean ± SEM. *In vitro* data (ELISA; western blot) were statistically examined using the non-parametric Mann-Whitney U test. Statistical evaluation for *in vivo* data was performed using two-way ANOVA and post-hoc the Sidak test, the Student's t test for unpaired data, or the Mann-Whitney U test, as appropriate and as indicated in the figure legends. Statistical analysis for histological quantification was conducted using one-way ANOVA and post-hoc the Dunnett test.

SUPPLEMENTAL INFORMATION

Supplemental Information includes one figure and four tables and can be found with this article online at https://doi.org/10.1016/j.omtm.2018.03.001.

AUTHOR CONTRIBUTIONS

C.F., D.F.E., L.U.W., and M.S. conceived and designed the experiments. C.F., F.L., and G.P. performed the experiments. C.F. and M.S. analyzed the data. T.F and W.J.B. contributed reagents/materials/analysis tools. C.F. and M.S. wrote the paper.

ACKNOWLEDGMENTS

This work has been supported by a grant from the European Community (FP7-PEOPLE-2011-IAPP project 285827 [EPIXCHANGE]) to M.S. and L.U.W.

REFERENCES

1. Simonato, M., Brooks-Kayal, A.R., Engel, J., Jr., Galanopoulou, A.S., Jensen, F.E., Moshé, S.L., O'Brien, T.J., Pitkanen, A., Wilcox, K.S., and French, J.A. (2014). The challenge and promise of anti-epileptic therapy development in animal models. Lancet Neurol. *13*, 949–960.

2. Simonato, M., Tongiorgi, E., and Kokaia, M. (2006). Angels and demons: neurotrophic factors and epilepsy. Trends Pharmacol. Sci. *27*, 631–638.

3. Sasi, M., Vignoli, B., Canossa, M., and Blum, R. (2017). Neurobiology of local and intercellular BDNF signaling. Pflugers Arch. *469*, 593–610.

4. Gu, F., Parada, I., Shen, F., Li, J., Bacci, A., Graber, K., Taghavi, R.M., Scalise, K., Schwartzkroin, P., Wenzel, J., and Prince, D.A. (2017). Structural alterations in fast-spiking GABAergic interneurons in a model of posttraumatic neocortical epilepsy. Neurobiol. Dis. *108*, 100–114.

5. Binder, D.K., and Scharfman, H.E. (2004). Brain-derived neurotrophic factor. Growth Factors *22*, 123–131.

6. Tongiorgi, E., Domenici, L., and Simonato, M. (2006). What is the biological significance of BDNF mRNA targeting in the dendrites? Clues from epilepsy and cortical development. Mol. Neurobiol. *33*, 17–32.

7. Greenberg, M.E., Xu, B., Lu, B., and Hempstead, B.L. (2009). New insights in the biology of BDNF synthesis and release: implications in CNS function. J. Neurosci. *29*, 12764–12767.
8. Racine, R.J. (1972). Modification of seizure activity by electrical stimulation. II. Motor seizure. Electroencephalogr. Clin. Neurophysiol. *32*, 281–294.
9. Sloviter, R.S. (2005). The neurobiology of temporal lobe epilepsy: too much information, not enough knowledge. C. R. Biol. *328*, 143–153.
10. Liu, G., Gu, B., He, X.P., Joshi, R.B., Wackerle, H.D., Rodriguiz, R.M., Wetsel, W.C., and McNamara, J.O. (2013). Transient inhibition of TrkB kinase after status epilepticus prevents development of temporal lobe epilepsy. Neuron *79*, 31–38.
11. Gu, B., Huang, Y.Z., He, X.P., Joshi, R.B., Jang, W., and McNamara, J.O. (2015). A peptide uncoupling BDNF receptor TrkB from phospholipase Cγ1 prevents epilepsy induced by status epilepticus. Neuron *88*, 484–491.
12. Paradiso, B., Marconi, P., Zucchini, S., Berto, E., Binaschi, A., Bozac, A., Buzzi, A., Mazzuferi, M., Magri, E., Navarro Mora, G., et al. (2009). Localized delivery of fibroblast growth factor-2 and brain-derived neurotrophic factor reduces spontaneous seizures in an epilepsy model. Proc. Natl. Acad. Sci. USA *106*, 7191–7196.
13. Kuramoto, S., Yasuhara, T., Agari, T., Kondo, A., Jing, M., Kikuchi, Y., Shinko, A., Wakamori, T., Kameda, M., Wang, F., et al. (2011). BDNF-secreting capsule exerts neuroprotective effects on epilepsy model of rats. Brain Res. *1368*, 281–289.
14. Palma, E., Torchia, G., Limatola, C., Trettel, F., Arcella, A., Cantore, G., Di Gennaro, G., Manfredi, M., Esposito, V., Quarato, P.P., et al. (2005). BDNF modulates GABAA receptors microtransplanted from the human epileptic brain to Xenopus oocytes. Proc. Natl. Acad. Sci. USA *102*, 1667–1672.
15. Palma, E., Roseti, C., Maiolino, F., Fucile, S., Martinello, K., Mazzuferi, M., Aronica, E., Manfredi, M., Esposito, V., Cantore, G., et al. (2007). GABA(A)-current rundown of temporal lobe epilepsy is associated with repetitive activation of GABA(A) "phasic" receptors. Proc. Natl. Acad. Sci. USA *104*, 20944–20948.
16. Hermann, B., Seidenberg, M., and Jones, J. (2008). The neurobehavioural comorbidities of epilepsy: can a natural history be developed? Lancet Neurol. *7*, 151–160.
17. Kleen, J.K., Scott, R.C., Lenck-Santini, P.P., and Holmes, G.L. (2012). Cognitive and behavioral co-morbidities of epilepsy. In Jasper's Basic Mechanisms of the Epilepsies, Fourth Edition, J.L. Noebels, M. Avoli, M.A. Rogawski, R.W. Olsen, and A.V. Delgado-Escueta, eds. (National Center for Biotechnology Information).
18. Radiske, A., Rossato, J.I., Gonzalez, M.C., Köhler, C.A., Bevilaqua, L.R., and Cammarota, M. (2017). BDNF controls object recognition memory reconsolidation. Neurobiol. Learn. Mem. *142* (Pt A), 79–84.
19. Francis, B.M., Kim, J., Barakat, M.E., Fraenkl, S., Yücel, Y.H., Peng, S., Michalski, B., Fahnestock, M., McLaurin, J., and Mount, H.T. (2012). Object recognition memory and BDNF expression are reduced in young TgCRND8 mice. Neurobiol. Aging *33*, 555–563.
20. Nagahara, A.H., Merrill, D.A., Coppola, G., Tsukada, S., Schroeder, B.E., Shaked, G.M., Wang, L., Blesch, A., Kim, A., Conner, J.M., et al. (2009). Neuroprotective effects of brain-derived neurotrophic factor in rodent and primate models of Alzheimer's disease. Nat. Med. *15*, 331–337.
21. Brandt, C., Gastens, A.M., Sun, Mz., Hausknecht, M., and Löscher, W. (2006). Treatment with valproate after status epilepticus: effect on neuronal damage, epileptogenesis, and behavioral alterations in rats. Neuropharmacology *51*, 789–804.
22. Tchekalarova, J., Atanasova, D., Nenchovska, Z., Atanasova, M., Kortenska, L., Gesheva, R., and Lazarov, N. (2017). Agomelatine protects against neuronal damage without preventing epileptogenesis in the kainate model of temporal lobe epilepsy. Neurobiol. Dis. *104*, 1–14.
23. Kaplan, D.R., and Miller, F.D. (2000). Neurotrophin signal transduction in the nervous system. Curr. Opin. Neurobiol. *10*, 381–391.
24. Scott, R.C. (2016). Network science for the identification of novel therapeutic targets in epilepsy. F1000Res. *5*, F1000 Faculty Rev-893.
25. Bassett, D.S., and Sporns, O. (2017). Network neuroscience. Nat. Neurosci. *20*, 353–364.
26. Lehmann, T.N., Gabriel, S., Kovacs, R., Eilers, A., Kivi, A., Schulze, K., Lanksch, W.R., Meencke, H.J., and Heinemann, U. (2000). Alterations of neuronal connectivity in area CA1 of hippocampal slices from temporal lobe epilepsy patients and from pilocarpine-treated epileptic rats. Epilepsia *41* (*Suppl 6*), S190–S194.
27. Danzer, S.C. (2016). Neurogenesis in epilepsy: better to burn out or fade away? Epilepsy Curr. *16*, 268–269.
28. Berghuis, P., Dobszay, M.B., Sousa, K.M., Schulte, G., Mager, P.P., Härtig, W., Görcs, T.J., Zilberter, Y., Ernfors, P., and Harkany, T. (2004). Brain-derived neurotrophic factor controls functional differentiation and microcircuit formation of selectively isolated fast-spiking GABAergic interneurons. Eur. J. Neurosci. *20*, 1290–1306.
29. Andrioli, A., Alonso-Nanclares, L., Arellano, J.I., and DeFelipe, J. (2007). Quantitative analysis of parvalbumin-immunoreactive cells in the human epileptic hippocampus. Neuroscience *149*, 131–143.
30. Paradiso, B., Zucchini, S., Su, T., Bovolenta, R., Berto, E., Marconi, P., Marzola, A., Navarro Mora, G., Fabene, P.F., and Simonato, M. (2011). Localized overexpression of FGF-2 and BDNF in hippocampus reduces mossy fiber sprouting and spontaneous seizures up to 4 weeks after pilocarpine-induced status epilepticus. Epilepsia *52*, 572–578.
31. Drexel, M., Preidt, A.P., Kirchmair, E., and Sperk, G. (2011). Parvalbumin interneurons and calretinin fibers arising from the thalamic nucleus reuniens degenerate in the subiculum after kainic acid-induced seizures. Neuroscience *189*, 316–329.
32. Soukupová, M., Binaschi, A., Falcicchia, C., Zucchini, S., Roncon, P., Palma, E., Magri, E., Grandi, E., and Simonato, M. (2014). Impairment of GABA release in the hippocampus at the time of the first spontaneous seizure in the pilocarpine model of temporal lobe epilepsy. Exp. Neurol. *257*, 39–49.
33. Drexel, M., Romanov, R.A., Wood, J., Weger, S., Heilbronn, R., Wulff, P., Tasan, R.O., Harkany, T., and Sperk, G. (2017). Selective silencing of hippocampal parvalbumin interneurons induces development of recurrent spontaneous limbic seizures in mice. J. Neurosci. *37*, 8166–8179.
34. Emerich, D.F., Orive, G., Thanos, C., Tornoe, J., and Wahlberg, L.U. (2014). Encapsulated cell therapy for neurodegenerative diseases: from promise to product. Adv. Drug Deliv. Rev. *67-68*, 131–141.
35. Karami, A., Eyjolfsdottir, H., Vijayaraghavan, S., Lind, G., Almqvist, P., Kadir, A., Linderoth, B., Andreasen, N., Blennow, K., Wall, A., et al. (2015). Changes in CSF cholinergic biomarkers in response to cell therapy with NGF in patients with Alzheimer's disease. Alzheimers Dement. *11*, 1316–1328.
36. Wahlberg, L.U., Lind, G., Almqvist, P.M., Kusk, P., Tornøe, J., Juliusson, B., Söderman, M., Selldén, E., Seiger, Å., Eriksdotter-Jönhagen, M., and Linderoth, B. (2012). Targeted delivery of nerve growth factor via encapsulated cell biodelivery in Alzheimer disease: a technology platform for restorative neurosurgery. J. Neurosurg. *117*, 340–347.
37. Fjord-Larsen, L., Kusk, P., Emerich, D.F., Thanos, C., Torp, M., Bintz, B., Tornøe, J., Johnsen, A.H., and Wahlberg, L.U. (2012). Increased encapsulated cell biodelivery of nerve growth factor in the brain by transposon-mediated gene transfer. Gene Ther. *19*, 1010–1017.
38. Kilkenny, C., Browne, W., Cuthill, I.C., Emerson, M., and Altman, D.G.; National Centre for the Replacement, Refinement and Reduction of Amimals in Research (2011). Animal research: reporting in vivo experiments—the ARRIVE guidelines. J. Cereb. Blood Flow Metab. *31*, 991–993.
39. Lidster, K., Jefferys, J.G., Blümcke, I., Crunelli, V., Flecknell, P., Frenguelli, B.G., Gray, W.P., Kaminski, R., Pitkänen, A., Ragan, I., et al. (2016). Opportunities for improving animal welfare in rodent models of epilepsy and seizures. J. Neurosci. Methods *260*, 2–25.
40. Angelucci, F., Aloe, L., Vasquez, P.J., and Mathé, A.A. (2000). Mapping the differences in the brain concentration of brain-derived neurotrophic factor (BDNF) and nerve growth factor (NGF) in an animal model of depression. Neuroreport *11*, 1369–1373.
41. Ellinwood, E.H., Jr., and Balster, R.L. (1974). Rating the behavioral effects of amphetamine. Eur. J. Pharmacol. *28*, 35–41.
42. Paxinos, G.W.C. (1998). The Rat Brain in Stereotaxic Coordinates, Fourth Edition (Academic Press).

Neurobiology of Disease

Long-Term, Targeted Delivery of GDNF from Encapsulated Cells Is Neuroprotective and Reduces Seizures in the Pilocarpine Model of Epilepsy

Giovanna Paolone,[1,3] Chiara Falcicchia,[1,3] Francesca Lovisari,[1] Merab Kokaia,[2] William J. Bell,[3] Tracie Fradet,[3] Mario Barbieri,[1] Lars U. Wahlberg,[3] Dwaine F. Emerich,[3] and Michele Simonato[1,4,5]

[1]Department of Medical Science, Section of Pharmacology, Neuroscience Center, University of Ferrara and National Institute of Neuroscience, 44121 Ferrara, Italy, [2]Epilepsy Centre, Department of Clinical Sciences, Lund University Hospital, 221 00 Lund, Sweden, [3]Gloriana Therapeutics, Inc. (formerly NsGene Inc.), Providence, Rhode Island 02905, [4]Laboratory of Technologies for Advanced Therapy (LTTA), Technopole of Ferrara, 44121 Ferrara, Italy, and [5]School of Medicine, University Vita-Salute San Raffaele, 20132 Milan, Italy

Neurotrophic factors are candidates for treating epilepsy, but their development has been hampered by difficulties in achieving stable and targeted delivery of efficacious concentrations within the desired brain region. We have developed an encapsulated cell technology that overcomes these obstacles by providing a targeted, continuous, *de novo* synthesized source of high levels of neurotrophic molecules from human clonal ARPE-19 cells encapsulated into hollow fiber membranes. Here we illustrate the potential of this approach for delivering glial cell line-derived neurotrophic factor (GDNF) directly to the hippocampus of epileptic rats. *In vivo* studies demonstrated that bilateral intrahippocampal implants continued to secrete GDNF that produced high hippocampal GDNF tissue levels in a long-term manner. Identical implants robustly reduced seizure frequency in the pilocarpine model. Seizures were reduced rapidly, and this effect increased in magnitude over 3 months, ultimately leading to a reduction of seizures by 93%. This effect persisted even after device removal, suggesting potential disease-modifying benefits. Importantly, seizure reduction was associated with normalized changes in anxiety and improved cognitive performance. Immunohistochemical analyses revealed that the neurological benefits of GDNF were associated with the normalization of anatomical alterations accompanying chronic epilepsy, including hippocampal atrophy, cell degeneration, loss of parvalbumin-positive interneurons, and abnormal neurogenesis. These effects were associated with the activation of GDNF receptors. All in all, these results support the concept that the implantation of encapsulated GDNF-secreting cells can deliver GDNF in a sustained, targeted, and efficacious manner, paving the way for continuing preclinical evaluation and eventual clinical translation of this approach for epilepsy.

Key words: **cell therapy; epilepsy comorbidity; GDNF; neurodegeneration; neuroprotection; temporal lobe epilepsy**

Significance Statement

Epilepsy is one of the most common neurological conditions, affecting millions of individuals of all ages. These patients experience debilitating seizures that frequently increase over time and can associate with significant cognitive decline and psychiatric disorders that are generally poorly controlled by pharmacotherapy. We have developed a clinically validated, implantable cell encapsulation system that delivers high and consistent levels of GDNF directly to the brain. In epileptic animals, this system produced a progressive and permanent reduction (>90%) in seizure frequency. These benefits were accompanied by improvements in cognitive and anxiolytic behavior and the normalization of changes in CNS anatomy that underlie chronic epilepsy. Together, these data suggest a novel means of tackling the frequently intractable neurological consequences of this devastating disorder.

Introduction

Epilepsy affects tens of millions of individuals across all ages, ethnic groups, and social classes. A significant portion of epilepsies in adults originate focally from mesial temporal lobe structures that include the hippocampus, entorhinal cortex, and

Received Feb. 16, 2018; revised Nov. 14, 2018; accepted Dec. 14, 2018.

Author contributions: G.P., L.U.W., D.F.E., and M.S. designed research; G.P., C.F., F.L., W.J.B., T.F., M.B., and D.F.E. performed research; G.P. analyzed data; G.P., M.K., L.U.W., D.F.E., and M.S. wrote the paper.

This research was supported by a grant from the European Community FP7-PEOPLE-2011-IAPP 536 project 285827 (EPIXCHANGE) to M.S. and L.U.W.

L.U.W. and D.F.E. are employees of Gloriana Therapeutics, Inc., a for-profit biotechnology company that is developing the encapsulated cell technology to treat CNS diseases. The authors declare no other competing financial interests.

amygdala (Stephen and Brodie, 2000; Sridharan, 2002). These so-called mesial temporal lobe epilepsies (mTLEs) cannot be cured, and the currently available pharmacological options cause significant unwanted side effects and are ineffective in up to one-third of the patients (Kwan and Brodie, 2000; Engel et al., 2012). These patients continue to experience seizures, and, in many cases, their seizures increase in frequency and are associated with significant cognitive decline and psychiatric disorders (Aldenkamp and Arends, 2004; Lin et al., 2012; Nogueira et al., 2017). The focal nature of mTLE opens the opportunity for direct therapeutic options including surgery, local radiation, and deep brain stimulation. More recently, gene therapy has emerged as a possible means of direct, local delivery of potentially therapeutic agents such as trophic proteins to the temporal lobe (Simonato et al., 2013). Gene therapy typically involves injecting a viral vector into the desired site to transduce local cells for producing the desired agent and achieving localized high levels of the agent itself (Kanter-Schlifke et al., 2009; Eriksdotter-Jönhagen et al., 2012; Tornøe et al., 2012; Nikitidou et al., 2014; Ledri et al., 2016). While promising, the limitation of this approach is its permanent, irreversible, and nonregulatable nature. Nonetheless, several studies have provided compelling proof of concept for these approaches in TLE (Simonato, 2014).

Recently, glial cell line-derived neurotrophic factor (GDNF) has emerged as a potential antiepileptic candidate. GDNF and its receptor are expressed within the temporal lobe, particularly the pyramidal and granule cells of the hippocampus. An association between GDNF and epilepsy is suggested by the observations that (1) seizures increase the expression of hippocampal GDNF mRNA and protein (Humpel et al., 1994; Kokaia et al., 1999) and (2) that chemically and electrically induced seizures can be suppressed by local infusion of GDNF or injection into the hippocampus of viral vectors expressing GDNF (Yoo et al., 2006; Kanter-Schlifke et al., 2007, 2009). Together, these data strongly indicate that locally increasing GDNF levels in the temporal lobe could represent a possible way of suppressing epileptic activity.

Here, we used an encapsulated cell approach for the delivery of GDNF (EC-GDNF) directly into the hippocampus of rats made epileptic by a systemic injection of pilocarpine. This approach is based on enclosing ARPE-19 cells genetically modified to secrete GDNF in an immunoprotective polymer membrane before transplantation (Fjord-Larsen et al., 2012; Tornøe et al., 2012; Emerich et al., 2014). Using this approach, we tested the following hypotheses: (1) that EC-GDNF can provide controlled, stable, and long-term delivery of GDNF to the hippocampus in a well tolerated manner; (2) that the targeted delivery of GDNF can elicit a significant and long-lasting reduction of pilocarpine-induced seizures while normalizing changes in anxiety and cognition; and (3) that these functional benefits are associated with improvements in quantifiable immunohistochemical indices of hippocampal morphology. The present findings are the first to demonstrate that encapsulated GDNF-secreting cells produce long-term and robust elevations in hippocampal GDNF that are well tolerated, efficacious, and perhaps disease modifying across a spectrum of epilepsy-relevant neurological measures. In addition, these neurological benefits were associated with GDNF receptor engagement and normalization of hippocampal morphology, Fluoro Jade C (FJC)-positive cells, neurogenesis, and the number of parvalbumin-expressing GABAergic neurons.

Correspondence should be addressed to Giovanna Paolone at giovanna.paolone@univr.it.
https://doi.org/10.1523/JNEUROSCI.0435-18.2018
 0270-6474/19/392145-13$15.00/0

Materials and Methods

Animals. Experiments were performed on adult male Sprague Dawley rats (Harlan Laboratories) weighing 225–250 g upon arrival. Rats were housed in a temperature- and humidity-controlled colony room maintained on a 12 h light/dark cycle (lights on at 7:00 A.M.). Food and water were available *ad libitum* throughout the experiment. All procedures were performed in adherence with the guidelines of the National Institute of Health and the European Community (EU Directive 2010/63/EU) on the Use and Care of Animals. The approved protocol from the University of Ferrara Committee on Animal Welfare was authorized by the Italian Ministry of Health (D.M. 246/2012-B). Furthermore, the Animal Research: Reporting In Vivo Experiments guidelines (Kilkenny et al., 2011) and the recommendations for improving animal welfare in rodent models of epilepsy and seizures (Lidster et al., 2016) have been followed. Following pilocarpine treatment, animals were randomly assigned to the experimental or control group.

Cell culture. ARPE-19 cells were cultured using standard procedures in T-175 flasks with 1× DMEM-GlutaMAX growth medium supplemented with 10% fetal bovine serum (catalog #10566-016, Invitrogen). Routine culture consisted of feeding the cells every 2–3 d and passaging them at 70–75% confluence. Cells were incubated at 37°C, 90% humidity, and 5% CO_2.

Cell line establishment. We generated clonal GDNF-secreting ARPE-19 cell lines using the sleeping beauty (SB) transposon expression system (Fjord-Larsen et al., 2010, 2012). Briefly, ARPE-19 cells were cotransfected with the plasmid pT2.CAn.hopp. GDNF, containing the entire GDNF sequence, and the SB vector pCMVSB100X. clones were selected using G418 (Sigma-Aldrich), and single colonies were expanded and isolated based on their GDNF release levels. Clonal cell lines producing high and stable levels of GDNF were further characterized *in vitro* and *in vivo*, and the GDNF clone used in the experiments was selected based on high GDNF secretion and long-term function in devices *in vivo*.

Device fabrication. Cells were encapsulated into hollow fiber membranes as previously described (Tornøe et al., 2012). Devices were manufactured from 7 mm segments of polysulfone membrane internally fitted with filaments of polyethylene terephthalate yarn scaffolding for cell adhesion. Before filling, cultured cells were dissociated and suspended in human endothelial (HE)-SFM (catalog #11111-044, Thermo Fisher Scientific), and 5×10^4 cells were injected into each device using a custom-manufactured automated cell-loading system. Devices were kept in HE-SFM at 37°C and 5% CO_2 for 2–3 weeks before surgical implantation. Devices loaded with nonmodified ARPE-19 cells were treated in the same manner and included as negative controls.

Surgical implantation and retrieval. In all efficacy studies, surgery for device implantation was performed 20 d after status epilepticus (SE), between two video monitoring sessions, as described below. Rats were placed into a stereotaxic instrument (Stoelting) and were continuously anesthetized with 1.5–2% isoflurane via a nose cone. Ophthalmic ointment was used to lubricate eyes. A midline incision was made in the scalp, and two bilateral holes were drilled through the skull. Devices filled with ARPE-19 GDNF cells or nonmodified ARPE-19 cells were bilaterally implanted into the hippocampus using a cannula mounted to the stereotaxic frame. The coordinates for implantation were as follows: anteroposterior (AP) −4.8 mm mediolateral (ML) ±4.1 with respect to bregma; and dorsoventral (DV) −7.0 mm below dura (Paxinos and Watson, 2007). After placement of the device, the skin was sutured closed. Animals received a postoperative injection of amikacin (250 mg/ml, 0.1 ml, i.p.) and buprenorphine (0.01 mg/kg/ml, i.p.), and the incision site was treated with neosporin. For retrieval, devices were removed by placing the anesthetized animal into the stereotactic frame, visualizing the proximal tip of the implant, and gently removing it using microforceps.

Rats used for video-EEG monitoring (experimental group, $n = 7$; control group, $n = 5$) were implanted with a bipolar electrode (PlasticsOne) in the right dorsal hippocampus during the surgery session of the device implantation. The coordinates for electrode implantation were AP −3.4 mm and ML −1.7 with respect to bregma; and DV −3.5 mm below dura. The ground wire was connected to five screws secured to the skull, and the electrode was fixed with dental cement.

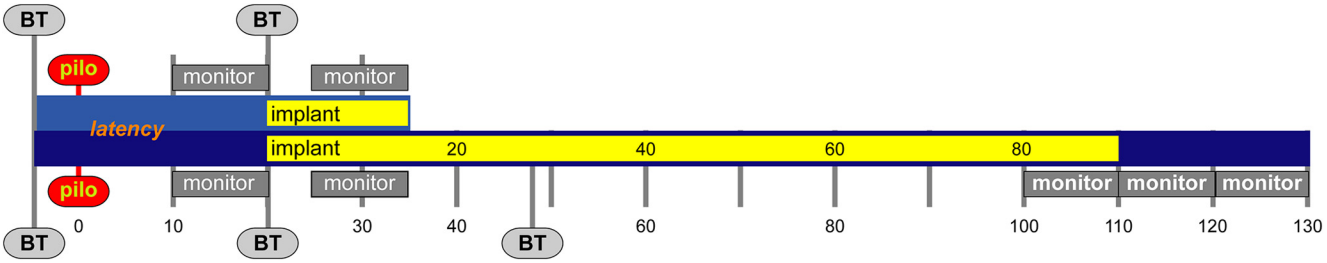

Figure 1. Experimental design. BT, Behavioral testing; pilo, pilocarpine.

ELISA. GDNF secretion from cell-loaded devices was verified before implantation and again following retrieval from the brain. Devices were incubated at 37°C in HE-SFM. Media samples (4 h incubation) were collected the next day to quantify GDNF release using a commercially available ELISA kit (DuoSet for human GDNF; catalog #DY212, R&D Systems). Previously implanted hippocampi were dissected free, transferred to vials containing 1 ml of Tissue Protein Extraction Reagent (T-PER; catalog #78510, Thermo Fisher Scientific), and flash frozen in liquid nitrogen. Supernatants from pulverized, and centrifuged tissue samples were assessed for GDNF levels using the ELISA kit mentioned above.

Long-term encapsulated cell function and tissue levels of GDNF in intact rats. We assessed the long-term (6 months) *in vivo* secretion of GDNF from cell-loaded devices, and the resulting levels of GDNF in the implanted hippocampi of intact rats (experimental group, $n = 36$; control group, $n = 4$). Devices were implanted as described above, and were removed at 1, 2, and 4 weeks postimplant, then monthly up to 6 months postimplant. The number of midline cage crossovers and the level of animal arousal were monitored for 60 s every 20 min for 2 h, at each time point. Behavior was rated using a modified version of the scale of Ellinwood and Balster (1974) i.e., 1, asleep (lying down, eyes closed); 2, awake/inactive (lying down, eyes open); and 3, crossing (moving, sniffing, rearing). Body weights were monitored biweekly. Four normal, intact animals were used as controls at each time point.

Pilocarpine treatment. Pilocarpine (340 mg/kg; catalog #P6503, Sigma-Aldrich) was administered intraperitoneally 30 min after a single subcutaneous injection of methylscopolamine (1 mg/kg), and the behavior of the rats was monitored and rated for several hours thereafter, using the scale of (Racine et al., 1972; Curia et al., 2008), as follows: 1, chewing or mouth and facial movements; 2, head nodding; 3, forelimb clonus; 4, generalized seizures with rearing; and 5, generalized seizures with rearing and falling. Within the first hour after pilocarpine injection, animals developed seizures that evolved into recurrent generalized (stage 4 and higher) convulsions (SE). Of the 60 animals administered pilocarpine, 95% (i.e., 57 animals) entered SE. SE was interrupted after 2 h by the administration of diazepam (10 mg/kg, i.p.). Twenty animals died during SE or in the following 3 d. Therefore, 37 animals were included in the study (allocation in the groups described below: 2 week implant experimental group, $n = 9$; 12 week implant experimental group, $n = 8$; control group, $n = 8$; video-EEG monitoring: experimental group, $n = 7$; control group, $n = 5$).

Video monitoring of seizure activity. Pilocarpine-treated animals were continuously video recorded for the quantification of generalized (class 4 or 5) seizures (Fig. 1). At the end of the latent phase (i.e., following the first spontaneous seizure; 10 ± 1 d after SE), the frequency and duration of generalized seizures were recorded through continuous video monitoring for 10 d. Animals then received bilateral intrahippocampal implants of devices or devices plus electrodes, and video or video-EEG monitoring was resumed 5 d after implantation for an additional 10 d. At the conclusion of monitoring (~35 d post-SE), animals were anesthetized and the devices were retrieved for confirmation of GDNF secretion. In a separate experiment, we examined the long-term effects of GDNF device implantation on seizures as well as the persistence of these effects after the devices were removed. SE was induced as described above, and animals were randomly divided into the following two treatment groups: bilateral implants of GDNF devices or of control devices loaded with the nonmodified parental ARPE-19 cell line. Animals were then monitored, and the seizure frequency and duration were recorded for two 10 d periods (days 5–15 and days 80–90 postimplantation; Fig. 1). After the second monitoring session, the devices were removed and the animals were monitored for an additional 20 d. At the conclusion of all experiments, hippocampi were removed and processed for quantification of GDNF levels.

For video-EEG monitoring, the rat headset was connected through a tripolar cable (PlasticsOne) to an EEG100C amplifier/MP150 Data Acquisition (Biopac) system, and signals were analyzed using AcqKnowledge version 5.0 software (Biopac). EEG seizures were defined as periods of paroxysmal activity of high frequency (>5 Hz) characterized by a more than threefold amplitude increment over baseline with progression of the spike frequency that lasted for a minimum of 5 s (Williams et al., 2009; Paradiso et al., 2011).

Open field arena and novel object recognition tests. The effects of GDNF on anxiety-like behavior and cognition were investigated using the open field (OF) and novel object recognition (NOR) tests, respectively (experimental group, $n = 13$; control group, $n = 14$). Each test was performed at the following three time points: before pilocarpine treatment (baseline); before device implantation (4 weeks after SE); and again 4 weeks after implant (Fig. 1). Before device implant, animals were randomly assigned to the following two groups: pilocarpine or pilocarpine + GDNF. For the OF test, animals were placed in an arena ($75 \times 75 \times 30$ cm) and video monitored for 30 min. Videos were analyzed (catalog #60201, ANY-maze) for distance moved, immobility, entries, and time spent in the center part of the arena. For the NOR, rats were tested in three phases. In the habituation phase (day 1), animals were allowed to freely explore the arena for 30 min. The following day, in the familiarization phase, rats were transferred for 5 min to the arena, where two identical objects were positioned in the central quadrant in opposite and symmetrical corners (A+A). In the testing phase (2 h later), animals were returned to the arena with one of the objects replaced with a novel one (A+B). The time spent exploring the objects was recorded by a blind investigator. To control for seizure effects in behavioral performance, rats were always tested at least 2 h after the last seizure.

Immunohistochemistry. A separate cohort of animals ($N = 25$; 2 week implant study: naïve, $n = 3$; pilocarpine, $n = 4$; pilo+GDNF, $n = 5$; 12 week implant study: naïve, $n = 3$; pilocarpine, $n = 4$; pilo+GDNF, $n = 6$) was unilaterally implanted with GDNF devices 20 d after pilocarpine-induced SE. After either 2 or 12 weeks, rats were deeply anesthetized and transcardially perfused with 200 ml of 0.9% ice-cold saline. Following saline perfusion, rats were decapitated and the devices removed. Brains were placed in Zamboni's fixative (catalog #NC9335034, Thermo Fisher Scientific) for 1 week, then were embedded in paraffin. The 8-μm-thick sections were cut coronally using a Leica RM2125RT microtome through the hippocampus (−2.3 to −5.8 mm from bregma; Paxinos and Watson, 2007). Sections were dewaxed and rehydrated as previously described (Paradiso et al., 2009): two 10 min washes in xylene (catalog #1330-20-7, Sigma-Aldrich), 5 min in 100% ethanol, 5 min in 95% ethanol, 5 min in 80% ethanol, and then rehydration in distilled water for 5 min. All antigens were unmasked using a commercially available kit (Unmasker; catalog #T0010, Diapath), according to the manufacturer instructions. After washing in PBS, sections were incubated at room temperature with Triton X-100 (0.3% in PBS; catalog #9002-93-1, Sigma-Aldrich) for 10 min, washed twice in PBS, and incubated with 5% bovine serum albumin and

5% serum of the species in which the secondary antibody was produced for 30 min. Sections were incubated overnight at 4°C in a humid atmosphere with a primary antibody specific for the following: glial fibrillary acid protein (GFAP; mouse polyclonal, catalog #AMAb91033, Atlas Antibodies; PRID:AB_2665775), 1:100; doublecortin (DCX; rabbit polyclonal; catalog #3973S, Cell Signaling Technology; PRID:AB_2276960), 1:400; parvalbumin (mouse monoclonal; catalog #235, Swant; PRID:AB_10000343), 1:100; phosphorylated receptor tyrosine kinase RET (rabbit polyclonal, catalog #sc-20252-R, Santa Cruz Biotechnology; PRID:AB_2179766), 1:100; and neural cell adhesion molecule (NCAM; mouse monoclonal; catalog #MAB5324, Millipore; PRID:AB:_11210572), 1:400. After 5 min rinses in PBS, sections were incubated with Triton (as above; 30 min), washed in PBS, and incubated with a goat anti-mouse Alexa Fluor 594 (catalog #A-11058, Invitrogen; PRID:AB_142540) or Alexa Fluor 488 (catalog #A-21125, Invitrogen; PRID:AB_141593) secondary antibody (1:250) for mouse primary antibodies, or with a goat anti-rabbit, Alexa Fluor 488 (catalog #A-11094, Thermo Fisher Scientific; PRID:AB_221544) or Alexa Fluor 594 secondary antibody (catalog #A-11012, Invitrogen; PRID:AB_141359, 1:250) for rabbit primary antibodies, at room temperature for 3 h. After staining, sections were washed in PBS, counterstained with 0.0001% 4′,6′-diamidino-2-phenylindole dihydrochloride (DAPI; catalog #D1306, Thermo Fisher Scientific; PRID:AB_2629482) for 15 min, and washed again before coverslipping. Omission of the primary antibody resulted in no specific staining.

Fluoro-Jade C staining. Slides were dewaxed and immersed for 5 min in a solution of 1% sodium hydroxide in 80% ethanol, then rinsed for 2 min in 70% ethanol, for 2 min in distilled water, and incubated in 0.06% potassium permanganate solution for 10 min. Slides were then transferred for 20 min into a 0.001% solution of FJC (catalog #AG325-30MG, Millipore) followed by three 1 min washes in distilled water. Slides were air dried on a slide warmer at 50°C for 5 min and cleared in xylene for 1 min. Coverslips were mounted using DPX (catalog #06522, Sigma-Aldrich) mounting media.

Morphological analyses. Quantitation of FJC, DCX, GFAP, PV, NCAM, and pRET-positive cells was performed by an investigator who was blinded to the experimental condition, using a Leica DMRA2 Microscope. Sections were collected for each stain at 500 μm intervals throughout the hippocampus (−2.3 to −5.3 mm relative to bregma; Paxinos and Watson, 2007), and the total numbers of immunopositive cells were counted bilaterally.

Hippocampal volumetry. FJC-stained sections were selected at three levels in the dorsal hippocampus (−2.8, −3.3, −3.8 mm relative to bregma; $N = 25$), and the area of the hippocampus was calculated (in square micrometers) on images obtained using the scan slide module of the MetaMorph software using a 6.3× objective. For volumetric analysis of the hippocampus, values were obtained by applying the formula $V = \frac{h}{3} \times (B_{max} + b_{min} + \sqrt{B_{max} \times b_{min}})$, where $h = 500$ μm.

Statistical methods. Mixed-design ANOVAs were used to determine the effects of treatment, time, and any treatment × time interactions. Table 1 statistical analyses performed. Where appropriate, *post hoc* comparisons were conducted using *t* test and Fisher's LSD test. Statistical analyses were performed using SPSS Statistics software (SPSS). All data were found to have a normal distribution, based on the Shapiro–Wilk test. In cases of the violation of the sphericity assumption, Huynh–Feldt corrected *F* values are given. The α value was set at 0.05, and exact *p* values are reported for significant results (Greenwald et al., 1996). Mean values and SEMs were calculated for each group and were expressed as the percentage of the naive group to facilitate statistical and graphic comparisons.

Results

Long-term encapsulated cell function and tissue levels of GDNF in normal rats

GDNF-secreting devices were implanted in naive rats and retrieved at different time points (1, 2, 4, 8, 16, or 24 weeks after implantation). All implanted devices were easily retrieved from the brain with no host tissue adhering to the capsule wall. All implants were located within the hippocampus and remained intact, with no evidence that any capsule broke either *in situ* or during the retrieval procedure. Quantification of device output confirmed a robust and sustained secretion of GDNF from the implanted devices (Fig. 2*A*). Before implantation, devices secreted 277.59 ± 10.72 ng/d GDNF. Explanted devices showed an initial increase in secretion peaking at ~2–8 weeks (28,451.50 ± 192.84 ng/24 h), then tapering to a sustained amount that remained well above preimplant levels for the 6 months of analysis (Fig. 2*A*; 566.79 ± 192.47 ng/24 h). The continued delivery of GDNF to the hippocampus significantly elevated local tissue concentrations of GDNF in a manner that paralleled device secretion (Fig. 2*B*). Tissue levels of GDNF were highly increased within 1 week following implantation and reached peak levels at 2–8 weeks (53.74 ± 8.89 ng), gradually decreasing while remaining elevated for at least 6 months postimplantation (9.04 ± 2.82 ng).

The prolonged and elevated levels of GDNF within the hippocampus were not associated with any changes in body weight or general behavioral activity. Indeed, over the 6 months of observation all rats gained weight at a typical rate that was indistinguishable between intact rats and those implanted with GDNF devices (Fig. 2*C*; $t_{(6)} = 0.27$; $p = 0.81$). Similarly, no differences were noted when animals were evaluated for time spent sleeping (Fig. 2*D*; $U = 15.50$, $z = -0.45$; $p = 0.65$), awake/inactive ($U = 15.00$, $z = -0.51$; $p = 0.65$), or moving across the cage ($U = 15.50$, $z = -0.45$; $p = 0.65$).

Seizures

Short-term (10 d) intrahippocampal implantation of GDNF devices dramatically reduced the frequency of motor seizures in pilocarpine-treated rats. Before GDNF treatment (first 10 d after the first spontaneous seizure; i.e., 10–20 d after SE), rats exhibited 2.34 ± 0.05 motor seizures/d. Five to 15 d following implantation (i.e., 25–35 d after SE), the frequency of motor seizures was reduced to 0.62 ± 0.14 seizures/d (Fig. 3*A*; main effect of treatment: $F_{(1,8)} = 189.16$; $p < 0.001$). This effect had a relatively rapid onset, as it was observed within the first week of implantation and was confirmed by the significant time × treatment interaction ($F_{(9,72)} = 2.14$; $p = 0.037$). While the frequency of motor seizures was reduced by ~75%, their duration was not altered relative to preimplantation (Fig. 3*B*; $t_{(8)} = 1.29$, $p = 0.23$). As expected, EEG monitoring detected a greater number of seizures (i.e., animals were experiencing nonmotor as well as motor seizures). Again, the frequency of EEG seizures was strongly reduced in animals implanted with GDNF devices compared with those implanted with nonmodified parental ARPE-19 cells (Fig. 4*A*), but their duration was identical in both groups (Fig. 4*B*). Representative EEG traces from nonmotor and motor seizures are shown in Figure 4, *C* and *D*. The magnitude of GDNF secretion from explanted devices (Fig. 3*C*; preimplant, 252.28 ± 7.34 ng/24 h; postimplant, 2339.26 ± 194.86 ng/24 h) and the levels of GDNF within the tissue (41.17 ± 3.69 ng; data not shown) were comparable to those observed in the intact, normal brain.

We then extended these observations to investigate longer lasting implantations and the postimplantation persistence of the effects. We implanted the devices as in the previous experiment, but left them in the brain much longer (90 d), while monitoring seizures in the following two epochs: 5–15 d (as above) and 80–90 d postimplantation. We then retrieved the devices and continued monitoring for 20 additional days. We found that the reduction in seizure frequency increased in magnitude over time, from 84% at 5–15 d postimplantation to 93% in the same animals at 80–90

Table 1. Effects of GDNF treatment on seizure frequency and histological analyses

Experiment	Treatment	Group size	Main effect of treatment	Treatment × time
Seizure frequency				
2 week implant	Pilo + GDNF	9	$F_{(1,8)} = 189.16; p < 0.001$	$F_{(9,72)} = 2.14; p = 0.037$
12 week implant	Pilo + Parental	8	$F_{(1,13)} = 698.62; p < 0.001$	$F_{(4,52)} = 240.56; p < 0.001$
	Pilo + GDNF	8		
Behavioral testing				
Open field	Pilo	14	$F_{(1.25)} = 4.46; p = 0.04$	$F_{(2,50)} = 11.12; p < 0.001$
	Pilo + GDNF	13		
Novel object recognition	Pilo	14	$F_{(1.25)} = 2.07; p = 0.04$	$F_{(2,50)} = 11.82; p < 0.001$
	Pilo + GDNF	13		
Hippocampal volume				
2 week implant	Naive	3		
	Pilo	4	$F_{(2,12)} = 7.23; p = 0.011$	NA
	Pilo + GDNF	5		
12 week implant	Naive	3		
	Pilo	4	$F_{(2,11)} = 96.87; p < 0.001$	NA
	Pilo + GDNF	5		
Histology				
2 week implant				Treatment × hippocampal level
FJ C	Naive	3		
	Pilo	4	$F_{(2,23)} = 17.59; p < 0.001$	$F_{(10,115)} = 2.51; p = 0.009$
	Pilo + GDNF	5		
PV	Naive	3		
	Pilo	4	$F_{(2,23)} = 17.54; p < 0.001$	$F_{(10,115)} = 3.42; p < 0.001$
	Pilo + GDNF	5		
GFAP	Naive	3		
	Pilo	4	$F_{(2,23)} = 0.14; p = 0.88$	NA
	Pilo + GDNF	5		
DCX	Naive	3		
	Pilo	4	$F_{(2,23)} = 6.67; p = 0.005$	$F_{(10,115)} = 3.88; p < 0.001$
	Pilo + GDNF	5		
NCAM	Naive	3		
	Pilo	4	$F_{(2,23)} = 22.41; p < 0.001$	$F_{(10,115)} = 2.06; p = 0.034$
	Pilo + GDNF	5		
pRET	Naive	3		
	Pilo	4	$F_{(2,23)} = 158.59; p < 0.001$	$F_{(10,115)} = 6.71; p < 0.001$
	Pilo + GDNF	5		
12 week implant				
FJ C	Naive	3		
	Pilo	4	$F_{(2,21)} = 9.71; p = 0.09$	NA
	Pilo + GDNF	6		
PV	Naive	3		
	Pilo	4	$F_{(2,21)} = 54.71; p < 0.001$	$F_{(10,105)} = 2.43; p = 0.012$
	Pilo + GDNF	6		
GFAP	Naive	3		
	Pilo	4	$F_{(2,21)} = 0.11; p = 0.90$	NA
	Pilo + GDNF	6		
DCX	Naive	3		
	Pilo	4	$F_{(2,21)} = 53.96; p < 0.001$	$F_{(10,105)} = 7.833; p < 0.001$
	Pilo + GDNF	6		
NCAM	Naive	3		
	Pilo	4	$F_{(2,19)} = 46.63; p < 0.001$	$F_{(10,95)} = 2.63; p = 0.04$
	Pilo + GDNF	6		
pRET	Naive	3		
	Pilo	4	$F_{(2,21)} = 205.86; p < 0.001$	$F_{(10,105)} = 22.70; p < 0.001$
	Pilo + GDNF	6		

NA, Not applicable; Pilo, pilocarpine.

d postimplantation (Fig. 5*A*; $F_{(1,13)} = 698.62, p < 0.001$). Implantation with control devices loaded with parental ARPE-19 cells did not alter seizure frequency at any time point. No change in seizure duration was observed at any time point in GDNF-treated animals and controls ($F_{(1,13)} = 0.57; p = 0.46$).

Interestingly, a persistent effect was observed when the GDNF devices were retrieved 90 d following implantation (Fig. 5*A*). Although the frequency of spontaneous seizures did increase over preremoval values, it was still significantly lower than in control epileptic animals (65% lower; Fig. 5*A*). Incidentally, it should be noted that, as previously reported (Soukupová et al., 2014), the frequency of seizures tended to increase in time in untreated animals.

At explant, the secretion of GDNF from devices remained high (Fig. 5*B*; preimplant, 283.36 ± 8.82 ng/24 h; postexplant, 4500.50 ± 410.93 ng/24 h). Relative to tissue levels measured

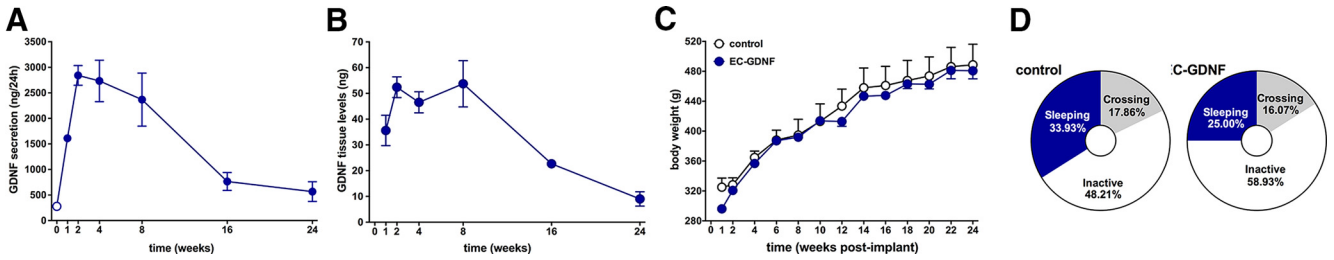

Figure 2. Encapsulated cell function, tissue levels of GDNF, body weight, and general behavioral activity in intact rats following bilateral intrahippocampal implantation of GDNF devices. ***A***, GDNF secretion from devices explanted from the hippocampus. Devices were implanted in intact rats and removed after 1, 2, 4, 8, 16, and 24 weeks. GDNF secretion dramatically increased over preimplant values at 2–8 weeks and then slowly declined a sustained amount that remained above preimplant levels for the 6 months of analysis. ***B***, Hippocampal tissue levels of GDNF during device implantation. Tissue levels were elevated within 1 week, reached and maintained a peak at 2–8 weeks, and then slowly decreased, remaining elevated for the duration of the experiment. ***C***, ***D***, Device implantation and elevation of tissue GDNF levels did not alter body weight (***C***) or affect the general pattern of behavioral activity (***D***; Mann–Whitney *U* test). All data are expressed as the mean ± SEM of 4 animals per time point in ***A*** and ***B***, and 40 animals in ***C*** and ***D***.

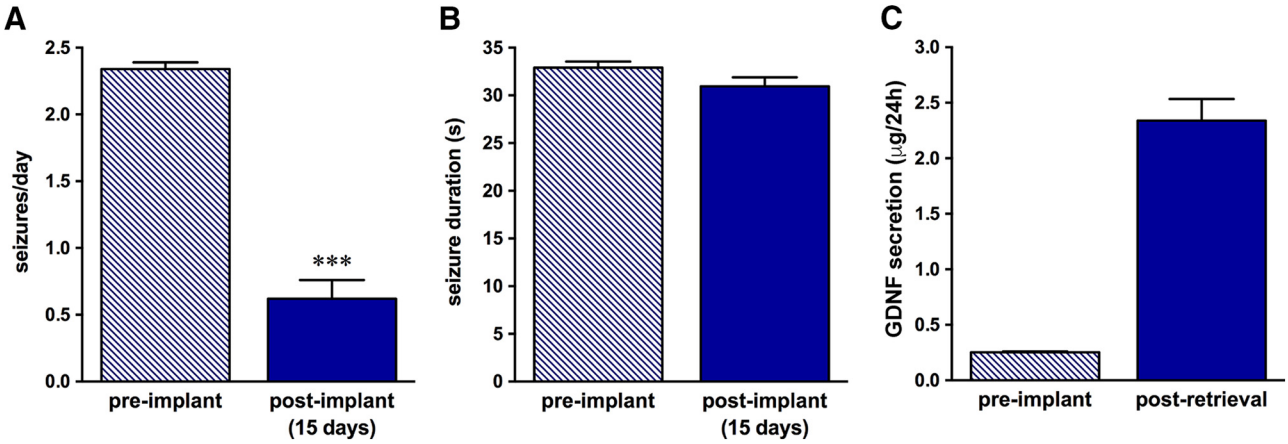

Figure 3. GDNF significantly reduces seizure frequency in pilocarpine-treated rats. Rats were video monitored before (10–20 d after SE) and following intrahippocampal GDNF device implantation (25–35 d after SE). ***A***, ***B***, The frequency of seizures was reduced by 84% relative to preimplantation levels (***A***), whereas seizure duration was not altered (***B***). ***C***, Levels of GDNF secretion before implantation and after retrieval at the conclusion of the video monitoring. Data are the mean ± SEM of nine animals monitored before and after GDNF treatment. ***$p < 0.001$ based on paired *t* test.

immediately after device retrieval, GDNF levels in the hippocampus were reduced by >98% when quantified 20 d after device removal (1.57 ± 1.01 ng; data not shown). This observation suggests that the persistent reduction in seizure frequency was not related to residual GDNF in the hippocampus.

Open field and novel object recognition

Pilocarpine-induced epilepsy produced significant impairments in the open-field and novel object recognition tests. Pilocarpine-treated rats alternated periods of hyperactivity and of freezing, spending significantly more time in the central part of the testing arena ($F_{(2,50)} = 11.12$; $p < 0.001$). In contrast, GDNF treatment prevented the development of this phenotype, with treated rats performing comparably to naive ones (Fig. 6*A*; $t_{(26)} = 10.35$; $p = 0.004$). Importantly, this change in behavior could not be attributed to alterations in general activity because, overall, the distance traveled and the immobility time did not change ($F_{(2,50)} = 0.54$, $p = 0.59$; and $F_{(2,50)} = 0.05$; $p = 0.95$; respectively; data not shown).

GDNF also reversed the cognitive impairment associated with pilocarpine-induced epilepsy. At baseline, all rats displayed a clear exploratory preference for the novel object, but this preference completely disappeared 4 weeks after SE ($F_{(2,50)} = 11.82$; $p < 0.001$). As shown in Figure 6*B*, pilocarpine-treated rats spent equal amounts of time exploring the new and the previously presented objects both 4 and 8 weeks after SE (i.e., 4 weeks after the implant of a control device; $t_{(26)} = 0.89$; $p = 0.38$). GDNF treatment reinstated the ability to distinguish between the novel and the familiar object (Fig. 6*B*; no GDNF: $t_{(13)} = 1.33$, $p = 0.21$; GDNF: $t_{(12)} = 7.07$, $p < 0.001$).

The findings described above were confirmed in the animals used for these behavioral experiments: the frequency of seizures was reduced by 74% relative to preimplantation ($t_{(8)} = 13.66$, $p < 0.001$), and the magnitude of GDNF secretion was monitored preimplantation and after retrieval of the device from the hippocampus were 144.03 ± 11.81 and 3641.70 ± 300.30 ng/24 h, respectively.

Immunohistochemistry

Neuroprotection

To analyze the morphological effects of GDNF on the epileptic hippocampal tissue, we implanted a single device in one hippocampus 20 d after pilocarpine-induced SE, and sacrificed the rats 2 and 12 weeks thereafter. GDNF treatment exerted a pronounced neuroprotective effect, as evidenced by the quantitation of hippocampal volume, the counts of degenerating neurons, and the counts of parvalbumin-positive cells. These effects were observed at both 2 and 12 weeks postimplantation and were comparable in magnitude between both the implanted and nonimplanted hemispheres. A generalized atrophy of the hippocampus was observed in epileptic animals. Compared with naive controls, the hippocampal volume of pilocarpine-treated

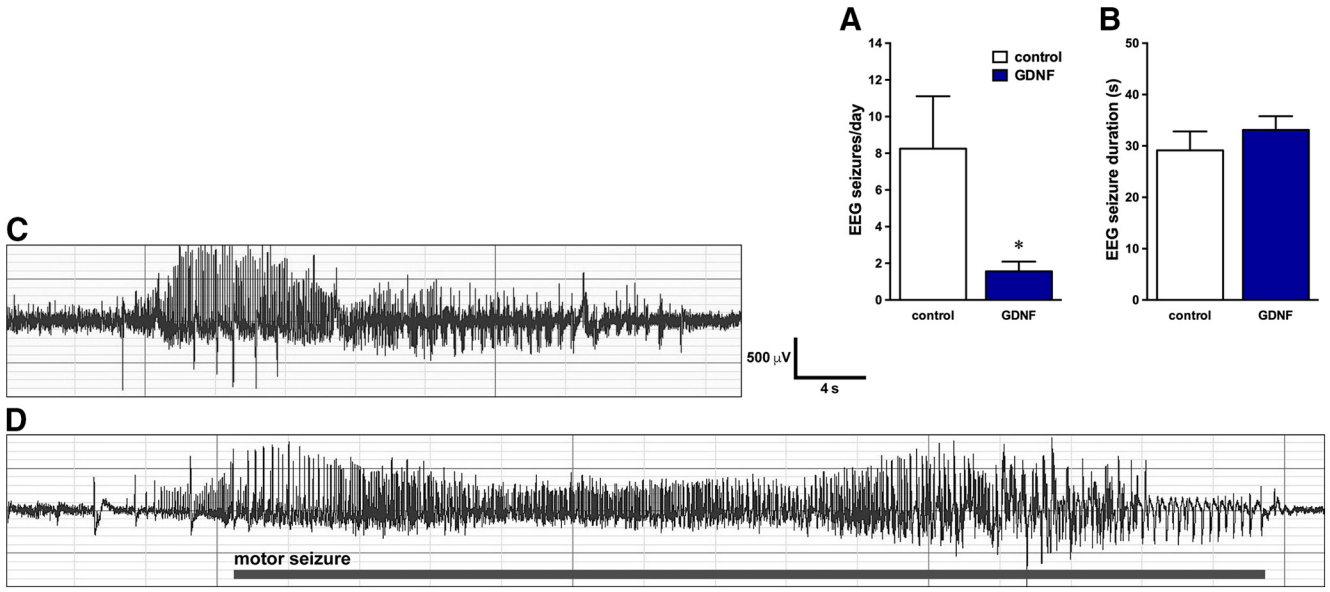

Figure 4. ***A***, ***B***, Electrical seizure frequency (***A***) and duration (***B***) were recorded 5–15 d after implantation with the nonmodified parental ARPE-19 cells or GDNF devices in chronically epileptic animals. ***C***, ***D***, Representative EEG patterns in the hippocampus during nonmotor (***C***) and motor (***D***) seizures in GDNF device-implanted animals. Identical patterns were observed in animals implanted with empty devices. The horizontal bar in ***D*** indicates the motor part of the seizure. All data are expressed as the mean ± SEM of seven animals per group. *$p < 0.05$. Student's *t* test for unpaired data.

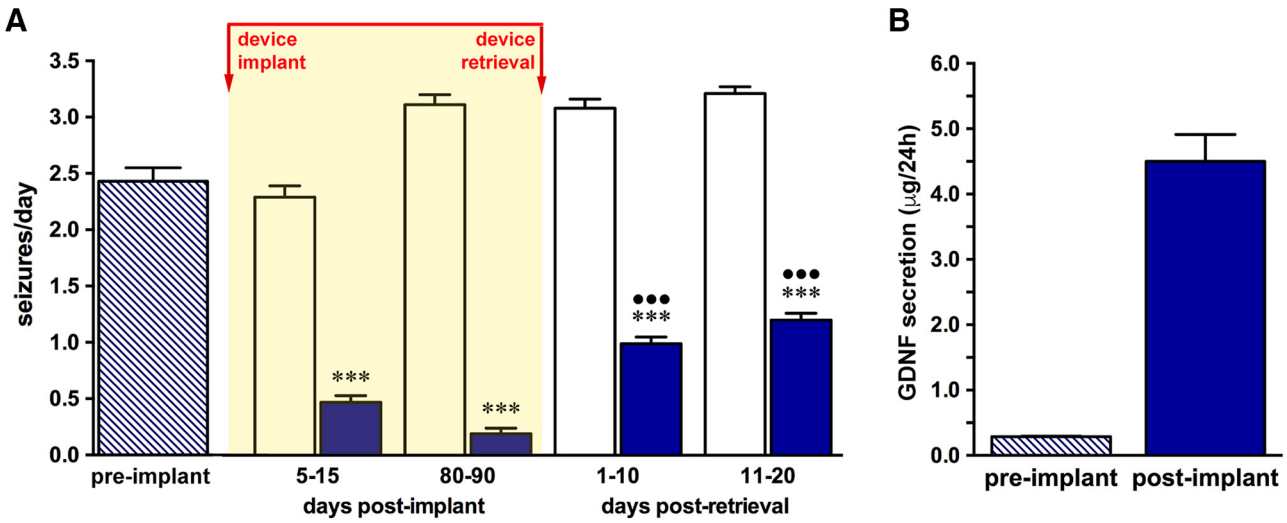

Figure 5. Long-term and persistent effects of GDNF on seizure frequency. Animals were implanted either with devices loaded with the nonmodified parental ARPE-19 cell line ($N = 8$) or with GDNF-secreting devices ($N = 8$), as in Figure 3. ***A***, Seizure frequency and duration were recorded before implantation (10–20 d after SE) and for two 10 d periods postimplantation (5–15 and 80–90 d after implantation; see text for details). At the conclusion of the second monitoring session (days 80–90), devices were retrieved and animals were monitored for an additional 20 d. Note that the effects of GDNF persisted even after device removal (65% decrease in seizure frequency relative to epileptic controls). ***B***, Levels of GDNF secreted before implantation and immediately following retrieval. All data are expressed as the mean ± SEM of 16 animals ***$p < 0.001$ compared with control devices; ●●●$p < 0.001$ compared with device preremoval values (80–90 d postimplant). Multiple comparisons were based on significant main effects or interactions resulting from the ANOVA described in the Materials and Methods and Results.

rats was reduced by ~20% 2 weeks after pilocarpine treatment, and by 33% after 12 weeks (2 weeks: $F_{(2,12)} = 7.23$; $p = 0.011$; 12 weeks: $F_{(2,11)} = 96.87$; $p < 0.001$; Figure 7). Treatment with GDNF reversed this loss of hippocampal volume (Fig. 7).

FJC staining was used to identify degenerating neurons and to determine the ability of GDNF to attenuate damage (Ehara and Ueda, 2009) (Fig. 8). Quantitative analysis revealed a significant increase in degenerating cells in CA1, CA3, and hilus of the dentate gyrus following pilocarpine treatment compared with naive cells (597% and 160% at 2 and 12 weeks after postpilocarpine treatment, respectively). Similar to the GDNF-induced prevention of hippocampal atrophy, a significant attenuation of neuronal degeneration was observed in treated rats, with a much smaller increase in FJC-positive cells (187% and 32% at 2 and 12 weeks, respectively) compared with cells from naive animals ($F_{(2,23)} = 17.59$, $p < 0.001$; and $F_{(2,21)} = 9.71$, $p = 0.09$, respectively).

Finally, because epilepsy has been consistently linked to changes in GABAergic neurotransmission, including a loss of PV and somatostatin cells (Mazzuferi et al., 2010; Soukupová et al., 2014), we quantified the ability of GDNF to protect this cell population. As shown in Figure 9, pilocarpine significantly reduced the number of PV-positive neurons in the hippocampus relative to naive rats (2 weeks: $F_{(2,23)} = 17.54$, $p < 0.001$; 12 weeks:

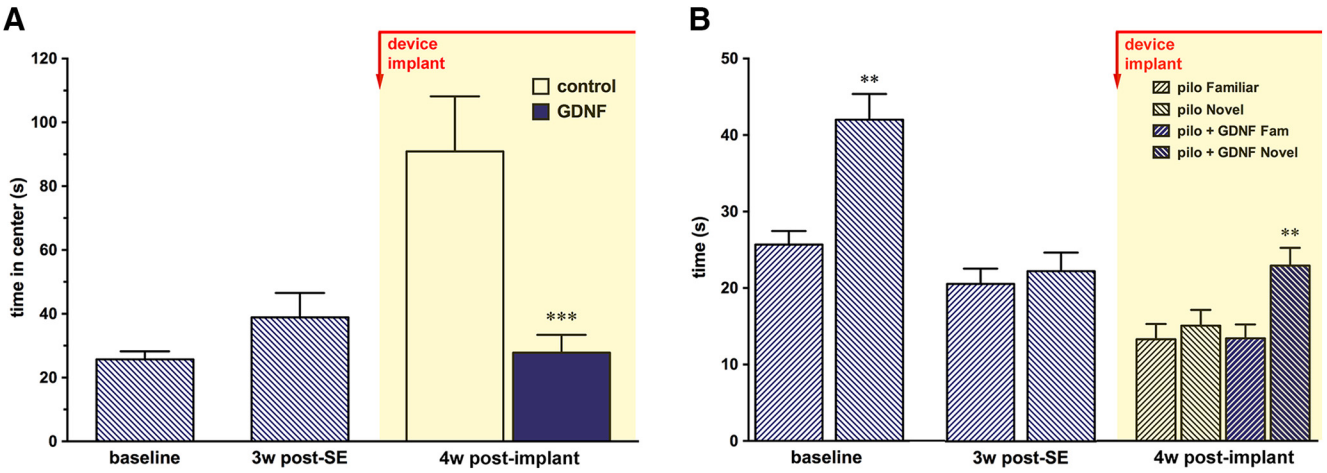

Figure 6. ***A***, ***B***, Effect of GDNF in the open field (***A***) and in the novel object recognition test (***B***). Rats ($N = 27$) were tested before any manipulation (baseline) and 4 weeks after pilocarpine-induced SE. Following the post-pilocarpine test session, a subgroup of animals ($n = 13$) was implanted with GDNF devices. Pilocarpine-induced epilepsy progressively reduced the natural tendency of the rat to avoid the central region of the arena and the exploratory preference for the novel object. ***A***, ***B***, GDNF restored a normal behavior both as measured by the time spent in the central region of the arena (***A***) and as the ability to distinguish new from familiar objects (***B***). All data are expressed as the mean ± SEM. $^{**}p < 0.01$; $^{***}p < 0.001$ of 27 animals. Multiple comparisons were based on significant main effects or interactions resulting from the ANOVAs described in the Materials and Methods and Results. w, Weeks.

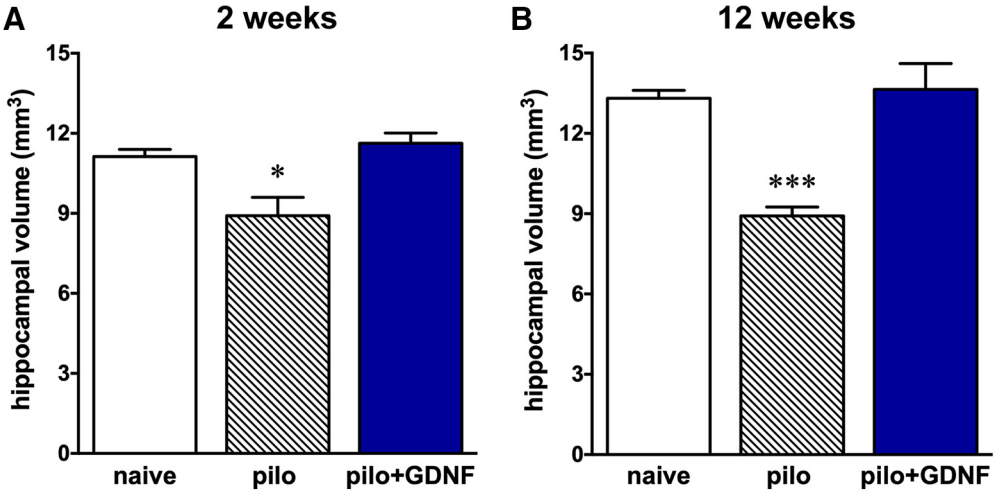

Figure 7. GDNF reverts the loss of hippocampal volume that occurs following pilocarpine. ***A***, ***B***, Sections were taken from the dorsal hippocampus of naive ($n = 3$), pilocarpine-treated ($n = 4$), and pilocarpine-treated rats treated with GDNF ($n = 5–6$) for either for 2 (***A***) or 12 (***B***) weeks. Data are presented as absolute values of hippocampal volumes. Because no differences were noted between the right and left hemispheres in any group, data from both hemispheres were combined. All data are expressed as the mean ± SEM. $^{*}p < 0.05$; $^{***}p < 0.001$ of 25 animals. Multiple comparisons were based on significant main effects resulting from the ANOVAs described in the Materials and Methods and Results. pilo, Pilocarpine.

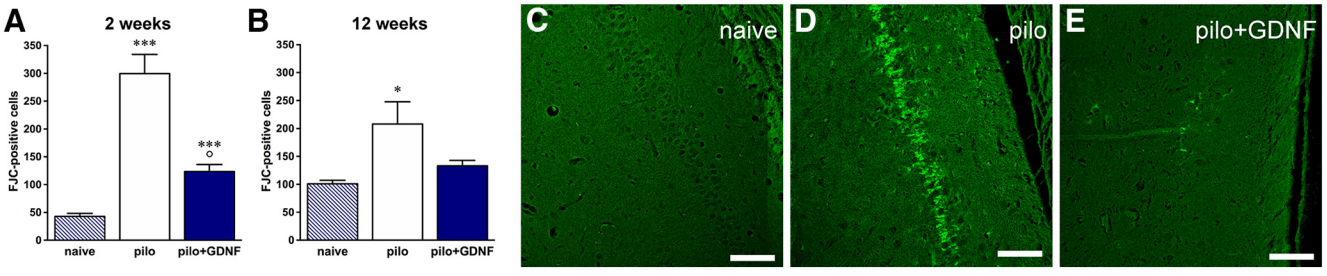

Figure 8. GDNF significantly reduces ongoing neuronal degeneration. ***A***, ***B***, The effects of pilocarpine and 2 (***A***) or 12 (***B***) weeks of treatment with GDNF on the total numbers of FJC-positive cells in the hippocampus. While pilocarpine significantly increased the numbers of degenerating FJC-positive neurons at both time points, this effect was significantly attenuated by GDNF. Data are expressed as the mean ± SEM of three to six animals per group. $^{*}p < 0.05$, $^{***}p < 0.001$ vs naive; $^{\circ}p < 0.05$ vs pilo. Multiple comparisons were based on significant main effects resulting from the ANOVAs described in the Materials and Methods and Results. Representative images taken from naive, pilocarpine-treated, and pilocarpine-treated rats treated with GDNF at 2 weeks are shown in ***C–E***. Scale bar, 500 μm. pilo, Pilocarpine.

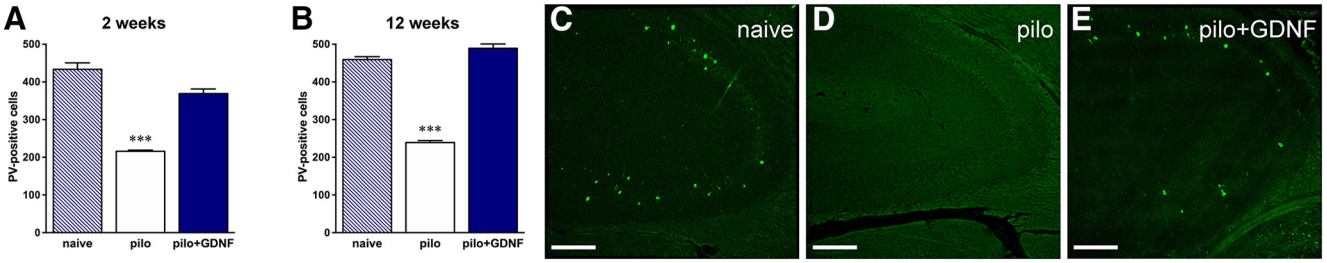

Figure 9. ***A***, ***B***, GDNF reverts pilocarpine (pilo)-induced degeneration of hippocampal parvalbumin (PV)-positive cells after both 2 weeks (***A***) and 12 weeks (***B***) of treatment. Data refers to the total number of positive cells and are expressed as the mean ± SEM of three to six animals per group.***$p < 0.001$. Multiple comparisons were based on significant main effects resulting from the ANOVAs described in the Materials and Methods and Results. ***C–E***, Representative images taken from the CA3 area of naive, pilocarpine-treated, and pilocarpine-treated rats treated with GDNF at 2 weeks are shown. Scale bar, 100 μm.

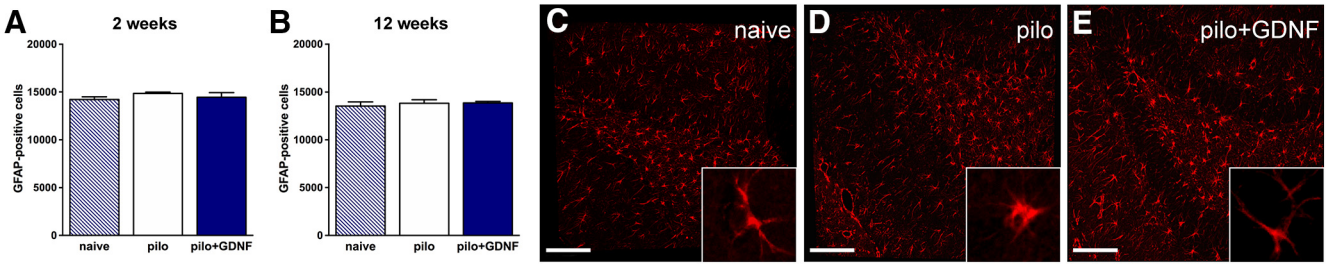

Figure 10. ***A***, ***B***, Astrocyte density in the hippocampus is not altered by treatment with either pilocarpine or GDNF for 2 (***A***) or 12 (***B***) weeks. Data refer to the total number of positive cells and are expressed as the mean ± SEM of three to six animals per group. ***C–E***, Representative images taken from the hilus of the dentate gyrus area of naive, pilocarpine-treated, and pilocarpine-treated rats treated with GDNF at 2 weeks are shown. Scale bar, 100 μm. Higher-magnification inserts illustrate the changes in the morphology of GFAP-positive cells.

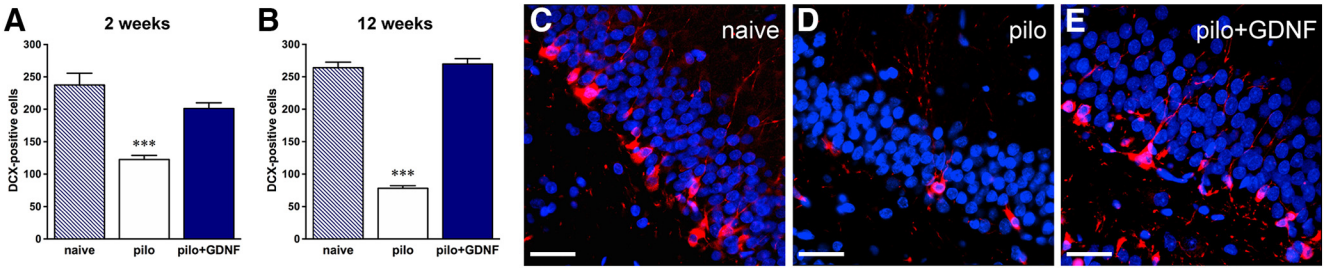

Figure 11. ***A***, ***B***, GDNF normalizes neurogenesis after 2 (***A***) and 12 (***B***) weeks of treatment. Data refer to the total number of positive cells and are expressed as the mean ± SEM of three to six animals per group. ***$p < 0.001$. Multiple comparisons were based on significant main effects resulting from the ANOVAs described in the Materials and Methods and Results. ***C–E***, Representative DCX immunofluorescence (in red) images taken from the granular zone of the dentate gyrus of naive, pilocarpine-treated, and pilocarpine-treated rats treated with GDNF at 2 weeks are shown. Nuclei are marked by DAPI (blue). DCX-positive cells in the naive dentate gyrus are located in the subgranular zone and present notable elongations across the granular layer. Pilocarpine causes a decrease in DCX-positive cells, which is associated with fewer elongations in the remaining cells. Treatment with GDNF reverses the loss of DCX-positive cells and normalizes cellular morphology. Scale bar, 20 μm. pilo, Pilocarpine.

$F_{(2,21)} = 54.71$, $p < 0.001$). GDNF reversed this loss of PV-positive cells.

Epilepsy-associated astrocytosis was evaluated using GFAP immunofluorescence (Vezzani et al., 2000). The quantification of GFAP-positive cells revealed that treatment with neither pilocarpine nor GDNF in pilocarpine-treated animals altered the number of astrocytes (Fig. 10*A*,*B*; 2 weeks: $F_{(2,23)} = 0.14$, $p = 0.88$; 12 weeks: $F_{(2,21)} = 0.11$, $p = 0.90$). However, many of the GFAP-positive cells in epileptic controls displayed short, thick processes, an indication of active astrocytosis (Fig. 10*D*, insert), whereas GFAP-positive cells of GDNF-treated rats were similar to those of naive animals, with a small cell body and thin processes (Fig. 10*C*,*E*, inserts).

Neurogenesis

As shown in Figure 11, GDNF treatment reversed the loss of DCX-positive cells that occurred following pilocarpine. In naive control rats, DCX-positive cells were present in the subgranular zone with notable elongations extending across the granular layer of the dentate gyrus region (Fig. 11*C*). In line with previous reports (Hattiangady et al., 2004), chronic epilepsy significantly decreased the numbers of these cells (by 48% and 70% at 2 and 12 weeks, respectively) and led to shorter and ectopic elongations. In contrast, treatment with GDNF restored the number of DCX-positive cells (2 weeks: $F_{(2,23)} = 6.67$, $p = 0.005$; 12 weeks: $F_{(2,21)} = 53.96$, $p < 0.001$). Qualitatively, these cells had their typical morphology with increased length and number of elongations, together with reduced cluster formation and reduced numbers of ectopic cells. The effects of GDNF were bilateral and more pronounced following 12 weeks of treatment.

Target engagement

Quantitative immunohistochemistry confirmed GDNF receptor engagement following GDNF device implantation. GDNF signals through a multicomponent receptor, first binding the Glycosylphosphatidylinisotol-anchored receptor α1 [GDNF family re-

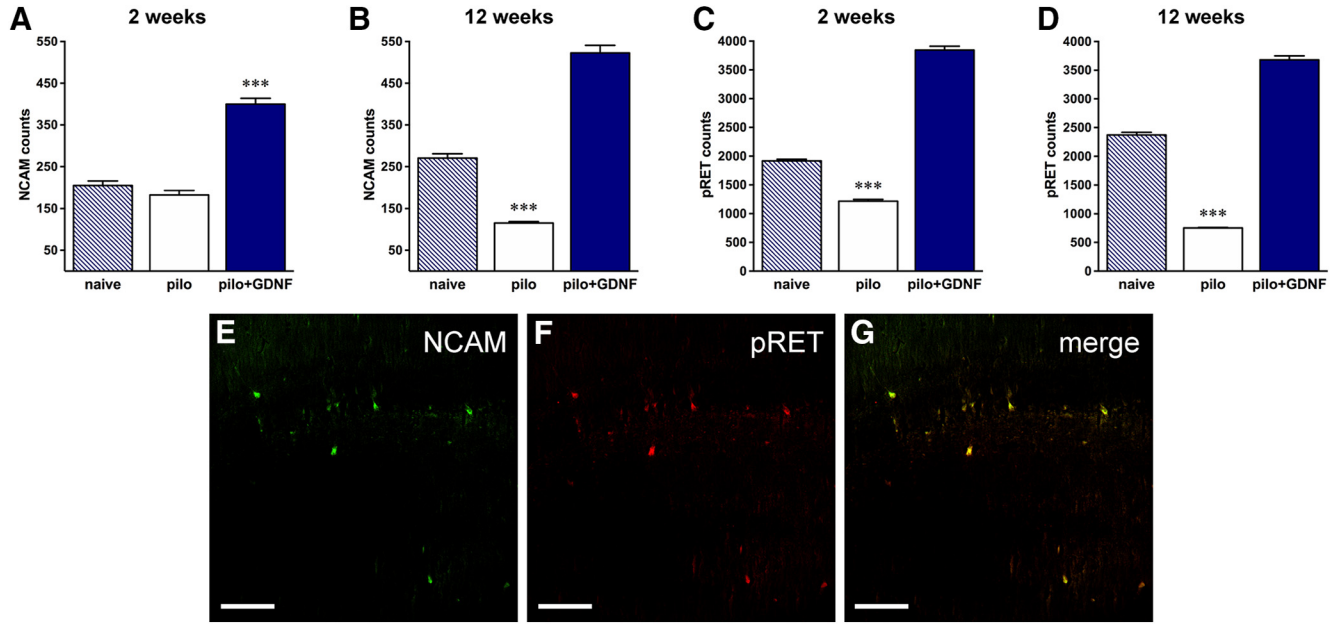

Figure 12. GDNF receptor engagement. ***A***, ***B***, Immunohistochemical quantification of NCAM expression after 2 (***A***) or 12 (***B***) weeks of GDNF treatment. Pilocarpine treatment significantly reduces the number of NCAM-positive cells at both time points. In contrast, GDNF increases NCAM expression above the levels observed in both the naive and pilocarpine-treated groups. ***C***, ***D***, Immunohistochemical quantification of phosphorylated Ret expression after 2 (***C***) or 12 (***D***) weeks of GDNF treatment. Pilocarpine treatment significantly reduces the number of pRet-positive cells at both time points. In contrast, GDNF increases pRET expression above the levels observed in both the naive and pilocarpine-treated groups. Data are expressed as the mean ± SEM of three to six animals per group. ***$p < 0.001$. Multiple comparisons were based on significant main effects resulting from the ANOVAs described in the Materials and Methods and Results. ***E***, ***F***, Representative images of NCAM and pRET double staining in GDNF-treated animals are shown. ***G***, The merged image. Similar patterns (although quantitatively different) were observed in naive and pilocarpine-treated animals. pilo, Pilocarpine.

ceptor α1 (GFRα1)], with the resulting complex recruiting the transmembrane receptor tyrosine kinase Ret or the NCAM to initiate downstream activation of FAK (focal adhesion kinase) and FYN (proto-oncogene tyrosine-protein kinase) signaling pathways (Airaksinen and Saarma, 2002; Paratcha et al., 2006; Duveau and Fritschy, 2010). To explore the role of NCAM-mediated GDNF effects on seizure frequency and neuroprotection, we quantified the numbers of NCAM-positive cells (Fig. 12*A*,*B*). In line with previous studies (Ledergerber et al., 2006), we observed a decrease in NCAM-positive cells in the hippocampus of pilocarpine-treated animals at both 2 and 12 weeks compared with naive animals (12% and 57%, respectively). In contrast, NCAM expression was dramatically increased by GDNF treatment (195% at 2 weeks and 193% at 12 weeks: 2 weeks: $F_{(2,23)} = 22.41$, $p < 0.001$; 12 weeks: $F_{(2,19)} = 46.63$, $p < 0.001$). A similar pattern was observed when the expression of phosphorylated Ret was assessed (Fig. 12*C*,*D*). Pilocarpine treatment significantly reduced the numbers of pRET-positive cells (by 37% and 68%, respectively, 2 and 12 weeks following administration). GDNF treatment resulted in a marked increase (100% and 55%, respectively, after 2 and 12 weeks of treatment; 2 weeks: $F_{(2,23)} = 158.59$, $p < 0.001$; 12 weeks: $F_{(2,21)} = 205.86$, $p < 0.001$).

Discussion

Current pharmacological therapies for epilepsy are palliative at best, frequently produce adverse effects, and are commonly completely ineffective. There is, accordingly, an urgent need for novel therapies in the treatment of epilepsy. Neurotrophic factors such as GDNF may have the capacity to provide therapeutic benefits, and encapsulated cell technologies might be able to provide a safe means of selectively targeting and continuously delivering GDNF to the epileptic area (Lindvall and Wahlberg, 2008; Eriksdotter-Jönhagen, 2012; Wahlberg et al., 2012; Orive et al., 2015). For these reasons, we engineered ARPE-19 cells to produce high levels of GDNF and enclosed them in a semipermeable capsule for implantation into the brain. The basic principle of this system is that the membrane allows oxygen and nutrients to enter and nourish the encapsulated cells while also allowing GDNF to leave the capsule and diffuse into the surrounding brain tissue, all the while eliminating exposure to the host immune system. This study provides important new data regarding the translation of this approach for continued development and human use. We report that GDNF devices can be implanted in the temporal lobe for prolonged periods of time while significantly elevating tissue levels of GDNF. The sustained delivery of GDNF was efficacious, as demonstrated by a pronounced and lasting reduction in seizure frequency. Importantly, nonmotor EEG seizure frequency was also reduced, indicating that the treatment actually suppresses seizures and does not merely attenuate their severity. This finding is in line with another study, in which we report that identical GDNF implants can also reduce the frequency of EEG seizures in the kainic acid model (Nanobashvili et al., 2018). In the present study, these favorable effects were rapid and progressive, with the seizure frequency reduced by 75% within 2 weeks after treatment and by 93% after 3 months of treatment. These effects are truly dramatic, considering that, in the pilocarpine model, only part of the seizures originates from the hippocampus (Toyoda et al., 2013). Therefore, this observation prompts the speculation that the hippocampus may also be implicated in seizures originating in other areas, and that treating the hippocampus may produce effects that surpass those expected (e.g., that the response to GDNF is nonlinear). The benefits of GDNF also appeared to extend beyond a simple symptomatic effect as it extended, even if in a less robust manner, well beyond removal of the devices. The concept of a potential disease-modifying effect is

further supported by the observation that the reduction in seizure frequency was accompanied by improvements in cognition and anxiety, both significant comorbidities of epilepsy (Strzelczyk et al., 2017; Michaelis et al., 2018). These benefits occurred without classic signs of mistargeted neurotrophic factor delivery such as alterations in food consumption, changes in daily activity, or other overt neurobehavioral changes. The observation that GDNF alleviated behavioral alterations, an expression of comorbidities of pilocarpine-induced epilepsy, is of particular importance. Although these comorbidities are well known and can even predate the diagnosis of epilepsy itself, no effective treatment has yet been developed. Once spontaneous seizures begin to occur and the diagnosis of epilepsy is made, the disease often progresses with increased severity of seizures and the appearance of neurological impairments. The etiology underlying these comorbid changes in humans is complex and includes numerous factors, like age of onset, seizure type/severity/duration, use of antiepileptic medications, and neuroanatomical changes (Pitkänen and Sutula, 2002; Aldenkamp and Arends, 2004; Elger et al., 2004; Lin et al., 2012). These neurobehavioral changes can also be either chronic, as part of the underlying etiology of the disease itself, or in constant dynamic evolution, due to recurrent seizures and interictal spikes. The complex interplay of chronic and dynamic underlying mechanisms has made it difficult to develop therapies capable of treating the broad spectrum of behavioral deficits in epilepsy, and the data provided here suggest that direct CNS delivery of trophic molecules such as GDNF can, at least in part, fulfill this requirement. In fact, pilocarpine SE induces a progressive increase in seizure frequency as well as significant impairments in the normal exploratory behavior (Brandt et al., 2006; Tchekalarova et al., 2017; avoidance of open space) and in the ability of the rat to use learning and recognition memory capabilities (Ainge et al., 2007; Wood et al., 2000), and all these signs of disease are strongly attenuated by GDNF.

The potential disease-modifying benefits of GDNF might be explained, at least in part, by long-lasting anatomical adaptations. A number of morphological changes can occur in epilepsy, including overt cell loss, synaptic reorganization, and neurogenesis. First, we applied volumetric and immunohistochemical analyses to both confirm the effects of pilocarpine on cellular degeneration and investigate whether GDNF can alter this pattern (Niessen et al., 2005). Consistent with reports of morphological changes in hippocampal volume and shape in TLE (Van Paesschen et al., 1995; Bernasconi et al., 2003; Hibar et al., 2016), we found that pilocarpine-induced SE produced a severe loss in hippocampal volume together with neurodegeneration and astrocytosis. Treatment with GDNF reversed both of these pathological changes and also reversed the loss of GABAergic parvalbumin-positive hippocampal cells that was previously found to continue for weeks after pilocarpine-induced SE (Soukupová et al., 2014). The roles of GABAergic transmission in epilepsy are complex, with some data indicating that increases in GABAergic activity occur during the interictal phase and just before seizure onset (D'Antuono et al., 2004; Ellender et al., 2014; Yekhlef et al., 2015; de Curtis and Avoli, 2016). Elevated GABAergic activity leads to increased extracellular potassium, which supports hyperexcitability and epileptiform synchronization (Zuckermann and Glaser, 1968; Fertziger and Ranck, 1970; de Curtis and Gnatkovsky, 2009). On the other hand, there are studies suggesting that the impaired GABAergic inhibition, related to a selective loss of inhibitory interneurons, accounts for epileptiform activity (Wendling et al., 2002; Forte et al., 2016). Although electrophysiological validations are required, it is tempting to speculate that the normalization of GABAergic transmission by GDNF prevents the broad spatial hypersynchronous recruitment of neurons and interneurons observed at the transition from interictal to ictal activity (Schevon et al., 2012; Fujita et al., 2014). GDNF can also promote the functional and morphological differentiation of GABAergic neurons via GFRα1 (Pozas and Ibáñez, 2005; Paratcha et al., 2006; Perrinjaquet et al., 2011). Because defects in cortical GFRα1 signaling increase excitability and sensitivity to subthreshold doses of epileptogenic agents (Canty et al., 2009), it can be hypothesized that GDNF, via GFRα1 activation, restores inhibitory neurotransmission in epileptic animals by supporting the survival of GABAergic neurons. As brain insults can induce neurogenesis of GABAergic cells (Magnusson et al., 2014), it is possible that exogenous GDNF-GFRα1 may redirect hippocampal granule cell neurogenesis after seizures toward inhibitory GABAergic cells (Marks et al., 2012).

The direct dependence of all the effects observed after GDNF treatment on GDNF receptors is difficult to assess with the currently available tools. Therefore, we attempted to at least demonstrate that the procedures led to target (GDNF receptor) engagement. To pursue this aim, we investigated the changes in NCAM and pRET. We found that GDNF reversed the decreased density of NCAM receptors and the expression of pRET in pilocarpine-treated animals, leading to levels well above those found in naive animals. These findings suggest a superactivation of GDNF receptors. In the adult hippocampal formation, NCAM is highly expressed in newly generated granule cells (Seki and Arai, 1993). The increased expression may reflect its role in regulating axonal outgrowth, synapse formation (Muller et al., 1996), and cell survival. The pattern was similar, with even more robust differences, when we assessed the expression of pRET. It has been previously reported that mRNA levels for GDNF and GDNF receptors (GFRα1 and RET) are region, cell, and insult specific (Reeben et al., 1998; Kokaia et al., 1999; Kanter-Schlifke et al., 2007). Here, we observe a robust increase of pRET expression indicating the activation of NCAM-independent GDNF signaling pathways.

The results described here form part of a program aimed at developing the use of polymer-encapsulated GDNF-secreting cells for direct and local delivery of GDNF to the brain of patients with epilepsy. These studies consistently demonstrated long-term and stable bioactive effects at doses shown to be safe in preclinical safety studies. To our knowledge, this is the first cellular delivery system capable of establishing the essential prerequisites of sustained, targeted, long-term delivery of sufficient quantities of GDNF to the temporal lobe. Based on the safety and efficacy of this platform technology, it represents a potentially novel and effective treatment for epilepsy.

References

Ainge JA, van der Meer MA, Langston RF, Wood ER (2007) Exploring the role of context-dependent hippocampal activity in spatial alternation behavior. Hippocampus 17:988–1002.

Airaksinen MS, Saarma M (2002) the GDNF family: signalling, biological functions and therapeutic value. Nat Rev Neurosci 3:383–394.

Aldenkamp A, Arends J (2004) The relative influence of epileptic EEG discharges, short nonconvulsive seizures, and type of epilepsy on cognitive function. Epilepsia 45:54–63.

Bernasconi N, Bernasconi A, Caramanos Z, Antel SB, Andermann F, Arnold DL (2003) Mesial temporal damage in temporal lobe epilepsy: a volumetric MRI study of the hippocampus, amygdala and parahippocampal region. Brain 126:462–469.

Brandt C, Gastens AM, Sun Mz, Hausknecht M, Löscher W (2006) Treatment with valproate after status epilepticus: effect on neuronal damage,

epileptogenesis, and behavioral alterations in rats. Neuropharmacology 51:789–804.
Canty AJ, Dietze J, Harvey M, Enomoto H, Milbrandt J, Ibáñez CF (2009) Regionalized loss of parvalbumin interneurons in the cerebral cortex of mice with deficits in GFRalpha1 signaling. J Neurosci 29:10695–10705.
Curia G, Longo D, Biagini G, Jones RS, Avoli M (2008) The pilocarpine model of temporal lobe epilepsy. J Neurosci Methods 172:143–157.
D'Antuono M, Louvel J, Köhling R, Mattia D, Bernasconi A, Olivier A, Turak B, Devaux A, Pumain R, Avoli M (2004) GABAA receptor-dependent synchronization leads to ictogenesis in the human dysplastic cortex. Brain 127:1626–1640.
de Curtis M, Avoli M (2016) GABAergic networks jump-start focal seizures. Epilepsia 57:679–687.
de Curtis M, Gnatkovsky V (2009) Reevaluating the mechanisms of focal ictogenesis: the role of low-voltage fast activity. Epilepsia 50:2514–2525.
Duveau V, Fritschy JM (2010) PSA-NCAM-dependent GDNF signaling limits neurodegeneration and epileptogenesis in temporal lobe epilepsy. Eur J Neurosci 32:89–98.
Ehara A, Ueda S (2009) Application of fluoro-jade C in acute and chronic neurodegeneration models: utilities and staining differences. Acta Histochem Cytochem 42:171–179.
Elger CE, Helmstaedter C, Kurthen M (2004) Chronic epilepsy and cognition. Lancet Neurol 3:663–672.
Ellender TJ, Raimondo JV, Irkle A, Lamsa KP, Akerman CJ (2014) excitatory effects of parvalbumin-expressing interneurons maintain hippocampal epileptiform activity via synchronous afterdischarges. J Neurosci 34:15208–15222.
Ellinwood EH Jr, Balster RL (1974) Rating the behavioral effects of amphetamine. Eur J Pharmacol 28:35–41.
Emerich DF, Orive G, Thanos C, Tornoe J, Wahlberg LU (2014) Encapsulated cell therapy for neurodegenerative diseases: from promise to product. Adv Drug Deliv Rev 67–68:131–141.
Engel J Jr, McDermott MP, Wiebe S, Langfitt JT, Stern JM, Dewar S, Sperling MR, Gardiner I, Erba G, Fried I, Jacobs M, Vinters HV, Mintzer S, Kieburtz K (2012) Early surgical therapy for drug-resistant temporal lobe epilepsy: a randomized trial. JAMA 307:922–930.
Eriksdotter-Jönhagen M, Linderoth B, Lind G, Aladellie L, Almkvist O, Andreasen N, Blennow K, Bogdanovic N, Jelic V, Kadir A, Nordberg A, Sundström E, Wahlund LO, Wall A, Wiberg M, Winblad B, Seiger A, Almqvist P, Wahlberg L (2012) Encapsulated cell biodelivery of nerve growth factor to the basal forebrain in patients with Alzheimer's disease. Dement Geriatr Cogn Disord 33:18–28.
Fertziger AP, Ranck JB Jr (1970) Potassium accumulation in interstitial space during epileptiform seizures. Exp Neurol 26:571–585.
Fjord-Larsen L, Kusk P, Tornøe J, Juliusson B, Torp M, Bjarkam CR, Nielsen MS, Handberg A, Sørensen JC, Wahlberg LU (2010) Long-term delivery of nerve growth factor by encapsulated cell biodelivery in the Göttingen minipig basal forebrain. Mol Ther 18:2164–2172.
Fjord-Larsen L, Kusk P, Emerich DF, Thanos C, Torp M, Bintz B, Tornøe J, Johnsen AH, Wahlberg LU (2012) Increased encapsulated cell biodelivery of nerve growth factor in the brain by transposon-mediated gene transfer. Gene Ther 19:1010–1017.
Forte N, Medrihan L, Cappetti B, Baldelli P, Benfenati F (2016) 2-Deoxy-d-glucose enhances tonic inhibition through the neurosteroid-mediated activation of extrasynaptic GABAA receptors. Epilepsia 57:1987–2000.
Fujita S, Toyoda I, Thamattoor AK, Buckmaster PS (2014) Preictal activity of subicular, CA1, and dentate gyrus principal neurons in the dorsal hippocampus before spontaneous seizures in a rat model of temporal lobe epilepsy. J Neurosci 34:16671–16687.
Greenwald AG, Gonzalez R, Harris RJ, Guthrie D (1996) Effect sizes and p values: what should be reported and what should be replicated? Psychophysiology 33:175–183.
Hattiangady B, Rao MS, Shetty AK (2004) Chronic temporal lobe epilepsy is associated with severely declined dentate neurogenesis in the adult hippocampus. Neurobiol Dis 17:473–490.
Hibar DP, Westlye LT, van Erp TG, Rasmussen J, Leonardo CD, Faskowitz J, Haukvik UK, Hartberg CB, Doan NT, Agartz I, Dale AM, Gruber O, Krämer B, Trost S, Liberg B, Abé C, Ekman CJ, Ingvar M, Landén M, Fears SC, et al (2016) Subcortical volumetric abnormalities in bipolar disorder. Mol Psychiatry 21:1710–1716.
Humpel C, Hoffer B, Strömberg I, Bektesh S, Collins F, Olson L (1994) Neurons of the hippocampal formation express glial cell line-derived neurotrophic factor messenger RNA in response to kainate-induced excitation. Neuroscience 59:791–795.
Kanter-Schlifke I, Georgievska B, Kirik D, Kokaia M (2007) Seizure suppression by GDNF gene therapy in animal models of epilepsy. Mol Ther 15:1106–1113.
Kanter-Schlifke I, Fjord-Larsen L, Kusk P, Angehagen M, Wahlberg L, Kokaia M (2009) GDNF released from encapsulated cells suppresses seizure activity in the epileptic hippocampus Exp Neurol 216:413–419.
Kilkenny C, Browne W, Cuthill IC, Emerson M, Altman DG (2011) Animal research: reporting in vivo experiments—the ARRIVE guidelines. J Cereb Blood Flow Metab 31:991–993.
Kokaia Z, Airaksinen MS, Nanobashvili A, Larsson E, Kujamäki E, Lindvall O, Saarma M (1999) GDNF family ligands and receptors are differentially regulated after brain insults in the rat. Eur J Neurosci 11:1202–1216.
Kwan P, Brodie MJ (2000) Epilepsy after the first drug fails: substitution or add-on? Seizure 9:464–468.
Ledergerber D, Fritschy JM, Kralic JE (2006) Impairment of dentate gyrus neuronal progenitor cell differentiation in a mouse model of temporal lobe epilepsy. Exp Neurol 199:130–142.
Ledri LN, Melin E, Christiansen SH, Gøtzsche CR, Cifra A, Woldbye DP, Kokaia M (2016) Translational approach for gene therapy in epilepsy: model system and unilateral overexpression of neuropeptide Y and Y2 receptors. Neurobiol Dis 86:52–61.
Lidster K, Jefferys JG, Blümcke I, Crunelli V, Flecknell P, Frenguelli BG, Gray WP, Kaminski R, Pitkänen A, Ragan I, Shah M, Simonato M, Trevelyan A, Volk H, Walker M, Yates N, Prescott MJ (2016) Opportunities for improving animal welfare in rodent models of epilepsy and seizures. J Neurosci Methods 260:2–25.
Lin JJ, Mula M, Hermann BP (2012) Uncovering the neurobehavioural comorbidities of epilepsy over the lifespan. Lancet 380:1180–1192.
Lindvall O, Wahlberg LU (2008) Encapsulated cell biodelivery of GDNF: a novel clinical strategy for neuroprotection and neuroregeneration in Parkinson's disease? Exp Neurol 209:82–88.
Magnusson JP, Göritz C, Tatarishvili J, Dias DO, Smith EM, Lindvall O, Kokaia Z, Frisén J (2014) A latent neurogenic program in astrocytes regulated by notch signaling in the mouse. Science 346:237–241.
Marks C, Belluscio L, Ibáñez CF (2012) Critical role of GFRα1 in the development and function of the main olfactory system. J Neurosci 32:17306–17320.
Mazzuferi M, Palma E, Martinello K, Maiolino F, Roseti C, Fucile S, Fabene PF, Schio F, Pellitteri M, Sperk G, Miledi R, Eusebi F, Simonato M (2010) Proc Natl Acad Sci U S A 107:3180–3185.
Michaelis R, Tang V, Wagner JL, Modi AC, Curt LaFrance W Jr, Goldstein LH, Lundgren T, Reuber M (2018) Cochrane systematic review and meta-analysis of the impact of psychological treatments for people with epilepsy on health-related quality of life. Epilepsia 59:315–332.
Muller D, Wang C, Skibo G, Toni N, Cremer H, Calaora V, Rougon G, Kiss JZ (1996) PSA-NCAM is required for activity-induced synaptic plasticity. Neuron 17:413–422.
Nanobashvili A, Melin E, Emerich D, Tornøe J, Simonato M, Wahlberg L, Kokaia M (2018) Unilateral ex vivo gene therapy by GDNF in epileptic rats. Gene Ther. Advance online publication. Retrieved November 21, 2018. doi: 10.1038/s41434-018-0050-7.
Niessen HG, Angenstein F, Vielhaber S, Frisch C, Kudin A, Elger CE, Heinze HJ, Scheich H, Kunz WS (2005) Volumetric magnetic resonance imaging of functionally relevant structural alterations in chronic epilepsy after pilocarpine-induced status epilepticus in rats. Epilepsia 46:1021–1026.
Nikitidou L, Torp M, Fjord-Larsen L, Kusk P, Wahlberg LU, Kokaia M (2014) Encapsulated galanin-producing cells attenuate focal epileptic seizures in the hippocampus. Epilepsia 55:167–174.
Nogueira MH, Yasuda CL, Coan AC, Kanner AM, Cendes F (2017) Concurrent mood and anxiety disorders are associated with pharmacoresistant seizures in patients with MTLE. Epilepsia 58:1268–1276.
Orive G, Santos E, Poncelet D, Hernández RM, Pedraz JL, Wahlberg LU, De Vos P, Emerich D (2015) Cell encapsulation: technical and clinical advances. Trends Pharmacol Sci 36:537–546.
Paradiso B, Marconi P, Zucchini S, Berto E, Binaschi A, Bozac A, Buzzi A, Mazzuferi M, Magri E, Navarro Mora G, Rodi D, Su T, Volpi I, Zanetti L, Marzola A, Manservigi R, Fabene PF, Simonato M (2009) Localized delivery of fibroblast growth factor–2 and brain-derived neurotrophic factor reduces spontaneous seizures in an epilepsy model. Proc Natl Acad Sci U S A 106:7191–7196.

Paradiso B, Zucchini S, Su T, Bovolenta R, Berto E, Marconi P, Marzola A, Navarro Mora G, Fabene PF, Simonato M (2011) Localized overexpression of FGF-2 and BDNF in hippocampus reduces mossy fiber sprouting and spontaneous seizures up to 4 weeks after pilocarpine-induced status epilepticus. Epilepsia 52:572–578.

Paratcha G, Ibáñez CF, Ledda F (2006) GDNF is a chemoattractant factor for neuronal precursor cells in the rostral migratory stream. Mol Cell Neurosci 31:505–514.

Paxinos G, Watson C (2007) The rat brain in stereotaxic coordinates. Amsterdam: Elsevier Academic.

Perrinjaquet M, Sjöstrand D, Moliner A, Zechel S, Lamballe F, Maina F, Ibáñez CF (2011) MET signaling in GABAergic neuronal precursors of the medial ganglionic eminence restricts GDNF activity in cells that express GFRα1 and a new transmembrane receptor partner. J Cell Sci 124:2797–2805.

Pitkänen A, Sutula TP (2002) Is epilepsy a progressive disorder? prospects for new therapeutic approaches in temporal-lobe epilepsy. Lancet Neurol 1:173–181.

Pozas E, Ibáñez CF (2005) GDNF and GFRalpha1 promote differentiation and tangential migration of cortical GABAergic neurons. Neuron 45:701–713.

Racine RJ, Gartner JG, Burnham WM (1972) Epileptiform activity and neural plasticity in limbic structures. Brain Res. 47:262–268.

Reeben M, Laurikainen A, Hiltunen JO, Castrén E, Saarma M (1998) The messenger RNAs for both glial cell line-derived neurotrophic factor receptors, c-ret and GDNFRalpha, are induced in the rat brain in response to kainate-induced excitation. Neuroscience 83:151–159.

Schevon CA, Weiss SA, McKhann G Jr, Goodman RR, Yuste R, Emerson RG, Trevelyan AJ (2012) Evidence of an inhibitory restraint of seizure activity in humans. Nat Commun 3:1060.

Seki T, Arai Y (1993) Highly polysialylated neural cell adhesion molecule (NCAM-H) is expressed by newly generated granule cells in the dentate gyrus of the adult rat. J Neurosci 13:2351–2358.

Simonato M (2014) Gene therapy for epilepsy. Epilepsy Behav 38:125–130.

Simonato M, Bennett J, Boulis NM, Castro MG, Fink DJ, Goins WF, Gray SJ, Lowenstein PR, Vandenberghe LH, Wilson TJ, Wolfe JH, Glorioso JC (2013) Progress in gene therapy for neurological disorders. Nat Rev Neurol 9:277–291.

Soukupová M, Binaschi A, Falcicchia C, Zucchini S, Roncon P, Palma E, Magri E, Grandi E, Simonato M (2014) Exp Neurol 257:39–49.

Sridharan R (2002) Epidemiology of epilepsy. Curr Sci 82:664–670.

Stephen LJ, Brodie MJ (2000) Epilepsy in elderly people. Lancet 355:1441–1446.

Strzelczyk A, Griebel C, Lux W, Rosenow F, Reese JP (2017) The burden of severely drug-refractory epilepsy: a comparative longitudinal evaluation of mortality, morbidity, resource use, and cost using German health insurance data. Front Neurol 8:712.

Tchekalarova J, Atanasova D, Nenchovska Z, Atanasova M, Kortenska L, Gesheva R, Lazarov N (2017) Agomelatine protects against neuronal damage without preventing epileptogenesis in the kainate model of temporal lobe epilepsy. Neurobiol Dis 104:1–14.

Tornøe J, Torp M, Jørgensen JR, Emerich DF, Thanos C, Bintz B, Fjord-Larsen L, Wahlberg LU (2012) Encapsulated cell-based biodelivery of meteorin is neuroprotective in the quinolinic acid ratmodel of neurodegenerative disease. Restor Neurol Neurosci 30:225–236.

Toyoda I, Bower MR, Leyva F, Buckmaster PS (2013) Early activation of ventral hippocampus and subiculum during spontaneous seizures in a rat model of temporal lobe epilepsy. J Neurosci 33:11100–11115.

Van Paesschen W, Sisodiya S, Connelly A, Duncan JS, Free SL, Raymond AA, Grünewald RA, Revesz T, Shorvon SD, Fish DR (1995) Quantitative hippocampal MRI and intractable temporal lobe epilepsy. Neurology 45:2233–2240.

Vezzani A, Moneta D, Conti M, Richichi C, Ravizza T, De Luigi A, De Simoni MG, Sperk G, Andell-Jonsson S, Lundkvist J, Iverfeldt K, Bartfai T (2000) Powerful anticonvulsant action of IL-1 receptor antagonist on intracerebral injection and astrocytic overexpression in mice. Proc Natl Acad Sci U S A 97:11534–11539.

Wahlberg LU, Lind G, Almqvist PM, Kusk P, Tornøe J, Juliusson B, Söderman M, Selldén E, Seiger Å, Eriksdotter-Jönhagen M, Linderoth B (2012) Targeted delivery of nerve growth factor via encapsulated cell biodelivery in alzheimer disease: a technology platform for restorative neurosurgery. J Neurosurg 117:340–347.

Wendling F, Bartolomei F, Bellanger JJ, Chauvel P (2002) Epileptic fast activity can be explained by a model of impaired GABAergic dendritic inhibition. Eur J Neurosci 15:1499–1508.

Williams PA, White AM, Clark S, Ferraro DJ, Swiercz W, Staley KJ, Dudek FE (2009) Development of spontaneous recurrent seizures after kainate-induced status epilepticus. J Neurosci 29:2103–2112.

Wood ER, Dudchenko PA, Robitsek RJ, Eichenbaum H (2000) Hippocampal neurons encode information about different types of memory episodes occurring in the same location. Neuron 27:623–633.

Yekhlef L, Breschi GL, Lagostena L, Russo G, Taverna S (2015) Selective activation of parvalbumin-or somatostatin-expressing interneurons triggers epileptic seizure-like activity in mouse medial entorhinal cortex. J Neurophysiol 113:1616–1630.

Yoo YM, Lee CJ, Lee U, Kim YJ (2006) Neuroprotection of adenoviral-vector-mediated GDNF expression against kainic-acid-induced excitotoxicity in the rat hippocampus. Exp Neurol 200:407–417.

Zuckermann EC, Glaser GH (1968) Hippocampal epileptic activity induced by localized ventricular perfusion with high-potassium cerebrospinal fluid. Exp Neurol 20:87–110.

Chapter 6: Conclusions and future perspectives

Epilepsy is a serious, heterogeneous neurological disorder affecting 1% of the population, from children to adults. Nowadays no cure is available. Traditional therapeutic approaches led to understand some of the mechanistic features of these diseases. However, anti-epileptic drugs (AEDs) do not offer seizure control in about 30% of epileptic patients [104]. Moreover, epilepsy is not just seizures, because this disease is characterized by a plethora of neurologic and psychiatric comorbidities, which are often not even referred to the doctors because of the strong stigma that accompanies this condition.

Our starting point is thus a complex disease, including different conditions with common symptoms but different etiologies and whose causal mechanisms are still little understood. We thought to apply the principles of systems genetics rather than looking at single mechanisms. Systems genetics allows to identify variations in the gene expression networks through transcriptome analysis, possibly leading to a better understanding of the mechanisms at the basis of a disease. Our systems genetics approach identified a master regulator of a network of pro-epileptic genes, SESN3, that is up-regulated in samples of TLE patients [42]. In order to better investigate on how the encoded protein actually can regulate and influence epilepsy development, we evaluated the phenotype of SESN3-knock-out (SESN3-KO) rats. Not only SESN3-KO rats were more resistant to SE induced by chemoconvulsants, but were also less susceptible to anxious behaviors. Because some compensatory mechanism may be in place in these KO animals, it would be interesting in the future to use conditional SESN3-KOs.

A systems genetics approach was also applied to investigate biomarkers of epileptogenesis, by analyzing RNA samples in plasma. This study was designed with the perfect control group, i.e. animals that experienced an epileptogenic brain insult but did not subsequently become epileptic. Four different laboratories throughout Europe put their efforts in this study. Biomarkers that could help identifying patients at risk of developing epilepsy are urgently needed, as they would offer the opportunity to preventively treat patients before they develop the disease. By performing a meta-analysis of the data, we identified five miRNAs (of which three are already known in literature) that were dysregulated in plasma samples of animals that were to become epileptic. Two of these miRNAs, namely miR-129-5p and miR-138-5p, were already reported to be dysregulated in brain samples from experimental models of TLE and/or surgical resection of epileptic focus in patients [85]. These two miRNAs are thought to be involved in pathophysiological

events leading to the transformation of a healthy brain into an epileptic one, such as neuroplasticity and neuroprotection processes controlled by MAP kinases [51,105]. However, it remains undetermined if the plasma levels of these miRNAs could be sign of modifications occurring in the brain during epileptogenesis. We are now planning to enlarge the cohort of cases to strengthen the data and extend them to other models of TLE.

Systems genetics cannot completely replace traditional investigation. On a more "classical" approaches, we thought to exploit the potential of neurotrophic factors (NTFs) for treating epileptic seizures and comorbidities. Brain-derived neurotrophic factor (BDNF) and glial-cell line derive neurotrophic factor (GDNF) may exert an anti-epileptic effect, because they are known to modulate mechanisms at the basis of epilepsy development and seizures occurrence. In addition to neurotrophic effects, these NTFs have effects that are more directly relevant for epilepsy. For examples, BDNF increases the function of parvalbumin interneurons, thereby potentiating GABA signal [99]. Chemically and electrically induced seizures can be suppressed by local infusion of GDNF or injection into the hippocampus of viral vectors expressing GDNF [106, 107, 108]. We demonstrated that the delivery of these neurotrophic factors, directly in the hippocampi of epileptic rats, dramatically reduced the frequency of epileptic seizures. Moreover, BDNF and GDNF were able to partially revert the cognitive impairment observed in the chronic phase of the diseases.

References

1. Pitkänen A, Lukasiuk K. Mechanisms of epileptogenesis and potential treatment targets. *The Lancet Neurology* 2011; **10**(2): 173-86.
2. Fisher RS, van Emde Boas W, Blume W, et al. Epileptic seizures and epilepsy: definitions proposed by the International League Against Epilepsy (ILAE) and the International Bureau for Epilepsy (IBE). *Epilepsia* 2005; **46**(4): 470-2.
3. Fisher RS. An overview of the 2017 ILAE operational classification of seizure types. *Epilepsy Behav* 2017; **70**(Pt A): 271-3.
4. Crowder KM, Gunther JM, Jones TA, et al. Abnormal neurotransmission in mice lacking synaptic vesicle protein 2A (SV2A). *Proc Natl Acad Sci U S A* 1999; **96**(26): 15268-73.
5. Liu G, Slater N, Perkins A. Epilepsy: Treatment Options. *Am Fam Physician* 2017; **96**(2): 87-96.
6. Villanueva V, Carreno M, Herranz Fernandez JL, Gil-Nagel A. Surgery and electrical stimulation in epilepsy: selection of candidates and results. *Neurologist* 2007; **13**(6 Suppl 1): S29-37.
7. Fan JJ, Shan W, Wu JP, Wang Q. Research progress of vagus nerve stimulation in the treatment of epilepsy. *CNS Neurosci Ther* 2019.
8. Salanova V. Deep brain stimulation for epilepsy. *Epilepsy Behav* 2018; **88S**: 21-4.
9. Lusardi TA, Akula KK, Coffman SQ, Ruskin DN, Masino SA, Boison D. Ketogenic diet prevents epileptogenesis and disease progression in adult mice and rats. *Neuropharmacology* 2015; **99**: 500-9.
10. Caraballo R, Vaccarezza M, Cersosimo R, et al. Long-term follow-up of the ketogenic diet for refractory epilepsy: multicenter Argentinean experience in 216 pediatric patients. *Seizure* 2011; **20**(8): 640-5.
11. Chen F, He X, Luan G, Li T. Role of DNA Methylation and Adenosine in Ketogenic Diet for Pharmacoresistant Epilepsy: Focus on Epileptogenesis and Associated Comorbidities. *Front Neurol* 2019; **10**: 119.
12. Freeman JM, Kossoff EH, Hartman AL. The ketogenic diet: one decade later. *Pediatrics* 2007; **119**(3): 535-43.
13. Blair RD. Temporal lobe epilepsy semiology. *Epilepsy Res Treat* 2012; **2012**: 751510.
14. Allone C, Lo Buono V, Corallo F, et al. Neuroimaging and cognitive functions in temporal lobe epilepsy: A review of the literature. *J Neurol Sci* 2017; **381**: 7-15.
15. Thom M. Review: Hippocampal sclerosis in epilepsy: a neuropathology review. *Neuropathol Appl Neurobiol* 2014; **40**(5): 520-43.
16. Pitkanen A, Lukasiuk K, Dudek FE, Staley KJ. Epileptogenesis. *Cold Spring Harb Perspect Med* 2015; **5**(10).
17. Dudek FE, Staley KJ. The Time Course and Circuit Mechanisms of Acquired Epileptogenesis. In: th, Noebels JL, Avoli M, Rogawski MA, Olsen RW, Delgado-Escueta AV, eds. Jasper's Basic Mechanisms of the Epilepsies. Bethesda (MD); 2012.
18. Kadam SD, Smith-Hicks CL, Smith DR, Worley PF, Comi AM. Functional integration of new neurons into hippocampal networks and poststroke comorbidities following neonatal stroke in mice. *Epilepsy Behav* 2010; **18**(4): 344-57.
19. Bertram E. The relevance of kindling for human epilepsy. *Epilepsia* 2007; **48 Suppl 2**: 65-74.
20. Pitkanen A, Sutula TP. Is epilepsy a progressive disorder? Prospects for new therapeutic approaches in temporal-lobe epilepsy. *Lancet Neurol* 2002; **1**(3): 173-81.

21. Jutila L, Immonen A, Partanen K, et al. Neurobiology of epileptogenesis in the temporal lobe. *Adv Tech Stand Neurosurg* 2002; **27**: 5-22.
22. Webster KM, Sun M, Crack P, O'Brien TJ, Shultz SR, Semple BD. Inflammation in epileptogenesis after traumatic brain injury. *J Neuroinflammation* 2017; **14**(1): 10.
23. Shetty AK. Hippocampal injury-induced cognitive and mood dysfunction, altered neurogenesis, and epilepsy: can early neural stem cell grafting intervention provide protection? *Epilepsy Behav* 2014; **38**: 117-24.
24. Santhakumar V, Aradi I, Soltesz I. Role of mossy fiber sprouting and mossy cell loss in hyperexcitability: a network model of the dentate gyrus incorporating cell types and axonal topography. *J Neurophysiol* 2005; **93**(1): 437-53.
25. Kanner AM. Management of psychiatric and neurological comorbidities in epilepsy. *Nat Rev Neurol* 2016; **12**(2): 106-16.
26. Korczyn AD, Schachter SC, Brodie MJ, et al. Epilepsy, cognition, and neuropsychiatry (Epilepsy, Brain, and Mind, part 2). *Epilepsy & Behavior* 2013; **28**(2): 283-302.
27. Sankar R, Mazarati A. Neurobiology of Depression as a Comorbidity of Epilepsy. In: th, Noebels JL, Avoli M, Rogawski MA, Olsen RW, Delgado-Escueta AV, eds. Jasper's Basic Mechanisms of the Epilepsies. Bethesda (MD); 2012.
28. Rider FK, Danilenko OA, Grishkina MN, et al. Depression and Epilepsy: Comorbidity, Pathogenetic Similarity, and Principles of Treatment. *Neuroscience and Behavioral Physiology* 2017; **48**(1): 78-82.
29. Vazquez B, Devinsky O. Epilepsy and anxiety. *Epilepsy & Behavior* 2003; **4**: 20-5.
30. Mazarati A. Epilepsy and forgetfulness: one impairment, multiple mechanisms. *Epilepsy Curr* 2008; **8**(1): 25-6.
31. Ben-Ari Y, Pradelles P, Gros C, Dray F. Identification of authentic substance P in striatonigral and amygdaloid nuclei using combined high performance liquid chromatography and radioimmunoassay. *Brain Res* 1979; **173**(2): 360-3.
32. Hamilton SE, Loose MD, Qi M, et al. Disruption of the m1 receptor gene ablates muscarinic receptor-dependent M current regulation and seizure activity in mice. *Proc Natl Acad Sci U S A* 1997; **94**(24): 13311-6.
33. Turski WA, Cavalheiro EA, Schwarz M, Czuczwar SJ, Kleinrok Z, Turski L. Limbic seizures produced by pilocarpine in rats: behavioural, electroencephalographic and neuropathological study. *Behav Brain Res* 1983; **9**(3): 315-35.
34. Racine RJ, Gartner JG, Burnham WM. Epileptiform activity and neural plasticity in limbic structures. *Brain Res* 1972; **47**(1): 262-8.
35. Gaitatzis A, Sisodiya SM, Sander JW. The somatic comorbidity of epilepsy: a weighty but often unrecognized burden. *Epilepsia* 2012; **53**(8): 1282-93.
36. Pitkanen A, Ekolle Ndode-Ekane X, Lapinlampi N, Puhakka N. Epilepsy biomarkers - Toward etiology and pathology specificity. *Neurobiol Dis* 2019; **123**: 42-58.
37. Taylor RS, Sander JW, Taylor RJ, Baker GA. Predictors of health-related quality of life and costs in adults with epilepsy: a systematic review. *Epilepsia* 2011; **52**(12): 2168-80.
38. Keezer MR, Sisodiya SM, Sander JW. Comorbidities of epilepsy: current concepts and future perspectives. *The Lancet Neurology* 2016; **15**(1): 106-15.
39. Steimer T. Animal models of anxiety disorders in rats and mice: some conceptual issues. *Dialogues Clin Neurosci* 2011; **13**(4): 495-506.

40. Chen SD, Wang YL, Liang SF, Shaw FZ. Rapid Amygdala Kindling Causes Motor Seizure and Comorbidity of Anxiety- and Depression-Like Behaviors in Rats. *Front Behav Neurosci* 2016; **10**: 129.
41. Hesdorffer DC, Ishihara L, Mynepalli L, Webb DJ, Weil J, Hauser WA. Epilepsy, suicidality, and psychiatric disorders: a bidirectional association. *Ann Neurol* 2012; **72**(2): 184-91.
42. Johnson MR, Behmoaras J, Bottolo L, et al. Systems genetics identifies Sestrin 3 as a regulator of a proconvulsant gene network in human epileptic hippocampus. *Nat Commun* 2015; **6**: 6031.
43. Rhee SG, Bae SH. The antioxidant function of sestrins is mediated by promotion of autophagic degradation of Keap1 and Nrf2 activation and by inhibition of mTORC1. *Free Radic Biol Med* 2015; **88**(Pt B): 205-11.
44. Citraro R, Leo A, Constanti A, Russo E, De Sarro G. mTOR pathway inhibition as a new therapeutic strategy in epilepsy and epileptogenesis. *Pharmacol Res* 2016; **107**: 333-43.
45. Talos DM, Jacobs LM, Gourmaud S, et al. Mechanistic target of rapamycin complex 1 and 2 in human temporal lobe epilepsy. *Ann Neurol* 2018; **83**(2): 311-27.
46. Li N, Lee B, Liu RJ, et al. mTOR-dependent synapse formation underlies the rapid antidepressant effects of NMDA antagonists. *Science* 2010; **329**(5994): 959-64.
47. Tchekalarova J, Moyanova S, Fusco AD, Ngomba RT. The role of the melatoninergic system in epilepsy and comorbid psychiatric disorders. *Brain Res Bull* 2015; **119**(Pt A): 80-92.
48. Porsolt RD. Animal model of depression. *Biomedicine* 1979; **30**(3): 139-40.
49. D'Aquila PS, Panin F, Serra G. Long-term imipramine withdrawal induces a depressive-like behaviour in the forced swimming test. *Eur J Pharmacol* 2004; **492**(1): 61-3.
50. Ennaceur A, Delacour J. A new one-trial test for neurobiological studies of memory in rats. 1: Behavioral data. *Behav Brain Res* 1988; **31**(1): 47-59.
51. Roncon P, Soukupova M, Binaschi A, et al. MicroRNA profiles in hippocampal granule cells and plasma of rats with pilocarpine-induced epilepsy--comparison with human epileptic samples. *Sci Rep* 2015; **5**: 14143.
52. Raedt R, Van Dycke A, Van Melkebeke D, et al. Seizures in the intrahippocampal kainic acid epilepsy model: characterization using long-term video-EEG monitoring in the rat. *Acta Neurol Scand* 2009; **119**(5): 293-303.
53. Curia G, Longo D, Biagini G, Jones RS, Avoli M. The pilocarpine model of temporal lobe epilepsy. *J Neurosci Methods* 2008; **172**(2): 143-57.
54. Dalina AA, Kovaleva IE, Budanov AV. Sestrins are Gatekeepers in the Way from Stress to Aging and Disease. *Molecular Biology* 2018; **52**(6): 823-35.
55. Narasimhan SD, Mukhopadhyay A, Tissenbaum HA. InAKTivation of insulin/IGF-1 signaling by dephosphorylation. *Cell Cycle* 2009; **8**(23): 3878-84.
56. Narasimhan SD, Yen K, Tissenbaum HA. Converging pathways in lifespan regulation. *Curr Biol* 2009; **19**(15): R657-66.
57. Huang LG, Zou J, Lu QC. Silencing rno-miR-155-5p in rat temporal lobe epilepsy model reduces pathophysiological features and cell apoptosis by activating Sestrin-3. *Brain Res* 2018; **1689**: 109-22.
58. Bragin A, Wilson CL, Almajano J, Mody I, Engel J, Jr. High-frequency oscillations after status epilepticus: epileptogenesis and seizure genesis. *Epilepsia* 2004; **45**(9): 1017-23.
59. Budanov AV. Stress-responsive sestrins link p53 with redox regulation and mammalian target of rapamycin signaling. *Antioxid Redox Signal* 2011; **15**(6): 1679-90.

60. Wang H, Quirion R, Little PJ, et al. Forkhead box O transcription factors as possible mediators in the development of major depression. *Neuropharmacology* 2015; **99**: 527-37.
61. Polter A, Yang S, Zmijewska AA, et al. Forkhead box, class O transcription factors in brain: regulation and behavioral manifestation. *Biol Psychiatry* 2009; **65**(2): 150-9.
62. Pineda EA, Hensler JG, Sankar R, Shin D, Burke TF, Mazarati AM. Interleukin-1beta causes fluoxetine resistance in an animal model of epilepsy-associated depression. *Neurotherapeutics* 2012; **9**(2): 477-85.
63. Zucchini S, Marucci G, Paradiso B, et al. Identification of miRNAs differentially expressed in human epilepsy with or without granule cell pathology. *PLoS One* 2014; **9**(8): e105521.
64. Tiwari D, Peariso K, Gross C. MicroRNA-induced silencing in epilepsy: Opportunities and challenges for clinical application. *Dev Dyn* 2018; **247**(1): 94-110.
65. Denli AM, Tops BB, Plasterk RH, Ketting RF, Hannon GJ. Processing of primary microRNAs by the Microprocessor complex. *Nature* 2004; **432**(7014): 231-5.
66. Zhang H, Kolb FA, Jaskiewicz L, Westhof E, Filipowicz W. Single processing center models for human Dicer and bacterial RNase III. *Cell* 2004; **118**(1): 57-68.
67. Meijer HA, Smith EM, Bushell M. Regulation of miRNA strand selection: follow the leader? *Biochem Soc Trans* 2014; **42**(4): 1135-40.
68. O'Brien J, Hayder H, Zayed Y, Peng C. Overview of MicroRNA Biogenesis, Mechanisms of Actions, and Circulation. *Front Endocrinol (Lausanne)* 2018; **9**: 402.
69. Pitkanen A, Henshall DC, Cross JH, et al. Advancing research toward faster diagnosis, better treatment, and end of stigma in epilepsy. *Epilepsia* 2019; **60**(7): 1281-92.
70. Engel J, Jr. Epileptogenesis, traumatic brain injury, and biomarkers. *Neurobiol Dis* 2019; **123**: 3-7.
71. Pitkänen A, Löscher W, Vezzani A, et al. Advances in the development of biomarkers for epilepsy. *The Lancet Neurology* 2016; **15**(8): 843-56.
72. Choy M, Dube CM, Patterson K, et al. A novel, noninvasive, predictive epilepsy biomarker with clinical potential. *J Neurosci* 2014; **34**(26): 8672-84.
73. Walker LE, Frigerio F, Ravizza T, et al. Molecular isoforms of high-mobility group box 1 are mechanistic biomarkers for epilepsy. *J Clin Invest* 2017; **127**(6): 2118-32.
74. Maroso M, Balosso S, Ravizza T, et al. Toll-like receptor 4 and high-mobility group box-1 are involved in ictogenesis and can be targeted to reduce seizures. *Nat Med* 2010; **16**(4): 413-9.
75. Pollard JR, Eidelman O, Mueller GP, et al. The TARC/sICAM5 Ratio in Patient Plasma is a Candidate Biomarker for Drug Resistant Epilepsy. *Front Neurol* 2012; **3**: 181.
76. Hsiao KY, Sun HS, Tsai SJ. Circular RNA - New member of noncoding RNA with novel functions. *Exp Biol Med (Maywood)* 2017; **242**(11): 1136-41.
77. Brennan GP, Dey D, Chen Y, et al. Dual and Opposing Roles of MicroRNA-124 in Epilepsy Are Mediated through Inflammatory and NRSF-Dependent Gene Networks. *Cell Rep* 2016; **14**(10): 2402-12.
78. Brandt C, Tollner K, Klee R, Broer S, Loscher W. Effective termination of status epilepticus by rational polypharmacy in the lithium-pilocarpine model in rats: Window of opportunity to prevent epilepsy and prediction of epilepsy by biomarkers. *Neurobiol Dis* 2015; **75**: 78-90.

79. Brandt C, Rankovic V, Tollner K, Klee R, Broer S, Loscher W. Refinement of a model of acquired epilepsy for identification and validation of biomarkers of epileptogenesis in rats. *Epilepsy Behav* 2016; **61**: 120-31.
80. van Vliet EA, Puhakka N, Mills JD, et al. Standardization procedure for plasma biomarker analysis in rat models of epileptogenesis: Focus on circulating microRNAs. *Epilepsia* 2017; **58**(12): 2013-24.
81. Bofill-De Ros X, Yang A, Gu S. IsomiRs: Expanding the miRNA repression toolbox beyond the seed. *Biochim Biophys Acta Gene Regul Mech* 2019: 194373.
82. Nemeth K, Darvasi O, Liko I, et al. Comprehensive analysis of circulating microRNAs in plasma of patients with pituitary adenomas. *J Clin Endocrinol Metab* 2019.
83. Rajman M, Metge F, Fiore R, et al. A microRNA-129-5p/Rbfox crosstalk coordinates homeostatic downscaling of excitatory synapses. *EMBO J* 2017; **36**(12): 1770-87.
84. Korotkov A, Mills JD, Gorter JA, van Vliet EA, Aronica E. Systematic review and meta-analysis of differentially expressed miRNAs in experimental and human temporal lobe epilepsy. *Sci Rep* 2017; **7**(1): 11592.
85. Srivastava PK, Roncon P, Lukasiuk K, et al. Meta-Analysis of MicroRNAs Dysregulated in the Hippocampal Dentate Gyrus of Animal Models of Epilepsy. *eNeuro* 2017; **4**(6).
86. Falcicchia C, Paolone G, Emerich DF, et al. Seizure-Suppressant and Neuroprotective Effects of Encapsulated BDNF-Producing Cells in a Rat Model of Temporal Lobe Epilepsy. *Mol Ther Methods Clin Dev* 2018; **9**: 211-24.
87. Paolone G, Falcicchia C, Lovisari F, et al. Long-Term, Targeted Delivery of GDNF from Encapsulated Cells Is Neuroprotective and Reduces Seizures in the Pilocarpine Model of Epilepsy. *J Neurosci* 2019; **39**(11): 2144-56.
88. Simonato M, Tongiorgi E, Kokaia M. Angels and demons: neurotrophic factors and epilepsy. *Trends Pharmacol Sci* 2006; **27**(12): 631-8.
89. Sutula TP, Hermann B. Progression in mesial temporal lobe epilepsy. *Ann Neurol* 1999; **45**(5): 553-6.
90. Parent JM, Yu TW, Leibowitz RT, Geschwind DH, Sloviter RS, Lowenstein DH. Dentate granule cell neurogenesis is increased by seizures and contributes to aberrant network reorganization in the adult rat hippocampus. *J Neurosci* 1997; **17**(10): 3727-38.
91. Simonato M, Zucchini S. Are the neurotrophic factors a suitable therapeutic target for the prevention of epileptogenesis? *Epilepsia* 2010; **51 Suppl 3**: 48-51.
92. Gotz R, Koster R, Winkler C, et al. Neurotrophin-6 is a new member of the nerve growth factor family. *Nature* 1994; **372**(6503): 266-9.
93. Kullander K, Carlson B, Hallbook F. Molecular phylogeny and evolution ofthe neurotrophins from monotremes and marsupials. *J Mol Evol* 1997; **45**(3): 311-21.
94. Mowla SJ, Farhadi HF, Pareek S, et al. Biosynthesis and post-translational processing of the precursor to brain-derived neurotrophic factor. *J Biol Chem* 2001; **276**(16): 12660-6.
95. Curtis R, Adryan KM, Stark JL, et al. Differential role of the low affinity neurotrophin receptor (p75) in retrograde axonal transport of the neurotrophins. *Neuron* 1995; **14**(6): 1201-11.
96. Binder DK, Scharfman HE. Brain-derived neurotrophic factor. *Growth Factors* 2004; **22**(3): 123-31.
97. Sariola H, Saarma M. Novel functions and signalling pathways for GDNF. *J Cell Sci* 2003; **116**(Pt 19): 3855-62.

98. Baloh RH, Enomoto H, Johnson EM, Jr., Milbrandt J. The GDNF family ligands and receptors - implications for neural development. *Curr Opin Neurobiol* 2000; **10**(1): 103-10.
99. Gu F, Parada I, Shen F, et al. Structural alterations in fast-spiking GABAergic interneurons in a model of posttraumatic neocortical epileptogenesis. *Neurobiol Dis* 2017; **108**: 100-14.
100. Kokaia Z, Airaksinen MS, Nanobashvili A, et al. GDNF family ligands and receptors are differentially regulated after brain insults in the rat. *Eur J Neurosci* 1999; **11**(4): 1202-16.
101. Martin D, Miller G, Rosendahl M, Russell DA. Potent inhibitory effects of glial derived neurotrophic factor against kainic acid mediated seizures in the rat. *Brain Res* 1995; **683**(2): 172-8.
102. Li S, Xu B, Martin D, Racine RJ, Fahnestock M. Glial cell line-derived neurotrophic factor modulates kindling and activation-induced sprouting in hippocampus of adult rats. *Exp Neurol* 2002; **178**(1): 49-58.
103. Emerich DF, Orive G, Thanos C, Tornoe J, Wahlberg LU. Encapsulated cell therapy for neurodegenerative diseases: from promise to product. *Adv Drug Deliv Rev* 2014; **67-68**: 131-41.
104. Engel J, Jr. What can we do for people with drug-resistant epilepsy? The 2016 Wartenberg Lecture. *Neurology* 2016; **87**(23): 2483-9.
105. Rajman M, Schratt G. MicroRNAs in neural development: from master regulators to fine-tuners. *Development* 2017; **144**(13): 2310-22.
106. Yoo YM, Lee CJ, Lee U, Kim YJ. Neuroprotection of adenoviral-vector-mediated GDNF expression against kainic-acid-induced excitotoxicity in the rat hippocampus. *Exp Neurol* 2006; **200**(2): 407-17.
107. Kanter-Schlifke I, Georgievska B, Kirik D, Kokaia M. Seizure suppression by GDNF gene therapy in animal models of epilepsy. *Mol Ther* 2007; **15**(6): 1106-13.
108. Kanter-Schlifke I, Fjord-Larsen L, Kusk P, Angehagen M, Wahlberg L, Kokaia M. GDNF released from encapsulated cells suppresses seizure activity in the epileptic hippocampus. *Exp Neurol* 2009; **216**(2): 413-9.

Video Article

Microdialysis of Excitatory Amino Acids During EEG Recordings in Freely Moving Rats

Marie Soukupová[1], Chiara Falcicchia[1], Francesca Lovisari[1], Selene Ingusci[1], Mario Barbieri[1], Silvia Zucchini[1], Michele Simonato[1]

[1]Department of Medical Sciences, Section of Pharmacology, Neuroscience Center, University of Ferrara and National Institute of Neuroscience

Correspondence to: Marie Soukupová at marie.soukupova@unife.it

URL: https://www.jove.com/video/58455
DOI: doi:10.3791/58455

Keywords: Neuroscience, Issue 141, microdialysis, glutamate, aspartate, epilepsy, pilocarpine model, stereotaxic surgery, potassium stimulation, electroencephalography, liquid chromatography

Date Published: 11/8/2018

Citation: Soukupová, M., Falcicchia, C., Lovisari, F., Ingusci, S., Barbieri, M., Zucchini, S., Simonato, M. Microdialysis of Excitatory Amino Acids During EEG Recordings in Freely Moving Rats. *J. Vis. Exp.* (141), e58455, doi:10.3791/58455 (2018).

Abstract

Microdialysis is a well-established neuroscience technique that correlates the changes of neurologically active substances diffusing into the brain interstitial space with the behavior and/or with the specific outcome of a pathology (*e.g.,* seizures for epilepsy). When studying epilepsy, the microdialysis technique is often combined with short-term or even long-term video-electroencephalography (EEG) monitoring to assess spontaneous seizure frequency, severity, progression and clustering. The combined microdialysis-EEG is based on the use of several methods and instruments. Here, we performed *in vivo* microdialysis and continuous video-EEG recording to monitor glutamate and aspartate outflow over time, in different phases of the natural history of epilepsy in a rat model. This combined approach allows the pairing of changes in the neurotransmitter release with specific stages of the disease development and progression. The amino acid concentration in the dialysate was determined by liquid chromatography. Here, we describe the methods and outline the principal precautionary measures one should take during *in vivo* microdialysis-EEG, with particular attention to the stereotaxic surgery, basal and high potassium stimulation during microdialysis, depth electrode EEG recording and high-performance liquid chromatography analysis of aspartate and glutamate in the dialysate. This approach may be adapted to test a variety of drug or disease induced changes of the physiological concentrations of aspartate and glutamate in the brain. Depending on the availability of an appropriate analytical assay, it may be further used to test different soluble molecules when employing EEG recording at the same time.

Video Link

The video component of this article can be found at https://www.jove.com/video/58455/

Introduction

To provide insight into the functional impairment of glutamate-mediated excitatory and GABAergic inhibitory neurotransmission resulting in spontaneous seizures in temporal lobe epilepsy (TLE),we systematically monitored extracellular concentrations of GABA[1] and later the levels of glutamate and aspartate[2] by microdialysis in the ventral hippocampus of rats at various time-points of the disease natural course, *i.e.*, during development and progression of epilepsy. We took advantage of the TLE pilocarpine model in rats, which mimics the disease very accurately in terms of behavioral, electrophysiological and histopathological changes[3,4] and we correlated the dialysate concentration of amino acids to its different phases: the acute phase after the epileptogenic insult, the latency phase, the time of the first spontaneous seizure and the chronic phass[5,6,7]. Framing the disease phases was enabled by long-term video-EEG monitoring and the precise EEG and clinical characterization of spontaneous seizures. Application of the microdialysis technique associated with long-term video-EEG monitoring allowed us to propose mechanistic hypotheses for TLE neuropathology. In summary, the technique described in this manuscript allows the pairing of neurochemical alterations within a defined brain area with the development and progression of epilepsy in an animal model.

Paired devices, made up of a depth electrode juxtaposed to a microdialysis cannula, are often employed in epilepsy research studies where changes in neurotransmitters, their metabolites, or energy substrates should be correlated to neuronal activity.In the vast majority of cases, it is used in freely behaving animals, but it can be also conducted in a similar way in human beings, *e.g.*, in pharmaco-resistant epileptic patients undergoing depth electrode investigation prior to surgery[8]. Both EEG recording, and dialysate collection may be performed separately (*e.g.*, implanting the electrode in one hemisphere and the microdialysis probe in the other hemisphere or even performing the microdialysis in one group of animals while performing the sole EEG in another group of animals). However, coupling the electrodes to probes may have multiple advantages: it simplifies stereotaxic surgery, limits tissue damage to only one hemisphere (while leaving the other, intact, as a control for histological studies), and homogenizes the results as these are obtained from the same brain region and the same animal.

On the other hand, the preparation of the coupled microdialysis probe-electrode device requires skills and time if it is home-made. One could spend relatively high amounts of money if purchased from the market. Moreover, when microdialysis probes (probe tips are typically 200-400 µm in diameter and 7-12 mm long)[9], and EEG electrodes (electrode tips are usually of 300-500 µm in diameter, and long enough to reach the brain structure of interest[10]) are coupled, the mounted device represents a bulky and relatively heavy object on one side of the head, which is troublesome for animals and prone to be lost especially when it is connected to the dialysis pump and the hard-wire EEG recording system.

This aspect is more relevant in epileptic animals that are difficult to handle and less adaptive to the microdialysis sessions. Proper surgical techniques and appropriate post-operative care can result in long-lasting implants that cause minimal animal discomfort and should be pursued for combinatory microdialysis-EEG experiments[10,11,12].

The advantages and limitations of the microdialysis technique have been reviewed in detail by many neuroscientists. Its primary advantage over other *in vivo* perfusion techniques (*e.g.*, fast flow push-pull or cortical cup perfusion) is a small diameter of the probe which covers a relatively precise area of interest[13,14,15]. Second, the microdialysis membrane creates a physical barrier between the tissue and the perfusate; therefore, high-molecular weight substances do not cross and do not interfere with the analysis[16,17]. Moreover, the tissue is protected from the turbulent flow of the perfusate[18]. Another important advantage is the possibility to modify the perfusate flow for maximizing the analyte concentration in the perfusate (*i.e.*, the process of microdialysis can be well defined mathematically and can be modified to yield high concentrations of the analyte in the sample)[19]. Finally, the technique may be used to infuse the drugs or pharmacologically active substances into the tissue of interest and to determine their effect at the site of intervention[20]. On the other hand, microdialysis has a limited resolution time (typically more than 1 min due to the time needed for collecting samples) in comparison to electrochemical or biological sensors; it is an invasive technique that causes tissue damage; it compromises the neurochemical balance within the space around the membrane due to the continuous concentration gradient of all soluble substances which enters the perfusate together with the analyte of interest. Finally, the microdialysis technique is highly influenced by the limits of the analytical techniques employed for the quantification of substances in the perfusate[9,21,22,23]. The high-performance liquid chromatography (HPLC) after derivatization with orthophthaldialdehyde for glutamate and aspartate analysis in biological samples has been well validated[24,25,26,27] and its extensive discussion is out of the scope of this manuscript, but the data produced by using this method will be described in detail.

When performed properly and without modifications of the perfusate composition, microdialysis can provide reliable information about the basal levels of neurotransmitter release. The largest portion of the basal levels is likely the result of the transmitter spillover from the synapses[9]. Because in many instances the simple sampling of the neurotransmitter in the extra synaptic space is not sufficient to pursue the goals of an investigation, the microdialysis technique can be also employed to stimulate neurons or to deprive them of important physiological ions such as K^+ or Ca^{2+}, in order to evoke or prevent the release of the neurotransmitter.

High K^+ stimulation is often used in neurobiology to stimulate neuronal activity not only in awake animals but also in primary and organotypic cultures. The exposure of a healthy central nervous system to solutions with high concentrations of K^+ (40-100 mM) evokes the efflux of neurotransmitters[28]. This ability of neurons to provide an additional release in response to high K^+ may be compromised in epileptic animals[1] and in other neurodegenerative diseases[29,30]. Similarly, the Ca^{2+} deprivation (obtained by perfusing Ca^{2+} free solutions) is used to establish calcium-dependent release of most neurotransmitters measured by microdialysis. It is generally believed that Ca^{2+} dependent release is of neuronal origin, whereas Ca^{2+} independent release originates from glia, but many studies raised controversy over the meaning of Ca^{2+}-sensitive measurements of e.g. glutamate or GABA[9]: thus, if possible, it is advisable to support microdialysis studies with microsensor studies, as these latter have higher spatial resolution and the electrodes allows to get closer to synapses[31].

Regarding microdialysis studies in epileptic animals, it is important to stress that the data obtained from most of them rely upon video or video-EEG monitoring of seizures, *i.e.*, of the transient occurrence of signs and/or symptoms due to abnormal excessive or synchronous neuronal activity in the brain[32]. There are some specifics of electrographic seizures in pilocarpine treated animals which should be considered when preparing the experiment. Spontaneous seizures are followed by depressed activity with frequent EEG interictal spikes[3] and occur in clusters[33,34]. Sham operated non-epileptic animals may exhibit seizure-like activity[35] and therefore the parameters for EEG recordings evaluation should be standardized[36] and, if possible, the timing of microdialysis sessions should be well defined. Finally, we highly recommend following the principles and methodological standards for video-EEG monitoring in control adult rodents outlined by experts of International League Against Epilepsy and American Epilepsy Society in their very recent reports[37,38].

Here, we describe microdialysis of glutamate and aspartate in parallel with the long-term video-EEG recordings in epileptic animals and their analysis in the dialysate by HPLC. We will emphasize the critical steps of the protocol that one should take care of for best result.

Protocol

All experimental procedures have been approved by the University of Ferrara Institutional Animal Care and Use Committee and by the Italian Ministry of Health (authorization: D.M. 246/2012-B) in accordance with guidelines outlined in the European Communities Council Directive of 24 November 1986 (86/609/EEC). This protocol is specifically adjusted for glutamate and aspartate determination in rat brain dialysates obtained under EEG control of microdialysis sessions in epileptic and non-epileptic rats. Many of the materials described here may be easily replaced with those that one uses in his laboratory for EEG recordings or microdialysis.

1. Assembly of the Microdialysis Probe-electrode Device

1. Use a 3-channel two-twisted electrode (with at least a 20 mm cut length of the registering electrode and a 10 cm long grounding electrode) and couple it to a guide cannula to prepare the device. See examples of 3-channel electrode and guide cannula for dialysis in **Figure 1A-1B.**
2. Remove (**Figure 1C**) and insert (**Figure 1D**) the metal guide cannula into the dummy plastic cannula a few times prior to the usage in order to ease its removal at the moment of its switch for microdialysis probe in animal.
3. Bend the twisted wires of registering electrode two times (**Figure 1E-1F**) in order to align the wires with the dummy cannula of the guide and cut the electrode tip (**Figure 1G**) to be 0.5 mm longer than the tip of the guide cannula (**Figure 1H**) using the digital caliper.
4. Have ready the 1 mm long silicon circlet (O.D. 2 mm, thickness 0.3 mm; **Figure 1I**) and insert the tip of the guide cannula and the tip of the twisted electrodes into the silicon circlet using the tweezers (**Figure 1J**). Fix it onto the foot of the guide cannula pedestal with polymer glue of rapid action or resin (**Figure 1K**). See the example of the completed devices in **Figure 1L and Figure 2A**.
5. Sterilize the device under germicidal UV light for 4 h. Turn over the device four times so as each of its sides is exposed to the light for 1 h. Note: Many home-made electrodes and microdialysis probes may be assembled in a similar way. The head of above described implant for rats has the following dimensions: 7 mm width x 5 mm depth x 10 mm length from the top to pedestal toe; the implant tip is about 11 mm

long, 600 µm in diameter and all the device weights about 330-360 mg. The device may be reused two or three times if (i) a sufficient length of the ground electrode is left on the skull during the surgery for the next use and (ii) when the animal is killed, and the device recovered together with the dental cement it is left in acetone overnight, such that the cement may be mechanically disaggregated, and the device washed and sterilized again.

2. Stereotaxic Surgery

1. Use a stereotaxic apparatus and probe clip holder (**Figure 2B**) for the device implantation following the contemporary standards for aseptic and pain-free surgeries[39,40,41].
    1. Anesthetize the adult Sprague-Dawley rats with ketamine/xylazine mixture (43 mg/kg and 7 mg/kg, i.p.) and fix it onto the stereotaxic frame. Add isoflurane anesthesia (1.4% in air; 1.2 mL/min) to initial ketamine/xylazine injection as it allows to control the depth of anesthesia in time. Shave the fur on animal's head.

2. Swab the head skin surface by iodine-based solution followed by 70% ethanol to prepare it for aseptic surgery[39].
    1. Implant the guide cannula-electrode device prepared in precedence (1.1 – 1.5) into the right ventral hippocampus using the following coordinates: nose bar + 5.0 mm, A – 3.4 mm, L + 4.5 mm, P + 6.5 mm to bregma[1,2]. Follow standard techniques for stereotaxic surgeries[10,11,12].
    2. Ensure that it does not cover the anchoring screws. When mounting it onto the stereotaxic apparatus, grasp the device for the guide cannula head as this may be easily aligned to the probe holder.

3. Anchor the device to the skull with at least four stainless screws screwing them into the skull bone (1 screw into the left and 1 screw into the right frontal bone plates, 1 screw into the left parietal and 1 screw into the interparietal bone plates). Add a drop of tissue glue to further fix each screw to the skull bone.
    1. Cover half of screw threads with methacrylic cement. Promote the binding of the cement by making shallow grooves in the bone to increase the adherence.

4. Once the tip of the device is positioned into the brain tissue, twist the wire of the ground electrode around 3 anchoring screws. Cover all mounted screws and the device with the dental cement[12,42,43].
5. Monitor the animals during the surgery and for about 1 h thereafter until upright and moving around the cage. Keep them on a warming pad to avoid hypothermia. Allow the rats to recover for at least 7 days after the device implantation.
6. Monitor the animals at least once daily for 3 days after the surgery for signs of pain or distress. Give the animals with the antibiotic cream (gentamycin 0.1%) close to the incised site to prevent the infection and an analgesic (tramadol 5 mg/kg, i.p.) for 3 days to prevent the post-surgical pain.

3. Temporal Lobe Epilepsy Induction by Pilocarpine and Assignment of Animals to Experimental Groups

1. After a week of post-surgical recovery, assign the animals randomly to groups: (i) control animals receiving vehicle and (ii) epileptic animals that will receive pilocarpine. Use a proportionally higher number of animals for epileptic group since not all of the pilocarpine administered rats will develop the disease.
2. Inject a dose of methylscopolamine (1 mg/kg, s.c.) and 30 min after, a single injection of pilocarpine (350 mg/kg, i.p.) to induce the status epilepticus (SE). Inject methylscopolamine and the vehicle (saline) to the control rats. Use 1 mL syringe with 25G needle for all i.p. administrations.
    1. Check visually the animals to start to have behavioral seizures (moving vibrissa within 5 min, nodding head, cloning the limbs) and within 25 min to clone continuously all the body (SE).

3. Arrest the SE 2 h after the onset to have a mortality about 25% and a mean latent period of approximately 10 days by administration of diazepam (20 mg/kg, i.p.). Observe and record any seizure behavior beginning immediately after the pilocarpine injection and continue for at least 6 h thereafter.
4. Give the animals saline (1 mL, i.p.) using 1 mL syringe with 25G needle and sucrose solution (1 mL, p.o.) using 1 mL syringe and flexible feeding 17G needle for 2-3 days after SE to promote the recovery of body weight loss.
    1. Exclude the animals that do not achieve the initial body weight within the first week after pilocarpine SE from the study (except for the acute group killed 24 h after SE, where the body weight follow up is not possible).

5. Assign post-SE animals randomly to different experimental groups (**Figure 3**): acute phase (where the microdialysis takes place 24 h after SE), latency (7-9 days after SE), first spontaneous seizure (approximately 11 days after SE), and chronic period (starts about 22-24 days after SE, i.e. about 10 days after the first seizure). Monitor the animals for the occurrence of spontaneous seizures.
NOTE: Use the following inclusion/exclusion criteria for further experiments in epileptic rats: development of convulsive SE within 1 h after pilocarpine administration; weight gain in the first week after SE and the correct positioning of the microdialysis probe and electrode.

4. Epileptic Behavior Monitoring and Analysis

1. Long-term monitoring of epileptic behavior
    1. Approximately 6 h after pilocarpine administration (*i.e.*, at the end of direct observation by the researchers), place the animals into the clean home cages and start the 24 h video monitoring.
    2. Continue the 24 h video monitoring until day 5, using a digital video surveillance system.
    3. Beginning at day 5, connect the rats in their home rectangular cages to tethered EEG recording system and continue the 24 h video monitoring.

4. Set the parameters on the amplifier positioned outside of the Faraday cage (set amplification factor on each channel according to the specificity of the EEG signal of each single animal) and start the EEG acquisition observing the EEG signal produced by unconnected cables. Use sampling rate 200 Hz and low pass filter set to 0.5 Hz.
5. Connect the animal to cables holding an animal's head between two stretched fingers of one hand and screwing down the connectors to the electrode pedestal using the other free hand. Start the acquisition.
   CAUTION: Ensure that the signal is free of artifacts. Common artifacts are the spikes greatly exceeding the scale.
6. A day before the microdialysis experiment, transfer the animals into the tethered EEG system equipped with plexiglass cylinders for microdialysis. Disconnect the animals from the EEG tethering system in home cage screwing up the connectors from the electrode without restrain the animal. Place the animal into the high plexiglass cylinders.

2. Monitoring of epileptic behavior a day before and during the microdialysis session
   1. Switch on the amplifier positioned outside of the Faraday cage. Open the EEG software. Start the EEG acquisition observing the EEG signal produced by unconnected cables.
   2. Connect the animal to the tethered EEG recording system holding an animal's head between two stretched fingers of one hand and screwing down the connectors to the electrode pedestal using the other free hand. Set an amplification factor (gain) on each channel of amplifier according to electrode signal of single animal so the EEG signal is in scale. Let the animal explore the new cage (cylinder) for at least 1 h under the direct observation of the researcher.
   3. **NOTE:** 24 h before the microdialysis experiment, the rats are briefly anesthetized with isoflurane for the switch of guide cannulas to microdialysis probe. Take advantage of the moment when they are anesthetized to connect them to the EEG recording system.
   4. Shorten or prolong pendulous cable according to animal's commodity. Make sure that the cables do not interfere with animal's movements and lying posture.
   5. Check for the correct image framing of the video cameras. Start the video-EEG recording.

3. Identification of seizures and EEG activity
   1. Use a software player to watch the videos. Scroll the movie 8 times faster than the real time playing and individuate the generalized seizures (see animal to rear with forelimb clonus or animal rearing and falling with forelimb clonus). Slow down the video and note the precise time of the beginning and of the end of the behavioral seizure.
   2. Process the data by counting the number of generalized seizures observed in 24 h of video records and express them in terms of seizure frequency and duration as mean values of all seizures observed in 24 h.
   3. Define the EEG seizures as the periods of paroxysmal activity of high frequency (>5 Hz) characterized by a >3-fold amplitude increment over baseline with progression of the spike frequency that lasts for a minimum of 3 s[2,44] or similar[28]. Use EEG software to process the raw EEG recordings. Split the EEG traces into 1 h fractions. Copy the EEG tracing fractions to file for software automatic spike analysis.
   4. Analyze the EEG activity data using EEG software and predefined parameters (4.3.3.). Conduct all video analyses in two independent investigators who are blind for the group of analyzed animals. In case of divergence, make them re-examine the data together to reach a consensus[45].

5. Microdialysis

1. *In vitro* probe recovery
   1. Prepare the probe for its first use according to the manufacturer's instructions, handling it in its protective sleeve.
   2. Run the experiment in triplicate: prepare three 1.5 mL test tubes loading them with 1 mL of Ringer's solution containing the mixture of standards (2.5 µM of glutamate and 2.5 µM of aspartate). Put three loaded 1.5 mL test tubes into the block heater set to 37 °C and position it on the stirrer.
      NOTE: Use the same standard solutions for chromatography calibrations.
   3. Seal the 1.5 mL test tubes with paraffin film and puncture it by sharp tweezers to make a hole of about 1 mm in diameter.
   4. Take the probe and insert it into the hole made in paraffin film. Immerse the membrane at least 2 mm under the solution level. Fix further the probe to 1.5 mL test tube by paraffin film.
      CAUTION: Ensure that the tip does not touch the walls of the 1.5 mL test tube.
   5. Connect the probe inlet to the syringe mounted on the infusion pump using FEP-tubing and tubing adapters. Optionally, use fine bore polythene tubing of 0.28 mm ID and 0.61 mm OD and colored tubing adapters (red and blue tubing adapters) for connections.
   6. Start the pump at 2 µL/min and let the fluid appear at the outlet tip. Connect the probe outlet to the 0.2 mL collecting test tube using FEP-tubing and tubing adapters.
      NOTE: Use FEP-tubing for all connections. Cut the desired length of tubing by using a razor blade. Use tubing adapters of different color for inlet and outlet of the probe. Let the pump run for 60 min. Check for leaks and air bubbles. These should not be present.
   7. Set the pump to the flow rate 2 µL/min and start to collect the samples on the outlet side of the tubing.
   8. Collect three 30 min perfusate samples and three equal volume samples of the solution in the 1.5 mL test tube. Take the equal volume samples from the 1.5 mL test tube every 30 min using the microsyringe immersed into the standard solution in the 1.5 mL test tube.
   9. Repeat the experiment (5.1.1-5.1.8) setting up the pump to the flow rate 3 µL/min (5.1.7) to have a probe recovery comparison when using two different perfusion flow rates.
   10. When finished, stop the pump and rinse the tubing with distilled water, 70% ethanol and push the air into it. Store the probe in a vial filled with clean distilled water. Rinse the probe thoroughly by perfusing it at 2 µL/min by distilled water prior the storage.
   11. Analyze the concentration of the glutamate and aspartate in the samples by chromatography (see the details below; 6.3).
   12. Calculate the recovery using the following equation:
       Recovery (%) = $(C_{perfusate} / C_{dialysed\ solution}) \times 100$.

2. Microdialysis sessions in freely moving rats
   1. Preparative procedures: probe insertion and testing, infusion pump setting and start

1. Prepare the microdialysis probes for the first use according to the manufacturer user's guide and fill them with Ringer's solution. Cut about 10 cm long pieces of FEP-tubing and connect them to inlet and outlet cannulas of the probe using the tubing adapters of different colors.
2. Make sure that the tubing touches the adapters with no dead space in all connections.
3. 5.2.1.3. 24 h before the microdialysis experiment, anesthetize briefly the animal with isoflurane (5% in air) in an induction chamber until recumbent. Remove the dummy cannula from its guide using the tweezers and holding the animal's head firmly. Insert the microdialysis probe, endowed with a dialyzing membrane, into the guide cannula and firm further the microdialysis cannulas inserted in their guide by modeling clay.
   CAUTION: Do not let the probe touch the walls of the protective probe sleeve when extracting.
4. Put the animal into the plexiglass cylinder and let it explore the new ambience. Connect the animal to the tethered EEG recording system as described above (follow the points 4.2.2 and 4.2.3).
5. Follow the awake and freely moving rat movements and connect the inlet of the probe to the 2.5 mL syringe with blunted 22G needle containing Ringer's solution using the tubing adapters. Push Ringer's solution inside the probe ejecting 1 mL of Ringer's solution in 10 s pushing continuously the piston of 2.5 mL syringe. Check for the drop of the liquid appearing on the outlet. The probe is now ready for use.
6. Fill up the 2.5 mL syringes connected to FEP-tubing by tubing adapters with Ringer's solution and mount them onto the infusion pump. Start the pump at 2 µL/min. Let it run overnight.
   NOTE: Use the desired length of all FEP-tubing but calculate the tubing dead volume to know when the high K^+ stimulation should be started and to correlate the quantification data with neurochemical changes in animal brain. Use the air bubble created in the tubing under the working flow to calculate this time.

2. Collection of samples during EEG recording and potassium stimulation
   1. Verify the absence of seizures in the 3 h preceding the onset of sample collection (video-EEG recordings) and continue to monitor seizure activity during microdialysis.
   2. Stop the pump carrying the FEP-tubing cannulated syringes filled up with Ringer's solution. Mount onto the pump another set of 2.5 mL syringes connected to FEP-tubing with tubing adapters filled up with a modified Ringer's solution containing 100 mM K^+ solution.
   3. Start the pump at 2 µL/min and let it run. For more rapid filling of the tubing, set the pump at 5 µL/min for the time of filling. Check for the absence of air bubbles in the system. Ensure that the tubing touches the adapters with no dead space in all connections.
   4. Test the probe if ready for use in animal as described above (5.2.1.5).
      NOTE: If for some reason the probe does not work, change it. For these cases, keep a few prepared microdialysis probes ready to use near the microdialysis-EEG workstation. Disconnect the animal from EEG cables and anesthetize it briefly with isoflurane if necessary to realize the change.
   5. Connect the FEP-tubing of syringes filled up with Ringer's solution to the inlet cannula of the probe in each animal and wait for the appearance of the liquid drop on the tip of the outlet.
   6. Connect the outlet of the probe to the FEP-tubing, which leads to collection in the test tube. Insert the FEP-tubing into the closed 0.2 mL test tube with a perforated cap. Ensure that the tube stays in the place by fixing with a piece of modeling clay.
   7. Continue to run the pump at 2 µL/min for 60 min without collecting samples to equilibrate the system (zero sample).
   8. Collect 5 consecutive 30 min dialysate samples (60 µL respective volume) under baseline conditions (perfusion with normal Ringer's solution). Store samples on ice.
   9. Calculate the time it takes liquid to pass from the pump into the animal's head (it depends on dead volume of tubing, *i.e.*, air bubble time) and switch the FEP-tubing that goes from the syringes containing normal Ringer's solution to syringes containing modified (100 mM K^+) Ringer's solution at this time without stopping the pump. Check for the absence of the air bubbles in the system. Let the pump run for 10 min.
      CAUTION: In 10 min of high K^+ stimulation, the animals tend to move themselves frenetically and usually present a great number of wet dog shakes (control and out of seizure cluster animals) or behavioral seizures (epileptic animals), so be ready to intervene to protect the tubing and cables from twisting.
   10. After 10 min, switch the tubing from the syringes containing 100 mM K^+ Ringer's solution to normal Ringer's solution and let the pump run. Do not turn off the pump during the solution changes so that that there will be a drop of the liquid at the end of the tubing to be connected in line.
   11. From the moment at which the dialysate contains high potassium, *i.e.*, after collection of the fifth post-equilibration dialysate, collect the dialysate fractions every 10 min (20 µL) for 1 h. Collect 3 additional 30 min dialysate samples and stop the pump. Store the samples on ice.
   12. Store the samples at -80 °C after the experiment until HPLC analysis.
   13. Repeat the microdialysis experiment for 3 consecutive days, except for the acute (24 h) and first seizure group, in which only one microdialysis session takes place 24 h after SE or within 24 h after the first spontaneous seizure (**Figure 3**).
   14. On completion of each experiment, euthanize the animal with an anesthetic overdose and remove the brain for verification of probe and electrode placement.

3. Post-microdialysis procedures
   1. Rinse the used microdialysis probes with distilled water and store them in a vial filled with clean distilled water until next use.
      NOTE: The reused membranes may have increased permeability; check for the probe recovery before its repeated use.
   2. Rinse the entire microdialysis set up (tubing, connectors and syringes) with distilled water followed by 70% ethanol. Replace ethanol with air and store the set up in a sterile environment.
   3. Split the basal dialysate samples into 20 µL fractions and use only one 20 µL fraction for amino acid basal concentration analysis. Store the remaining sample volume for further or confirmatory analysis at -80 °C.
   4. Fix the brains in 10% formalin and preserve them by paraffin-embedding[1]. Coronally section the brains into slices and stain them with hematoxylin and eosin. Examine the brains for correct probe and electrode placement[1,2].

NOTE: Fix the brains in cooled 2-methylbutane and store them at -80 °C. Use any other proven staining on the nervous tissue sections which permits to visualize the probe and electrode tract.

6. Chromatographic Analysis of Glutamate and Aspartate

1. Preparation of derivatizing agent
    1. Mix the respective volumes 20:1 (v/v) of orthophthaldialdehyde reagent (OPA) and 2-mercaptoethanol (5-ME) in the vial. Close the vial using the cap and air tight septum.
    CAUTION: Work under the chemical hood.
    2. Vortex the prepared solution and put it into the autosampler into the position for derivatizing agent.

2. Preparation of dialysate samples
    1. Put the glass insert with bottom spring into the 2 mL brown autosampler vial. Prepare the vials for all samples measured in one batch.
    2. Take the 20 µL dialysis samples from -80 °C freezer and let them melt. Remove 1 µL of the solution and add 1 µL of internal standard (IS) L-Homoserine (50 µM) to 19 µL of the sample, thus the sample contains 2.5 µM of IS. Pipette 20 µL of the dialysis sample into the glass insert in vial and seal it with an air tight septum.
    3. Place the vials containing the samples into the autosampler using the chromatographic software to label the samples in their positions.

3. Chromatographic analysis of samples to determine glutamate and aspartate concentration
    1. Run the analyses on the liquid chromatograph system with spectrofluorometric detection. Detect the amino acids after 2 min pre-column derivatization with 20 µL of orthophthaldialdehyde/5-mercaptoethanol 20:1 (v/v) added to 20 µL of sample.
    2. Prepare the system for amino acids analysis. Switch on the autosampler, the pump, the degasser, the detector and controlling unit together with computer.
    3. Immerse the siphons into the bottles containing the mobile phase and purge the channels of the chromatographic pump to be used for the analysis.
    4. Start to increase the flow of the mobile phase checking the pressure on the column (*e.g.*, start at 0.2 mL/min and increase the flow for additional 0.2 mL/min every 5 min until achieving the working flow). Let the system run at working flow 0.8 mL/min for at least 1 h to equilibrate the column.
    CAUTION: Unstable pressure indicates the presence of the air in the system. The pressure should not exceed 25 MPa.
    5. Set the gain, high sensitivity and the excitation and emission wavelengths on the detector to 345/455 nm respectively. Reset the detector signal (AUTOZERO).
    6. Using the chromatographic software, send the method to the instrument. Now, the chromatograph should be ready to measure.
    7. Separate the dialysate samples, standard spiked dialysate samples as well as standards (0.25 µM – 2.5 µM aspartate and glutamate in Ringer's solution) on the appropriate chromatographic column. Calibrate the chromatographic method and establish the detection and quantification limits before any dialysis samples analysis.
    8. Activate the single analysis or create the sequence of the samples to be analyzed using the chromatography software and run the sequence.
    CAUTION: Run more than one blank sample and different standard samples within the sequence of dialysate samples in order to control the method accuracy.
    9. Once the chromatograms are acquired, analyze them with chromatography software. Check the integration of the peaks of the interest into the calibration plot. Use peak height or peak area for quantification.
    10. Once the sample recording is finished fill the column and the system with an organic solvent (*e.g.*, 50% acetonitrile in ultrapure water) to prevent its aging and mold growth in it.
    11. Shut down the system.

Representative Results

Probe recovery

The mean recovery (*i.e.,* the mean amino acid content in the perfusate as a percentage of the content in an equal volume of the vial solution) was 15.49 ± 0.42% at a flow rate of 2 µL/min and 6.32 ± 0.64 at 3 µL/min for glutamate and 14.89 ± 0.36% at a flow rate of 2 µL/min and 10.13 ± 0.51 at 3 µL/min for aspartate when using the cuprophane membrane probe. If using the polyacrylonitrile membrane probe, the mean recovery was 13.67 ± 0.42% at a flow rate of 2 µL/min and 6.55 ± 1.07 at 3 µL/min for glutamate and 14.29 ± 0.62% at a flow rate of 2 µL/min and 8.49 ± 0.15 at 3 µL/min for aspartate (**Figure 4A-4B**). As it can be clearly seen in **Figure 4A**, the slower flow rate (2 µL/min) enhances the dialyzing performance of both probes. For the following experiments the cuprophane membrane endowed probe perfused at a flow rate 2 µL/min was chosen, because its mean recovery was higher (even if not significantly) at this flow rate for both analytes and because of experimental continuity (these probes were used for analyzing GABA in precedence[1]).

Seizures development and progression of the disease after status epilepticus

The behavioral and EEG monitoring of seizures, their evaluation, was done in all the animals employed in this study to confirm the development and progression of TLE disease in these.

The robust convulsive SE, that was interrupted after 3 h using diazepam, occurred 25±5 min after the pilocarpine injection. Then, all the animals entered a latency state in which they were apparently well and they were continuously video-EEG monitored in order to verify that no spontaneous seizures occurred in the first 9 days or to identify the first spontaneous seizure, respectively for the latency and the first seizure group. The first spontaneous seizure occurred 11.3 ± 0.6 days after SE (mean ± SEM, n=21). Thereafter, seizures occurred in clusters, and aggravated in time. In late chronic phase (days 55-62 after SE) the epileptic rats experienced 3.3±1.2 (mean ± SEM, n=12) generalized seizures

daily. There was a clear progression of the disease. Many, but not all EEG seizures, corresponded with behavioral seizure activity. **Figure 5B** shows the recorded paroxysmal epileptiform activity that was observed about 500 ms before and during behavioral seizures. **Figure 5A** shows control traces in non- epileptic rats.

Representative basal values of amino acids found in microdialysis perfusate and potassium stimulated release of glutamate

Basal glutamate concentration found in chronic epileptic rats (0.87 ± 0.06 µM) was significantly higher than in control animals (0.59 ± 0.03 µM; $p < 0.05$ vs. controls; one-way ANOVA and post hoc Dunnett's test). There was no statistically significant difference between chronic epileptic (0.31 ± 0.04 µM) and non-epileptic animals (0.30 ± 0.05 µM) in basal or high K^+ evoked aspartate concentrations. See the original article for details[2]. The reported basal levels of glutamate in control rats are in line with those found by others in similar studies (*i.e.*, about 0.75 µM when using a 2 µL/min flow and membranes of 2 mm effective length)[46,47,48,49,50,51,52,53]. However, many different factors can influence the results of microdialysis, for example the effective length of the probe and the membrane cut off.

High K^+-evoked an additional release of glutamate for about 30 min in control rats and for about 60 min in chronic epileptic rats (**Figure 6**). See the original article for details[2]. As can be seen from the depicted time course, the 10 min time resolution of microdialysis was sufficient to capture the variances in glutamate release found in both groups of animals.

HPLC calibration and limits

The data were calculated based on calibration curves obtained with standard solutions of glutamate and aspartate and the internal standard L-homoserine. The concentration of the neurotransmitters glutamate and aspartate in the perfusates was expressed in absolute values (µmol/L). Each calibration plot was constructed by analysis of solutions of glutamate and aspartate at four concentration levels (five replicates at each level).Regression coefficients were calculated for calibration plots: $y = \mathbf{k}x + \mathbf{q}$, where x was the concentration ratio of aspartate or glutamate to L-homoserine (IS) and y was the corresponding peak-area ratio of aspartate or glutamate to L- homoserine (IS). The coefficient of determination (r^2) was calculated. The applicability of HPLC method was within the limits; the lower limit of quantification was determined as the lowest concentration in the standard calibration curve and the upper limit of quantification as the highest used concentration of amino acid analytes for calibration, respectively. Limit of detection (LOD) was also calculated. Some of these values are delineated in **Table 1**. A model chromatogram of blank sample, standards sample and collected dialysis sample obtained with above described method are shown in **Figure 7**.

Probe localization

Microdialysis probe and recording electrode were implanted into the right ventral hippocampus and their correct placement was verified. Only those animals where the implantation was maximally in 500 µm distant from stabilized coordinates (see **Figure 8**) were included in analysis.

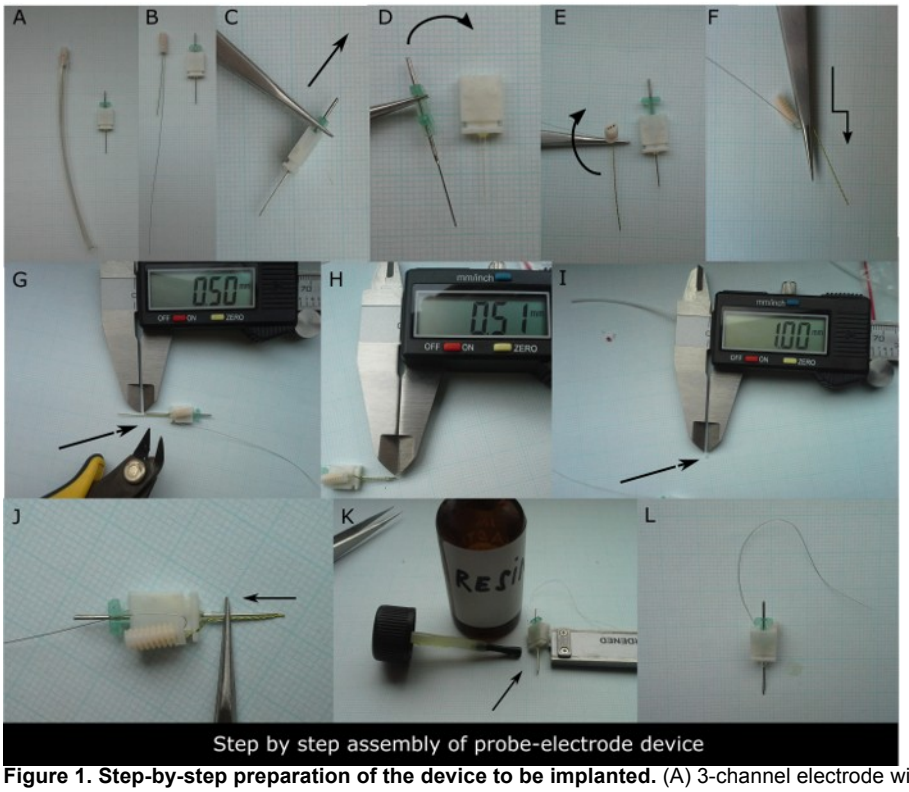

Figure 1. Step-by-step preparation of the device to be implanted. (A) 3-channel electrode with 10 cm long grounding electrode in its protective sleeve on the left and guide cannula for microdialysis on the right needed to assemble the device. (B). The bare electrode and guide cannula in detail. The first step is to remove (C) and insert (D) the metal guide cannula from and into its plastic dummy few times to ease its release once implanted into the animal's head. The second step is to bend two times the twisted registering electrode to be aligned to dialysis guide cannula (E, F). (G) The electrode tip should be cut to be 0.5 mm longer than the tip of the metal guide cannula. (H) Check for the precision of the cut using the digital caliper. Subsequently, about 1 mm long silicon circlet should be used to fix the alignment of electrode to guide cannula foot (I). (J) The photograph showing how to ring the electrode and guide cannula shaft. The final step is to put a drop of resin or glue onto the guide cannula pedestal fixing the silicon circlet to it (K). (L) Assembled device ready to be sterilized. Please click here to view a larger version of this figure.

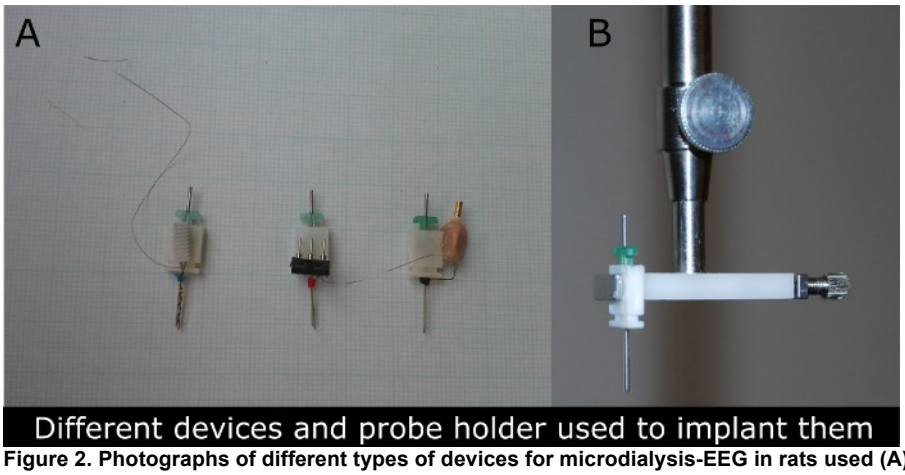

Figure 2. Photographs of different types of devices for microdialysis-EEG in rats used (A) and the photograph of the probe clip holder (B) used to implant these devices. (A) The guide cannula (in green) is replaced by a microdialysis cannula typically 24 h before the experiment. The electrical connector of the device (first left was used for the recordings described in this manuscript) permits the attachment of wires that conduct electrical signal to amplifier and data collection equipment. The device is surgically attached to the skull of anesthetized rats and recordings may be obtained later without causing pain or discomfort in freely behaving rats. Please click here to view a larger version of this figure.

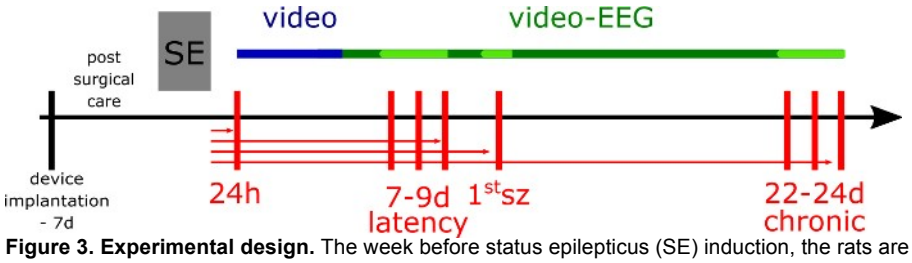

Figure 3. Experimental design. The week before status epilepticus (SE) induction, the rats are implanted with the device. SE is induced by pilocarpine and animals (if not dialyzed and killed at 24 h after SE; the rats from acute group) are video monitored for 5 days (blue line), then video-EEG monitored to assess the seizure frequency and duration in their home cages (green line). For the microdialysis experiment, the epileptic and respective non-epileptic control rats are transferred to another EEG set up equipped with cylinder cages in 24 h before the microdialysis session and still video-EEG monitored (light green line). The vertical red lines represent the dialysis sessions at different time-points of epileptic disease development. The horizontal red lines represent the different groups of epileptic animals (and respective non-epileptic animals), where the arrow indicates the last day of the microdialysis and the day of animal's death. Please click here to view a larger version of this figure.

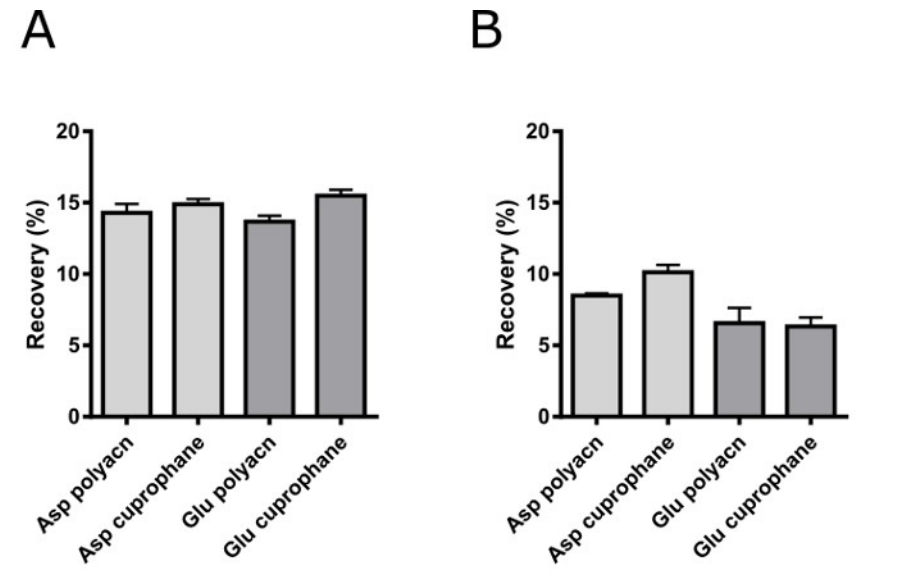

Figure 4. *In vitro* recovery of two dialysis probes. Mean *in vitro* recovery (%) of aspartate and glutamate using two different commercially available microdialysis probes (both endowed with 1 mm long dialyzing membrane) at (A) 2 µL/min and (B) 3 µL/min flow rate. Data are the mean ± SEM of 3 independent experiments run in triplicates. There are not statistically significant differences between the efficiency of various probes (Student's unpaired t-test, $p<0.05$).Using a flow rate 2 µL/min the glutamate recovery increased about 5% compared to 3 µL/min flow rate, thus the slower flow rate was used for microdialysis experiments. Please click here to view a larger version of this figure.

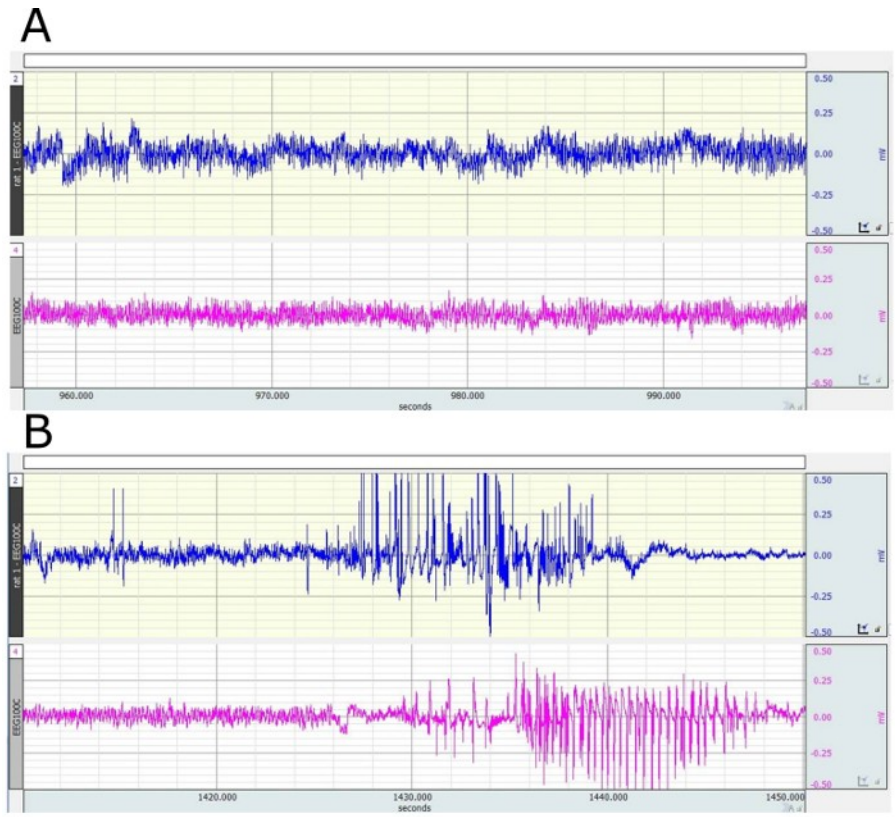

Figure 5. Illustrative EEG recordings from ventral hippocampus of paraoxystic activities as can be seen at chronic phase in control and epileptic rats. (A) Two representative traces recorded in two saline treated non-epileptic rats. (B) Traces recorded in two epileptic rats. Epileptiform discharges correspond with class 3 behavioral seizures in these rats. Please click here to view a larger version of this figure.

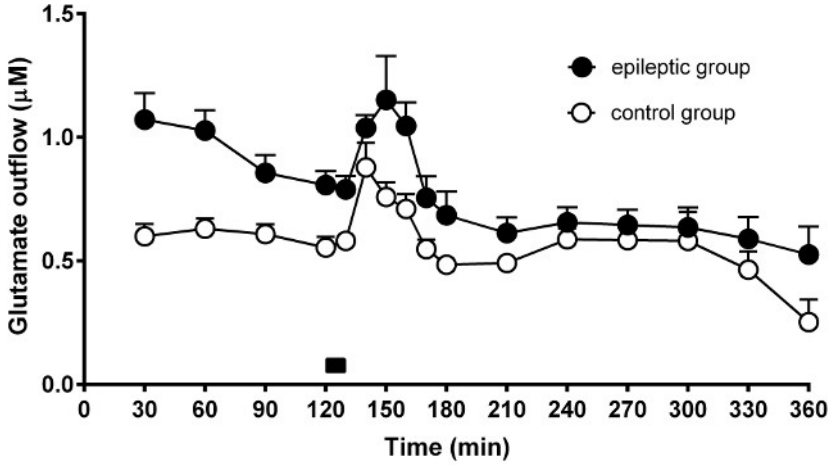

Figure 6. Time-course of the effect of potassium stimulation on glutamate release from the rat hippocampus. Representative result of the microdialysis experiment performed in 6 control (open circles) and 6 chronic epileptic rats (black circles). The graph shows the temporal changes of dialysate glutamate concentration in the course of microdialysis experiments and during high 100 mM K^+ stimulation. The time of high K^+ stimulus (10 min) is indicated by the black bar on bottom of the graph. The data are the means ± SEM of 6 animals per group. Please click here to view a larger version of this figure.

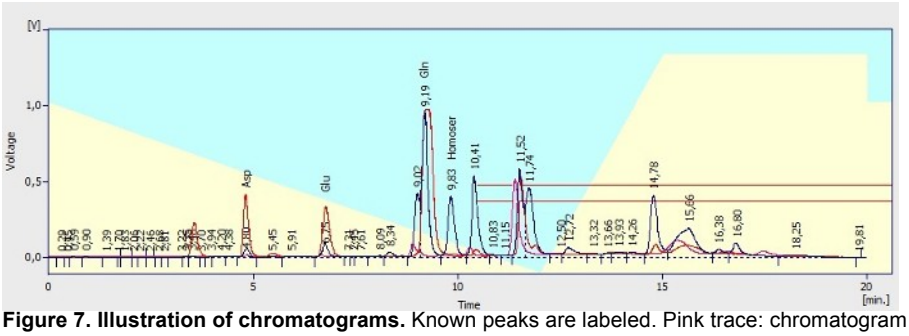

Figure 7. Illustration of chromatograms. Known peaks are labeled. Pink trace: chromatogram of Ringer's solution without intentionally added amines after OPA/5-ME derivatization (blank sample). Blue trace: chromatogram of dialysate sample after derivatization showing the peaks of amino acids: aspartate (t_R 4.80 min), glutamate (t_R 6.75 min) and glutamine (t_R 9.19 min) and the peak of IS L-homoserine (2.5 µM, retention time, t_R 9.83 min). Red trace: Chromatogram of standard of aspartate (2.5 µM) and glutamate (2.5 µM) in Ringer's solution. Azure and yellow background of the picture stands for mobile phase A (azure) and mobile phase B (yellow) portion used for analytes elution. A red rectangle indicated area (t_R 10.41 min and further) shows the peaks of unknown substances and OPA degradation products. All injection volumes were 20 µL. The derivatives were separated at a flow rate of 0.8 mL/min. Please click here to view a larger version of this figure.

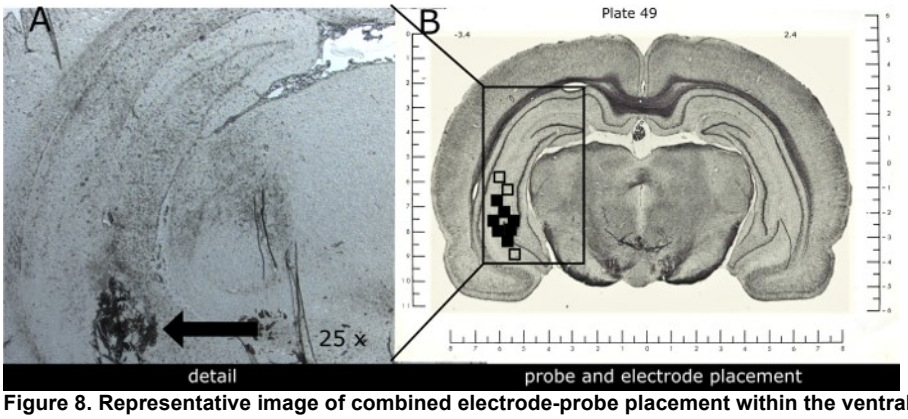

Figure 8. Representative image of combined electrode-probe placement within the ventral hippocampus. (A) Photograph shows the scare left by the device tip in detail (black arrow). (B) Schematic illustration of the electrode-probe tip positions within the implanted ventral hippocampus of 12 rats. The solid squares (some overlapping) indicate correctly localized probe-electrode tips. Open squares indicate incorrectly localized probe-electrode tips in animals excluded from the study (n=3). Coronal brain slices containing probes and recording sites were processed after experiments for histological analysis. The numbers above the illustration show the distance from Bregma (according to Pellegrino *et al.* 1979 atlas of rat brain; nose bar + 5.0 mm, co-ordinates used: A -3.4 mm, L+5.4 mm; P + 7.5 mm from dura). Please click here to view a larger version of this figure.

Analyte	c (µmol/l)	*k*	*q*	r^2	LOD (pmol/l)
Glutamate	0.25-2.5	5.215	1043.79	0.999	19.4
Aspartate	0.25-2.5	2.258	1994.72	0.998	31.7

Table 1. Quantification characteristics of HPLC method used for amino acids determination. Concentration range of standards (c), slope (k), intercept (q), coefficient of determination (r^2) and limit of detection (LOD) describing the calibration plots obtained with standard solutions of glutamate and aspartate (0.25, 0.5, 1.0 and 2.5 µM) and internal standard L-homoserine (2.5 µM) using the described HPLC method with spectrofluorometric detection.

Discussion

In this work, we show how a continuous video-EEG recording coupled with microdialysis can be performed in an experimental model of TLE. Video-EEG recording techniques are used to correctly diagnose the different phases of the disease progression in animals and the microdialysis technique is used to describe the changes in glutamate release that occur in time (no changes have been found for aspartate in a previously published study[2]). We strongly recommend the use of a single device/implant to perform them both in each animal for the reasons discussed in the Introduction.

Whenever available, radiotelemetry should be preferred to tethered systems for chronic EEG recording as it minimizes interferences with behavior and reduces harm risk and distress for the animals[54]. However, the tethered EEG recording is much less expensive than telemetry.

In our laboratory, we use the connectors to the EEG recording system and microdialysis tubing in parallel, such that wires and tubings are attached to two different swivels. This is the most critical issue for these experiments: the wires and tubing tend to cross frequently due to the animal's movements. Therefore, we use connectors and tubing long enough to let the animal chase its own tail (a behavior that is typically observed with potassium stimulation) or fall down and roll during generalized epileptic seizures. It is advisable to firm further the microdialysis cannulas inserted in their guide by modeling clay, in order to strengthen their contact with the guide (sometimes, microdialysis cannulas are

bumped against the walls of the cage during generalized seizures and may slip off). On the other hand, it is advisable to keep the tubing as short as possible, to minimize the delay between neurochemical time and collection time. This is particularly important when collection periods are short. In general, the microdialysis tubing should be of adequate length and capacity to ensure that the sampling time does not exceed the time between dialysis outlet and collection. It was observed that the solutes tend to diffuse more between some plugs if the tubing dead time is superior to the sampling rate[55]. Therefore, the experimental dead time/volume of microdialysis tubing should be reduced as much as possible and determined very precisely in order to correlate the neurochemistry data with the animal's behavior. Finally, it is important to note that both swivels and electrodes coupled with cannula for combined EEG and microdialysis studies are commercially available. Therefore, whenever possible, set up the EEG system with the option to perform the microdialysis experiments.

The minor recommendations are: (i) before beginning any experiment, check that the EEG recording system and/or microdialysis set up are functioning properly and troubleshoot any problem; we suggest that having one reserve set up ready (another pump with syringes mounted on and completed of tubing filled up with working solutions) when performing the experiment, as well as a sufficient number of ready to use microdialysis probes for changing broken ones; (ii) when transferring animal into the working EEG-microdialysis cage it is helpful to have a second person assisting and starting the acquisitions; (iii) make sure that the column and autosampler reached the appropriate temperatures before chromatography; in addition, use standards and construct the calibration plots before any dialysate samples are injected on the chromatographic column; (v) whenever needed, try to develop the chromatographic or other analytical method to measure multiple analytes at the same time.

Alterations in neurotransmission have implications in many CNS disorders (including epilepsy) and there has been a great interest over the decades to quantify these changes during the progression from a healthy to a diseased phenotype. Today, only a few techniques allow the measurement of changes in neurotransmitter levels over days or months. Microdialysis is one of these techniques. In a large number of cases, like that described here, it is performed in freely moving animals and coupled to conventional offline analytical assays like high performance liquid chromatography (HPLC) or capillary electrophoresis (CE), with which it reaches 5-30 min temporal resolution[31,56]. Clearly, these sampling intervals do not reflect the rapid neurotransmitter dynamics in the vicinity of synapses, but may be convenient for some long term microdialysis applications (*e.g.*, disease development or drug effect studies) which require coupling neurochemical, EEG and behavioral data. However, other studies are primarily concerned with measuring real-time or close to real-time changes in neurotransmitter release. For these, the microdialysis technique must be refined to increase the speed of sampling (therefore decreasing sample volumes). Indeed, the classic microdialysis technique is often criticized for its poor temporal (minutes) and spatial resolution (the conventional probe is much larger than the synaptic cleft)[9,21,56,57]. However, it is the mass sensitivity of the analytical method coupled to microdialysis what determines the microdialysis time resolution (*i.e.*, its resolution is equal to the time required to have enough sample to be detected by an analytical technique[56]). Thus, when the microdialysis produces tiny amounts of samples, the sensitivity of quantification techniques must be increased. To date, such improvements in temporal resolution of the microdialysis technique followed 3 different lines. One of these is represented by miniaturization of the columns and/or detection cells of classic HPLC methods; these are called UHPLC (ultra-performant HPLC) techniques and allow to achieve 1-10 min time resolution[58,59,60]. Another approach is to couple a classic HPLC to mass spectrometry (MS) or tandem (MS/MS) for multiplex analysis of neurotransmitters in brain dialysates. Combined HPLC-MS assays have an excellent sensitivity and reach about 1-5 min time resolution[56,61,62,63]. A third line of improvement exists in modifications of capillary electrophoresis (CE). If CE uses laser induced fluorescence detection (CE-LIFD), it enables the determination of submicromolar concentrations of various neurotransmitters in nanoliter fractions obtained every 5 min[55,64,65] or even at 10 s intervals[56]. A clear advantage that emerges from UHPLCs or advanced CEs analytical approaches is that the sampling may be done in freely moving animals, not compromising experiments in which spontaneous behavior must be observed and analyzed. On the other hand, there are methods that permits the brain dialysate sampling at even hundred milliseconds temporal resolution (*e.g.,* enzyme reactor based on-line assays or droplet collection of dialysate coupled to MS techniques), but these are typically used in restrained animals[66] or under general anesthesia[67,68,69], not allowing to couple microdialysis with behavioral studies.

When considering the second most important weakness of microdialysis, *i.e.,* relatively low spatial resolution due to the membrane dimensions (often about 0.5 mm in diameter and 1-4 mm long), an alternative may be the microprobes developed with low-flow push-pull sampling. These probes consist of two silica capillaries (of 20 µm ID and 200 µm OD) fused side-by-side and sheathed with a polymeric tubing. During the experiment, these capillaries are perfused at very low flow rates, such that fluid is pulled out of one capillary and a sample is retrieved from the other at the same flow rate. Because the sampling occurs only at the probe tip, the spatial resolution is greater than with the probe for microdialysis[70]. Another possibility is to switch from miniaturized probes to microelectrode arrays (biosensors) for real-time neurotransmitter evaluation. Different electrochemical techniques (based principally on voltammetry or amperometry) permit analyte sampling very close to the synapse (micron scale) and in less than 1 s[31,70,71]. These devices can measure the concentration of multiple analytes from multiple brain regions. However, they also require some refinements, for example to avoid artifacts and a relatively rapid deterioration.

Considering the latest advances in *in vivo* neurochemical monitoring, it seems likely that the different transmitter sampling methods will be combined in one sensor in the near future. The work on microfabricated sampling probes has already started, and we believe that further progress in microfabrication technologies together with analytical advances will further facilitate *in vivo* neurochemical monitoring investigation. At this time, however, the conventional microdialysis correlated to EEG remains a valid method for many neuroscience applications.

Disclosures

The authors have nothing to disclose.

Acknowledgements

The authors wish to thank Anna Binaschi, Paolo Roncon and Eleonora Palma for their contribution to manuscripts published in precedence.

References

1. Soukupova, M., *et al.* Impairment of GABA release in the hippocampus at the time of the first spontaneous seizure in the pilocarpine model of temporal lobe epilepsy. *Experimental Neurology.* **257** 39-49 (2014).
2. Soukupova, M., *et al.* Increased extracellular levels of glutamate in the hippocampus of chronically epileptic rats. *Neuroscience.* **301** 246-253 (2015).
3. Curia, G., Longo, D., Biagini, G., Jones, R. S., & Avoli, M. The pilocarpine model of temporal lobe epilepsy. *Journal of Neuroscience Methods.* **172** (2), 143-157 (2008).
4. Scorza, F.A., *et al.* The pilocarpine model of epilepsy: what have we learned? *Anais da Academia Brasileira de Ciencias.* **81** (3), 345-365 (2009).
5. Pitkanen, A., & Sutula, T. P. Is epilepsy a progressive disorder? Prospects for new therapeutic approaches in temporal-lobe epilepsy. *The Lancet Neurology.* **1** (3), 173-181 (2002).
6. Pitkanen, A., & Lukasiuk, K. Mechanisms of epileptogenesis and potential treatment targets. *The Lancet Neurology.* **10** (2), 173-186 (2011).
7. Reddy, D. S. Role of hormones and neurosteroids in epileptogenesis. *Frontiers in Cellular Neuroscience.* **7** (115) (2013).
8. Engel, J., Jr. Research on the human brain in an epilepsy surgery setting. *Epilepsy Research.* **32** (1-2), 1-11 (1998).
9. Watson, C. J., Venton, B. J., & Kennedy, R. T. In vivo measurements of neurotransmitters by microdialysis sampling. *Analytical Chemistry.* **78** (5), 1391-1399 (2006).
10. Jeffrey, M., *et al.* A reliable method for intracranial electrode implantation and chronic electrical stimulation in the mouse brain. *BMC Neuroscience.* **14** 82 (2013).
11. Oliveira, L. M. O., & Dimitrov, D. Surgical techniques for chronic implantation of microwire arrays in rodents and primates. *Frontiers in Neuroscience.Methods for Neural Ensemble Recordings. 2nd edition. Boca Raton (FL): CRC Press/Taylor & Francis; 2008. Chapter 2.* (2008).
12. Fornari, R.V., *et al.* Rodent stereotaxic surgery and animal welfare outcome improvements for behavioral neuroscience. *Journal of Visualized Experiments: JoVE.* (59), e3528 (2012).
13. Horn, T. F., & Engelmann, M. In vivo microdialysis for nonapeptides in rat brain--a practical guide. *Methods.* **23** (1), 41-53 (2001).
14. Kennedy, R. T., Thompson, J. E., & Vickroy, T. W. In vivo monitoring of amino acids by direct sampling of brain extracellular fluid at ultralow flow rates and capillary electrophoresis. *Journal of Neuroscience Methods.* **114** (1), 39-49 (2002).
15. Renno, W. M., Mullet, M. A., Williams, F. G., & Beitz, A. J. Construction of 1 mm microdialysis probe for amino acids dialysis in rats. *Journal of Neuroscience Methods.* **79** (2), 217-228 (1998).
16. Nirogi, R., *et al.* Approach to reduce the non-specific binding in microdialysis. *Journal of Neuroscience Methods.* **209** (2), 379-387 (2012).
17. Zhou, Y., Wong, J. M., Mabrouk, O. S., & Kennedy, R. T. Reducing adsorption to improve recovery and in vivo detection of neuropeptides by microdialysis with LC-MS. *Analytical Chemistry.* **87** (19), 9802-9809 (2015).
18. Wisniewski, N., & Torto, N. Optimisation of microdialysis sampling recovery by varying inner cannula geometry. *Analyst.* **127** (8), 1129-1134 (2002).
19. Morrison, P. F., *et al.* Quantitative microdialysis: analysis of transients and application to pharmacokinetics in brain. *Journal of Neurochemistry.* **57** (1), 103-119 (1991).
20. Westerink, B. H., & De Vries, J. B. A method to evaluate the diffusion rate of drugs from a microdialysis probe through brain tissue. *Journal of Neuroscience Methods.* **109** (1), 53-58 (2001).
21. Chefer, V. I., Thompson, A. C., Zapata, A., & Shippenberg, T. S. Overview of brain microdialysis. *Current Protocols in Neurosciences.* **Chapter 7** Unit 7.1 (2009).
22. Westerink, B. H. Brain microdialysis and its application for the study of animal behaviour. *Behavioural Brain Research.* **70** (2), 103-124 (1995).
23. Zhang, M. Y., & Beyer, C. E. Measurement of neurotransmitters from extracellular fluid in brain by in vivo microdialysis and chromatography-mass spectrometry. *Journal of Pharmaceutical and Biomedical Analysis.* **40** (3), 492-499 (2006).
24. Allison, L. A., Mayer, G. S., & Shoup, R. E. o-Phthalaldehyde derivatives of amines for high-speed liquid chromatography/electrochemistry. *Analytical Chemistry.* **56** (7), 1089-1096 (1984).
25. Boyd, B. W., Witowski, S. R., & Kennedy, R. T. Trace-level amino acid analysis by capillary liquid chromatography and application to in vivo microdialysis sampling with 10-s temporal resolution. *Analytical Chemistry.* **72** (4), 865-871 (2000).
26. Hanczko, R., Jambor, A., Perl, A., & Molnar-Perl, I. Advances in the o-phthalaldehyde derivatizations. Comeback to the o-phthalaldehyde-ethanethiol reagent. *Journal of Chromatography A.* **1163** (1-2), 25-42 (2007).
27. Molnar-Perl, I. Quantitation of amino acids and amines in the same matrix by high-performance liquid chromatography, either simultaneously or separately. *Journal of Chromatography A.* **987** (1-2), 291-309 (2003).
28. Solis, J.M., *et al.* Variation of potassium ion concentrations in the rat hippocampus specifically affects extracellular taurine levels. *Neuroscience Letters.* **66** (3), 263-268 (1986).
29. Boatell, M. L., Bendahan, G., & Mahy, N. Time-related cortical amino acid changes after basal forebrain lesion: a microdialysis study. *Journal of Neurochemistry.* **64** (1), 285-291 (1995).
30. Sutton, A.C., *et al.* Elevated potassium provides an ionic mechanism for deep brain stimulation in the hemiparkinsonian rat. *The European Journal of Neuroscience.* **37** (2), 231-241 (2013).
31. Hascup, K. N., & Hascup, E. R. Electrochemical techniques for subsecond neurotransmitter detection in live rodents. *Comparative Medicine.* **64** (4), 249-255 (2014).
32. Fisher, R.S., *et al.* Epileptic seizures and epilepsy: definitions proposed by the International League Against Epilepsy (ILAE) and the International Bureau for Epilepsy (IBE). *Epilepsia.* **46** (4), 470-472 (2005).
33. Goffin, K., Nissinen, J., Van Laere, K., & Pitkanen, A. Cyclicity of spontaneous recurrent seizures in pilocarpine model of temporal lobe epilepsy in rat. *Experimental Neurology.* **205** (2), 501-505 (2007).
34. Pitsch, J., *et al.* Circadian clustering of spontaneous epileptic seizures emerges after pilocarpine-induced status epilepticus. *Epilepsia.* **58** (7), 1159-1171 (2017).

35. Pearce, P.S., *et al.* Spike-wave discharges in adult Sprague-Dawley rats and their implications for animal models of temporal lobe epilepsy. *Epilepsy and Behavior.* **32** 121-131 (2014).
36. Twele, F., Tollner, K., Bankstahl, M., & Loscher, W. The effects of carbamazepine in the intrahippocampal kainate model of temporal lobe epilepsy depend on seizure definition and mouse strain. *Epilepsia Open.* **1** (1-2), 45-60 (2016).
37. Kadam, S.D., *et al.* Methodological standards and interpretation of video-electroencephalography in adult control rodents. A TASK1-WG1 report of the AES/ILAE Translational Task Force of the ILAE. *Epilepsia.* **58 Suppl 4** 10-27 (2017).
38. Hernan, A.E., *et al.* Methodological standards and functional correlates of depth in vivo electrophysiological recordings in control rodents. A TASK1-WG3 report of the AES/ILAE Translational Task Force of the ILAE. *Epilepsia.* **58 Suppl 4** 28-39 (2017).
39. Bernal, J., *et al.* Guidelines for rodent survival surgery. *Journal of Investigative Surgery: the official journal of the Academy of Surgical Research.* **22** (6), 445-451 (2009).
40. Flecknell, P. Rodent analgesia: Assessment and therapeutics. *Veterinary Journal (London, England: 1997).* **232** 70-77 (2018).
41. Miller, A. L., & Richardson, C. A. Rodent analgesia. *The Veterinary Clinics of North America. Exotic Animal Practice.* **14** (1), 81-92 (2011).
42. Geiger, B. M., Frank, L. E., Caldera-Siu, A. D., & Pothos, E. N. Survivable stereotaxic surgery in rodents. *Journal of Visualized Experiments: JoVE.* (20) (2008).
43. Gardiner, T. W., & Toth, L. A. Stereotactic Surgery and Long-Term Maintenance of Cranial Implants in Research Animals. *Contemporary Topics in Laboratory Animal Science.* **38** (1), 56-63 (1999).
44. Williams, P.A., *et al.* Development of spontaneous recurrent seizures after kainate-induced status epilepticus. *The Journal of Neuroscience: The official journal of the Society for Neuroscience.* **29** (7), 2103-2112 (2009).
45. Paradiso, B., *et al.* Localized overexpression of FGF-2 and BDNF in hippocampus reduces mossy fiber sprouting and spontaneous seizures up to 4 weeks after pilocarpine-induced status epilepticus. *Epilepsia.* **52** (3), 572-578 (2011).
46. Kanamori, K. Faster flux of neurotransmitter glutamate during seizure - Evidence from 13C-enrichment of extracellular glutamate in kainate rat model. *PLoS One.* **12** (4), e0174845 (2017).
47. Kanamori, K., & Ross, B. D. Chronic electrographic seizure reduces glutamine and elevates glutamate in the extracellular fluid of rat brain. *Brain Research.* **1371** 180-191 (2011).
48. Kanamori, K., & Ross, B. D. Electrographic seizures are significantly reduced by in vivo inhibition of neuronal uptake of extracellular glutamine in rat hippocampus. *Epilepsy Research.* **107** (1-2), 20-36 (2013).
49. Luna-Munguia, H., Meneses, A., Pena-Ortega, F., Gaona, A., & Rocha, L. Effects of hippocampal high-frequency electrical stimulation in memory formation and their association with amino acid tissue content and release in normal rats. *Hippocampus.* **22** (1), 98-105 (2012).
50. Mazzuferi, M., Binaschi, A., Rodi, D., Mantovani, S., & Simonato, M. Induction of B1 bradykinin receptors in the kindled hippocampus increases extracellular glutamate levels: a microdialysis study. *Neuroscience.* **135** (3), 979-986 (2005).
51. Meurs, A., Clinckers, R., Ebinger, G., Michotte, Y., & Smolders, I. Seizure activity and changes in hippocampal extracellular glutamate, GABA, dopamine and serotonin. *Epilepsy Research.* **78** (1), 50-59 (2008).
52. Ueda, Y., *et al.* Collapse of extracellular glutamate regulation during epileptogenesis: down-regulation and functional failure of glutamate transporter function in rats with chronic seizures induced by kainic acid. *Journal of Neurochemistry.* **76** (3), 892-900 (2001).
53. Wilson, C.L., *et al.* Comparison of seizure related amino acid release in human epileptic hippocampus versus a chronic, kainate rat model of hippocampal epilepsy. *Epilepsy Research.* **26** (1), 245-254 (1996).
54. Lidster, K., *et al.* Opportunities for improving animal welfare in rodent models of epilepsy and seizures. *Journal of Neuroscience Methods.* **260** 2-25 (2016).
55. Parrot, S., *et al.* High temporal resolution for in vivo monitoring of neurotransmitters in awake epileptic rats using brain microdialysis and capillary electrophoresis with laser-induced fluorescence detection. *Journal of Neuroscience Methods.* **140** (1-2), 29-38 (2004).
56. Kennedy, R. T., Watson, C. J., Haskins, W. E., Powell, D. H., & Strecker, R. E. In vivo neurochemical monitoring by microdialysis and capillary separations. *Current Opinion in Chemical Biology.* **6** (5), 659-665 (2002).
57. Kennedy, R. T. Emerging trends in in vivo neurochemical monitoring by microdialysis. *Current Opinion in Chemical Biology.* **17** (5), 860-867 (2013).
58. Ferry, B., Gifu, E. P., Sandu, I., Denoroy, L., & Parrot, S. Analysis of microdialysate monoamines, including noradrenaline, dopamine and serotonin, using capillary ultra-high performance liquid chromatography and electrochemical detection. *Journal of Chromatography B, Analytical Technologies in the Biomedical and Life Sciences.* **951-952** 52-57 (2014).
59. Jung, M. C., Shi, G., Borland, L., Michael, A. C., & Weber, S. G. Simultaneous determination of biogenic monoamines in rat brain dialysates using capillary high-performance liquid chromatography with photoluminescence following electron transfer. *Analytical Chemistry.* **78** (6), 1755-1760 (2006).
60. Parrot, S., Lambas-Senas, L., Sentenac, S., Denoroy, L., & Renaud, B. Highly sensitive assay for the measurement of serotonin in microdialysates using capillary high-performance liquid chromatography with electrochemical detection. *Journal of Chromatography B, Analytical Technologies in the Biomedical and Life Sciences.* **850** (1-2), 303-309 (2007).
61. Hershey, N. D., & Kennedy, R. T. In vivo calibration of microdialysis using infusion of stable-isotope labeled neurotransmitters. *ACS Chemical Neuroscience.* **4** (5), 729-736 (2013).
62. Vander Weele, C.M., *et al.* Rapid dopamine transmission within the nucleus accumbens: dramatic difference between morphine and oxycodone delivery. *The European Journal of Neuroscience.* **40** (7), 3041-3054 (2014).
63. Zestos, A. G., & Kennedy, R. T. Microdialysis Coupled with LC-MS/MS for In Vivo Neurochemical Monitoring. *The AAPS journal.* **19** (5), 1284-1293 (2017).
64. Benturquia, N., Parrot, S., Sauvinet, V., Renaud, B., & Denoroy, L. Simultaneous determination of vigabatrin and amino acid neurotransmitters in brain microdialysates by capillary electrophoresis with laser-induced fluorescence detection. *Journal of Chromatography B, Analytical Technologies in the Biomedical and Life Sciences.* **806** (2), 237-244 (2004).
65. Chefer, V., *et al.* Repeated exposure to moderate doses of ethanol augments hippocampal glutamate neurotransmission by increasing release. *Addiction Biology.* **16** (2), 229-237 (2011).
66. Morales-Villagran, A., Pardo-Pena, K., Medina-Ceja, L., & Lopez-Perez, S. A microdialysis and enzymatic reactor sensing procedure for the simultaneous registration of online glutamate measurements at high temporal resolution during epileptiform activity. *Journal of Neurochemistry.* **139** (5), 886-896 (2016).
67. Petit-Pierre, G., *et al.* In vivo neurochemical measurements in cerebral tissues using a droplet-based monitoring system. *Nature Communication.* **8** (1), 1239 (2017).

68. Renaud, P., Su, C. K., Hsia, S. C., & Sun, Y. C. A high-throughput microdialysis-parallel solid phase extraction-inductively coupled plasma mass spectrometry hyphenated system for continuous monitoring of extracellular metal ions in living rat brain. *Nature Communication.* **1326** 73-79 (2014).
69. Zilkha, E., Obrenovitch, T. P., Koshy, A., Kusakabe, H., & Bennetto, H. P. Extracellular glutamate: on-line monitoring using microdialysis coupled to enzyme-amperometric analysis. *Journal of Neuroscience Methods.* **60** (1-2), 1-9 (1995).
70. Ngernsutivorakul, T., White, T. S., & Kennedy, R. T. Microfabricated Probes for Studying Brain Chemistry: A Review. *Chemphyschem: a Eurepean journal of chemical physics and physical chemistry.* **19** (10), 1128-1142 (2018).
71. Mirzaei, M., & Sawan, M. Microelectronics-based biosensors dedicated to the detection of neurotransmitters: a review. *Sensors (Basel, Switzerland).* **14** (10), 17981-18008 (2014).

(*Acknowledgments*:

This part is written in Italian, unless my beloved Mara wouldn't understand.

Giunta alla fine di questo percorso credo sia doveroso ringraziare tutti colore che, in un modo o nell'altro, mi hanno supportata (e sopportata) in questi tre anni.

Michele, se non fosse stato per te questa tesi di dottorato non esisterebbe nemmeno. Mi hai dato l'opportunità di crescere e migliorare giorno per giorno, lasciandomi sbagliare ed imparare dai miei errori. Credo non avrei potuto trovare un gruppo migliore con cui passare questo dottorato.

Silvia e **Michela**, sempre pronte a rincuorarmi nei momenti no e a spronarmi quando le cose mi sembravano insormontabili.

Chiara, **Marie** e **Anna**, è grazie a voi che oggi posso dire di saper fare questo lavoro; mi mancate, tantissimo, siete colleghe speciali e non sarebbe stato lo stesso senza di voi.

Sele, amica mia, compagna di questo folle percorso, non riesco davvero ad immaginare come sarebbe andata se tu non fossi stata sempre al mio fianco.

Stefano, **Nunzia**, **Gianluca**, **Barbara** e chiunque sia passato per il nostro lab anche solo per un breve periodo, grazie perchè non dev'essere facile lavorare con una come me.

Marta e tutti gli studenti che in questi anni hanno imparato da me e da tutti noi, perchè mi avete insegnato sicuramente più di quanto io abbia insegnato a voi.

Lorenzo, grazie per le ore a cantare, le mattinate insieme al brico, per avermi insegnato a montare armadi e perchè mi hai insegnato che perseverare alla fine ripaga. Sono orgogliosissima di te.

Carola, bene più prezioso che Unife mi ha donato, senza di te questamiamilano non sarebbe diventata presto casa. Ringrazio infinitamente quell'esame di Farmacologia che ci ha unite.

Paolo, che hai iniziato tutto ciò che ho scritto fino a qui, e per fortuna mi ricordi ogni giorno di sentirmi libera di sbagliare.

Gli amici di Ferrara: Anna, Silvia, Marti, Isa, Vir. Grazie perchè avete contribuito a rendere Fe il mio luogo sicuro.

Michela, **Giulia**, **Giovanni**, **Sofia** tutti gli altri del 5 Novembre. Credevo non avrei mai ringraziato il diabete per qualcosa. E invece.

Alice, che hai sempre creduto in tutto ciò di pazzo io mi inventassi, mi hai ascoltata

nelle mie paranoie, non mi hai mai concesso di mollare. Grazie.

Laura, per essere al mio fianco da più di 15 anni, e per esserti sorbita i miei sfoghi pur non

Università degli Studi di Ferrara

Sezioni

Dottorati di ricerca

Il tuo indirizzo e-mail

francesca.lovisari@unife.it

Oggetto:

Dichiarazione di conformità della tesi di Dottorato

Io sottoscritto Dott. (Cognome e Nome)

Lovisari Francesca

Nato a:

Rovigo

Provincia:

Rovigo

Il giorno:

21/12/1990

Avendo frequentato il Dottorato di Ricerca in:

Neuroscienze Traslazionali e Neurotecnologie

Ciclo di Dottorato

32

Titolo della tesi:

microRNAs, gene networks and cell therapy: promises and challenges for treating epilepsies and their comorbidities

Titolo della tesi (traduzione):

microRNA, network genetici e terapia cellulare: sfide e speranze per trattare epilessia e le sue comorbidità

Tutore: Prof. (Cognome e Nome)

Simonato Michele

Settore Scientifico Disciplinare (S.S.D.)

BIO/14

Parole chiave della tesi (max 10):

epilepsy, comorbidities, gene networks, microRNAs, biomarkers, BDNF, GDNF

Consapevole, dichiara

CONSAPEVOLE: (1) del fatto che in caso di dichiarazioni mendaci, oltre alle sanzioni previste dal codice penale e dalle Leggi speciali per l'ipotesi di falsità in atti ed uso di atti falsi, decade fin dall'inizio e senza necessità di alcuna formalità dai benefici conseguenti al provvedimento emanato sulla base di tali dichiarazioni; (2) dell'obbligo per l'Università di provvedere al deposito di legge delle tesi di dottorato al

fine di assicurarne la conservazione e la consultabilità da parte di terzi; (3) della procedura adottata dall'Università di Ferrara ove si richiede che la tesi sia consegnata dal dottorando in 2 copie, di cui una in formato cartaceo e una in formato pdf non modificabile su idonei supporti (CD-ROM, DVD) secondo le istruzioni pubblicate sul sito : http://www.unife.it/studenti/dottorato alla voce ESAME FINALE – disposizioni e modulistica; (4) del fatto che l'Università, sulla base dei dati forniti, archivierà e renderà consultabile in rete il testo completo della tesi di dottorato di cui alla presente dichiarazione attraverso l'Archivio istituzionale ad accesso aperto "EPRINTS.unife.it" oltre che attraverso i Cataloghi delle Biblioteche Nazionali Centrali di Roma e Firenze. DICHIARO SOTTO LA MIA RESPONSABILITA': (1) che la copia della tesi depositata presso l'Università di Ferrara in formato cartaceo è del tutto identica a quella presentata in formato elettronico (CD-ROM, DVD), a quelle da inviare ai Commissari di esame finale e alla copia che produrrà in seduta d'esame finale. Di conseguenza va esclusa qualsiasi responsabilità dell'Ateneo stesso per quanto riguarda eventuali errori, imprecisioni o omissioni nei contenuti della tesi; (2) di prendere atto che la tesi in formato cartaceo è l'unica alla quale farà riferimento l'Università per rilasciare, a mia richiesta, la dichiarazione di conformità di eventuali copie. PER ACCETTAZIONE DI QUANTO SOPRA RIPORTATO

Dichiarazione per embargo

12 mesi

Richiesta motivata embargo

1. Tesi in corso di pubblicazione

Liberatoria consultazione dati Eprints

Consapevole del fatto che attraverso l'Archivio istituzionale ad accesso aperto "EPRINTS.unife.it" saranno comunque accessibili i metadati relativi alla tesi (titolo, autore, abstract, ecc.)

Firma del dottorando

Ferrara, li 07/02/2020 Firma del Dottorando ____Francesca Lovisari 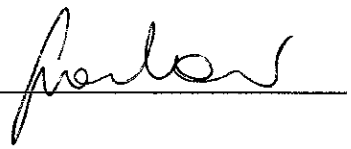

Firma del Tutore

Visto: Il Tutore Si approva Firma del Tutore ____Michele Simonato